THE INTEGRATION OF BOTTOM-UP AND TOP-DOWN SIGNALS IN HUMAN PERCEPTION IN HEALTH AND DISEASE

Rimona Sharon Weil

Wellcome Trust Centre for Neuroimaging

Institute of Cognitive Neuroscience

Institute of Neurology

University College London

Prepared under the supervision of:

Professor Geraint Rees

Professor Ray Dolan

Submitted to UCL for the Degree of PhD

DECLARATION

I, Rimona Weil, confirm that the work presented in this thesis is my own. Where information has been derived from other sources, I confirm that this has been indicated in the thesis.

The study described in Chapter 5 of this thesis was performed in collaboration with Victoria Wykes. I designed and constructed the stimuli, ran the experiment on some participants, analysed the data and wrote the manuscript which has been submitted for publication by Visual Cognition. The collection of data for the rest of the participants was performed by Victoria Wykes.

The study presented in Chapter 7 has been submitted for publication by Cerebral Cortex.

The work presented in Chapters 3, 4 and 6 has been published in the following peer reviewed papers:

Weil RS, Kilner J, Haynes JD, Rees G. Neural correlates of perceptual filling-in of an artificial scotoma in humans. *Proc Natl Acad Sci USA* 2007; 104:5211-6.

Weil RS, Watkins S and Rees G. Neural correlates of perceptual completion of an artificial scotoma in human visual cortex measured using functional MRI. *Neuroimage.* 2008;42(4):1519-28

Weil RS, Plant GT, James-Galton M and Rees G. Neural correlates of hemianopic completion across the vertical meridian. *Neuropsychologia.* 2009;47(2):457-64

ACKNOWLEDGEMENTS

Above all, I would like to thank my supervisor Geraint Rees. I cannot imagine a more encouraging, supportive and inspiring supervisor, or anyone as able to see the positive in almost any situation. In addition I am grateful to my second supervisor, Ray Dolan, for helpful and timely advice and to Jon Driver for astute input just when it was needed.

I would also like to thank the members of the Rees lab – Richard, Su, David, Bahador, Marieke, Chris, Lauri, Ayse, Sharon, Sam, Frank, Claire, Elaine, John and Vic for all their help and advice and for many eventful lab meetings.

I would also like to thank many people at the FIL especially the Dolan Group, particularly Mkael Symmonds and Steve Fleming. Also at the FIL, I would like to thank Jenny, Fiona, Bogdan, Nick, Ferath, Guillaume and Jean. Thanks also to the FIL support staff – Peter, Holly, Eric, Marcia, David, Jan, Amanda, Sheila, Kristjan, Gareth, Chris and Rachel. Special thanks to James Kilner for much needed help and support in MEG analysis and to Ric for practical support for a myriad of technical issues

Thank you to all the volunteers prepared to lie for many hours in the scanners and special thanks to patient POV for coming back several times to be scanned and always managing to be cheerful.

Thanks also to the Medical Research Council for funding me.

I would also like to thank my family and friends. In particular, thank you Jonnie, for always asking the questions I don't have the answers for and being prepared to challenge, inspire and support me. Thank you to Elia and Adina for giving me a sense of perspective. Finally thank you to my parents who always believed in me.

ABSTRACT

To extract a meaningful visual experience from the information falling on the retina, the visual system must integrate signals from multiple levels. Bottom-up signals provide input relating to local features while top-down signals provide contextual feedback and reflect internal states of the organism.

In this thesis I will explore the nature and neural basis of this integration in two key areas. I will examine perceptual filling-in of artificial scotomas to investigate the bottom-up signals causing changes in perception when filling-in takes place. I will then examine how this perceptual filling-in is modified by top-down signals reflecting attention and working memory. I will also investigate hemianopic completion, an unusual form of filling-in, which may reflect a breakdown in top-down feedback from higher visual areas.

The second part of the thesis will explore a different form of top-down control of visual processing. While the effects of cognitive mechanisms such as attention on visual processing are well-characterised, other types of top-down signal such as reward outcome are less well explored. I will therefore study whether signals relating to reward can influence visual processing.

To address these questions, I will employ a range of methodologies including functional MRI, magnetoencephalography and behavioural testing in healthy participants and patients with cortical damage. I will demonstrate that perceptual filling-in of artificial scotomas is largely a bottom-up process but that higher cognitive

functions can modulate the phenomenon. I will also show that reward modulates activity in higher visual areas in the absence of concurrent visual stimulation and that receiving reward leads to enhanced activity in primary visual cortex on the next trial.

These findings reveal that integration occurs across multiple levels even for processes rooted in early retinotopic regions, and that higher cognitive processes such as reward can influence the earliest stages of cortical visual processing.

CONTENTS

LIST OF FIGURES

LIST OF TABLES

CHAPTER 1: GENERAL INTRODUCTION

1.1 Introduction

Our experience of the world as a series of meaningful objects and scenes is constructed by the visual system from the dauntingly complex pattern of light and dark edges transmitted by the retina. Transforming these complicated signals into meaningful information and experiences requires complex multilevel neural interactions with bottom-up processing, informed by the properties of the sensory signals themselves; and top-down influences whereby internal states such as attention, motivation and reward can influence the processes taking place at earlier stages of the visual pathway. In this way, information can be integrated from different regions and processes to arrive at a coherent output.

In this thesis, I will examine the influences of top-down (internal states) and bottom-up processing on both behavioural measures of awareness and on signals from early (retinotopic) and later visual cortices. I will examine two very different model systems, perceptual filling-in and reward processing, providing converging evidence about their respective behavioural and neural effects on human visual cortex using multiple experimental techniques including functional MRI (fMRI) with retinotopic mapping, magnetoencephalography (MEG) and behavioural experiments.

The first part of this thesis examines the neural basis of perceptual filling-in. This involves the interpolation of missing information to make sense of a world where

visual information is frequently absent or objects are occluded behind other objects. It provides a unique substrate for investigating this integration of bottom-up and top-down neural processes as it involves the extraction of local feature information, lateral propagation of signals, and feedback from higher regions to constrain and inform feature recognition. I will begin examining whether the earliest stages of cortical processing are involved in perceptual filling-in. I will then look for evidence of top-down control of this phenomenon by examining how attention and working memory affect the process of perceptual filling-in of artificial scotomas

In the second part of the thesis, I will turn to study top-down influences on visual cortical processing more directly, but using some of the experiment tools, techniques and procedures learnt in the first part. Rather than focus on relatively well-studied top-down influences such as attention and working memory, here I will focus on the potential influence of receiving reward on visual processing. Humans in common with other animals, optimise their behaviour to maximise the pleasurable experience that is reward. It might be predicted, therefore, that receiving a reward could guide performance to bring about future reward. In the context of visual processing, where a task is associated with a pleasurable outcome, this might be expected to influence future performance of that visual task. Such a role for reward outcome as a top-down modulator of visual processing has not been explicitly examined previously in humans. I will therefore examine how reward outcome influences visual cortex activity at the point of reward feedback and the effect of reward receipt on retinotopic visual cortex activity during subsequent performance of a visual task.

1.1.1 Bottom-up processing: the organisation of the visual cortex

Current knowledge of the organization of the visual system originates from behavioural, anatomical and neurophysiological studies in monkeys. These have revealed two processing pathways both originating in primary visual cortex (V1) (Ungerleider and Mishkin, 1982): the ventral stream which identifies objects and projects from V1 through areas V2 and V4 to the inferior temporal cortex; and the dorsal stream which projects through areas V2 and V3 to the middle temporal area and on to the superior temporal and parietal cortex and processes spatial relations of objects and guides object-related movement. There is a largely hierarchical organisation of information processing within both streams, progressing from simple local attributes by cells in V1 to more global feature detection in inferior temporal cortex (Tanaka, 1993) and direction and velocity of motion in the middle temporal area (Mikami *et al.*, 1986). There is also an associated increase in receptive field size with progression from V1 towards the temporal and parietal lobes (Gattass *et al.*, 1981;Gattass *et al.*, 1988).

Neuroimaging studies in humans reveal extensive similarities between the human and monkey visual systems, with similar ventral and dorsal streams (Ungerleider and Haxby, 1994). For example, tasks requiring the perception of object characteristics such as colour or faces lead to activity in area V4 and more anterior ventral stream regions (Zeki *et al.*, 1991;Kanwisher *et al.*, 1997) whereas those requiring motion perception are associated with activity in the dorsal stream, especially in a region homologous to monkey MT (Zeki *et al.*, 1991;Tootell *et al.*, 1995). Moreover, the increasing complexity of processing seen in the progression from posterior to more

anterior areas in monkey visual cortex is also found in humans with more global feature processing such as face or object detection in more anterior regions (Kanwisher *et al.*, 1997;Grill-Spector *et al.*, 1998) with associated increases in receptive field size (Tootell *et al.*, 1997).

However, it is clear that bottom up mechanisms alone cannot provide flexible and responsive information in a rapidly changing internal as well as external environment. Consistent with this idea, anatomical studies in monkeys reveal that almost all connections between regions in the ventral stream are reciprocal (Felleman and Van Essen, 1991), with further feedback projections from areas outside this processing pathway, such as from prefrontal and parietal cortex (Cavada and Goldman-Rakic, 1989;Ungerleider et al., 1989), providing potential pathways for top-down processing of visual information.

1.1.2 Top-down processing of visual information

Extensive neurophysiological and neuroimaging studies support the idea that visual processing in humans is also subject to top-down influences, whereby internal states such as attention or motivation which reflect our internal representation of the world can modulate the simpler processes occurring at earlier stages (for a review see (Gilbert and Sigman, 2007)). There are several well-studied examples of these higher cognitive functions such as attention (Moran and Desimone, 1985;Treue and Maunsell, 1996) and working memory (Desimone, 1996;Soto *et al.*, 2007) influencing

earlier stages of visual processing. Here I will now briefly review some of the evidence for the effects of attention on visual processing and awareness.

Single cell recordings in monkeys and neuroimaging studies in humans demonstrate that selective attention modulates neural processing in visual cortex. Directing attention to a stimulus causes neural responses in monkeys to be enhanced in V1 (Motter, 1993), V2 (Motter, 1993;Luck *et al.*, 1997) and in V4 (Haenny *et al.*, 1988;Spitzer *et al.*, 1988). Similar enhancement with increased spatial attention is seen for neurons in MT (Treue and Maunsell, 1996) and the lateral intraparietal area (Colby *et al.*, 1996). Similarly in humans, attention enhances fMRI responses in primary visual cortex (Gandhi *et al.*, 1999;Watanabe *et al.*, 1998;Somers *et al.*, 1999) and beyond (Tootell et al., 1998a;Martinez et al., 1999b), with a gradient in the influence of attention as one moves up the hierarchy from V1 (Tootell *et al.*, 1998a).

Initial studies of the top-down effects of attention on visual processing focussed on spatial attention, but it has become clear that feature-based non-spatial attention also modulates visual processing in monkeys (Motter, 1994;Treue and Martinez Trujillo, 1999) and in humans (Corbetta *et al.*, 1990;O'Craven *et al.*, 1997). Attention can even influence visual processing in the absence of any visual stimulation. Neurophysiological studies show increased firing rates for V2 and V4 neurons when an animal is cued to attend to a location within the neuron's receptive field, before the stimulus is presented (Luck et al., 1997;Treue and Martinez Trujillo, 1999) and similar effects are seen in humans (Kastner *et al.*, 1999).

However, attention is just one example of top-down control on early sensory processing. Other influences include expectation, or prior experience, where previous experience of representations of objects or scenes shapes how they are segregated (Dolan *et al.*, 1997) and working memory, which influences visual processing independently from attention (Soto *et al.*, 2007). However, it is not yet clear whether other higher cognitive processes can influence visual processing, and in particular, whether processes such as reward can modulate the earliest cortical stages of visual processing is still unknown.

This thesis is concerned with exploring the integration of bottom-up and top-down signals in visual processing by exploring two key areas: the first is perceptual filling-in, where the visual system interpolates information across visual space where that information is physically absent. The second will explore an intriguing aspect of top-down processing: the influence of higher processes such as the effect of reward on visual cortex activity in the absence of concurrent visual stimulation.

1.2 Perceptual filling-in

Perceptual filling-in is the interpolation of missing information across visual space. It is a ubiquitous process in the visual system, necessary to make sense of the world. Light from portions of objects and scenes often falls upon interferences in the retina, such as the blind spot or retinal vessels; or falls behind objects in the real world and the visual system must process information across these occluders so that they are perceived as complete and not fragments. It is an extremely effective process, as most

of the time we are entirely unaware that it is taking place. It is also a natural process which takes place all the time, but researchers have observed that certain stimuli can be configured to promote perceptual filling-in. These may exploit some of the same mechanisms underlying other forms of filling-in.

Perceptual filling-in is a heterogeneous phenomenon. Here I will discuss different forms of filling-in and present a new framework for categorising the various types of perceptual filling-in. I propose that this system, by grouping together common aspects of filling-in and separating out contrasting features, may provide some insights into possible mechanisms underlying the different forms of perceptual filling-in.

1.2.1 Nomenclature of perceptual filling-in

There is some confusion in the literature regarding nomenclature, with the terms filling-in, perceptual filling-in and perceptual completion all being used to describe the interpolation of missing information across visual space but sometimes for different forms of filling-in. In particular, some groups use filling-in to refer to surfaces (Sasaki and Watanabe, 2004) and perceptual completion to refer to contours (Sergent, 1988), but many influential groups use the terms interchangeably (Pessoa *et al.*, 1998;De Weerd, 2006). Here I will use the terms perceptual completion and perceptual filling-in interchangeably to refer to the perceptual experience of interpolation of information across visual space, for both contours and surfaces. It is also important to distinguish perceptual filling-in from *neural* filling-in (Pessoa *et al.*,

1998). Perceptual filling-in here refers to the perceptual experience of interpolation and does not imply anything about neural mechanisms. Where mechanisms are being considered, this will be explicitly stated in the text. Note, perceptual filling-in here refers only to situations where there is a conscious experience of the image, as occurs in illusory contours, but also occurs for occluded objects; for example, there is a subjective experience of seeing a whole car, even if it is obscured by a tree. This is not the case, however, for the information behind the back of the head. We do not have a perceptual experience of things happening behind us. It is possible to imagine or infer what happens in the space behind our heads, but to experience it, we have to turn around. For this reason, in this thesis, perceptual filling-in does not include the processing of information from the space behind our head or other similar forms of gleaning of absent information. Filling-in is also used in areas of visual neuroscience to refer to aspects of surface perception (Neumann et al., 2001;Paradiso and Hahn, 1996). Although perceptual filling-in may share some of the same mechanisms that are involved in normal surface perception, this is not being explored here.

1.2.2 Current theories of mechanisms of perceptual filling-in

Two main hypotheses have been discussed in the literature for perceptual filling-in. The first hypothesis, described by Dennet (Dennett, 1991) and extended by others (Kingdom and Moulden, 1988;O'Regan, 1992), suggests that neural filling-in does not occur, but that the visual system simply ignores the absence of information across the scotoma or blind spot and labels or 'tags' the region with the information in the surround ('more of the same'). According to this theory, also termed the symbolic or

cognitive theory, there would be no retinotopic representation of the filled-in surface in earlier visual regions, but activity related to filling-in might be found in higher visual areas representing objects. However, substantial evidence is accumulating for an active process for perceptual filling-in, with point-for-point representations of filled-in regions in retinotopic cortex.

The second hypothesis is the isomorphic model that suggests a point-for-point representation of the filled-in surface will be found in early retinotopic regions. This might be achieved by lateral propagation of neural signals, with the spread of activation across the retinotopic map from the border to interior surface of the filled-in figure (Gerrits and Vendrik, 1970;De Weerd et al., 1995). Alternatively, this might be achieved by passive remapping of receptive fields (Chino *et al.*, 2001) such that visual input from the region surrounding the scotoma or blind spot is displaced so that it infiltrates the cortical region representing the blind spot or scotoma.

1.2.3 Previous taxonomies of perceptual filling-in

Taxonomies of perceptual filling-in have been proposed previously. Pessoa (Pessoa *et al.*, 1998) proposed two general divisions: modal versus amodal completion and boundary versus featural completion. However, this taxonomy has been criticised as being unnecessarily complicated (Birgitta Dresp 1998, commentary on (Pessoa *et al.*, 1998)) and the major division of modal/amodal as unhelpful (Carol Yin 1998, commentary on (Pessoa *et al.*, 1998)).

Dresp proposed a taxonomy based purely on psychophysical evidence rather than phenomenology. She proposed divisions based on area, surface and contour completion, where area completion involves spreading of contrast into regions without clearly defined boundaries; surface completion involves the perception of figures from real or apparent contours and contour completion involves the perceptual grouping of collinear lines. However, it is not clear that the distinction between area and surface completion is helpful and dismissing all phenomenological differences between types of perceptual filling-in misses the aim of a framework to explore commonalties and differences to better understand underlying mechanisms.

Yin proposed a taxonomy reflecting the goals of visual completion: unity, shape and perceptual quality. However, this taxonomy is very similar to the original Pessoa taxonomy (with shape determination closely linked to boundary completion and perceptual quality determination linked to featural completion) and it has been suggested that unity does not necessarily involve perceptual completion as disparate fragments may be experienced as unified without any visual completion taking place (for example when a group of dots moving coherently are experienced as unified) (Pessoa *et al.*, 1998).

1.2.4 A framework for categorising different forms of perceptual filling-in

Here I propose a new framework for perceptual filling-in based on phenomenological and psychophysical characteristics. I suggest that this framework provides some

insight into the possible underlying processes involved in filling-in by grouping the various types of perceptual completion.

Perceptual filling-in can be broadly separated on phenomenological and psychophysical grounds into two types: perceptual filling-in which takes place instantly and perceptual filling-in which is delayed as it requires prolonged fixation before it can occur. These can each be further subdivided according to whether perceptual filling-in will occur only in the presence of specific stimulus configurations (stimulus dependent) or will occur regardless of stimulus configuration (stimulus independent, often due to a deficit or particular feature of the visual system, see Table 1.1). I will now explore the current understanding of perceptual filling-in within these categories and consider how this categorisation helps understanding of the processes involved in perceptual filling-in. This review is not intended to be exhaustive, but will provide examples for each type of perceptual filling-in (instant versus delayed; stimulus dependent and stimulus independent) where these help to illustrate common and distinct features of filling-in.

	Stimulus dependent	Stimulus independent
Instant	Illusory contours Illusory surfaces Neon colour spreading Craik-O'Brien-Cornsweet effect Afterimage colour filling-in Amodal completion	Filling-in at the blind spot Filling-in of retinal scotomas
Delayed	Troxler fading Artificial scotomas Motion induced blindness	Stabilised retinal images

Table 1.1 Framework for categorising different types of perceptual filling-in, according to whether perceptual filling-in occurs instantly or is delayed and only occurs after prolonged fixation; and according to whether perceptual filling-in occurs only with specific stimulus configurations or will occur independent of the particular stimulus used.

1.2.5 Instant perceptual filling-in dependent on stimulus configuration

a) illusory contours

One type of instant perceptual filling-in is the perceptual completion of illusory contours (also termed modal completion (Michotte *et al.*, 1991)). These are edges which are perceived in the absence of physical boundaries. They are induced by an appropriate arrangement of local elements, or inducers, causing the perception of a

surface overlaying these inducing elements. A classic example of illusory contours is the Kanizsa figure. This is generated by a particular configuration of high contrast figures, such as incomplete and co-aligned black circles, which induce the illusory perception of a light shape (Kanizsa, 1979)(see Fig 1.1).

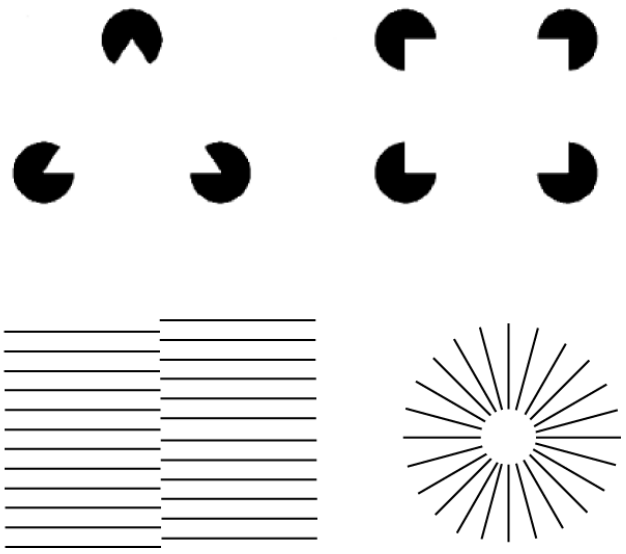

Figure 1.1 Kanizsa figures and other examples of illusory contours

Illusory contours can also be generated by displaced gratings, which can form edges or circular boundaries, depending on the configuration of the inducing gratings (see Fig 1) and can even be defined by depth cues (Mendola *et al.*, 1999). This type of perceptual completion, in addition to inducing the appearance of a complete contour or shape, is also characterised by the striking phenomenon that the region intervening between the inducers is filled-in with illusory brightness and colour that is determined by the inducers (Davis and Driver, 2003).

One area of debate is whether illusory contours are processed at the same anatomical level as real contours. Purely psychophysical studies in normal human vision suggest

a locus of perceptual completion in earlier visual areas as the tilt after-effect and motion after-effects can be generated with illusory as well as real contours (Smith and Over, 1975;Smith and Over, 1979) and tilt after-effects cross over between illusory and real contours (Berkley *et al.*, 1994). Furthermore, Kanizsa figures are detected without attention in a visual search paradigm (Davis and Driver, 1994;Senkowski et al., 2005) and if the high contrast inducers are placed on a checkerboard background which is misaligned with the inducing elements, the illusory contour disappears (Ramachandran *et al.*, 1994), consistent with a close interaction between illusory contour processing and processes extracting local feature information. Moreover, perceptual completion of illusory contours is worse across the vertical meridian (Pillow and Rubin, 2002), reflecting limitations in cross-hemispheric integration and therefore a locus more likely to be in V1 or V2, areas which are more sensitive to this hemispheric divide. Finally, patients with visuospatial neglect show improved performance on line bisection tasks when illusory contours are present, despite being unaware of their presence (Mattingley *et al.*, 1997;Vuilleumier *et al.*, 2001), consistent with a preattentive locus of boundary completion.

Electrophysiological studies in animals have explored the type and location of neurons involved in perception of illusory contours (for a review see (Nieder, 2002)). An illusory bar induced by aligned corners placed outside the classical receptive field of V2 neurons yields significant responses (Von der Heydt and Peterhans, 1989). Subsequent experiments in cats and monkeys have shown that both V1 and V2 neurons carry signals related to illusory contours, although signals in V2 are more robust that those in V1(Redies *et al.*, 1986;Sheth *et al.*, 1996;Ramsden *et al.*, 2001). More recent studies have suggested the presence of interactions between V1 and V2

neurons in illusory contour processing, with responses occurring earlier in V2 (70-95 ms) than in V1 (100-200 ms) (Lee and Nguyen, 2001). However, a recent report of illusory contour processing in monkeys instead implicates inferior temporal neurons (Sary *et al.*, 2007) and lesions of monkey IT (which may be homologous to human lateral occipital complex (LOC) (Denys *et al.*, 2004;Sawamura *et al.*, 2005)) impair illusory contour discrimination (Huxlin *et al.*, 2000).

Illusory contours have been extensively studied in human neuroimaging experiments with conflicting results, some of which may be explained by confounding methodological issues, particularly differences in stimuli, such as stimulus size, ratio between inducers and total length of illusory figure and different types of inducers, such as static and moving features (for a review see (Seghier and Vuilleumier, 2006)). Some studies have shown specific activations in response to illusory contours within area V1 (Larsson et al., 1999;Seghier et al., 2000) and the timing of responses seen in MEG and ERP studies is consistent with involvement of early cortical visual areas (Herrmann and Bosch, 2001;Ohtani et al., 2002;Proverbio and Zani, 2002;Murray et al., 2006). However, other studies do not show the involvement of V1 during perception of static (Ffytche and Zeki, 1996;Kruggel et al., 2001;Stanley and Rubin, 2003) or moving illusory contours (Goebel *et al.*, 1998). As with neurophysiological studies on primates, the involvement of area V2 in illusory contour perception has been more consistently shown, with most neuroimaging studies demonstrating activation of this region (Ffytche and Zeki, 1996;Goebel et al., 1998;Hirsch et al., 1995;Larsson et al., 1999), although some studies did not find reliable evidence for involvement of V2 (Mendola *et al.*, 1999).

Higher level regions have also been implicated in illusory contour processing. One study found activations specifically associated with illusory contour processing in putative areas V7 and V8, and overlapping with the lateral occipital complex (Mendola *et al.*, 1999). A similar region was identified in other studies (Murray et al., 2002a;Stanley and Rubin, 2003;Murray et al., 2004) and using ERP source mapping (Murray *et al.*, 2004). It is possible that this area was activated partly due to object processing within the Kanizsa figure. Interestingly, an MEG study using line gratings but no illusory figure failed to detect activity within the LOC (Ohtani *et al.*, 2002) and when illusory contour formation was prevented using misaligned inducers (Stanley and Rubin, 2003), LOC was still activated, suggesting that LOC activity may not be specific to illusory contour processing.

Other higher-tier visual areas that have been implicated in processing illusory contours include the right fusiform gyrus (Larsson et al., 1999;Halgren et al., 2003) and the kinetic occipital region (also called area V3B), which is activated by the perception of moving (Seghier *et al.*, 2000) and static illusory contours (Kruggel *et al.*, 2001) and a recent study (Montaser-Kouhsari *et al.*, 2007) found orientation-selective adaptation to illusory contours in a range of higher tier visual areas (V3, V4, VO1, V3A/B, V7, LO1 and LO2) as well as V1 and V2, with an increase in orientation-selective adaptation in higher regions.

Taken together, electrophysiological and neuroimaging studies suggest that illusory contour processing is associated with activity of neuronal populations in early visual areas, especially V2; and may also involve more global, high-level processing in higher visual areas, which may then feed back to the lower visual regions.

b) Illusory surfaces

i) Neon colour spreading

Neon colour spreading is a striking and beautiful phenomenon whereby the neon-like glow of a colour escapes the boundaries of a real figure and seems to fill the surrounding area until it is limited by the boundaries of an illusory figure (for a review see (Bressan *et al.*, 1997) (see Fig 1.2).

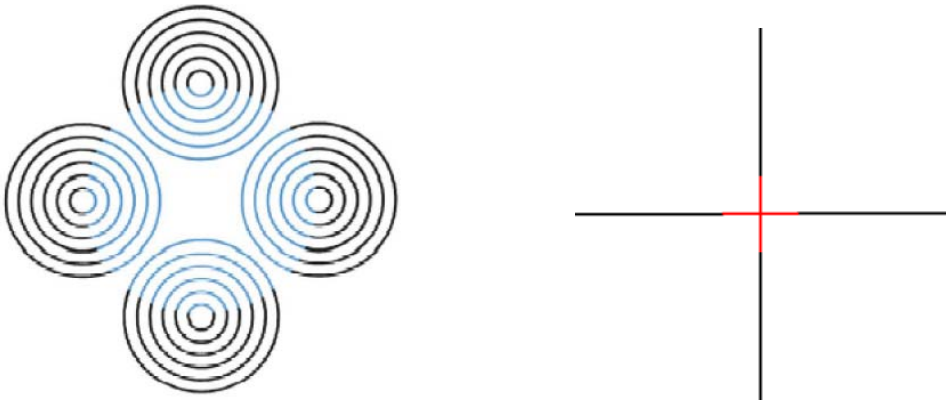

Figure 1.2. Neon colour spreading. a) The central virtual circle appears as a transparent blue surface overlapping the black rings. Adapted from (Pinna and Grossberg, 2005). b) The Ehrenstein figure: red colour from the inner red segments of the cross seems to leak into its surround to produce the impression of a central red disc.

This effect, first observed by Dario Varin in 1971 (Varin, 1971) and Harrie van Tuijl (van Tuijl, 1975), also occurs for achromatic figures, with illusory brightness spreading induced by grey segments on black inducers. The illusion is strongest when the lines and segments are continuous, collinear and equally thick and the effect disappears if the subjective figure is encircled by a ring (Redies and Spillman, 1982). Others have shown that depth cues are important in producing this effect, with neon

spreading only occurring if the coloured elements are phenomenally in front of the inducing areas (Nakayama et al., 1990;Meyer and Dougherty, 1987) (although see also (Bressan and Vallortigara, 1991)). The rules for whether colour or brightness spreading will take place seem to represent the colour and luminance prerequisites for perceiving a transparent subjective figure, as spreading usually occurs when the luminance of the segments is between the luminance of the embedding lines and that of the background (Bressan *et al.*, 1997).

Illusory contours seem to play a crucial role in delimiting the spread of neon colour illusions, with spreading particularly vivid when coloured segments are inserted into the blank area of a figure that otherwise would produce a colourless illusory figure (Watanabe and Sato, 1989;Watanabe and Takeichi, 1990).

Neon colour spreading seems to involve very early visual processes: if the coloured cross and black arms are presented to different eyes but aligned to form a fused image, an illusory contour is perceived, but no colour spreading occurs (Takeichi *et al.*, 1992) and neon colour filling-in (and the related, but contrasting watercolour illusion) has recently been explained in terms of competition within boundary perception (Pinna and Grossberg, 2005). Specifically, boundaries of lower contrast edges might be weakened by spatial competition more than boundaries of higher contrast edges and this induces spreading of colour across boundaries, producing the illusion. However, in a recent neuroimaging study in humans, neon colour spreading was associated with activity in V1 only when attention was controlled with a task at fixation (Sasaki and Watanabe, 2004), consistent with a process involving early visual regions but influenced by higher cortical functions.

ii) Craik-O'Brien-Cornsweet illusion

The Craik-O'Brien-Cornsweet effect occurs when regions of the same luminance appear to differ in brightness because of differences in luminance at the borders between these regions (Craik, 1966;O'Brien, 1958;Cornsweet, 1970) (see Fig 1.3). For example, in Figure 1.3, the bars appear to alternate between light and dark despite the fact that the central portion of the bars are of equal luminance. Thus the impression is similar to a square-wave grating of alternating uniformly luminant bars. This effect is abolished if the edges are occluded.

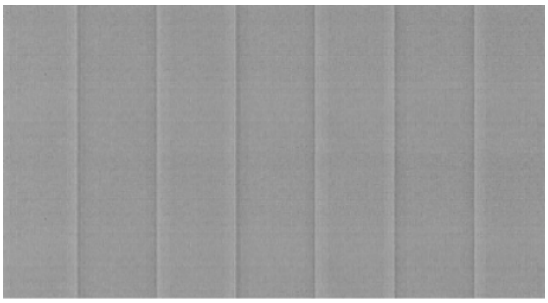

Figure 1.3. A Craik-O'Brien-Cornsweet effect grating. Note that although the luminance in the central regions of each panel is identical, alternate bars appear darker or lighter due to differences at the edges of the bars.

It has been proposed that this effect is mediated by a form of cortical filling-in (Cohen and Grossberg, 1984;Gerrits and Vendrik, 1970) and this is consistent with psychophysical studies showing that brightness propagates at a fixed speed across the central retinal field (Davey *et al.*, 1998) (but see also (Devinck *et al.*, 2007) and (Dakin and Bex, 2003)). An alternative hypothesis is that an abstract process occurs whereby a label such as 'brightness' is attached to one region (Burr, 1987), possibly at a later stage of visual processing, similar to the symbolic theory of filling-in.

In cats, brightness responses due to the Cornsweet effect are seen in Area 18 and to a lesser extent in Area 17 (Hung *et al.*, 2001), consistent with local processes propagating brightness information. More recently, the same group showed in macaque that V2 thin stripe regions are responsive to Cornsweet-induced brightness (as well as true luminance brightness) whereas V1 blob regions respond only to real brightness, suggesting that V1 responses reflect luminance properties signalled by local inputs, whereas V2 confers higher-order properties resulting from integration of non-local inputs (Roe *et al.*, 2005).

However, in humans, a recent study examining specific fMRI responses to edges in the Craik-O'Brien-Cornsweet illusion (Perna *et al.*, 2005) found that the caudal region of the intraparietal sulcus and the lateral occipital sulcus responded specifically to the illusion. They found that earlier visual areas, including V1, responded as strongly to the location of the edge as to a line of matched contrast and detectability, rather than to the brightness illusion, consistent with the suggestion that V1 does not encode illusory brightness, but that regions higher than V2 compute surface brightness. Conversely, a recent study using high spatial resolution fMRI shows that the brightness filling-in seen in the Craik-O'Brien-Cornsweet illusion arises instead from signals in populations of monocular neurons early in human lateral geniculate nucleus (Anderson, Dakin and Rees JOV 2009, in revision).

iii) Afterimage colour filling-in

A recent and striking perceptual filling-in phenomenon has been described (van Lier *et al.*, 2009) whereby afterimage colours can spread to previously uncoloured areas, when constrained by contours presented after the coloured image (Fig. 1.4), demonstrating the important role of boundaries in constraining perceptual filling-in of afterimages.

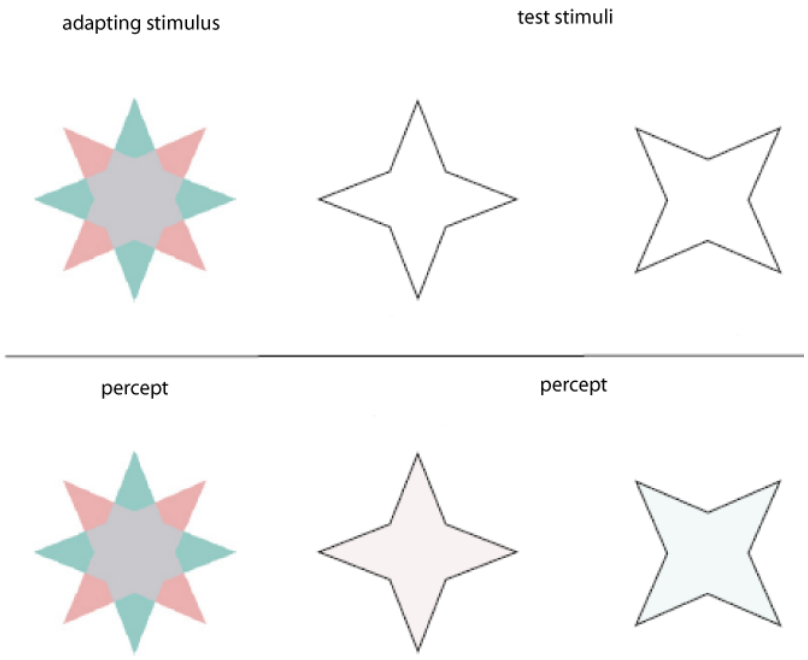

Figure 1.4 Illustration of colour afterimages After adapting to the adapting stimulus, the test outlines are presented alternately. The two outlines cause the appearance of a red and then a cyan afterimage, including in the centre of the figure, where previously no colour was present. Adapted from (van Lier *et al.*, 2009).

Taken together, perceptual filling-in of surfaces seems to be closely linked to boundary perception (real or illusory) and is likely to entail a multilevel process involving higher regions feeding back to earlier visual regions.

c) Perceptual filling-in behind occluders: amodal completion

Objects in the natural world do not present themselves in isolation, but are often occluded by other objects. Yet we do not have the impression of being surrounded by object fragments as the visual system perceptually fills-in the missing information to interpret the objects as complete (Fig 1.5).

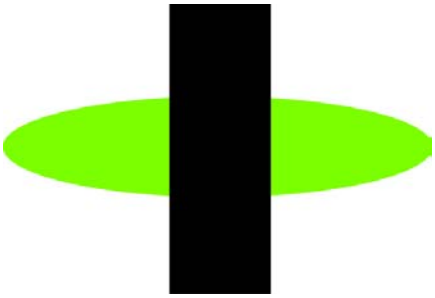

Figure 1.5 Example of amodal completion The appearance is of a green oval behind a black rectangle, although the oval is not seen in full.

This type of perceptual filling-in, where fragments are taken to be the visible portions of an occluded object, is termed amodal completion. Several theories have been proposed to explain this linkage of image fragments. One classic theory is that local image cues are used to determine object relationships. For example, T-junctions are often present when an object is perceived as occluded and are likely to represent contour discontinuity (Kellman and Shipley, 1991;Nakayama et al., 1989). Another local cue is the relative orientation of image contours (Kellman and Shipley, 1991): objects are more likely to complete behind an occluder if the angle between their extensions behind the occluder is greater than 90^{o}, such that good contour continuation is more likely. However, important exceptions can be shown where completion takes place in the absence of T-junctions or good contour continuation and

conversely, where relatable edges are present but completion is not perceived (see (Boselie and Wouterlood, 1992;Tse, 1999) for examples).

Another theory emphasises the importance of more global cues in causing perceptual completion, such as symmetry, regularity or simplicity (Sekular *et al.*, 1994;van Lier *et al.*, 1994). According to this theory, completion tends to produce the impression of the most regular shapes (Buffart and Leeuwenberg, 1981). However, other researchers have shown that observers do not always perceive the most regular shapes (Boselie and Wouterlood, 1992). Other theories ascribe amodal completion to the use of volume cues to form the image (Tse, 1999) or common depth planes (Nakayama and Shimojo, 1992). Indeed, the presence of a depth-appropriate occluder plays a critical role in determining whether completion takes place (Johnson and Olshausen, 2005).

Amodal completion seems to take place early on in visual processing. For example, when subjects are asked to search for a notched circle in an array of circles and squares, if the notched circle abuts the edge of a square so that it seems to be occluded by it, the notched circle takes longer to find (see Fig 1.6) (Rensink and Enns, 1998) as it is perceived as a complete circle in a sea of complete circles.

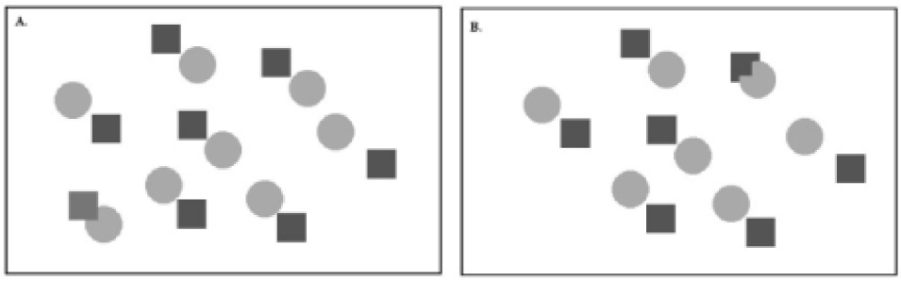

Figure 1.6 Visual search for amodally completed target. Identifying the notched circle is harder in (A) as it is amodally completed and perceived as a circle among the other circles. In (B), the notched circle 'pops out'. Search display similar to those used in (Rensink and Enns, 1998), adapted from (Driver et al., 2001a).

Neurophysiological studies support the notion that amodal completion involves early visual processes, with evidence of amodal contour responses about 100 ms after presentation of occluded images in macaque V1 cells (Lee and Nguyen, 2001) and V1 monkey cells fire in response to an amodally completed bar behind a square (Sugita, 1999). V2 neurons in macaque also respond to partially occluded contours (Bakin *et al.*, 2000). Moreover, in humans, ERP differences between occluded images and their deleted counterparts are seen as early as 130 ms after presentation (Johnson and Olshausen, 2005).

Initial neuroimaging studies seemed to contradict these findings with some studies showing increased activity in LOC for occluded compared to scrambled images with identical local features (Lerner *et al.*, 2002). Yet the same authors found that completion effects occur very rapidly following stimulus onset (Lerner *et al.*, 2004). More recently, fMRI adaptation paradigms have been used to show that the representation of an amodally completed figure evolves over time (Rauschenberger *et al.*, 2006), with physical properties of the stimulus processed first (before 100 ms)

followed by the amodal completion of the stimulus (within 250 ms). These findings were extended by a study identifying regions in early visual cortex involved in processing of local contour information during amodal completion and regions in inferior temporal cortex responding to the amodally completed shape (Weigelt *et al.*, 2007) consistent with both local and global processing in amodal completion. Conversely, a recent study used a stereoscopic manipulation to reveal that LOC and dorsal object-selective foci are specifically responsive to completed occluded objects (Hegde *et al.*, 2008).

Taken together, the process of filling-in behind occluders is likely to involve a large number of information processing steps in early and higher regions of visual cortex. These might involve distinguishing between the boundaries of the occluded and the occluding object, assigning each of the resulting partial views a surface and then filling-in the missing information of each part (Johnson and Olshausen, 2005) using clues from depth disparity and collinear edges and representing the fully completed shape.

i) A common mechanism for modal and amodal completion?

A subject of intense debate is whether modal and amodal completion share a common mechanism as both involve the connection of disjoint image fragments into a coherent representation of an object, surface or contour. Kellman and Shipley (Kellman and Shipley, 1991;Kellman et al., 1998) have argued in their 'identity hypothesis' that the same interpolation mechanism is responsible for both processes, but that the

difference in appearance arises from depth of placement of completed contours and surfaces. However, others have shown that there may be differences in the mechanisms underlying modal and amodal completion. For example, Davis and Driver (Davis and Driver, 1994) found that search for modally completed figures is more efficient than for amodally completed counterparts. Similarly, neurophysiological studies show a dissociation in responses to modal and amodal completion at the earliest stages of visual processing (Sugita, 1999;Von der Heydt and Peterhans, 1989) and in a series of experiments, Anderson and colleagues (Anderson *et al.*, 2002;Singh, 2004) provide evidence for different mechanisms for the two processes. Nevertheless, a recent study has refuted these claims and proposes a model consistent with both Kellman's identity hypothesis and Anderson's unstable percepts whereby V1 and V2 cells receive feedback from higher visual areas modulating responses to modal and amodal completion (Albert, 2007).

1.2.6 Instant perceptual filling-in independent of stimulus configuration

a) Filling-in at the blind spot

The blind spot is the part of the retina where the optic nerve leaves the eye. It is devoid of photoreceptors and therefore carries no visual information from the corresponding region in visual space. It measures roughly 5^{o} in diameter and its centre lies 15^{o} medial to the fovea, slightly above the horizontal meridian. In normal binocular vision, the cortical representation of the other eye compensates for this lack

of visual information. Interestingly however, monocular viewing does not lead to the appearance of a blank patch in the visual field as the visual system perceptually fills-in visual information across the blind spot from the surrounding colour and texture (Ramachandran, 1992) (Fig 1.7), as long as coherent elements are presented on both sides of the blind spot (WALLS, 1954).

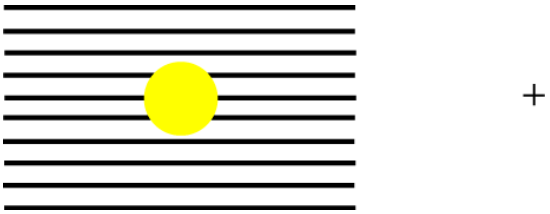

Figure 1.7. Example of perceptual filling-in at the blind spot. Hold the page 15 cm from your face, fixate the cross and close your right eye. When the yellow disc falls across the blind spot, it will seem to disappear and be perceptually filled-in by the horizontal bars. Adapted from (Komatsu, 2006).

Behavioural studies suggest that this is an early, preattentive process involving sensory rather than cognitive mechanisms. If several rings are viewed, with one ring positioned over the blind spot, this will 'pop out' as it is perceived as a disc in a background of rings (Ramachandran, 1992)). Even an extremely narrow border (0.05 deg) surrounding the blind spot, will generate the appearance of uniform colour filling-in the blind spot (Spillmann *et al.*, 2006), consistent with the theory that this form of filling-in depends on local processes generated at the edge of the blind spot representation in early visual cortex. Studies also indicate that this is an active process, as the perception of filled-in motion at the blind spot causes a motion after-effect in the other eye suggesting that perceptual filling-in can cause adaptation of motion-sensitive neurons (Murakami, 1995). Perceptual filling-in at the blind spot induces little or no distortion of the surrounding region (Tripathy *et al.*, 1996) which

would argue against remapping or 'sewing up' of the region corresponding to the blind spot. Moreover, spatial alignment thresholds are lower across the blind spot than across intact retina (Crossland and Bex, 2009), consistent with involvement of a low-level mechanism in perceptual filling-in at the blind spot.

Single cell recordings from anaesthetised monkeys show that when filling-in takes place at the blind spot, neural responses are generated at the retinotopic representation of the blind spot in primary visual cortex (Fiorani et al., 1992;Matsumoto and Komatsu, 2005;Komatsu et al., 2002). Some V1 neurons activated during perceptual filling-in at the blind spot have large receptive fields, extending out of the blind spot (Komatsu *et al.*, 2002), suggesting the passive importing of information from the surrounding visual field. Conversely, there is also strong evidence consistent for an active neural completion process as stronger activity is associated with bars spanning both sides of the blind spot than for bars stimulating only one side of the blind spot (Fiorani et al., 1992;Matsumoto and Komatsu, 2005). Moreover, this most recent study (Matsumoto and Komatsu, 2005) demonstrated response latencies in V1 that were 12 ms slower for stimuli presented to the blind spot eye than to the other eye. These response latencies did not increase when more distal regions of the receptive field were stimulated, suggesting that they were not due to long-range horizontal connections, but might instead reflect feedforward signals to V2 which then feedback to V1.

In humans, fMRI studies demonstrate the presence of a weakly responsive region in V1 corresponding to the cortical representation of the blind spot that is no longer evident in V2 (Tong and Engel, 2001;Tootell et al., 1998b). A more recent study

using fMRI (Awater *et al.*, 2005) failed to find distortions of representation around the blind spot during stimulation of the two sides of the blind spot independently. This is consistent with neurophysiological studies showing that perceptual completion at the blind spot is likely to occur through an active completion mechanism (Fiorani et al., 1992;Matsumoto and Komatsu, 2005), although, crucially that fMRI study did not examine cortical representation around the blind spot during perceptual filling-in at the blind spot. Consistent with previous studies, they also showed that by V2, the gap in cortical representation corresponding to the blind spot was no longer present.

Taken together, these studies suggest that perceptual filling-in at the blind spot is likely to reflect active processes, probably comprising lateral propagation signals but also possibly involving feedback signals from extrastriate regions.

b) Filling-in across retinal scotomas

Patients with retinal scotomas due to macular degeneration or toxoplasma infection also experience perceptual filling-in (Zur and Ullman, 2003;Gerrits and Timmerman, 1969;Alvarenga et al., 2008) which is instant, improves with increasing density and regularity of the filled-in patterns and occurs for scotomas as large as 6 degrees, at less than 2 mm from the fovea (Zur and Ullman, 2003). Retinal scotomas are also associated with a twinkle after-effect, for areas as large as 20 degrees (Crossland *et al.*, 2007), consistent with an active completion process, but possibly in extrastriate areas, given the large area of this effect. Interestingly, alignment thresholds over pathological retinal scotomas are not lower than across intact retina

(Crossland and Bex, 2009;Alvarenga et al., 2008), suggesting that perceptual filling in across retinal scotomas does not include low-level receptive field organisation.

Single cell recordings in mammalian visual cortex have revealed conflicting results. In monkeys, cells within primary visual cortex representing the edge of the lesions expand their receptive fields within minutes after inducing bilateral retinal lesions (Gilbert and Wiesel, 1992) and several months after the lesion, the receptive fields have expanded and shifted to outside the lesion. Similar reports of receptive field reorganisation in V1 have been shown following monocular retinal lesions in cats (Chino *et al.*, 1992) and following cortical lesions in kittens (Zepeda *et al.*, 2003). Importantly, in adult mammals, this reorganisation occurs within hours of the lesion (Chino *et al.*, 1992), but only if associated with absence of input from the fellow eye. However, other studies have failed to observe topographic remapping effects in V1 after monocular retinal lesions (Murakami *et al.*, 1997) or even following bilateral retinal lesions (Smirnakis *et al.*, 2005), causing some significant controversy (Calford et al., 2005;Giannikopoulos and Eysel, 2006).

In humans, reports are also inconsistent. Visual cortex (including V1) deprived of retinal input due to macular degeneration shows increased activation with functional MRI to stimuli outside the corresponding region in visual space (Baker *et al.*, 2005;Baker *et al.*, 2008). Reorganisation also occurs following loss of visual input due to optic radiation damage following stroke (Dilks *et al.*, 2007). However, other studies have failed to find consistent evidence for cortical reorganisation in macular degeneration (Sunness *et al.*, 2004;Masuda *et al.*, 2008) and a recent study suggests

that large scale cortical reorganisation may only occur in association with the complete absence of functional foveal vision (Baker *et al.*, 2008).

Thus, the mechanisms underlying perceptual filling-in associated with retinal scotomas remain unclear. If any reorganisation occurs in early visual areas, it is likely to be augmented by feedback projections from higher visual areas with larger receptive fields (Baker *et al.*, 2008).

1.2.7 Delayed perceptual filling-in, dependent on stimulus configuration

a) Troxler fading and artificial scotomas

Troxler fading or perceptual filling-in refers to the tendency of stimuli placed in peripheral vision to gradually fade from view with maintained central fixation (Troxler, 1804)(Fig 1.8). Stimuli are more likely to fade if they are peripheral, have indistinct edges (Friedman *et al.*, 1999) and when the luminance (Sakaguchi, 2001) and contrast difference between the target and surround is reduced (Sakaguchi, 2006). The faded percept returns with eye movements or blinking and is counteracted by microsaccades (Martinez-Conde *et al.*, 2006).

Figure 1.8. Example of Troxler fading. Hold the page 20cm away from your face, fixate the cross with both eyes open, after a few seconds, the blue pattern will fade and disappear.

This perceptual filling-in can be made even more striking if the background is replaced by dynamic twinkling noise (Ramachandran and Gregory, 1991), which causes perceptual filling-in to occur more rapidly (Spillmann and Kurtenbach, 1992) and the percept is then termed an artificial scotoma (Ramachandran and Gregory, 1991) (see Fig. 1.9).

The perceptual filling-in of artificial scotomas is similar in many ways to that which occurs with Troxler fading. Both require prolonged fixation before perceptual filling-in of the peripheral target can take place. Both require the target to be in the near periphery and both processes are disrupted by eye movements and counteracted by microsaccades. Perceptual filling-in of artificial scotomas occurs earlier than for a target of equivalent size and eccentricity to fade and perceptual filling-in of artificial scotomas occurs more consistently for salient targets (e.g. red or flickering targets) than would occur for Troxler fading. Phenomenologically, a possible difference is that during perceptual filling-in of an artificial scotoma, the background is perceived at the position previously occupied by the target. Furthermore, researchers have argued that the filling-in of an artificial scotomas is less likely to be due to adaptation as the border between the target and the surround is constantly refreshed (Spillmann and Kurtenbach, 1992). However, it is not entirely clear that these two phenomena

are distinct and are not due to similar underlying neural processes. For the purposes of this thesis, they will be considered as separate processes, but experimental findings will be discussed for both processes together, where this is helpful to understand the underlying mechanisms of either process.

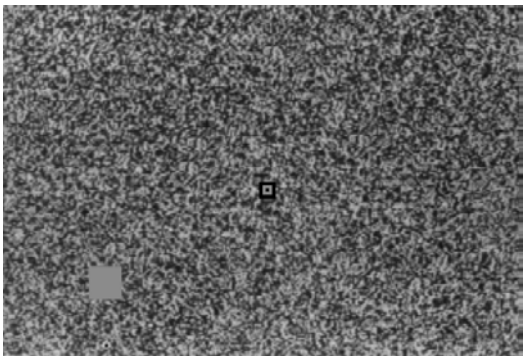

Figure 1.9 Example of an artificial scotoma. A target is placed in the near periphery on the background of dynamic twinkling noise. Participants fixate centrally and the target gradually fades and disappears. Adapted from (Ramachandran and Gregory, 1991).

Behavioural studies suggest that perceptual filling-in of artificial scotomas is associated with activity in early retinotopic cortex as filling-in is influenced by low-level sensory factors such as eccentricity and boundary length (De Weerd et al., 1998;Welchman and Harris, 2001) as well as increased differences in luminance or motion contrast between the target and its surround (Welchman and Harris, 2001). Similarly, the relative salience of the target compared to its background influences time to filling-in, with increasing perceptual salience associated with an increased fading time (Sturzel and Spillmann, 2001;Welchman and Harris, 2001).

Detection thresholds for Gabor patches presented within artificial scotomas are elevated by dynamic noise surrounds (Mihaylov *et al.*, 2007) and after Troxler fading, participants are less able to detect a probe presented within a perceptually filled-in

target (Lleras and Moore, 2006), suggesting suppression of target-associated signals during the subjective experience of perceptual completion. However, an earlier study (Kapadia *et al.*, 1994) used a 3 line bisection task to measure distortions around artificial scotomas and found the apparent position of the middle line segment was drawn towards the interior of the artificial scotoma, suggesting possible reorganisation around the perceptually filled-in target. This is also consistent with a more recent behavioural study suggesting cortical reorganisation surrounding perceptually filled-in targets (Tailby and Metha, 2004).

Artificial scotomas can also induce after-effects (Reich et al., 2000;Hardage and Tyler, 1995), consistent with an active process. Furthermore, high-level factors have also been shown to influence perceptual filling-in (De Weerd *et al.*, 2006;Lou, 1999) as directing spatial attention to the peripheral target increases the probability of it perceptually filling-in. Taken together, these studies are consistent with perceptual filling-in of peripheral targets occurring in retinotopic visual cortex, possibly with some contribution from higher visual areas, but the mechanism remains elusive.

Physiological studies do not yet reveal a consistent pattern of neural activity associated with perceptual filling-in of artificial scotomas. In monkey, single neurons in V2 and V3 whose receptive fields overlap an achromatic target placed on dynamic noise increased their firing after a few seconds of eccentric fixation (De Weerd *et al.*, 1995). However, it is not clear whether such changes correspond to perceptual completion as the monkeys did not report their perception and conversely, in responding monkeys, V1 and V2 boundary neurons show decreased activity during Troxler colour filling-in (Von der Heydt *et al.*, 2003).

In humans, luminance filling-in (filling-in of an achromatic target on a uniform achromatic background) is associated with a generalized (non-retinotopic) decrease in activation in V1 and V2, and increased activity in higher visual areas (Mendola *et al.*, 2006) but the neural correlates of perceptual filling-in of artificial scotomas have not yet been directly measured in humans. Thus, the processes underlying perceptual filling-in of peripheral targets remain unclear. In particular, whether perceptual filling-in occurs in retinotopic cortex, is associated with increased or suppressed activity and the role of higher cortical functions in the process are still unknown.

b) Motion-induced blindness

Motion induced blindness (MIB) is a striking phenomenon in which a perceptually salient target repeatedly disappears and then reappears when superimposed on a field of moving distractors, after a period of maintained central fixation (Bonneh *et al.*, 2001) (Fig 1.10). Target disappearance is influenced by low-level sensory factors such as eccentricity (Hsu *et al.*, 2004) and size (Bonneh *et al.*, 2001), the boundary adaptation effect (Hsu *et al.*, 2006) and also placing the target behind the distractors (Graf *et al.*, 2002).

However, several features of MIB distinguish it from other forms of peripheral perceptual filling-in such as Troxler fading and perceptual filling-in of artificial scotomas. Unlike peripheral perceptual filling-in, MIB targets perceptually fill-in more readily if they are of increased luminance and contrast compared to the

background (Bonneh *et al.*, 2001) and MIB occurs after briefer periods of prolonged fixation. Furthermore, if MIB targets are surrounded by a region without any distractor targets, this region is spared from any perceptual filling-in.

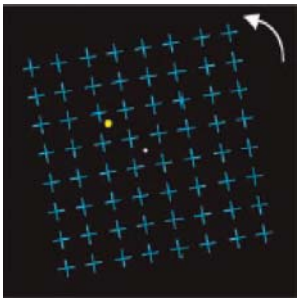

Figure 1.10 Example of motion induced blindness. The grid of blue crosses rotates and participants fixate the central white point while attending to the yellow disc. The yellow disc intermittently disappears and reappears. (Adapted from (Scholvinck and Rees, 2009b)).

MIB is unlikely to reflect local adaptation processes, as it persists for moving or flickering targets and even when targets and distracters are spatially separated (Bonneh *et al.*, 2001). Furthermore, high level factors seem to play an important role in MIB: disappearance of the target is subject to grouping effects, with targets tending to disappear together rather than separately if they form good gestalts (Bonneh *et al.*, 2001) and when two Gabor patches are presented as targets, they disappear together if they are collinear and in alternation if their orientation is orthogonal (Bonneh *et al.*, 2001). Even when targets are invisible, they can still generate orientation-specific after-effects (Montaser-Kouhsari *et al.*, 2004) or negative afterimages (Hofstoetter *et al.*, 2004), suggesting that MIB occurs beyond the cortical site of these after-effects. Finally, attended targets are more likely to disappear than unattended targets (Scholvinck and Rees, 2009a).

Functional MRI studies have shown conflicting results. One study (Donner *et al.*, 2008) found decreased activity associated with target disappearance in the region of V4 corresponding to the target, but increased responses with target disappearance in regions of dorsal visual areas corresponding to the mask, particularly in areas V3A and B and the posterior intraparietal sulcus. These responses were superimposed on a delayed and spatially non-specific response in visual areas V1-3. In contrast, a more recent study found that disappearance of the target was associated with increased activity in V1 and V2 regions corresponding to the target and in V5/MT contralateral to the target (Scholvinck and Rees, 2009b).

1.2.8 Delayed perceptual filling-in independent of stimulus configuration

a) Stabilised retinal images

When an image of an object is stabilised on the retina (for example using an optical lever system to ensure that the stimulus moves opposite to eye movements to cancel out eye movements), after a few seconds, it gradually fades away and is replaced by the texture or colour of the surrounding visual field (DITCHBURN and GINSBORG, 1952;RIGGS et al., 1953). Notably, complete stabilisation of the image (for example by projecting the internal structure of the eye onto the retina) causes images to disappear and never return (Campbell and Robson, 1961). Within a stabilised image, single lines tend to disappear as units and parallel lines tend to disappear and reappear together. The length of time that the target remains visible is partly a function of the

complexity of the target and meaningful figures remain visible for longer than meaningless figures (PRITCHARD et al., 1960). Studies have also shown features of interocular transfer (Krauskopf and Riggs, 1959;COHEN, 1961) consistent with a cortical locus for the phenomenon. Moreover, the part of the image to which the participant is directing attention remains in view longer than other parts and stimulating other modalities such as a sudden noise, causes reappearance of the image (PRITCHARD et al., 1960) consistent with involvement of higher regions in the disappearance of the images.

This phenomenon may be an adaptive mechanism to prevent retinal vessels from interrupting our view of the world and also demonstrates the importance of constant eye movements in continually stimulating the visual system and preventing the apparent disappearance of visual scenes. It is possible that other forms of perceptual filling-in following maintained fixation share some common mechanisms with the fading of stabilized retinal images.

1.2.9 Using this framework for perceptual filling-in to explore possible underlying mechanisms

The framework described above is a new and useful way of categorising all forms of perceptual filling-in. By considering perceptual filling-in within these categories, the commonalties and differences between the various forms of filling-in become apparent, which is essential in considering the mechanisms underlying perceptual filling-in. Perceptual filling-in can be considered as an abnormal form of surface and

contour perception, as contours or surfaces are perceived where they do not actually exist in visual space. It can be instant or delayed, and as becomes apparent from the framework described above, this depends on the presence or absence of existing boundaries. Where perceptual filling-in occurs in the absence of real boundaries it will occur instantly. For example, if the perceptual completion involves the formation of new boundaries (as in illusory contours, where no boundary is present), or the spread of surface in the absence of a boundary (as in the blind spot), perceptual filling-in is instant.

Conversely, where perceptual filling-in occurs in the presence of an existing boundary, it will only occur after prolonged fixation, as this boundary must first be broken down by adaptive mechanisms, before perceptual filling-in can occur. For example perceptual filling-in of artificial scotomas only occurs after prolonged fixation, as the boundary of the figure being filled-in must first be degraded by adaptive mechanisms. Similarly for Troxler fading and even for stabilised retinal images

This importance of boundaries in preventing interpolation processes has been discussed previously in the context of filling-in of artificial scotomas (De Weerd et al., 1995;Spillman and De Weerd, 2003), where a model has been proposed for a two stage process involving adaptation of figure boundaries followed by a faster interpolation process where the background fills-in the area previously occupied by the figure. However, the importance of boundaries has not previously been applied systematically to all forms of perceptual filling-in. By considering perceptual filling-

in within this framework, the importance of boundary adaptation as a predictor of the timing of filling-in becomes immediately apparent.

1.2.10 Perceptual filling-in in the context of general perception of contours and surfaces

In order to understand perceptual filling-in, it is helpful to consider perceptual filling-in in the context of processes involved in general perception of contours and surfaces. One influential model of general perception is FACADE (Form-And-Color-And-DEpth) theory, described by Grossberg (Grossberg, 1994;Grossberg, 1997;Grossberg, 2003). This theory describes two main systems in visual processing: The Boundary Contour System and the surface system, termed the Feature Contour System. According to FACADE theory, all boundaries are in fact invisible and edges are only perceived as such as they arise as coherent patterns of excitatory and inhibitory signals across a feedback network from the retina through the LGN and V1 interblob and V2 interstripe areas (see Fig. 1.11). Long-range cooperative interactions build boundaries across space while interacting with shorter-range inhibitory competitive interactions suppressing boundary groupings. These boundaries are, in a sense, invisible, as they are insensitive to contrast polarity, but simply pool information from cells sensitive to the same orientation but not necessarily of the same contrast polarities (Grossberg, 2003).

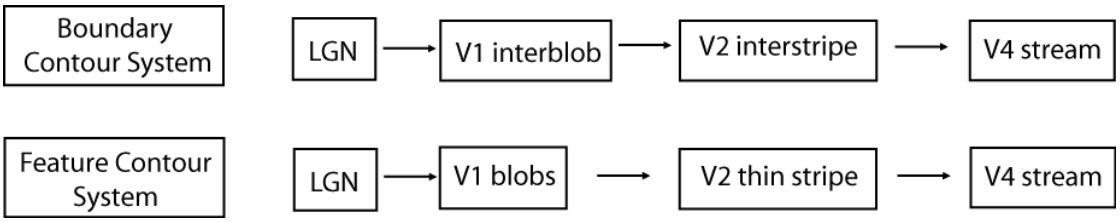

Figure 1.11 Schematic diagram of the Feature Contour System and the Boundary Contour System. (Adpated from (Grossberg, 2003)).

The surface system, on the other hand, termed the Feature Contour System, operates as a network from the retina, via the LGN to the V1 blob, V2 thin stripe and then V4 stream. It relies on discounting the illumination, to compensate for variable illumination and then filling-in the surface with colour or brightness, in a form of diffusion across visual space. The surface system interacts with the Boundary Contour System to limit the diffusive spread of surface information. Conversely, the Boundary Contour System becomes visible through interactions with the surface system.

FACADE theory has been applied to perceptual filling-in previously (Grossberg, 2003). Here I extend it by applying it to the new system for categorising perceptual filling-in presented here and use it to make predictions for all forms of perceptual filling-in. Where perceptual filling-in occurs for specific stimulus configurations following a delay, as in Troxler fading or filling-in of artificial scotomas, boundaries are invariably present. As discussed above and by others (De Weerd *et al.*, 1998), in order for perceptual filling-in to take place, these boundaries must first be adapted, or broken down, thus explaining the initial delay.

Where filling-in occurs instantly but is dependent on stimulus configuration, as in illusory contours and neon colour spreading, boundaries and surfaces are formed where they do not physically exist. This may explain why filling-in occurs instantly. Moreover, these illusions exploit specific feature configurations which in the real world often signify borders and surfaces, such as in the context of camouflaged or occluded objects and are therefore interpreted by the visual system as the most likely natural configuration to explain the existing set of boundaries and surfaces.

It is likely that forms of perceptual filling-in that are dependent on stimulus configuration exploit common mechanisms to those underlying perceptual filling-in independent of stimulus configuration which have been developed by the visual system to overcome deficits to visual system input. Thus, in instant filling-in independent of stimulus configuration, as in the filling-in that takes place across the blind spot, the Feature Contour System is not limited by any boundaries, so filling-in continues almost instantly across regions of visual space.

Conversely, retinal vessels do provide a boundary that would otherwise limit the spread of visual information. The visual system has therefore developed mechanisms to prevent such interruptions to vision by causing images stabilised on the retina to fade and disappear over time. These mechanisms are exploited in illusions such as Troxler fading and the disappearance of artificial scotomas.

1.2.11 Overview of thesis structure

In the first part of this thesis I will examine the role of the bottom-up contribution to visual processing. I will do this by exploring how stimulus-driven signals from artificial scotomas influence the perception of the stimulus that becomes invisible due to perceptual filling-in. I will look for evidence of a neural signature of filling-in, evidence that it is an active process and attempt to determine the locus of perceptual filling-in. In addition, I will explore whether the top-down influences of perceptual load and working memory load have any impact on the process of perceptual filling-in. In this section I will also examine an unusual and contrasting type of perceptual filling-in seen in the context of hemianopia, which may reflect the perceptual effects of a breakdown in top-down processing due to brain injury.

In the second part of the thesis I will turn to the question of whether receiving reward can act as a top-down influence on visual responses, by exploring whether visual cortex activity can be modulated by reward outcome.

1.3 Reward influences on visual processing

1.3.1 Processes involved in reward-seeking behaviour

A reward is any pleasurable event or experience that is obtained when a requisite task has been satisfied. Most animals, including humans, will seek out rewards, performing tasks in order to obtain them. To coordinate this behaviour, a set of

processes must be in place. These include: the ability to represent the value of rewarding stimuli, the ability to predict when and where rewards might occur and to use these predictions to form decisions that will guide future behaviour (O'Doherty, 2004). Extensive neurophysiological, neuroimaging and lesion studies in humans have identified a group of brain structures including the ventromedial prefrontal cortex (encompassing both the orbital and medial prefrontal regions), the amygdala, striatum and dopaminergic parts of the midbrain as being essential components of an integrated network processing reward information (see Fig. 1.12). Notably, this putative reward network does not involve sensory cortices, with neither primary nor association sensory cortices included. The specific brain regions involved in each of these reward-associated processes will be reviewed in the next section.

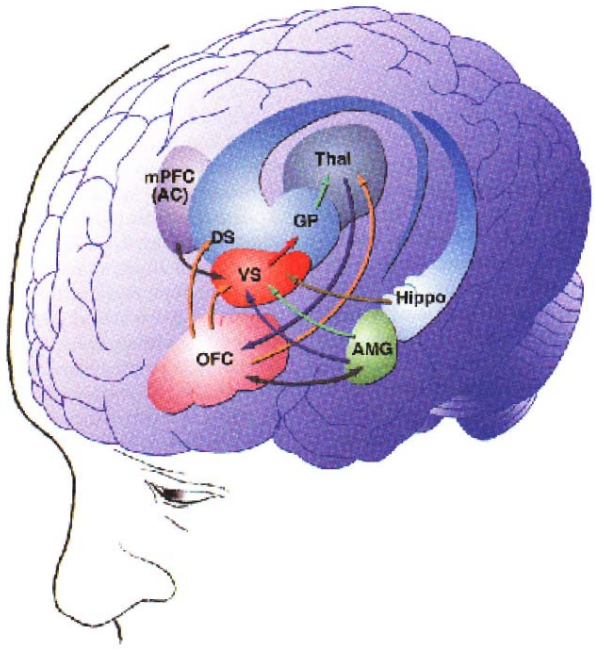

Figure 1.12 Representation of cortical and subcortical structures involved in reward processing. OFC, orbitofrontal cortex; AMG, amygdala; VS, Ventral striatum; DS, Dorsal striatum; mPFC, medial prefrontal cortex; GP, Globus pallidus; Thal, Thalamus; Hippo, Hippocampus. (Adapted from (Koob *et al.*, 2008).

1.3.1.1 Brain structures involved in representing reward value

The orbitofrontal cortex (OFC) has a key role in representing the reward value of a stimulus. In macaque, neurons within orbitofrontal cortex respond more strongly during fruit juice consumption when monkeys are hungry than when they are satiated (Rolls *et al.*, 1989). Similarly in humans, fMRI responses in OFC decrease when a liquid food is eaten to satiety (Kringelbach *et al.*, 2003). This role has been confirmed in other modalities in neuroimaging studies in humans, including visual (comparing neutral and happy expressions (O'Doherty *et al.*, 2003)) and auditory stimuli (Blood *et al.*, 1999).

The amygdala may also be involved in processing reward value (for a review see (Holland and Gallagher, 2004)). Rats with lesions to the amygdala show impaired performance in coding specific reinforcing outcomes (Balleine *et al.*, 2003;Malkova *et al.*, 1997), suggesting a role in learning the association between stimuli and the value of particular food rewards. Similarly, in humans, hunger modulates fMRI responses in the amygdala to food stimuli (LaBar *et al.*, 2001). However, this role has recently been called into question by a study dissociating the effects of intensity and valence in olfaction (Anderson *et al.*, 2003). This study found amygdala activation is associated with the intensity and not valence of the stimuli and that, in contrast, OFC activation is associated with the valence rather than the intensity of stimuli, suggesting a primarily sensory rather than affective role for the amygdala in stimulus processing (see also (Small *et al.*, 2003), for similar findings using gustatory stimuli),

although it could be argued that reward value depends not only on the nature of the reward but also on the amount of reward available (O'Doherty, 2004).

1.3.1.2 Brain structures involved in predicting rewarding events

Reward can be predicted when a neutral stimulus is followed by a reward in a contingent way. After learning, this neutral stimulus becomes predictive of reward. In humans, neuroimaging studies show that the amygdala, OFC and ventral striatum are involved in reward prediction (Knutson *et al.*, 2001;O'Doherty *et al.*, 2002;Gottfried *et al.*, 2002), with learning-related changes in neural activity in response to conditioned stimuli in the OFC (Gottfried *et al.*, 2002) and increased activity in dopaminergic midbrain, amygdala, striatum and OFC during anticipation of a taste reward (O'Doherty *et al.*, 2002).

1.3.1.3 A dissociation between reward expectation and reward receipt

A longstanding area of controversy concerns the nature of responses to conditioned stimuli (previously neutral stimuli which after becoming associated with rewarding events, themselves become associated with reward-seeking behaviour). Specifically, researchers have debated whether a conditioned stimulus itself acquires value and produces the same responses as the unconditioned stimulus (rewarding event) (Pavlov, 1927;Zener, 1937). Neuroimaging studies seem to be consistent with distinct representation of conditioned stimuli, as the ventral striatum and amygdala respond to

predictors of reward but not to reward itself (Knutson *et al.*, 2003) (O'Doherty *et al.*, 2002).

1.3.1.4 Brain structures involved in reward-guided behaviour

Having predicted that a stimulus is likely to lead to a reward, one must then act on this prediction. Neuroimaging studies suggest a role for dorsal striatum in these response-reward associations (Haruno *et al.*, 2004;Elliott *et al.*, 2004). However, action preparation in response to rewarding stimuli is associated with enhanced activity in prestriate visual cortex, premotor cortex and lateral prefrontal cortex (Ramnani and Miall, 2003). This finding suggests that reward-associated stimuli may influence regions beyond the established reward-processing network to bring about behaviour that is likely to produce more rewards in the future.

1.3.2 Could reward influence the earliest stages of visual processing?

Increasing reward has been shown to improve performance and even increase activity in primary somatosensory cortex during reward feedback, following a tactile discrimination task in humans (Pleger *et al.*, 2008) and other mammals (Pantoja *et al.*, 2007).

Recently, reward expectation has been shown to modulate activity in primary visual cortex. When rats are presented with a visual stimulus associated with a reward, a proportion of neurons in primary visual cortex begin to express activity that predicts

the timing of the reward (Shuler and Bear, 2006). In humans, visual selective attention is modulated by the possibility of financial reward (Della and Chelazzi, 2006) and visual cortex shows increased activity when reward is expected in a spatial-attention task (Small *et al.*, 2005). Similarly, during stimulus presentation, activity is increased in stimulus-selective regions of visual cortex for rewarded compared to non-rewarded trials (Krawczyk *et al.*, 2007) and prestriate visual cortex shows enhanced activity during the motor preparation stage for trials when reward is expected (Ramnani and Miall, 2003). More recently, visual cortex activity was enhanced during presentation of visual stimuli previously associated with reward (Serences, 2008).

Crucially, all these studies examined responses during the presentation of visual stimuli and therefore could not dissociate effects of reward outcome per se on the visual system. These studies also do not clearly distinguish the effects of attention from those of reward, as higher reward values are likely to be associated with increased attention during presentation of a visual stimulus. A recent behavioural study has attempted to remove the effects of attention by rendering rewarded stimuli invisible by presenting continuously flashing contour rich stimuli to the other eye (Seitz *et al.*, 2009). The experimenters found that reward pairing, even in the absence of awareness, led to improvement in a visual task, showing that reward can influence visual processing even in the absence of awareness.

In the second part of this thesis, I will use functional MRI to examine whether and how reward can influence BOLD signals in different areas of human visual cortex, but in the absence of concurrent visual stimulation. Note that I will be examining

responses to reward outcome. This is where correct performance in a visual task is followed by a cue informing participants that they have won a specified amount of money. Although they will not physically be given the money during the trial, they will receive it at the end of the experiment. This form of reward outcome has been validated in many previous studies (Pleger *et al.*, 2008;Knutson *et al.*, 2001;Petrovic *et al.*, 2008).

Critically, in the experiment presented in this thesis, I will distinguish between signals associated with the visual stimulus and those attributable to later non-visual reward feedback by employing a design separating these signals in time. I will also examine whether reward on one trial can influence activity in visual cortex during the next trial. One possibility is that reward modulates activity at later stages of visual processing, which in turn may affect behavioural measures of visual perception. Alternatively, reward may influence the earliest cortical stages of visual processing, either at the point of feedback or during visual performance at the next trial.

1.4 Summary of studies presented in this thesis

The first part of this thesis will explore top-down and bottom-up processes in perception using two forms of perceptual filling-in as model systems. I will explore neural correlates of filling-in and consider evidence for boundary breakdown followed by lateral spreading as possible mechanisms. The studies will use a combination of methods including functional MRI, MEG and behavioural studies in normal human participants and in patients.

The basis of fMRI and MEG acquisition and analysis as well as retinotopic mapping is summarised in Chapter 2.

Chapter 3 presents a study using magnetoencephalography to examine brain responses during perceptual filling-in of an artificial scotoma. By isolating neural population signals entrained at the frequency of flicker of the filled-in target, I will be able to track specific responses to that target and specifically compare activity between times in the trial when the target is present and visible and when it is present but invisible because it has perceptually filled-in.

Chapter 4 presents a study exploring the neural location of perceptual filling-in of artificial scotomas. Specifically, I will use high field functional MRI (fMRI) to examine Blood Oxygenation Level Dependent (BOLD) signals in retinotopic visual cortex during perceptual filling-in. By using an almost identical paradigm to that used in Chapter 3, I will be able to compare the MEG and fMRI findings and provide converging evidence from these contrasting techniques for the pattern of neuronal responses during perceptual filling-in.

Chapter 5 will turn to the question of how higher cortical functions can modulate visual processing in the context of perceptual filling-in. In this chapter I will explore behaviourally the influence of two contrasting top-down manipulations on the latency and probability of perceptual filling-in of an artificial scotoma.

Chapter 6 presents a study of a different and unusual form of perceptual completion: hemianopic completion. This occurs in the context of hemianopia, where a figure is perceived as complete, despite only half a figure being presented. I will use functional MRI to explore the neural structures mediating this form of completion in a patient with hemianopia. I will consider this phenomenon in the context of the integration of information from object sensitive areas in the damaged brain.

The second part of the thesis will address the top-down influences on visual cortical processing more directly, but instead of examining the relatively well-studied influences of attention and working memory, I will instead examine the potential influence of reward on visual performance and visual cortical processing.

In Chapter 7 I will use functional MRI to investigate the possible effects of reward feedback on activity in human visual cortex while separating reward events (presented via auditory feedback) from visual events and assessing both within and trial-to-trial effects.

1.5 Conclusion

Visual processing requires complex multilevel computations to make sense of the information transmitted about the world around us from the retina. This includes integration of information from early sensory processing with modulating influences from higher cognitive regions in order to interpolate information across visual space to compensate for deficits in visual information. Moreover, higher cognitive regions can influence early visual processing even in the absence of concurrent visual

stimulation, but whether other cognitive influences, including processes such as reward can influence visual processing remains unknown. Taken together, the series of experiments outlined above will explore the neural basis of the integration of bottom-up and top-down signals to interpolate missing information and the role of reward feedback in influencing visual processing in the absence of any visual stimulation.

CHAPTER 2: GENERAL METHODS

2.1 Introduction

This chapter describes the physics underlying functional MRI (fMRI), the analysis of fMRI data using statistical parametric mapping (SPM) and the localisation of early cortical visual areas in individual subjects using retinotopic mapping. These methods were used in several of the experiments presented in this thesis. Other methods used in individual studies, including long-range infrared eye tracking and preprocessing of the abnormal brain will be discussed in the relevant chapters where these techniques were used. The precise methods used in individual experiments varied and additional methods were often used; therefore, each experimental chapter in this thesis also contains a methods section describing the relevant methods in detail. This chapter also describes the neurophysiology underlying magnetoencephalography (MEG), the analysis of MEG data using event related fields, time-frequency analysis and the localisation of MEG signals.

2.2 Functional MRI

2.2.1 Physics of MRI

MRI (magnetic resonance imaging) is a technique used to produce high quality images of the human body. It is based on the principles of nuclear magnetic

resonance, whereby hydrogen nuclei (protons) have magnetic properties called nuclear spin. When protons are placed within a large external magnetic field (often called B_0) they align with or against the external field. The frequency of rotation (termed precession) about the axis (z) of the B_0 field is termed the Larmor or resonance frequency (ω_0) and is proportional to the strength of the external magnetic field:

$\omega_0 = \gamma B_0$

More spins are aligned parallel to than against the large external magnetic field, resulting in a longitudinal component aligned with B_0, but the phase of the precessing protons is randomly distributed so the net transverse magnetization (M_0, orthogonal to B_0) is zero.

If an electromagnetic radio frequency (RF) pulse is then applied perpendicular to B_0, at the resonance frequency, the protons will absorb this energy (excitation) and the net magnetization vector spirals down from the equilibrium position to the XY plane. When the RF pulse is turned off, there is a return of the net magnetization to equilibrium over several seconds. During this process, called relaxation, the absorbed RF energy is retransmitted, as the MRI signal. Relaxation involves two processes:

Longitudinal relaxation occurs as the spinning protons and the surrounding tissue (or lattice) returns to thermal equilibrium. As the spins move from a high to low energy state, they release RF energy back into the surrounding lattice. This recovery rate is characterised by a time constant T1, which is different for every tissue, enabling MRI to differentiate between tissue types. T1 values are longer at higher field strengths.

Transverse relaxation occurs as the protons begin to spin out of phase, with the magnetic fields of the spinning protons interacting (spin-spin interaction) to modify their rate of precession. This causes a cumulative loss of phase, producing transverse magnetization decay, which is characterised by the time constant T2, which (like T1) is also tissue specific, but is unrelated to field strength. The signal unaffected by any magnetic gradient is termed the Free Induction Decay (FID).

In practice, the MRI signal decays faster than T2 would predict based on a purely homogenous external magnetic field, and decreases exponentially at the time constant T2*. T2* takes into account imperfections in the homogeneity of the magnetic field which arise due to flaws in the magnetic field and distortions at the tissues borders, as well as tissue-specific spin-spin relaxation which are responsible for pure T2 decay. Of particular significance to functional MRI, T2* is also affected by magnetic susceptibility variations in blood vessels, where the level of deoxyhaemoglobin in the blood affects the T2* in the vessels and is the basis behind BOLD (blood oxygen level dependent) imaging. For this reason, T2* imaging is used for functional MRI sequences. T2 imaging uses a spin-echo technique to reverse the spins and compensate for these local field inhomogeneities. T2* imaging is used for functional MRI sequences and is performed without refocusing the spins, sacrificing image resolution for additional sensitivity for the T2 relaxation processes.

2.2.2 Formation of images using MRI

To produce an image, spatial information must be encoded into the MRI signal. This is done by collecting signal from slices (slice selection) and then extracting information from the columns and the rows separately.

Slice selection is performed by applying a second magnetic field gradient perpendicular to the slice plane. This causes all the planes perpendicular to the gradient to have different precessional frequencies. In this way, when the RF pulse is applied, only protons within the desired slice will be excited as they will be at the same frequency.

A magnetic field gradient is then applied in the direction of the columns, by passing currents through coils placed around the subject. This causes a change in phase which is proportional to the distance (thus termed *phase-encoding*). The final step of spatial localisation is *frequency encoding*. This is performed perpendicular to the phase-encoding and gives spatial information in the x-plane. These discrete increases in frequency and phase encoding divide each slice into small cubes, called voxels (volume elements). All the protons within a voxel experience the same frequency and phase encoding. The MR signal is therefore a mix of RF waves with varying amplitudes, frequencies and phases, containing spatial information. This is then digitised and written into a matrix known as k-space, which is equivalent to a Fourier plane. The k-space data is reconstructed into the original image using a 2D inverse Fourier transform.

2.2.3 Contrast

The main source of contrast in MRI is spin density contrast where the image intensity is proportional to the local density of spins (known as proton density contrast). Most proton signal comes from water, but there is not a great range in water content between tissues, apart from bone. Other ways are therefore needed to differentiate between tissues. These include relaxation times, contrast agents and blood oxygenation contrast. For the studies in this thesis, contrast introduced by relaxation times and blood oxygenation are of most significance. Different tissues have different MRI relaxation times which can be used to provide contrast based on differences in T1, T2 or T2*. Relaxation time contrast is achieved by changing two sequence timing parameters: the repeat time between RF pulses (TR) and the time to echo following the excitation pulse (TE). (One can also introduce relaxation time contrast by using other methods which will not be discussed here).

T1-weighted contrast is achieved by reducing the value of TR. If the TR is shorter than the tissue T1, longitudinal magnetization will not have recovered by the next excitation and the signal in those regions will be reduced and appear darker in colour, as higher signal causes the MR image to appear brighter. T2-weighted contrast is introduced by increasing the echo time (TE). A longer TE for regions with short T2, will lose signal and appear darker. (Long TR is used here to minimise unwanted T1 weighting).

T2*-weighting can result when gradient echo sequences are used with a long TE. (Here TE is the time between the initial excitation of spins and the centre of the

gradient echo). For long TE, tissues with long T2* will have higher signal. T2* contrast caused by gradients around blood vessels are the basis of the BOLD signal.

2.2.4 Echo-planar imaging

Echo-planar imaging is a way of acquiring brain images very rapidly, with a complete slice acquired in less than 100 ms. This is achieved by encoding all the lines of k-space in a singe pulse, unlike other sequences which acquire one line per slice. This is at the expense of limited spatial resolution and increased susceptibility to field inhomogeneities. With its low acquisition time, EPI is most suitable for recording dynamic brain function. All the fMRI experiments in this thesis were carried out using EPI sequences.

2.2.5 The basis of the BOLD signal

A fundamental principle underlying fMRI is the neurovascular coupling in the brain which ensures that blood flow and energy metabolism are tightly linked to neuronal activity. Therefore by measuring changes in the blood supply, neuronal activity can be indirectly determined. A second important principle, first observed by Pauling and Coryell (Pauling and Coryell, 1936) is that oxygenated and deoxygenated haemoglobin have different paramagnetic properties. Deoxyhaemoglobin has paramagnetic properties and increases the spin phase dispersion and therefore reduces transverse (T2) relaxation and T2*, resulting in a reduced T2*-weighted MRI signal.

Thus, deoxygenated blood produces a reduced BOLD signal compared to oxygenated blood in T2* sensitive images. This was first exploited by Ogawa and colleagues in mice (Ogawa *et al.*, 1990), later in cats (Turner *et al.*, 1991), and subsequently in humans (Kwong *et al.*, 1992;Ogawa *et al.*, 1992), demonstrating that MRI can show blood oxygenation level dependent (BOLD) signal changes in the living brain.

The haemodynamic response to neuronal activity is thought to consist of three stages (Heeger and Ress, 2002):

1) An initial small decrease in signal below baseline, corresponding to the increase in deoxygenated haemoglobin due to oxygen consumption (Malonek *et al.*, 1997).

2) This is followed by a large increase in signal above baseline caused by vasodilation and increased blood flow resulting in a net increase in oxyhaemoglobin, despite the oxygen uptake by the surrounding tissues (Fox and Raichle, 1986;Malonek et al., 1997).

3) Finally, there is a decrease in signal back to below the baseline after the supply of oxygenated blood has reduced. This pattern of an initial dip, followed by a rise and then a decrease below the baseline is known as the Haemodynamic Response Function (HRF). The increase in BOLD signal is delayed in time with respect to neuronal activity, with a peak 4-6 seconds after the onset of neuronal activity. The difference in susceptibility between oxygenated and deoxygenated blood is very small (about 0.02×10^{-6} cgs units (Turner *et al.*, 1998)), thus image intensity changes are very small, no more than 2-4% at 1.5T (although signal loss is enhanced with increased static magnetic field of the scanner).

2.2.6 Neural basis of the BOLD signal

2.2.6.1 Mechanisms underlying vascular response to neuronal activity

The neurophysiological mechanisms causing the increase in blood flow in response to brain activity are still unclear and whether it reflects a response to synaptic or neuronal activity is also debated. Blood flow has been shown to increase in proportion to glucose consumption (Fox *et al.*, 1988). This has added weight to suggestions that the increase in blood flow is a result of synaptic rather than neuronal activity as glucose metabolism is tightly linked to synaptic activity (Schwartz et al., 1979;Shulman and Rothman, 1998) and astrocytes, which are crucial for neurotransmitter recycling, rely on glycolysis (Magistretti and Pellerin, 1999).

An alternative possibility is that the blood flow delivers oxygen required by neurons as initial studies suggested that the increase in blood flow is a direct result of the oxygen consumption of the tissues (Hoge *et al.*, 1999;Davis *et al.*, 1998). This theory is supported by the observation that oxygen consumption increases with neuronal activity (although less than blood flow) and by estimates of brain metabolism suggesting that most energy is used by neurons, whose energy consumption is closely linked to firing rates, with only a small proportion of energy being used for neurotransmitter recycling by astrocytes (Attwell and Laughlin, 2001).

However, both these theories are based on the assumption that the blood flow response is causally related to glucose or oxygen consumption, when the evidence shows only correlation. Furthermore studies have shown that the blood flow response

is not affected by sustained hypoxia (Mintun *et al.*, 2001) or by hypoglycaemia (Powers *et al.*, 1996), suggesting that other factors are likely to be involved. Moreover, the blood flow response is extremely slow relative to the underlying neuronal activity (Heeger and Ress, 2002) and although oxygen usage co-localises with neuronal activity, the increase in blood flow occurs in a larger area (Malonek and Grinvald, 1996). Therefore blood flow must be controlled by factors other than reduced energy.

Another possibility is that cerebral blood flow is controlled locally by glutamate and possibly by GABA, as nitric oxide (an inhibitor of non-NMDA glutamate receptors) blocks the increase in blood flow (Akgoren *et al.*, 1994;Yang *et al.*, 1999) and exogenous glutamate or NMDA dilates pial arterioles (Yang and Iadecola, 1996). According to this theory, a glutamate-evoked calcium ion influx in postsynaptic neurons activates the production of NO, adenosine and arachidonic acid metabolites. These agents cause vasodilatation and thus reflect both the activity of neurons presynaptic to the cells releasing the metabolites and the level of depolarization of the postsynaptic cells (Attwell and Iadecola, 2002). Other studies have suggested lactate release by astrocytes which would suggest a close link between BOLD signal and synaptic activity. It is possible that all these processes are involved in modulating blood flow, with other, as yet unidentified mechanisms.

2.2.6.2 The relationship between BOLD signal and neuronal activity

It is clearly important to understand the relationship between the BOLD signal and the underlying neuronal responses, in order to compare fMRI studies with electrophysiological and MEG experiments. Several studies have shown a linear relationship between neuronal activity and haemodynamic changes in monkeys (Rees *et al.*, 2000) and in rats (Mathiesen *et al.*, 1998;Ogawa *et al.*, 1990).

One highly influential study (Logothetis *et al.*, 2001) examined the relationship between the BOLD signal and neuronal activity which was simultaneously recorded using a microelectrode in monkey primary visual cortex. They recorded both multiunit activity (MUA), which is thought to reflect the spiking activity of neurons near the electrode tip (within 200μm) (Legatt *et al.*, 1980); and the local field potential (LFP), the low frequency component of the electrophysiological signal, thought to reflect synchronised dendritic currents averaged over a large volume of tissue (Mitzdorf, 1987), likely to reflect inputs and intracortical activity. They found that the LFP and MUA were both correlated with the BOLD response, but that the LFPs correlated slightly better. This might suggest that the BOLD signals reflect the input and intracortical processing rather than just the spiking output of neurons.

A recent study has added further to the controversy surrounding the link between neural activity and blood flow (Sirotin and Das, 2009). This showed that the vascular response in visual cortex is modulated by the expectation of the task, but without any neural modulation, suggesting that the vascular response might be primed by a part of

the brain anticipating neural activity. Further studies will be needed to clarify this complex relationship between neuronal activity and the BOLD response.

2.2.7 Resolution of fMRI in visual cortex

The spatial and temporal resolution of fMRI is limited by the spatio-temporal properties of the haemodynamic response to neural activity. Within visual cortex, the spatial resolution is able to distinguish between stimuli 1.5mm apart (Engel *et al.*, 1997) and the temporal resolution within calcarine cortex has been estimated to have a delay of approximately 2.5s which rises to a peak 3 seconds later (Boynton *et al.*, 1996).

2.3 FMRI analysis

All fMRI data acquired for the experiments in this thesis were analysed, at least in part, using Statistical Parametric Mapping software, developed at the Wellcome Trust Centre for Neuroimaging (http://www.fil.ion.ucl.ac.uk/spm/). SPM is a set of software tools implemented in MATLAB which allow preprocessing of raw fMRI data and subsequent statistical analysis. Two different versions of this software were used in the experiments in this thesis, SPM2 and SPM5, according to the timing and requirements of the individual experiments.

The fundamental principle of fMRI analysis is the same for all experiments: first the preprocessing of the raw fMRI data. This involves a series of spatial transformations to align each individual participant's data and then warp it either to the subject's own anatomical space or to a standardised anatomical space. These data are then smoothed in some, but not all experiments.

Next, a model is created of the hypothesised BOLD signal changes during each condition of the experiment and the data generated by the experiment is fitted to this model using a General Linear Model (see below). In some experiments, activation maps are generated from the resulting parameter estimates and tested for statistical significance. In other experiments, the analysis of parameter estimates is only carried out on pre-defined regions of interest (retinotopic visual cortex in individual participants) and tested for statistical significance across participants.

The stages of preprocessing and subsequent analysis differ slightly between experiments and will be discussed in detail for each experiment separately. Here I describe the overall aim of the individual stages and the motivation for performing them.

2.3.1 Preprocessing

2.3.1.1 Spatial realignment

Despite head restraints, all participants move their heads a few millimetres during scanning, causing neighbouring brain regions to move in and out of the voxel being analysed, which is a potentially serious confound. This is partly overcome using realignment. This process realigns the time-series of images by applying a rigid-body transformation to realign each scan with a reference scan (either the first scan or the mean of all the scans) and then resampling the data using tri-linear, sinc or spline interpolation. Six parameters are used to transform the image, representing adjustments in pitch, yaw, roll and in the X, Y and Z planes. These are estimated iteratively to minimise the sum of the squares of the difference between each successive scan and the reference scan (Friston, 1995). However, even after realignment, significant movement-related signals persist, which are non-linear and therefore cannot be accounted for by an affine linear transformation (Friston *et al.*, 1996). These are due to the position of each voxel within the magnetic field, as the image intensity depends on the present and previous position of a brain volume (termed spin-excitation history), as well as movements between slice acquisitions. To correct for these non-linear movement-related effects, the estimated movement parameters from the realignment procedure are estimated and subtracted from the original data in the design matrix during the model estimation stage of the analysis (Friston *et al.*, 1996).

2.3.1.2 Unwarping

The magnetic field in the head is not homogeneous, which causes geometric distortion of the image. Echo-planar sequences are especially susceptible to geometric distortions, particularly close to regions with tissue/air interfaces (such as the sinuses). To reduce this distortion, a field map is acquired. This involves combining additional EPI images with different gradient echo weightings. In this way, an image is produced showing the magnitude of deviation in magnetic field at each voxel. The magnetic field deviation is proportional to the extent of distortion. The image can then be transformed by warping the distorted voxel positions to non-distorted voxel positions by calculating the magnitude of distortion. The resulting images can be aligned better with the structural image.

2.3.1.3 Coregistration to T1 structural image

Coregistration is used to co-register each subject's functional images with their own structural images. In a similar way to realignment, it is achieved by applying a rigid-body transformation to the mean functional image (created during realignment) and interpolating over the borders of old voxels using nearest neighbour, B-spline, trilinear or sinc interpolation. The mismatch between the source and reference images is then calculated, and the parameters of the transform matrix required to reduce the mismatch are estimated. The parameters can then be adjusted iteratively until the mismatch is minimised.

2.3.1.4 Spatial Normalisation

Spatial normalisation is used to warp images from several participants into the same standard space to enable signal averaging across subjects. This also allows sites of activation to be reported using coordinates within a standard space. This is achieved by first determining the optimum 12-parameter affine transformation which will map the mean image (created during realignment) onto a standard anatomical template image. Unlike coregistration where the images to be matched are from the same subject, the image needs to be warped using zooms and shears to register heads of different shapes and sizes. A Bayesian framework is used where the registration searches for the solution which maximises the *a posteriori* probability of it being correct (Friston, 1995). Next, non-linear registration is used to correct for differences in head shapes not accounted for by the affine transformation. This is modelled by combinations of cosine transform basis functions and involves minimising the residual squared difference between the images and the template (Ashburner and Friston, 1999). The estimated warp is then applied to all the functional images.

The template used for normalisation is that defined by the Montreal Neurological Institute (MNI). Voxel location is expressed using an *x,y,z* coordinate system, where *x* values indicate distance to the right (positive) and left (negative) of the mid-sagittal plane; *y* values indicate distance anterior (positive) and posterior (negative) to the vertical plane through the anterior commissure; and *z* values indicate distance above (positive) and below (negative) the inter-commissural line. The origin (0,0,0) is located at the anterior commissure.

2.3.1.5 Spatial smoothing

Spatial smoothing or filtering is achieved by convolving each volume with a Gaussian-shaped kernel, with the width of the kernel at full width half maximum (FWHM) determining the extent of spatial blurring. Usually a kernel of 6-10 FWHM mm is used. There are several reasons for spatially smoothing:

1) To improve the signal-to-noise ratio. By local averaging, the noise values will cancel each other out, leaving relatively more signal. Ideally, the filter kernel should match the size of the signal.

2) Statistical parametric analysis requires the data to be smooth as it relies on the underlying assumption that errors are normally distributed.

3) Smoothing the data compensates for small variations in anatomy between subjects, reducing the variation in the localisation of activations across participants.

4) Smoothing also reduces the number of resolution elements (resels) which are assumed to be independent and are used for correction of multiple comparisons during later analysis.

2.3.2 Statistical Parametric Mapping

2.3.2.1 Overview

Once the images have been pre-processed, statistical analysis is performed to identify voxels activated during the experiment. In this thesis, Statistical Parametric Mapping

(SPM) has been used to analyse the fMRI data. This uses estimates of brain responses at every voxel and analyses these using a standard univariate statistical test (termed the General Linear Model, GLM). The resulting statistical parameters are then displayed as a three-dimensional image, called a Statistical Parametric Map (SPM), which identifies the voxels in the image where the brain has been activated by the task. The Gaussian Random Field (GRF) theory is then used to solve the problem of multiple comparisons which arises when multiple statistical tests are performed on continuous data (as in images of brain responses). This takes into account the spatial smoothness of the statistical map and thereby estimates the number of statistically independent voxels. It also takes into account the size of the clusters of activation. In this way, it corrects for multiple comparisons but in a more appropriate way than the very stringent Bonferroni correction, given the inter-relatedness of neighbouring voxels.

2.3.2.2 General Linear Model

General linear modelling is a way of setting up a model of what would be expected to be seen in the data and then fitting this model to the data. For example, one aspect of the model is derived from the timing of the stimulus and a good fit would suggest that the data were likely to have been caused by that stimulus. GLM is used here (and usually) in a univariate way. This means that the model is applied to the time course of the responses from each voxel separately.

A simple example is:

$y = \beta * x + c + e$

Where y is the time course of the BOLD signal at a particular voxel, x is the model, with a value for each time point. β is the parameter estimate for x, which is the value that x must be multiplied by to fit the data and therefore reflects the contribution of the variable x to the data; c is a constant and corresponds to the baseline of the data; e is the error in the model fitting which is assumed to be independent and identically distributed with zero mean and variance (Kiebel and Holmes, 2003). For several explanatory variables (L) and several time points (j) the formula would be:

$$Y_j = x_{j1}\,\beta_1 + x_{j2}\,\beta_2 + \ \ldots + x_{jl}\,\beta_l + \ \ldots x_{jL}\,\beta_L + e_j$$

The GLM can also be expressed in matrix notation:

$$Y = X\beta + \varepsilon$$

Where Y is the vector of observations or time course at a particular voxel and β is the vector of parameters to be estimated. ε is the vector of error terms and X is the design matrix which has one row per observation and one column per model parameter (x), also referred to as explanatory variables, covariates or regressors.

Regressors are created for every factor manipulated in the experiment by placing a stimulus function at the time point which corresponds to the effect of interest. This is then convolved with a Haemodynamic Response Function (HRF) to account for the delayed and dispersed form of the BOLD response. The HRF is modelled in SPM

using a multivariate Taylor expansion of a combination of gamma functions (Friston *et al.*, 1998). Other effects, including those which are not experimentally interesting such as movement parameters, are also included into the design matrix to account for as much variance in the data as possible and minimise effects of no interest. Before fitting the model, the fMRI data are high-pass filtered to remove low frequencies which would be attributed to scanner drift, cardiac and respiratory artefacts and the data are low-pass filtered to reduce high-frequency noise in the time series. Finally, the beta parameters (also called betas) for each voxel are estimated by multiple linear regression to minimise the sum of the squares of the differences between the observed data and the values predicted by the model.

2.3.2.3 t and F statistics

The betas, or parameter estimates (PE) from the β vector are converted into a useful statistic by comparing each value with the uncertainty of its estimation to produce a T value where:

T=PE / standard error (PE).

A significant fit with the data is where the PE is high relative to its uncertainty. In this way, inferences about the relative contribution to the data of each regressor can be made. An F-statistic can be used to test the null hypothesis that the parameter estimates are zero, to produce an SPM{F} image. Parameter estimates can be compared directly to test whether one regressor fits more closely to the data than another by using a contrast. This is done by subtracting one PE from another and calculating a new standard error for this value. A t-statistic can be used to test the null hypothesis that there is no difference between the two conditions and used to generate

an SPM{t} image. The statistical map can then be thresholded to determine, at a given level of significance, which areas are activated by a particular contrast. Thresholding is performed by selecting a significance level, usually using Gaussian Random Field theory, to take into account the spatial smoothness of the statistical map, but avoid the multiple comparison problem.

2.4 Retinotopic mapping

2.4.1 Retinotopic organisation of visual areas

Human visual cortex is organised into multiple areas, each representing the visual field, but with neurons within the different visual areas responding in different ways. This varies from receptive field size, which increases from primary visual cortex to the higher visual areas V2, V3 and beyond (Smith *et al.*, 2001); to more complex attributes such as modulation by directed attention (Kastner and Pinsk, 2004). Human primary visual cortex (V1) occupies an area approximately 4-8 cm at the posterior end of the occipital lobe in each hemisphere, with most of V1 falling within the calcarine sulcus. Studies of patients with occipital lobe lesions have established that the receptive fields of neurons in V1 are retinotopically organised (Holmes, 1918;Horton and Hoyt, 1991). This means that the receptive fields are organised to form a continuous map within the cortical surface of the contralateral visual field. Thus, from posterior to anterior cortex the representation of the visual field moves from the centre to the periphery. In addition, the central fovea is represented by a larger proportion of cortical surface than a comparable region in the peripheral visual field.

Animal experiments have subsequently uncovered multiple maps with V2 adjacent and surrounding V1 (THOMPSON et al., 1950;Cowey, 1964;Essen and Zeki, 1978) and V3 adjacent and surrounding V2 (Hubel and Wiesel, 1965) and many more maps beyond these, extending to higher visual areas (Allman and Kaas, 1971;Gattass et al., 2005). The consistent topographic organisation is used to accurately determine boundaries between these multiple visual areas in the human brain (Engel *et al.*, 1994;Sereno *et al.*, 1995).

There are several important reasons for performing retinotopic mapping in this thesis and in other experiments:

1) The differences in response properties of neurons in different visual regions means that they should be analysed separately as differences in activation can provide important insights for the particular experimental question.

2) There is wide inter-subject variability in the precise anatomical location and size of the different visual areas (Dougherty *et al.*, 2003). It is therefore not possible to assign borders based on normalised coordinates. To compare activation in a particular region between individuals, it is necessary to determine where that region is in each individual separately.

3) It is often necessary to localise the responses within a specific region in the visual field (for example to compare responses between different parts of the visual field).

The retinotopic organisation of the visual areas allows the accurate delineation of the different visual areas. This has traditionally been performed using phase-encoded mapping, whereby a contracting ring stimulates the visual field from the periphery to the fovea, thus creating a travelling wave of activity from anterior to posterior cortex, along the dimension of eccentricity. The second dimension, of angular position, is represented by a path that spans from the lower to the upper lip of the calcarine sulcus, from the upper vertical, through the

horizontal to the lower vertical meridian (see Figure 2.1), determined by using a rotating wedge to stimulate the neurons.

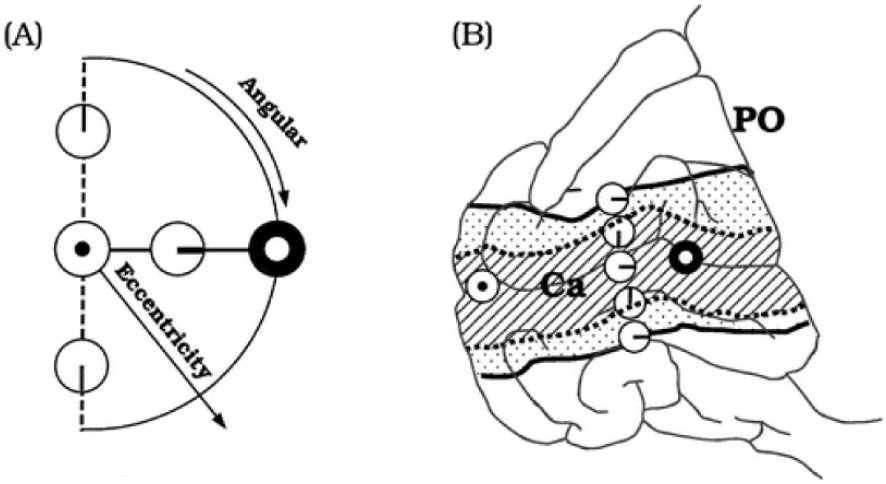

Figure 2.1 Retinotopic organisation of visual areas in the left hemisphere. (A) Representation of the visual field with icons representing the horizontal and vertical meridians and the central fixation (black dot, white surround) and periphery (white dot, black surround). **(B)** The position of V1 (diagonal shading) and V2 (dotted shading) on a sketch of the medial surface of the left occipital lobe. The visual field icons indicate on the sketch the retinotopic organisation of areas V1 and V2, with the horizontal meridian in the middle of V1, at the depth of the calcarine sulcus and the vertical meridians at the borders between V1 and V2. Note that central fixation is represented at the occipital pole and the periphery is more anterior. The positions of the calcarine sulcus (Ca) and parieto-occipital sulcus (PO) are indicated (adapted from (Wandell, 1999)).

The travelling wave reverses direction at the border between V1 and V2, and at the border between V2 and V3. As the experiments in this thesis are mostly concerned with defining the borders between the visual areas, and not with precise locations within the visual areas, a simpler, more rapid method was used to define the borders, which is based on the same principles as phase-encoded mapping. This method is meridian mapping, whereby the horizontal and vertical meridians are used to define the borders between visual areas: the midline of V1 represents the horizontal meridian

and the border between V1 and V2 represents the vertical meridian, both dorsally and ventrally. Instead of a rotating wedge, stimuli representing the horizontal and vertical meridians are used (see Figures 2.2 and 2.6).

Figure 2.2 Visual stimuli used to identify cortical visual areas in human visual cortex

2.4.2 Meridian mapping

As described above, the aim of meridian mapping is to accurately determine, on a subject-by-subject basis, the boundaries of the early visual areas. A high resolution structural scan and functional meridian mapping scans responding to stimuli in the horizontal and vertical meridians are collected for each participant (details are described in the Methods section of each experimental chapter). These provide BOLD response patterns in 3D volumetric space which can then be projected onto the 3-dimensional reconstruction of the anatomical image. However, retinotopic information is better described in two-dimensional space on the cortical surface, as adjacent points on the cortical surface represent adjacent points in the visual field. Therefore, retinotopic mapping requires flattening of the cortical surface. Two methods have been used in this thesis, for different experiments. These will each be described here in turn.

2.4.2.1 Meridian mapping using MrGray

This method uses MrGray software developed at Stanford (Teo *et al.*, 1997;Wandell *et al.*, 2000)(http://white.stanford.edu/~brian/mri/segmentUnfold.htm) and requires several stages:

1) The grey and white matter in the T1 structural scan is segmented semi-automatically by defining the white matter using luminance values and using MrGray software to 'grow' a grey layer over this (see Fig. 2.3). The resulting grey and white matter is checked manually for every participant and discrepancies with the structural scan corrected manually.

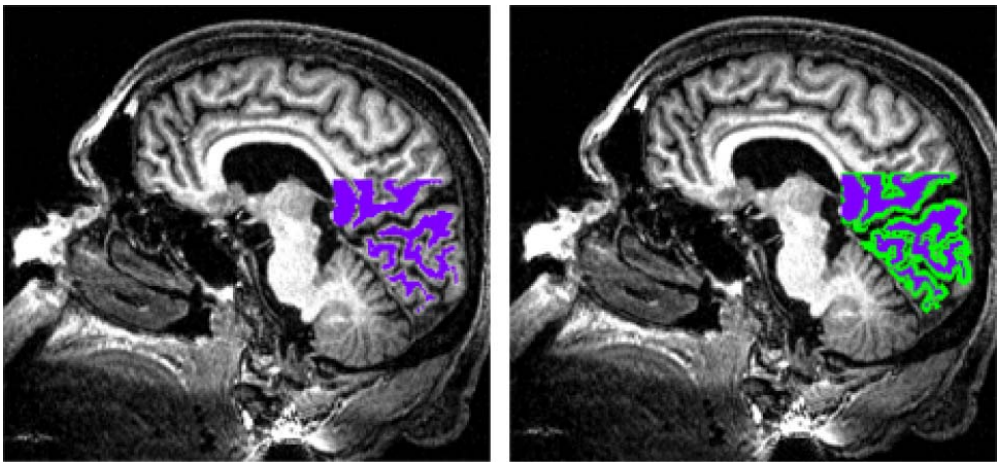

Figure 2.3 White and grey matter segmentation using MrGray

The T1-weighted structural image of one participant, viewed using Mr Gray software, is shown in both panels. Within a volume of interest (here defined as most of the occipital and part of the parietal lobes), the white matter is defined according to luminance values and checked manually for each participant individually. The segmented white matter is shown here in purple. The grey matter is then 'grown' by the MrGray software onto the defined white matter surface (here shown in green), as shown in the right panel. This is then checked manually, for each participant individually and any discrepancies between the automatically generated grey matter and the participant's anatomy are corrected manually.

2) The white/grey interface generated during the semi-automatic segmentation step is then used to reconstruct the surface anatomy of the occipital lobe (Figure 2.4). A mesh is also generated, covering the surface of the portion of the cortical area to be flattened and onto which the grey matter nodes can be mapped.

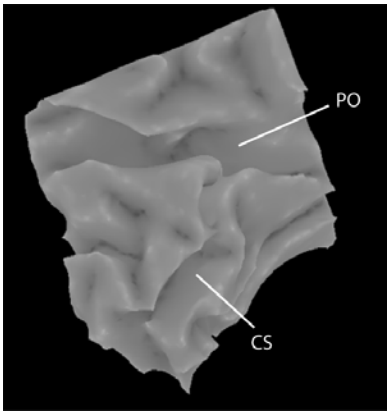

Figure 2.4 3D rendering of the cortical surface of the right occipital lobe of one participant, generated following the segmentation process in MrGray.

PO, parieto-occipital sulcus, CS, calcarine sulcus. Note this is the right occipital lobe but is shown on the left side as in radiological convention, with the medial surface on the right.

3) Next, the 3D mesh is unfolded or flattened maintaining the distance between adjacent grey matter nodes using mrFlatMesh software (http://white.stanford.edu/~brian/mri/segmentUnfold.htm). Grey layers are then mapped onto the flattened mesh to generate a flatmap, with a greyscale system where black represents sulci and white, gyri (see Fig. 2.5).

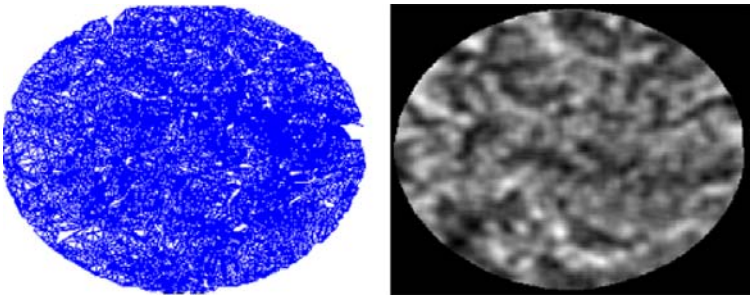

Figure 2.5 Flattened representations of occipital lobe generated using mrFlatMesh software

Unfolded mesh (left panel) of the occipital lobe from a participant and flatmap from the same participant (right panel).

4) Finally, the functional activations generated by the contrast of horizontal compared to vertical, and vertical compared to horizontal stimulation are displayed on the flattened representation of the occipital cortex using in-house software code (see Fig. 2.6).

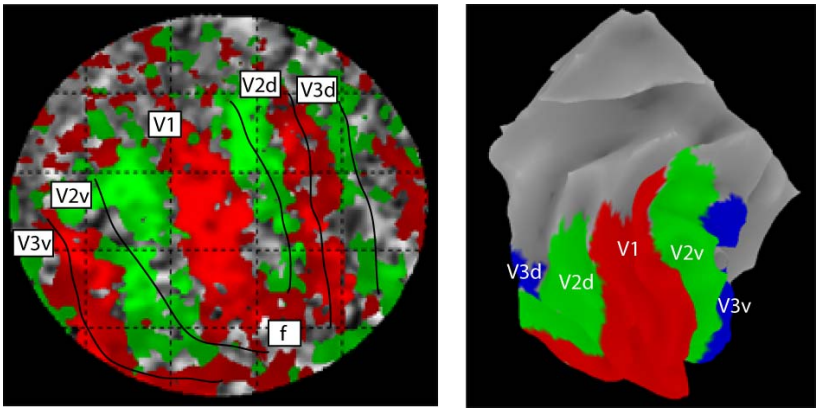

Fig 2.6 Functional data from meridian mapping projected onto the flatmap and 3D representation of the occipital lobe of a participant. Left panel: Functional data from horizontal (red) and vertical (green) meridian mapping projected onto the flatmap of a participant's right occipital lobe. These data are used to delineate boundaries between the different visual areas V1-V3. Right panel: 3D reconstruction of the same participant's right occipital lobe with the regions defined using the flatmap now projected onto the surface. Note how V1 (red) lies within the calcarine sulcus and V2v and V2d (green) surround this region.

As described above, the boundaries between the visual areas lie at the most vertically responsive regions. These activations can therefore be used to divide the flattened cortex into the early visual areas and the voxels within them exported as mask images.

2.4.2.2 Meridian mapping using Freesurfer

This method uses FreeSurfer software developed at Harvard (Dale *et al.*, 1999) (http://surfer.nmr.mgh.harvard.edu/). The cortical reconstruction and volumetric segmentation is automatically performed by the FreeSurfer software. This involves removal of non-brain tissue using a deformation procedure (Segonne *et al.*, 2004), followed by automated Talarirach transformation, segmentation of the subcortical white matter and deep gray matter structures (Fischl *et al.*, 2002;Fischl *et al.*, 2004), intensity normalisation (Sled *et al.*, 1998) and tessellation of the gray/ white matter boundary. There is an automated topology correction (Fischl *et al.*, 2001;Segonne *et al.*, 2007) and surface deformation is performed following intensity gradients to optimally place the grey/white and grey/CSF borders (Dale et al., 1999;Fischl and Dale, 2000). This automated procedure generates a cortical model, the surface of which can then be inflated (Fischl *et al.*, 1999) to better visualise the sulci. Curvature information is added using intensity and continuity information from the segmentation and deformation procedure (Fischl and Dale, 2000). Functional data in the form of activations responding to horizontal and vertical meridian stimuli are superimposed onto the inflated cortical surface. These are used to delineate the boundaries of the early visual areas as described in the alternative method above (see Figure 2.7). The

surface regions are then converted to volumes using FreeSurfer software for use as mask images in later analyses.

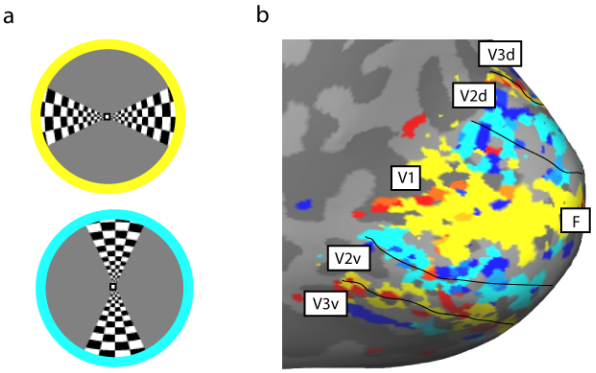

Fig 2.7 Meridian mapping projected onto inflated hemisphere created using FreeSurfer The patterns of activation elicited by horizontal (shown in yellow) and vertical (shown in blue) meridian stimuli from a single participant are overlayed onto the inflated surface of the right occipital lobe of the same representative participant. As can be seen from images generated using MrGray, the horizontal stimulus activates the midpoint of the calcarine sulcus and the vertical stimulus activates the gyri on each side.

2.5 MAGNETOENCEPHALOGRAPHY

2.5.1 Introduction

Magnetoencephalography (MEG) is a non-invasive brain imaging tool which records the weak magnetic fields generated by neuronal activity. These magnetic signals are detected with superconducting coils connected to SQUIDs (superconducting quantum interference devices), which are extremely sensitive to changes in magnetic fields, detecting signals which are 1 million to 1 billion times smaller than the surrounding noise (Vrba and Robinson, 2001). These SQUIDs are usually arranged within helmets in arrays of over 300 SQUIDs to record simultaneously from the whole cortex.

The main advantage of MEG over fMRI is its excellent temporal resolution, of the order of milliseconds, unlike fMRI which has a temporal resolution of approximately 1 second. This allows MEG to follow rapid changes in cortical activity which might not be possible using fMRI. MEG, like EEG (electroencephalography), is also a direct measure of neural activity, rather than the associated haemodynamic or metabolic effects measured by fMRI.

One of the main disadvantages of MEG is its relatively poor spatial resolution compared with fMRI. However, unlike electric signals of EEG, magnetic fields are not distorted as they pass through the scalp and skull. This allows more accurate solutions to the inverse problem for source localisation than can be achieved using

EEG, as will be discussed below. A further feature of MEG is that it can only detect fields that originate from neurons oriented tangentially to the scalp. Thus MEG is particularly well suited to investigating brain regions within the cortical sulci. MEG therefore provides information that is complementary to fMRI and within this thesis the two methodologies will be used to provide, in some instances, convergent evidence for presented theories.

2.5.2 Neurophysiological basis of MEG signal

The human cortex contains millions of pyramidal cells (approximately 10^5 per mm^2) arranged perpendicular to the cortical surface. Nerve cells receive information in the form of electrical signals from other cells via synapses on their dendrites. Within each cell, equilibrium exists between ions diffusing in and out of the cell, producing a negative potential of -70 mV within the cell. When a neuron is excited by another neuron via an action potential, an excitatory postsynaptic potential (EPSP) is generated at the apical dendritic tree. The apical dendritic membrane becomes transiently depolarised and electronegative with respect to the cell body and basal dendrites. This potential difference causes a current to flow from the non-excited membrane of the soma and basal dendrites to the apical dendritic tree. Some of this current takes the shortest route and flows within the dendritic trunk (also called the primary current). The current loop must be closed to conserve electric charges, therefore extracellular currents flow even through the most distant part of the volume conductor (also called secondary or return currents) (see Figure 2.8a).

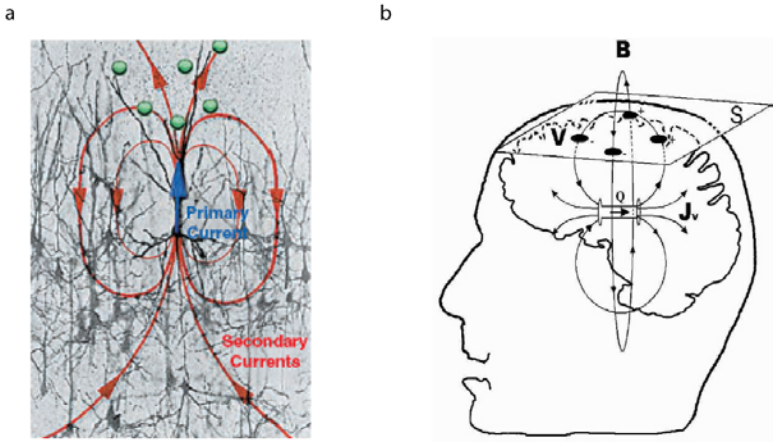

Figure 2.8 (a) Current dipole around a single neuron. Primary current flows across the shortest route, with return currents flowing outside the cell. Adpated from (Baillet *et al.*, 2001). **(b) The relationship between the current in the brain and magnetic field detected outside the head**. A current source with strength Q causes a current flow Jv inside the brain. This produces a potential difference V on the scalp (which can be measured using EEG) and a magnetic field B outside the head. Adapted from www1.aston.ac.uk/lhs/research/centres-facilities/meg/introduction/.

Primary and secondary currents contribute to the magnetic fields detected outside the head, but the spatial arrangement of the cells are crucial in determining which currents produce fields outside the scalp. For an individual cell arranged perpendicularly to the cortical surface, this current flows perpendicular to the cortex. However, the cortical surface is intricately convoluted into sulci and gyri, such that the current can be tangential or perpendicular to the scalp surface, depending on the location of the cell. Only currents tangential to the scalp will result in fields outside the scalp (see Figure 2.8b). Radial dipoles are oriented perpendicular to the surface of the skull and will therefore produce no magnetic field outside the skull.

The potential produced by an individual neuron is weak and the current-dipole moments required to explain the magnetic fields measured outside the scalp are of the order of 10nAm (Hamalainen *et al.*, 1993). Therefore, for fields to be detectable, a very large number of neurons ($10^4 – 10^5$) must be simultaneously activated (Wilkswo, 1989).

2.5.3 MEG acquisition

2.5.3.1 Detection of brain magnetic fields

Magnetic fields produced by neuronal activity are very small, even when multiple neurons are activated simultaneously, and the only detectors with adequate sensitivity are Superconducting Quantum Interference Devices or SQUID sensors. A SQUID is a superconducting ring with one or two weak links known as Josephson Junctions (Josephson, 1962), these limit the flow of the supercurrent. The voltage in the loop changes as a function of the magnetic flux passing through it. (See (Hamalainen *et al.*, 1993) for review).

The SQUIDS are coupled to the magnetic fields by flux transformers. These are also superconducting and consist of a pickup coil, which is exposed to the magnetic field, leads and a coupling coil which inductively couples the flux transformer to the SQUID ring. Flux transformers operate based on the fact that distant noise sources have a spatially uniform magnetic field at the pickup coil, whereas brain sources close to the gradiometer have comparatively large spatial gradients. This helps reduce noise from distant sources. They can take various configurations (see Figure 2.9). The simplest configuration of a flux transformer is the magnetometer, others include axial

and planar gradiometers which are better at compensating for variations in the background field. For example, an axial first-order gradiometer consists of a pick-up coil and a compensation coil which are identical and connected in series but wound in opposing directions. This makes them insensitive to changes which affect both coils identically, but sensitive to inhomogeneous changes. Thus the pickup coil detects the signal and the compensation coil compensates for variations in the background field.

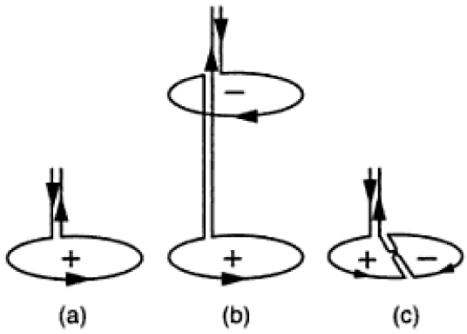

Figure 2.9 Flux transformer configurations. (a) A magnetometer. (b) An axial first-order gradiometer. (c) A first-order planar gradiometer. Arrows indicate current direction in the wires. Plus and minus signs indicate magnetic fluxes of opposite polarities. Adapted from (Hamalainen and Hari, 2002).

The CTF system at the Wellcome Trust Centre for Neuroimaging uses third-order axial gradiometers. The locating accuracies of axial and planar gradiometers are essentially the same (Carelli and Leoni, 1986), although the planar gradiometers collect their signals from a more restricted area near their sources.

2.5.3.2 Set-up of the MEG system

A multichannel MEG system comprises more than 100 channels within a helmet to record the magnetic field distribution all around the brain simultaneously. At the

Welcome Trust Centre for Neuroimaging, the Omega275 CTF MEG system (VSMmedTech, Vancouver, Canada) is used. This has 275 3rd order axial gradiometers arranged to cover the entire brain.

Both SQUIDs and flux transformers can only operate at extremely low temperatures, usually at 4K (-269^{o}C). They are therefore immersed in cryogen (usually liquid Helium). The cryogen is enclosed in a thermally insulated container (known as a dewar), which is electromagnetically transparent to allow brain signals to reach the flux transformers and SQUID detectors. The dewar is mounted in a movable gantry to allow for horizontal or seated positions. This is often placed in a magnetically shielded room (MSR) to remove extraneous magnetic fields (see below). The MEG signals are transmitted from the MSR to the computers for data analysis. The MSR also contains a screen for stimulus delivery (see Figure 2.10).

Figure 2.10 Participant in MEG system in magnetically shielded room Plastic overshoes are worn to prevent inadvertent introduction of ferromagnetic elements into the MSR.

The participant is able to move their head within the MEG helmet and it is therefore important to accurately measure the head position relative to the sensors. This is achieved by using three small coils (1 at each pre-auricular point, and one at the nasion). During MEG acquisition, excitation currents are fed to these coils and the resultant magnetic field is measured to determine the head position. This is measured routinely at the beginning and end of each recording to ensure stable head position, requiring the participant to keep their head still throughout the MEG recording. This places some additional limits on source modelling, as even cooperative participants find it difficult to keep their head still and fast methods are being developed to measure head position continuously.

2.5.3.3 Noise reduction

The magnetic signals from the brain are extremely weak, typically 50-500 fT (Hamalainen *et al.*, 1993) compared to the ambient magnetic field (for example urban magnetic noise ranges between 1 nT to 1 micro tesla (Vrba and Robinson, 2001)) and there are many sources for this magnetic noise including the earth's geomagnetic field, cars, radio and power fields and even the human heart. It is therefore extremely important to eliminate external noise as far as possible.

One step in reducing environmental noise is using a magnetically shielded room. This uses various technologies including μ-metal which shields the inside of the room from low frequency magnetic fields; and thick layers of high-conductivity metals to set up eddy currents shielding against higher frequency magnetic interference. Active

electronic circuits can also be used to cancel external disturbances. In addition to the external active shielding, the MEG system itself can be equipped with compensation sensors, to detect background signals distant from the head. A proportion of the output of these compensation signals can then be added to the output of the sensors detecting brain signals.

2.5.4 MEG analysis

2.5.4.1 Data Acquisition and sampling

During acquisition, the analog signals are digitised. Data are collected at a sampling rate of 240-480 Hz. This rate determines the highest frequency of signal that can be collected undistorted, as sampling at too low a frequency can cause aliasing (detection of frequencies not actually present in the signal). According to the Nyquist criterion, the sampling rate must be at least double the highest frequency in the sampled data, thus the sampling rates used in practice are well above this requirement.

2.5.4.2 Signal processing

The data are then band-pass filtered, usually at 1-45 Hz (Butterworth) to attenuate low- and high-frequency components. Epochs are then extracted from the data at points time-locked to the stimulus and baseline corrected. The data are often then downsampled to reduce file sizes.

2.5.4.3 Artefact detection

Artefacts in MEG are any magnetic activity recorded by MEG equipment that does not originate from cerebral sources. These can distort the ERF (event related field) and it is therefore necessary to detect and remove them. They are typically generated by external sources such as eye movements, muscular activity or recording equipment. Blinks and eye movements are particularity important sources of biological artefacts as they may be time-locked to the stimuli and can be of large amplitude. They can be reduced by avoiding contact lenses where possible and building blink breaks into the paradigm and should be monitored and removed by recording eye movements and pupil diameter during MEG acquisition. Trials with blinks or eye movements greater than a specified threshold can then be rejected. Other sources of artefacts include cardiac artefacts (stronger in the left than the right hemisphere channels) and artefacts due to muscular tension (EMG artefacts, which are weaker than in EEG) and artefacts due to respiration movements if the body or clothing contains magnetic material.

EMG artefacts are reduced by asking participants to sit comfortably, relax and open their mouth slightly. Other artefacts can be removed by rejecting trials with ERFs greater than a specified threshold, indicating channel drift or excessive muscle activity.

2.5.4.4 Event related fields (ERFs)

Event-related fields are the small changes in magnetic fields detected outside the head time-locked to a specific stimulus event. They are equivalent to event related potentials measured using EEG. The evoked event-related fields in response to a single stimulus are very small relative to background activity (even after noise removal, filtering, and artefact detection) and therefore ERFs are extracted from the background MEG waveform and averaged together over many trials to increase the signal to noise ratio. Averaging will enhance the signal providing that the following assumptions are met (Spencer, 2005): that the signal in each trial has stable characteristics; that the background activity is random and uncorrelated with the signal and that the signal and noise linearly sum to produce the EEG or MEG waveform.

The event related field is therefore a time-series plotting scalp magnetic field (in femtoTesla) over time (milliseconds), where fluctuations provide information about the internal state of the participant. By recording from multiple sensors simultaneously, a spatial dimension is also introduced. Thus MEG analysis involves analysis in the temporal and spatial domains.

Temporal analysis of ERFs involves examining how waveforms recorded at a particular sensor vary over time across one or more experimental conditions. This usually involves quantification of amplitude and latency characteristics of specific ERF components, which are positive and negative-going deflections in the ERF-

waveform (Spencer, 2005). However, this type of analysis is not possible with the experimental set-up in this thesis. ERFs were measured time-locked to a continuous flickering stimulus and therefore all of the characteristic components usually seen following presentation of a single visual stimulus are removed by baseline correction. Therefore the analysis was limited to a qualitative comparison of the ERF waveforms between conditions and performed more detailed, quantitative analyses on data in the frequency domain.

2.5.4.5 Steady state analysis

MEG, like EEG, can be analysed in the frequency domain. This is of particular relevance to the experiment presented in Chapter 3 of this thesis as this involved neural responses to the perception of a stimulus flickering at a known frequency. Oscillations can be classified as spontaneous, induced or evoked according to the extent of phase locking to the stimulus (Galambos, 1992). Spontaneous activity is completely uncorrelated with experimental condition, induced activity is correlated with experimental condition but not phase-locked to the onset and therefore cannot be observed in averaged signals. Evoked activity is phase-locked to the onset of an experimental condition. Thus, it starts at the same time after every stimulation, has identical phase and may be visible in the averaged ERF. In Chapter 3, evoked activity was measured.

The MEG waveform can be decomposed into sinusoidal oscillations of different frequencies using various methods including filtering, Fourier transformation and

wavelet analysis. In this thesis, wavelet analysis was used as it retains time course information. Wavelets are simple oscillating amplitude functions of time, with a zero mean amplitude (Samar *et al.*, 1999). They are relatively localised in time and frequency space with large fluctuating amplitudes during a restricted time period and very low or zero amplitude outside that time period (see Figure 2.11). This localisation property allows one to follow the time course of component structures in the MEG signal. Wavelets can take a variety of shapes. For the analysis in this thesis, the Morlet wavelet, also known as the Gabor wavelet, is used. These are complex functions with real and imaginary parts consisting of a harmonic oscillation windowed in time by a Gaussian envelope. They are particularly suitable for analysis of oscillatory activity due to their sinusoidal nature (see Figure 2.11).

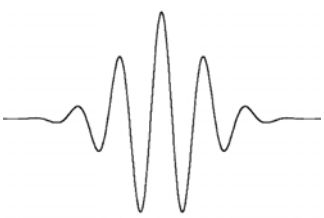

Figure 2.11 A Morlet wavelet

To perform a wavelet transform, the original time series is convolved with a scaled and translated version of the wavelet function. This generates a new signal of wavelet coefficients which are measures of how much the wavelet at that scale and position is included in the MEG waveform at each point (for an overview see (Herrmann *et al.*, 2005)). Convolutions with Morlet wavelets can be computed to generate a time-frequency representation of the signal.

The output of a wavelet transform is the wavelet power spectrum. This is a measure of the signal energy contained in the time-frequency bin covered by the transform. To represent evoked (phase-locked) activity, the wavelet transform is computed on the averaged signal.

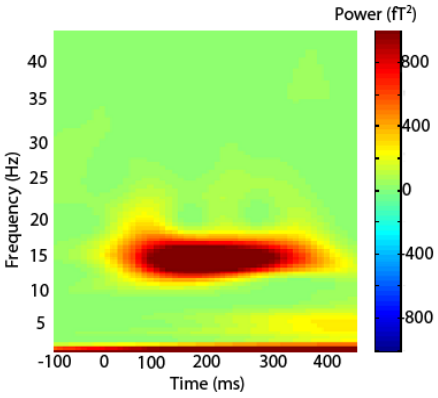

Figure 2.12 Example of time-frequency spectrum from an occipital sensor during presentation of stimulus flickering between black and white at 7.5 Hz. Clear response at 15 Hz (double the stimulating frequency), throughout the time-window, reflecting response to every change in stimulus from black to white and white to black.

2.5.4.6 Source analysis

2.5.4.6.1 The inverse problem

The aim of source analysis in MEG is to estimate the source current density underlying the MEG signals measured outside the head. However, to identify the location orientation and time-courses of the source of MEG data, one deals with the 'inverse problem' that there are an infinite number of possible neuronal source combinations within the brain which can give rise to a particular pattern of MEG

signals (von Helmholtz, 1853). Therefore additional physiological information is often used to constrain the problem and help facilitate a solution.

One approach to solving the inverse problem is to model the generators on a small number of sources or current dipoles, which represent neural activity in a few discrete brain regions, and finding the best fitting current dipole or equivalent current dipole. This is done by estimating the predicted output of that particular configuration of sources (the solution to the 'forward problem') and comparing this with the observed recording. The precise anatomical locations, orientations and strengths of the MEG sources can then be estimated iteratively using the least squares method to minimise the difference between the observed and predicted MEG recording (Marquardt, 1963). In practice this method is based on several assumptions including a limited number of sources and approximations of head shape, so results need to be interpreted with caution. Additional constraints can be placed on the model based on information from functional neuroimaging and neurophysiological data and by using the MRI of the participant to reconstruct the cortical surface, leading to more stable and more accurate source localisation. However, even with these constraints, finding the best fitting model for a time-varying signal is very challenging and the standard least squares approach may not yield the best estimate for the given parameters. More complex algorithms are used to take into account the physiological characteristics of particular experimental questions (Huang *et al.*, 2000;Aine *et al.*, 2000). Even with these advanced methods, however, the equivalent current dipole approach may not adequately model the underlying MEG sources. Competing solutions with different source configurations may be indiscernible based on the given

magnetoencephalographic output. Perhaps more crucially, the actual source distribution may not be adequately approximated by a dipole.

An alternative approach, used in this thesis, is to assume that the sources are distributed within a surface or a volume, often called the source space, and use estimation techniques to find the most likely source distribution. In this way, a reasonable estimate of even complex source configurations can be achieved without having to resort to dipole fitting. In this thesis, a mesh of 3004 vertices based on the cortical surface from individual participants' structural MRI, is used as the source space. This limits the inverse problem by assuming the sources lie within the cortical grey matter and allows any configuration of sources, rather than the small number used in the equivalent dipole model. However, an enormous number of possible solutions can be generated by this approach and a framework for constraining solutions is required. This can be achieved using a Bayesian framework, whereby constraints or priors can be introduced probabilistically. With this approach, any number of priors on the source or noise covariance matrices can be introduced in terms of variance components estimated from the data and an expectation maximisation algorithm is used to obtain a restricted maximum likelihood (ReML) estimate of the hyperparameters associated with each constraint. This enables the maximum *a posteriori* solution for the sources to be calculated uniquely and efficiently (Phillips *et al.*, 2002). Values can then be converted into voxel space and smoothed for further analysis.

2.5.4.6.2 Group analysis of source data using SPM

Group analysis can then be performed in a similar way to analysis of functional MRI data, using Statistical Parametric Mapping. Multiple linear regression is used to generate parameter estimates for each condition at every voxel for every participant. The resulting parameter estimates for each condition at each voxel can then be entered into a second level analysis where each participant serves as a random effect in a one-tailed t-test and appropriate corrections made for non-sphericity and correlated repeated measures. The resulting statistical parameters can then be displayed as a Statistical Parametric Map (SPM) to find the voxels within the image consistently identified as sources across all participants.

CHAPTER 3: EXAMINING THE NEURAL CORRELATES OF FILLING-IN OF ARTIFICIAL SCOTOMAS IN HUMANS USING MAGNETOENCEPHALOGRAPHY

3.1 Introduction

Artificial scotomas are a form of perceptual completion seen in normal human vision. They were first described by Ramachandran and Gregory(Ramachandran and Gregory, 1991) and involve a uniform target placed in the visual periphery on a background of dynamic luminance noise. After a few seconds of peripheral viewing, the target seems to fade, to be replaced by the background (Ramachandran and Gregory, 1991), thus leading to an "artificial scotoma" in the visual field. This form of filling-in is a useful model system with which to probe the neural mechanisms underlying perceptual completion. Unlike other forms of perceptual completion (e.g. across the blind spot), texture filling-in has a clearly defined latency and onset (De Weerd et al., 1998;Welchman and Harris, 2001), making it possible to study how it unfolds in time. It can also provide insight into the neural mechanisms of visual awareness in general, because changes in awareness occur without any change in physical (retinal) stimulation.

3.1.1 Previous studies of the mechanism of filling-in of artificial scotomas

Very little is known about the mechanism of filling-in of artificial scotomas. Psychophysical studies have shown that it is fixation-dependent (Spillmann and

Kurtenbach, 1992;De Weerd et al., 1998), promoted by a dynamic background (Spillmann and Kurtenbach, 1992) and that the time taken for the target to fill-in with surrounding texture is linearly related to the length of its bounding contour as projected onto visual cortex (De Weerd *et al.*, 1998). This strongly implicates retinotopic cortex as the neural substrate for such perceptual completion, but does not provide any insight into the processes taking place during filling-in of artificial scotomas.

Neurophysiological investigations of texture filling-in have produced conflicting results. In non-responding monkeys, filling-in of artificial scotomas is associated with increased activity in V2 or V3 (De Weerd *et al.*, 1995). Conversely, Troxler colour fading (filling-in of uniform chromatic targets on chromatic backgrounds) in responding monkeys is associated with no changes in activity in V1 and V2 corresponding to the centre of the coloured target, but decreased activity in V1 and V2 neurons responding to the boundary of the target (Von der Heydt *et al.*, 2003). In humans, in luminance filling-in (filling-in of an achromatic target on an untextured achromatic background) V1/V2 activity is reduced and activity increases in higher visual areas, but with little evidence for any retinotopic specificity of these effects (Mendola *et al.*, 2006).

3.1.2 The challenge of examining activity associated with perceptual filling-in

All of these previous studies have focused on measuring cortical activity associated with perceptual completion that was retinotopically specific to the area of the

scotoma. This has the potential disadvantage that it necessarily conflates the neural correlates of two distinct perceptual phenomena. First, the 'positive effects' associated with filling-in of the textured background into the region of the visual field occupied by an achromatic surface. Second, the 'negative effects' associated with the physically present achromatic surface that is no longer perceived. To differentiate these two factors, some way of distinguishing signals evoked by the perceptually filled-in target from the perceptually completed background is required. Retinotopic location alone cannot distinguish these signals because the positive and negative effects of texture completion occur at the same location in the visual field.

In this study, this problem was overcome by using frequency-tagged magnetoencephalography (MEG) (Tononi *et al.*, 1998;Chen *et al.*, 2003;Cosmelli *et al.*, 2004). A uniform target was flickered at 7.5 Hz and steady-state responses specific to this stimulus frequency were measured in contralateral posterior MEG channels. These responses allowed the assessment of how stimulus-related signals changed when perceptual completion unfolded in time. Because the signals were specific to the stimulus (and its corresponding retinotopic location), and not the background (which had a broad frequency spectrum), it was possible to evaluate whether steady-state neuromagnetic responses persisted after perceptual completion. The presence of such signals would indicate an unconscious representation of the perceptually completed stimulus (Gerrits and Vendrik, 1970;De Weerd et al., 1995;Matsumoto and Komatsu, 2005).

3.2 Methods

3.2.1 Participants

Seventeen neurologically normal adults (five females, 18 to 36 years old) with normal or corrected-to-normal vision gave written informed consent to participate in the study, which was approved by the local ethics committee. One participant was rejected due to excessive head movement (mean>1.5mm), one was rejected due to falling asleep during the experiment and one was rejected due to misunderstanding experimental instructions. Fourteen participants (four females, 18-36 years old) were therefore included in the analyses reported here.

3.2.2 Stimuli

Stimuli consisted of full-field random dynamic achromatic noise (subtending 33x24.8 degrees) with a red central fixation cross (0.2 degrees) and a flickering peripheral target. Stimuli were projected using an LCD projector (Sanyo PRO xtraX, refresh rate 60Hz, screen resolution 640x480) through a porthole and two mirrors onto a projection screen mounted in front of the participant. All stimuli were presented with MATLAB (Mathworks Inc.) using the COGENT 2000 toolbox (www.vislab.ucl.ac.uk/Cogent2000/index.html). To generate random dynamic noise, 30 arrays of 200x200 pixels were created, each measuring 0.165 by 0.124 degrees that were randomly assigned a grey-scale at the start of each run. These 30 arrays were then presented in a random order at the screen refresh rate (60Hz) to give the

appearance of random dynamic noise with a mean luminance of 20.7cd/m^2. An artificial scotoma was created by placing a small flickering square achromatic target (1.12 by 1.12 degrees) on the background in the lower left visual field at 9.43 degrees eccentricity (8 degrees across, 5 degrees down) flickering between black (luminance 2.5cd/m^2) and white (luminance 98.4cd/m^2) at a rate of 7.5 Hz (8 screen refresh cycles). This frequency was chosen because it produces the largest amplitude oscillatory MEG signal (Pastor *et al.*, 2003). The lower half of the visual field was chosen for placement of the target, as filling-in has been shown to be more robust (Mendola *et al.*, 2006) and because MEG signals have been shown to be stronger for stimuli presented in the lower visual field (Portin *et al.*, 1999). Behavioural experiments prior to scanning confirmed that the target was small enough to allow filling-in to occur, despite the pertinent flickering.

3.2.3 Procedure

On each trial, participants were presented with a screen of dynamic noise and a flickering target in the near periphery. Participants were instructed to fixate centrally and indicate the disappearance of the peripheral target using a button press ('2' on the keypad) (see Figure 3.1). On some occasions, the stimulus was perceived to fade for a short time before disappearing and participants could indicate this fading with a different button press ('1' on the keypad). Participants indicated any re-appearance of the target (for example following loss of central fixation) with a third button press ('3' on the keypad). These button presses were used to define time-periods of 'flicker visible', 'flicker-faded', 'flicker filled-in' and 'flicker returned'. Each trial lasted 10 seconds and was followed by a 500 ms interval during which a grey screen

(luminance 15.0 cd/m^2) was presented. A small red fixation mark was always present centrally. Optimal trial length was determined prior to scanning. In a proportion of trials (27%) the peripheral flickering stimulus *physically* disappeared 5 seconds after trial onset, whether the participant was reporting filling-in or not. As the target had been flickering, there were no stimulus-contingent after-effects. The periods of time after the stimulus had physically disappeared were defined as 'flicker absent' time periods. Each participant completed five runs, each comprising 55 trials, and received quantitative feedback at the end of every run as a percentage of trials where they had reported filling-in for longer than 1 second. Participants were encouraged to blink during specific rest periods during recording, but were not told to abstain from blinking during the rest of the experiment. All participants received training prior to scanning, to ensure they could experience disappearance of the stimulus and assign consistent responses to different perceptual states.

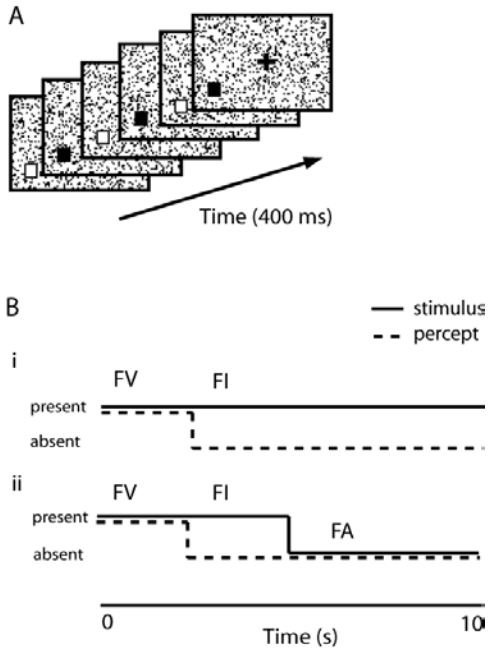

Figure 3.1 (A) **Stimulus configuration**. Visual stimuli consisted of full-field random dynamic achromatic noise with a small square achromatic target in the lower left visual field flickering at a rate of 7.5Hz. (B) **Procedure**. (i) Normal trials: During each 10s trial, participants fixated centrally and indicated the *perceived* disappearance of the flickering target. Time periods were defined as "flicker visible" (FV) whilst the target was present and perceived and "filled-in" (FI), whilst the target was present but not perceived. This filling-in occurred at a variable time after stimulus presentation, depending on participants' perception. (ii) Catch trials: During 27% of trials, the flickering target was *physically* removed 5 seconds after the onset of the trial. During these trials, periods were defined as "flicker visible", for target present and perceived, "filled-in" for target present but not perceived and "flicker absent" (FA), for target absent and not perceived.

3.2.4 MEG acquisition

MEG data were recorded using 275 3rd order axial gradiometers using the Omega275 CTF MEG system (VSMmedTech, Vancouver, Canada) at a sampling rate of 240 Hz within an electromagnetically shielded dimly lit room. Participants were seated and

viewed computer-generated stimuli projected through a porthole and two mirrors onto a screen at a distance of 57cm. Trigger events were recorded at every change of the target from black to white, where the stimulus was visible, and at the equivalent time when the flickering target was absent. Each participant's head position was determined using three coils attached to anatomical landmarks (nasion, right and left pre-auricular points), at the beginning and end of every run. In a separate session, a photodiode was placed on the screen at the position of the flickering target to record the precise timing of the flicker and determine screen latency.

3.2.5 MRI acquisition

T1-weighted volumetric anatomical images were acquired with either a 3T Siemens Allegra system (n=11) or a 1.5T Siemens Sonata system (n=3), according to scanner availability. (Dimensions 224x256x176, slice thickness=1mm). Fiducial points were marked using vitamin E capsules.

3.2.6 MEG analysis

MEG data were analysed using SPM5 (Wellcome Department of Imaging Neuroscience, London, UK. www.fil.ion.ucl.ac.uk/spm). For all analyses, each ten second trial was divided into separate time-periods according to the participants' button press responses, and taking into account any times where the target had been physically removed from the screen (see above). Thus, three different time-periods, or conditions, were defined across all trials as follows:

1. “Flicker visible”. In this time period the flickering target was present on-screen and participants indicated that they clearly perceived it, by the lack of button-press.

2. “Flicker filled-in”. In this time period the flickering target was present on-screen but participants indicated that it was invisible, with the dynamic noise appearing in its location through perceptual completion. This condition is physically identical to ‘flicker visible’ but differs in conscious perceptual state.

3. “Flicker absent”. In this time period the flickering target was absent and replaced by dynamic noise. Note that this condition is perceptually identical to ‘flicker filled-in’ but differs in physical stimulation due to the absence (versus presence) of the flickering target. (Fig 3.1B).

Time-periods between ‘flicker-faded’ and ‘flicker filled-in’ button presses were discarded as these were most variable between and within individuals in terms of subjective experience. Furthermore, as the participants improved at the task, the transition between faded and filled-in became increasingly short, so that for most participants, the flickering stimulus disappeared without fading.

3.2.7 Event-Related Fields

For the computation of event-related fields the data were band-pass filtered at 1-45 Hz (Butterworth) and from each time period defined by participant responses, 180ms epochs were extracted from the time series, 50ms prior to the trigger event, when the target changed from black to white and 130ms after the trigger event. Short epochs were used to capture the first trigger-related responses, to avoid loss of signal due to jitter. Extracted data were baseline corrected and downsampled and individual 180ms epochs containing blinks or saccades greater than 2 degrees were discarded. An artefact criterion of ±950 fTesla (n=12) or ±1150 fTesla (n=2) was used to reject trials with excessive EMG or other noise transients. Data were then averaged across trials for the same condition and a grand mean for all participants was calculated for each condition.

3.2.8 3D Source Reconstruction of ERFs

Source reconstruction was performed in SPM5 (Wellcome Department of Imaging Neuroscience, London, UK www.fil.ion.ucl.ac.uk/spm) using a distributed source solution based on a mesh of 3004 vertices derived from each individual participant's structural MRI. Event-related fields were then coregistered into structural MRI space using a landmark-based coregistration based on fiducial position (nasion and left and right pre-auricular). Fiducials in MEG space were matched to the corresponding MRI space using rigid transformation matrices. The same transformation was then applied to the sensor positions. Forward computation was performed using a single sphere

method. Inverse reconstruction of the evoked response used an empirical Bayesian approach (Mattout *et al.*, 2006). The entire time series for each condition was reconstructed. The peak absolute value for each condition in each participant was found and the source estimation for that time-point used in further analyses. Values were normalised to the mean and then converted into voxel space and smoothed with a 12mm FWHM Gaussian kernel. Multiple linear regression was then used to generate parameter estimates for each condition at every voxel for every participant. The resulting parameter estimates for each condition at each voxel were then entered into a second level analysis where each participant served as a random effect in a one-tailed t-test. Appropriate corrections were made for non-sphericity and correlated repeated measures (Friston *et al.*, 2002). For these whole brain analyses, a statistical threshold of $p<0.001$ corrected for multiple comparisons was used.

3.2.9 Steady state analysis

Data were band-pass filtered at 1-45 Hz (Butterworth) and from each of the time periods defined by participant responses, consecutive, non-overlapping 500 ms epochs were extracted from the time series. Each epoch was extracted exactly at one of the trigger events, where the target changed from black to white, to ensure phase-locked averaging (Herrmann, 2001), with epochs starting 100 ms prior to the trigger and lasting until 400 ms after the trigger. As epochs were non-overlapping, not every trigger was used as a start-point to extract data. The first 500ms epoch from every 10 second trial was discarded to remove onset effects and allow build up of steady-state. The extracted data were baseline corrected and downsampled to 100 Hz. Epochs

containing blinks or saccades greater than 2 degrees were discarded. Artefacts were also discarded using thresholds specific for individual participants, as above. These epochs were then averaged across trials for the same condition. Mean number of epochs per condition was 1207 (SEM=91.5) for flicker visible, 1708 (SEM=174) for filled-in and 529.9 (SEM=34.1) for the flicker absent condition. Quantification of the evoked oscillatory activity was performed using a wavelet decomposition of the averaged MEG signal across a 2-45 Hz frequency range, using a complex Morlet wavelet, with a width of 7 cycles (as used elsewhere (Gross *et al.*, 2004;Busch *et al.*, 2004;Jensen *et al.*, 2002).

Prior to statistical testing, the frequency spectra were normalised to the mean of the power at 30 to 45 Hz at the middle 20 ms of each 500 ms epoch (140-160 ms) at each of 58 sensors in a quadrant over the right posterior cortex (Fig 3.4A). As the steady-state phenomenon ran across the whole of each condition, the middle of each epoch was chosen to avoid loss of specificity at the borders of the epochs. All analyses were carried-out on power data, and therefore included no negative values, such that averaging did not result in cancellation of field patterns. Differences between pairs of conditions, for the mean of sensors in the right posterior quadrant (Fig 3.4), were tested for statistical significance using a one-tailed paired Student's t test, with $p<0.05$ indicating significance.

Topographies were produced by linearly interpolating sensor information at 14-16 Hz at the middle 20 ms time point onto sensor space. These were then smoothed using a Gaussian kernel (FWHM 6 mm) and normalised to the mean of the power at 30-45 Hz. The power at 15 Hz was examined. This is double the stimulus frequency of 7.5

Hz, as the fundamental response to patterned stimuli occurs at double the stimulus frequency (Fawcett *et al.*, 2004).

3.2.10 Eye movement recording and analysis

During scanning, eye position and pupil diameter were continually sampled at 60Hz using infrared video-oculography (Iview X Hi Speed Tracking System, Tracksys Ltd, SensoMotoric Instruments). Eye movements were monitored on-line via a video screen for 11 participants. Due to technical reasons eye movement data could not be recorded in 3 of the included participants.

Eye tracking data were analyzed with MATLAB (Mathworks Inc, Sherborn, MA). Epochs with blinks and saccades greater than 2 degrees were removed from the MEG data. Mean rejection rate due to blinks and saccades was 21.2% for flicker visible (SEM=3.95), 19.7% for filled-in (SEM=3.53), and 25.4% for flicker absent conditions (SEM=3.20). Mean eye position, expressed as distance from fixation, was then computed for the residual eye tracking data, for each condition and every participant from whom data were available. A repeated measures ANOVA was used to establish whether mean eye position deviated significantly from fixation or between conditions.

3.3 Results

3.3.1 Behavioural findings

All participants reported reliable filling-in throughout the experiment, and that they were unable to distinguish between periods of perceptual completion where the stimulus was physically present but perceptually filled-in and periods where the stimulus was physically absent. No visual after-effects from the flickering stimulus were reported.

Perceptual completion was reliably experienced in the majority of trials, with at least 1 second of filling-in on 92.6% (SEM=2.29) of trials. Within each trial, perceptual completion occurred with variable latency but the change from beginning to fade, to filled-in completely, was rapid, with mean time from onset of fading to completely filled-in of 0.75s (SEM=0.16). Perceptual completion occurred at a mean latency across participants of 4.0s (SEM=0.23) after trial onset; mean duration of filling-in was 5.0s (SEM=0.39), persisting to the end of the trial on most occasions.

3.3.2 Eye position data

Repeated measures ANOVA showed no significant differences in grand mean eye movement from fixation between conditions for eleven (out of 14) participants for whom eye-tracking data were available ($F(2,20) = 2.56$, $p=0.102$). Thus, fixation was well maintained throughout, consistent with the high proportion of trials on which reliable filling-in was reported.

3.3.3 Event-Related Fields

Figure 3.2B shows the grand mean ERF across all participants from a representative posterior sensor, time-locked to the change in the flickering target from black to white, for each of the three conditions separately. During time-periods where the flickering target was present and consciously perceived, a clear sinusoidal event-related field was identified. When the flickering target was not perceived and when the target was absent, no clear event-related field was seen. This effect was qualitatively present in 12/14 participants in the right posterior sensors, but was not seen in any participants in frontal sensors (where no stimulus-evoked activity would be expected) (Fig 3.2B).

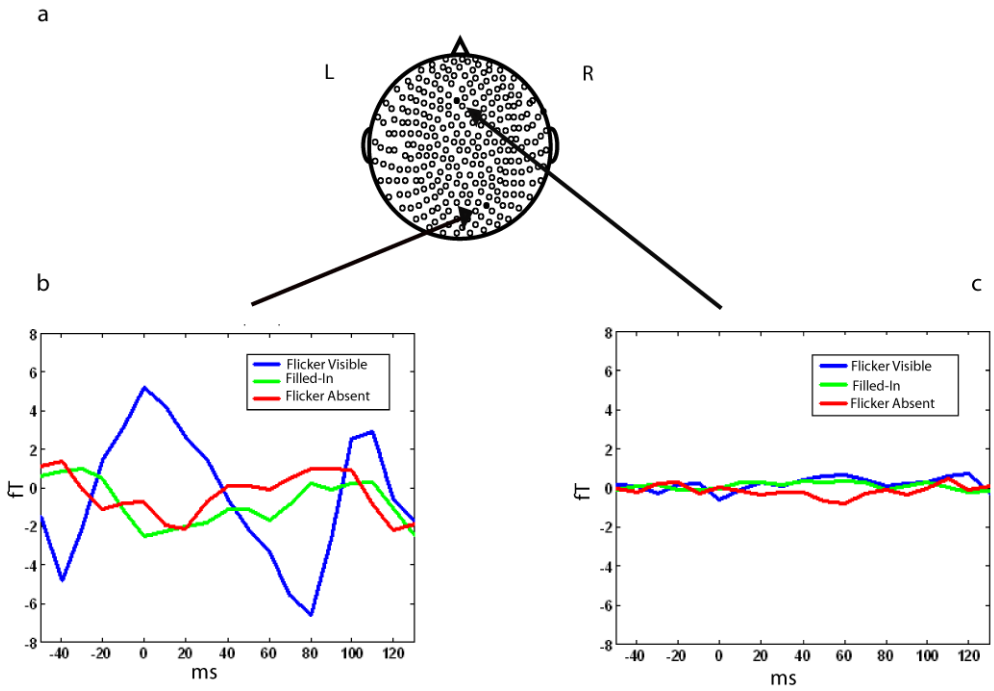

Figure 3.2 (A) Schematic topographic representation of the 275 channels in the MEG array. The locations of the representative sensors MRO22 and MLC11 have been highlighted. (L, Left, R, Right) (B) Grand mean event-related fields time-locked to the change in stimulus for 14 participants recorded at MRO22, which was representative of right posterior channels during epochs when the peripheral flickering target was visible (blue), filled-in (green) and absent (red). Note that a sinusoidal event-related field is seen, which is less prominent when the flickering target was filled-in and absent. (C) Grand mean event-related fields for 14 participants in a representative frontal channel, sensor MLC11, with minimal separation between the event-related fields in the three conditions.

Statistical parametric maps (Figure 3.3) of the reconstructed putative 3D sources (see Methods) of these event-related fields revealed that the most reliable generator (at a threshold of $p<0.001$, corrected) in occipital cortex for flicker visible and filled-in conditions was located in the upper bank of the right calcarine sulcus, consistent with the location of the flickering stimulus in the lower left visual field. In the filled-in conditions, additional generators were also identified in more lateral areas of occipital cortex. Taken together, these findings suggest that signals associated with texture

completion in humans may originate from structures including primary visual cortex. However, caution is required in interpreting these findings due to the very close proximity of the likely retinotopic sources for the stimulus, plus the known extensive inter-subject variability in the spatial extent of retinotopic areas (Dougherty *et al.*, 2003) even after spatial normalisation. Nevertheless, these preliminary findings suggest that investigation of texture completion using a technique with higher spatial resolution such as functional MRI may be promising.

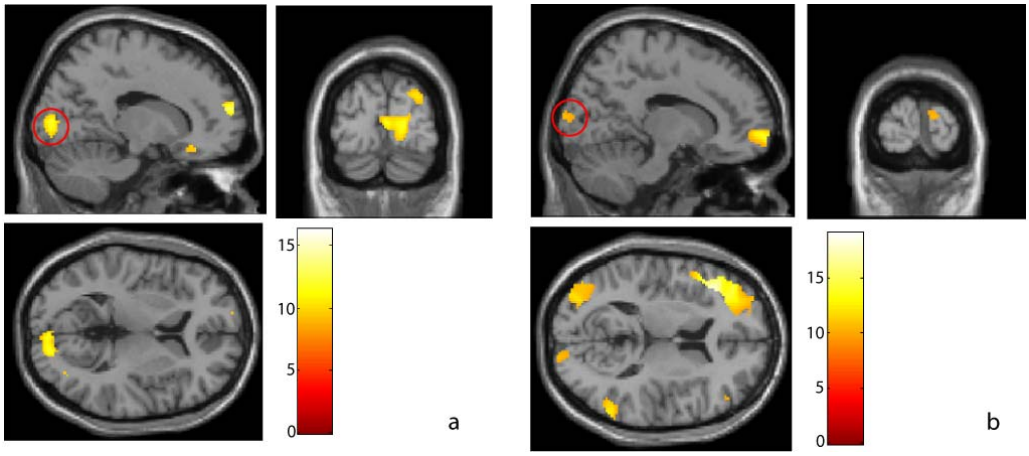

Figure 3.3 Loci whose activity is significantly (P<0.001, corrected for multiple comparisons) associated with the putative generators of the event-related fields measured in flicker visible (a) and filled-in (b) conditions (see Methods for details). Normalised data from all subjects is shown, overlaid on a canonical T1-weighted structural image. The left hemisphere is presented on the left. Colour represents the t-value, as indicated by the scale bar. A statistically reliable source in the upper right calcarine sulcus (within red circle on sagittal view) is identified in both conditions, consistent with a V1 generator associated with the flickering stimulus which was placed in the left lower visual field. In the filled-in condition, additional generators located in more lateral occipital cortex are also apparent. However, caution is required in interpreting these data due to the significant inter-subject variability in retinotopic visual areas (Dougherty *et al.*, 2003) and the close proximity of the likely retinotopic sources associated with the stimulus in V1-V3.

3.3.4 Steady state analysis

Grand mean power spectra of steady-state evoked responses recorded from sensors over right posterior cortex (i.e. contralateral to the field of stimulation; see Methods) for the three conditions are shown in figure 3.4B. An overall 1/f pattern was apparent across all three conditions, as reported previously for steady-state responses to visual flicker (Herrmann, 2001). However, during epochs where the flickering target was clearly visible to the participants, two additional peaks were seen, at 7.5 Hz (the frequency of change in the target from white to black), and at 15 Hz (the frequency of any change, i.e. from white to black and from black to white).

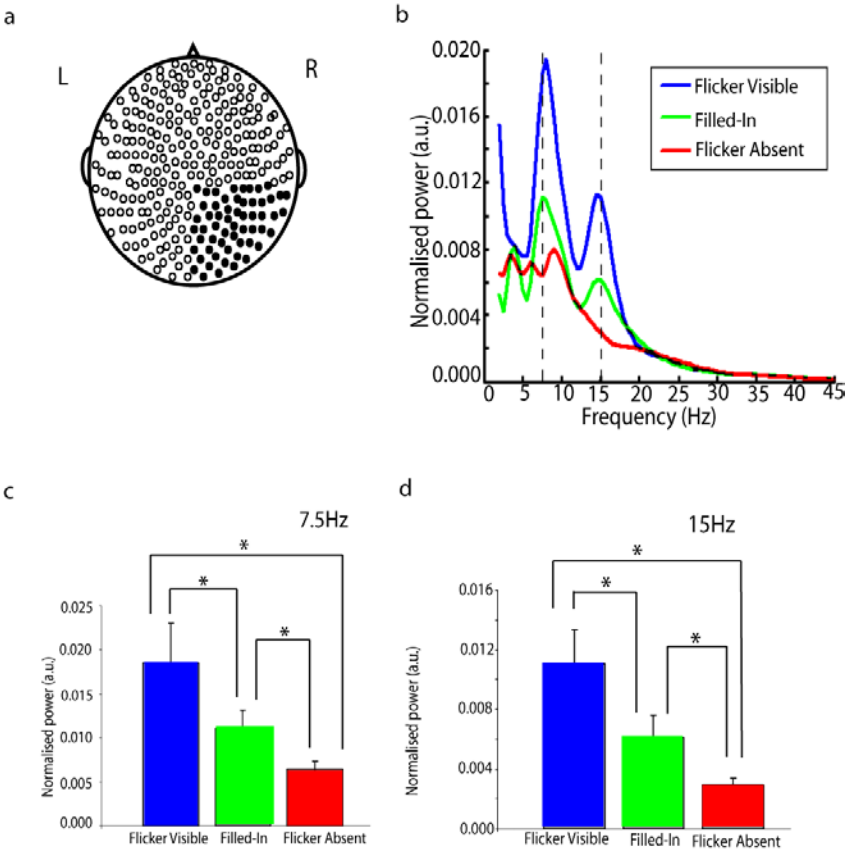

Figure 3.4 (a) Schematic topographic representation of the 275 channels in the MEG array. The locations of the right posterior channels used in further analyses have been highlighted. (b) Mean power-frequency spectra for steady-state evoked responses recorded from all channels in the right posterior quadrant and averaged across 14 participants, during epochs where a peripheral flickering target was visible (blue), filled-in (green) and absent (red). Note the peaks at 7.5Hz and at 15Hz during epochs when the target was visible. (Flickering frequency white to black was 7.5Hz and frequency of any change was 15Hz). A small peak in the alpha range (9-11Hz) is most prominent in the flicker absent condition. Dashed lines indicate 7.5Hz and 15Hz. (c) Normalised power in right posterior sensors at 7.5Hz and at 15Hz (d) compared between flicker visible (blue), filled-in (green) and flicker absent (red) conditions. Data shown are averaged across 14 participants with error bars representing standard error of the mean and the symbol '*' indicating statistical significance in a one-tailed paired t test ($p<0.05$). Normalised power is in arbitrary units.

When the flickering target was physically present but perceptually filled-in by the background, smaller peaks in the power spectrum at 7.5 Hz and 15 Hz were seen

compared to when the stimulus was clearly visible. However when the flickering stimulus was physically removed (but the filled-in background dynamic noise remained visible), these peaks were no longer present. Clearly visible stimuli evoked significantly greater power at stimulation frequencies compared to perceptually filled-in but physically present stimuli ($t(13) = 2.0$, $p=.027$ for 7.5 Hz, one-tailed t test; $t(13) = 2.1$, $p=.035$ for 15 Hz, one-tailed t test). Similarly, when stimuli were physically present but phenomenally filled-in there was significantly greater activity than for the same perceptual appearance but with the stimulus was physically absent ($t(13) = 1.8$, $P=.046$ for 7.5Hz; $t(13) = 2.087$, $P=.029$ for 15Hz).

3.3.4 Topographic displays

Figure 3.5 shows interpolated topographic maps of normalised power at 15 Hz, the frequency of any change in the target, corresponding to epochs where the flickering target was visible, filled-in and physically absent. During epochs where the stimulus was physically present, greatest power was seen in the right posterior quadrant, contralateral to the visual field of stimulation. This is consistent with (but not proof of) the retinotopic specificity of the effects. During epochs when the stimulus was filled-in, the greatest power was still seen in the right posterior quadrant, but the power was reduced compared to epochs where the flickering stimulus was perceived. The topographic map for epochs where the stimulus was physically removed demonstrates low power bilaterally in the posterior cortex. Qualitatively similar maps were apparent for smoothed normalised power at 7.5 Hz. Similar topography across

all conditions suggests that similar neural generators are responsible for the differences in power in the frequency-tagged spectral components identified above.

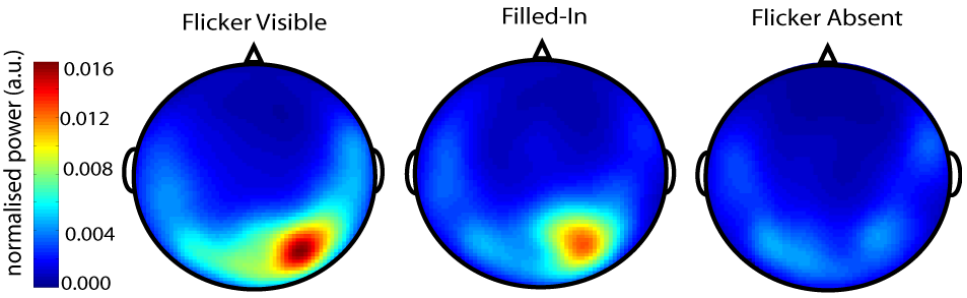

Figure 3.5 Topographic display of smoothed interpolated normalised power at 15Hz at the middle time-point within the epoch averaged across 14 participants. (See Methods). Colour indicates normalised power in arbitrary units. During epochs where the stimulus was physically present (flicker visible), greatest power is seen in the right posterior quadrant, contralateral to the visual field of stimulation. During epochs when the stimulus was filled-in, greatest power is still seen in the right posterior quadrant, but the power is reduced compared to epochs where the flickering stimulus was perceived. Where the stimulus was physically removed, (flicker absent) low power is seen bilaterally in the posterior cortex. Note that with the axial gradiometer MEG system used, these data should not be interpreted as suggesting that the hotspot overlies the area of maximal activity.

3.4 Discussion

The neural correlates of perceptual completion were examined in this study using frequency-tagged MEG to isolate neural representations of a flickering target placed on a dynamic noise background. Power in posterior sensors contralateral to the target was significantly reduced when the flickering target was filled-in, consistent with stronger neural representation in visual cortex for visible compared to perceptually filled-in stimuli. However, the flickering target still evoked neural signals (compared

to a no-stimulus baseline) even when subjectively invisible and filled-in. Note that signals from epochs where the target was gradually fading from awareness were removed from the analyses, so these findings reflect activation associated with epochs when the target was entirely invisible. There was therefore a persistent neural representation of the invisible target. Consistent with previous reports, modulation of stimulus-associated signals by conscious perception was stronger than by physical stimulus characteristics (Ress and Heeger, 2003).

3.4.1 Visual cortex activity is reduced during filling-in in humans

The neural mechanisms of such texture completion in humans have only rarely been studied. Consistent with the findings presented in this chapter, fMRI signals from contralateral V1/V2 are reduced for perceptual completion of small grey targets placed eccentrically on a uniform achromatic background (Mendola *et al.*, 2006). However, such reductions in signal are not confined to the retinotopic location of the target but extend into representations of the background. Due to the point-spread of the haemodynamic response (Disbrow *et al.*, 2000) it remains unclear to what degree these effects are contaminated by signals from the immediate surround, or reflect signals originating from the retinotopic location of the filled-in surface. In contrast, this study overcame this problem by using frequency-tagged MEG. The spatial resolution of MEG is poor compared to fMRI. But because the target flickered at a specific frequency, neural populations responding specifically to the target and not the background could be isolated even *after* filling-in had occurred. It is possible that frequency-specific responses might spread over the cortical surface beyond the

precise retinotopic location of the target; but critically, such responses were specifically associated with the target and not the background.

3.4.2 Neurophysiological studies show increased V2/V3 activity during filling-in

This study examined how the population responses of neurons in visual cortex entrained by the flickering target changed as a function of participants' perceptual reports. In contrast, previous studies in monkey examined perceptual completion in anaesthetised animals that did not report their perceptual state (De Weerd et al., 1995;Gilbert and Wiesel, 1992;DeAngelis et al., 1995). During texture filling-in, neurons in V2/V3 show increased firing over a time course comparable to filling-in reported behaviourally in humans (De Weerd *et al.*, 1995). However, during chromatic filling-in, neurons in V1 with receptive fields at the target borders exhibit reduced firing, while those with receptive fields at the target centre show no change in firing rates (Von der Heydt *et al.*, 2003). Differences between studies may arise from the different visual paradigms used to elicit perceptual completion. Nevertheless, without clear and consistent behavioural reports of whether perceptual filling-in occurred in all these previous studies, it is difficult to draw firm conclusions. In contrast, the present study combined behavioural reports with measures of population activity to show that filling-in is specifically associated with a reduction in activity of neural representations of the filled-in target.

3.4.3 Other types of filling-in cause increased activity in human V1 and V2

The extent to which other types of filling-in share common neural mechanisms with the texture completion investigated in this study remains to be established. In humans, completion of moving gratings across a blank gap (Meng *et al.*, 2005) and filling-in associated with motion induced blindness (Scholvinck and Rees, 2009b) is associated with enhanced activity in the retinotopic location where completion takes place. Unlike the present study, these previous studies did not explicitly 'tag' signals associated with the target that was filled-in. Thus signals associated with perceptual completion in V1 may represent the neural correlates of the perception of the filled-in background, rather than the overwritten target. Furthermore, enhanced activity in those studies may represent neuronal population responses to more salient signals after filling-in (a moving grating compared to a blank target and a moving background compared to a static yellow dot, for each study respectively).

3.4.4 Other invisible stimuli are associated with reduced signal in human visual cortex

The finding of reduced MEG power when a previously visible stimulus became invisible due to filling-in of an artificial scotoma suggests a reduction in the strength of neural representation in visual cortex for invisible (versus visible) stimuli. Consistent with this, frequency-tagged EEG and MEG studies also demonstrate reduced power for stimuli that become invisible during binocular rivalry (LANSING, 1964;Tononi et al., 1998). Moreover, recent fMRI studies consistently find that

signals from human ventral visual cortex are reduced when stimuli are invisible, compared to identical physical stimulation that results in conscious perception (Moutoussis and Zeki, 2002;Haynes and Rees, 2005). Thus, a consistent general feature of the human visual system is of stronger neural activity associated with conscious perception of a stimulus compared to equivalent physical stimulation that remains unconscious (Haynes and Rees, 2006). Moreover, MEG and fMRI studies are consistent, despite the very different aspects of population neural responses recorded by the different techniques. Some studies have also shown that additional areas of parietofrontal cortex are activated when a visual stimulus is consciously perceived (Lumer and Rees, 1999;Vandenberghe et al., 2000;Beck et al., 2001). In the present study, increased power associated with target visibility was restricted to contralateral occipital sensors. However, the frequency tagging approach deliberately isolated signals where neuronal population responses are entrained by the frequency of visual stimulation. Thus it would not be expected to reveal activity associated with perceptual completion in neuronal populations that are not strongly driven by retinal input (Herrmann, 2001), such as those outside occipital cortex.

3.4.5 Persistent representation of invisible stimuli

Target-specific responses were reduced but not eliminated during filling-in. This indicates the presence of a persistent neural representation of a subjectively invisible stimulus. Consistent with this, several fMRI and EEG studies have shown that ventral visual cortex can retain a neural representation of subjectively (and objectively) invisible stimuli (Driver et al., 2001b;Moutoussis and Zeki, 2002;Fang and He,

2005;Haynes and Rees, 2005;Sergent et al., 2005). These findings go beyond this earlier work by extending such observations to the new situation of low-level perceptual completion further confirming that activation in visual cortex is not sufficient for conscious awareness.

3.4.6 Other possible causes of reduced power during filling-in

Filling-in of the flickering stimulus necessarily followed a period when the stimulus was visible. However, these findings of maintained but reduced power following filling-in cannot be due to entrainment of MEG responses when the stimulus was visible persisting into the period of perceptual completion. To rule this out, the first 400ms of data recorded after filling-in or after the physical withdrawal of the target were removed. Findings were unchanged compared to when these data were included in the analysis, suggesting that continued power measured at 7.5Hz during filling-in was not due to entrainment. Furthermore, these findings of reduced power when the stimulus became invisible during filling-in, was in the opposite direction to the recognised increase in power that occurs with visual steady-state responses during the first few seconds of stimulus presentation (Heinrich and Bach, 2001) (Although an adaptation decline does occur, this begins only *after* 10 seconds of stimulation, which is longer than the duration of the entire trial in the current experiment). Such a tendency to increase would in any case be in the opposite direction to the observed reduction in power when the stimulus became invisible due to filling-in.

Eye movements were monitored throughout. Accurate fixation is necessary for filling-in and participants were asked to continually monitor the target location even after disappearance to ensure continued invisibility. Consistent with this, no significant differences were found in eye position or movements comparing the three different perceptual states (target visible, invisible or absent). The angular resolution of the infrared eye tracker was insufficient to rule out the possibility that there were different frequencies of microsaccades in the different perceptual states (Martinez-Conde *et al.*, 2006). However, any such microsaccades will not occur at a precise regular frequency of 7.5Hz or 15Hz, and so can neither account for the finding of decreased power at the specific frequency tagged by the flickering target during filling-in, nor for a persistent frequency-tagged representation of the invisible stimulus.

The frequency-tagging approach isolated signals specifically associated with the target. After filling-in had occurred, participants nevertheless perceived the textured background at the location in the visual field previously occupied by the (now invisible) target. The continuing presence of a target-specific MEG response to this invisible target therefore indicates that a retinotopically specific representation of the target co-exists with a phenomenal percept of a different texture at the same location in the visual field. This may provide some constraints for theoretical or computational accounts of perceptual completion. Specifically, it is not consistent with accounts that posit that the phenomenal experience of perceptual completion is just the brain 'ignoring an absence' (Dennett, 1991). Instead, the findings presented in this chapter are more consistent with filling-in being associated with neural signals that represent a presence rather than ignoring an absence (De Weerd et al., 1998;Spillman and De Weerd, 2003). However, the persistence of the invisible target signal during

perceptual completion suggests that there must be additional brain mechanisms that suppress the target in awareness in favour of the background. These could include feedback connections from higher brain areas reflecting top-down control of this process taking place in early visual cortex. Future research will be needed to specifically examine this possibility.

3.5 Conclusion

This chapter provides evidence that target-specific responses of human contralateral visual cortex are reduced when a target is rendered invisible by perceptual completion. However, even when invisible, target-specific responses remain, demonstrating persistent representation of the now invisible target. The next chapter will use functional MRI and retinotopic mapping to explore in more detail the spatial location of perceptual completion within human visual cortex.

CHAPTER 4: LOCALISING THE PROCESS OF FILLING-IN

4.1 Introduction

The previous chapter demonstrated that target-specific responses in contralateral posterior cortex are reduced when a target is filled-in. However, the low spatial resolution afforded by MEG also raises the possibility that the signals associated with perceptual completion of the artificial scotoma arose from higher visual areas or from broader neural networks entrained by the frequency tagging approach. Evidence was also presented for a persistent target-specific representation of the now invisible target. One central question is whether the perceptual completion of the target with dynamic noise is associated with changes in early retinotopic areas representing the location of the target. In addition it remains unclear whether signals from retinotopic visual cortex continue to represent the invisible target once it has been filled-in by dynamic noise.

This chapter will explore these questions in more detail by examining activity in visual cortex representing the now invisible target using functional MRI and retinotopic mapping.

4.1.1 Evidence for involvement of retinotopic cortex in perceptual completion

Purely behavioural studies show that the latency to report perceptual completion of an artificial scotoma is directly related to the size of the perceptually filled-in target as projected onto visual cortex (De Weerd *et al.*, 1998) and occurs at different times

when more than one target is presented (De Weerd *et al.*, 2006). These findings are consistent with an early retinotopic locus for the process underlying perceptual completion of an artificial scotoma.

Physiological studies do not yet reveal a consistent pattern of neural activity associated with perceptual filling-in of artificial scotomas. In monkey, single neurons in V2 and V3 whose receptive fields overlap an achromatic target placed on dynamic noise increased their firing after a few seconds of eccentric fixation (De Weerd *et al.*, 1995). However, it is not clear whether such changes correspond to perceptual completion as the monkeys did not report their perception. The previous chapter, described how, in humans, frequency-tagged signals measured with magneto-encephalography (MEG) corresponding to a target placed on dynamic noise are reduced but not eliminated in posterior sensors when subjects report perceptual filling-in of the target (Weil *et al.*, 2007). However, due to the low spatial resolution of MEG it is not possible to be certain of the origin of these signals associated with filling-in of the artificial scotoma.

Other forms of perceptual completion that may be related to that seen in artificial scotomas have also been studied, with a similarly mixed picture. In responding monkeys, V1 and V2 boundary neurons show decreased activity during Troxler colour filling-in (Von der Heydt *et al.*, 2003). In humans, luminance filling-in (filling-in of an achromatic target on a uniform achromatic background) is associated with a generalized (non-retinotopic) decrease in activation in V1 and V2, and increased activity in higher visual areas (Mendola *et al.*, 2006). Conversely,

perceptual completion of moving gratings across a blank gap *increases* activity in early visual areas representing the blank gap region (Meng *et al.*, 2005).

It therefore remains unclear whether retinotopic cortex is involved in the perceptual completion of an artificial scotoma and whether early visual cortex continues to represent the invisible target.

To resolve these questions, Blood Oxygenation Level Dependent (BOLD) signals were studied before and after healthy participants had reported filling-in of an artificial scotoma using functional MRI. Inducing reliable perceptual filling-in of an artificial scotoma requires a relatively small and eccentric target (De Weerd *et al.*, 1998) to be surrounded by dynamic white noise, thus introducing particular technical challenges for functional MRI due to the cortical magnification factor and strong responses of visual cortex to dynamic noise. This study used individual retinotopic analyses to examine the modulatory effects of filling-in of an artificial scotoma on early visual areas.

4.2 Methods

4.2.1 Participants

Twelve neurologically normal adults (five females, 19 to 37 years old) with normal or corrected-to-normal vision gave written informed consent to participate in the study, which was approved by the local ethics committee.

4.2.2 Stimuli

Stimuli were identical to those used in the previous chapter for compatibility and consisted of full-field random dynamic achromatic noise (subtending 33x24.8 degrees) with a red central fixation cross (0.2 degrees) on which was superimposed a small square achromatic flickering peripheral target in the lower left visual field (measuring 1.2 x 1.2 degrees at 8.75 degrees eccentricity, 7.5 degrees across and 4.5 degrees down) (Figure 4.1a). The target flickered between black (luminance 0.10 cd/m^2) and white (luminance 13.64 cd/m^2) at a rate of 7.5Hz (8 screen refresh cycles) in order to maximally stimulate voxels within the cortical target representation, and for direct comparability with the previous chapter (Weil *et al.*, 2007). The lower half of the visual field was chosen for placement of the target, as filling-in is more robust for stimuli presented in the lower visual field (Mendola *et al.*, 2006). To generate random dynamic noise, 30 arrays of 200x200 pixels were created, each measuring 0.165 by 0.124 degrees. These were randomly assigned a grey-scale at the start of each trial. These 30 arrays were then presented in a random order at the screen refresh rate (60Hz) to give the appearance of random dynamic noise with a mean luminance of 3.68 cd/m^2. Stimuli were projected using an LCD projector (NEC LT158, refresh rate 60Hz, screen resolution 640x480) onto a circular projection screen at the rear of the scanner. Participants viewed the screen via a mirror positioned within the head coil. All stimuli were presented with MATLAB 6.5.1 (Mathworks Inc.) using the COGENT 2000 toolbox (www.vislab.ucl.ac.uk/Cogent2000/index.html).

4.2.3 Experimental paradigm

On each trial in the main experiment, participants were presented with a screen of dynamic noise for fourteen seconds. After 2.8s a flickering target appeared in the near periphery, on the background of the dynamic noise. Participants were instructed to fixate centrally and report by a series of button presses what happened after the flickering target appeared. One button press indicated the first time the flickering target began to perceptually complete ('1' on the keypad). A different button press was used to report when the target was completely filled-in by the surrounding dynamic noise ('2' on the keypad). A third button indicated whether the target subsequently re-appeared before the end of the trial (for example, after a blink) ('3' on the keypad) (Figure 4.1b). Participants were instructed to be conservative in their responses and only indicate that the target had filled-in when it was definitely no longer visible. It was thus possible to determine behaviourally on a trial-by-trial basis the latency at which perceptual completion first began to occur; the duration over which completion took place; and those trials on which the target re-appeared after initially being completed. For analysis of the imaging data, the sequence of button presses was then used on a trial-by-trial basis to define different time-periods during which the target was physically absent or physically present and either perceived clearly or perceptually completed and invisible.

Each trial lasted 14 seconds and was followed by a 500ms interval during which a grey screen (luminance 3.66 cd/m^2) was presented. As the target had been flickering, there were no stimulus-contingent after-effects. A small red fixation mark was always present centrally. Optimal trial length was determined prior to scanning. In a quarter

of trials the peripheral stimulus was *physically* removed 7 seconds after trial onset, whether the participant was reporting perceptual completion or not (Figure 4.1b). The periods of time after the stimulus had been physically removed were defined as 'target removed' time periods.

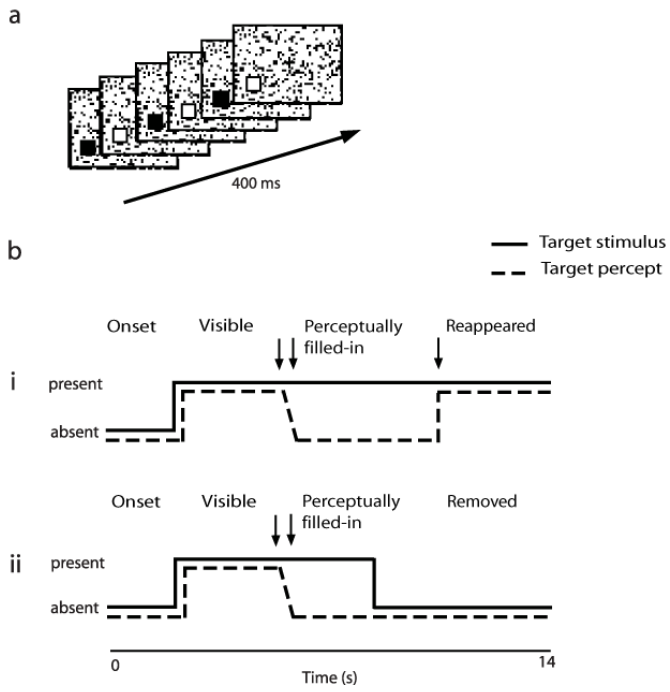

Figure 4.1 (a) Stimulus configuration. Visual stimuli consisted of full-field random dynamic achromatic noise with a flickering achromatic target (when present) placed in the lower left visual field. **(b) Procedure**. (i) Normal trials: During each trial, participants fixated centrally and reported perception of the target using different button presses (indicated here by down arrows). The first button indicated initial fading of the target, the second indicated when the target was completely perceptually filled-in and participants could press a third button if the target reappeared. Time periods were defined as "onset", when the target had not yet appeared; "visible", when the target was present and perceived, prior to any button presses; and "perceptually filled-in", when the target was present but not perceived as it was completely perceptually filled-in. Note that periods between the first and second button press, which represented the time from initial fading of the target to completely perceptually filled-in, were excluded from analysis as they were very short and represented a mix of

different percepts. Also note that the dynamic noise was present throughout the trial. (ii) Catch trials: In 25% of trials, the target was physically removed 7s after the onset of the trial ("removed").

Every participant completed six runs, each comprising 36 trials, and received quantitative feedback at the end of every run as the percentage of trials where they had reported perceptual completion for longer than 1 second. Participants were encouraged to blink during specific rest periods during scanning, but were not told to abstain from blinking during the rest of the experiment. All participants received training prior to scanning, to ensure they could experience perceptual completion of the artificial scotoma and assign consistent button press responses to different perceptual states.

4.2.4 Imaging and preprocessing

A 3T Siemens Allegra system was used to acquire both T2*-weighted echo planar images (EPI) with blood oxygenation level-dependent contrast (BOLD) and T1-weighted anatomical images. Each EPI image comprised thirty-two 3-mm axial slices with an in-plane resolution of 3×3mm. The main experiment was split into six runs, each consisting of 280 volumes. This was followed by three runs to functionally localize the target for subsequent region-of-interest (ROI) analyses. The first five volumes of each run were discarded to allow for T1 equilibration effects. Volumes were acquired continuously with a TR of 2.08 s per volume.

Functional localizer scans were used to independently identify areas in retinotopic visual cortex responding to stimulation of the visual field location of the artificial scotoma in the main experiment. In a separate scanning run, participants fixated

centrally while viewing a square checkerboard the same size and location as the target in the main experiment (1.2 degrees by 1.2 degrees at 8.75 degrees eccentricity, 7.5 degrees across, 4.5 degrees down, in the lower left visual field), with a check size of 0.6 degrees, contrast-reversing at 10Hz on a grey background (luminance 3.66 cd/m^2). The checkerboard stimulus was presented in 10 epochs of 15 s blocks interleaved with 15 s rest periods with no checkerboard displayed. A central red fixation cross was present throughout and participants performed a simple central fixation task to ensure fixation was maintained whereby a button press was required whenever a 0.15 by 0.15 degree square appeared within a quadrant of the fixation cross. The whole localizer experiment comprised 160 volumes (fMRI sequence and parameters were identical to the main experiment).

During scanning, eye position and pupil diameter were continually sampled at 60Hz using long-range infrared video-oculography (ASL 504LRO Eye Tracking System, Mass) to ensure participants maintained fixation. Eye movements were monitored on-line via a video screen for all participants. Eye position was not recorded in five participants for technical reasons.

4.2.5 Data analysis: eye tracking data

Eye tracking data were analyzed with MATLAB 6.5.1 (Mathworks Inc., Sherborn, MA). Blinks and periods of signal loss were removed from the data. Mean eye position, expressed as distance from fixation, was then computed for each condition and every participant from whom data were recorded. A repeated measures ANOVA

was used to establish whether mean eye position deviated significantly from fixation or between conditions.

4.2.6 Data analysis: fMRI preprocessing

Functional imaging data were analyzed using Statistical Parametric Mapping software (SPM2, Wellcome Trust Centre for Imaging Neuroscience, University College London). All image volumes were realigned spatially to the first and resulting image volumes were coregistered to each participant's structural scan. Box-car regressors were then generated that represented the timing and duration of each of the different perceptual states on a trial-by-trial basis, convolved with a synthetic haemodynamic response and mean corrected. Specifically, the button-press responses on each trial from each participant were used to define four distinct regressors:

1. "Onset". This regressor represented activity evoked from the beginning of each fourteen second trial until onset of the target, during which time full-field dynamic luminance noise and the fixation cross were displayed.

2. "Target visible". This regressor represented activity associated with a visible eccentric target i.e. between the times when the target was physically presented (2.8s after trial onset) until the participant reported fading or disappearance by button press.

3. "Target filled-in". This regressor represented any activity associated with the perceptually completed (filled-in) target i.e. between the times of the second

button press (indicating that the participant no longer perceived the target) and (on a trial-by-trial basis) either the third button press (indicating that the target had re-appeared) or physical removal of the target (on a quarter of trials; see above) or the end of the trial. Note that 'target visible' and 'target filled-in' conditions reflect physically identical stimulation (dynamic noise background, flickering eccentric target and fixation cross) but differ only in perceptual state (target either visible or filled-in)

4. "Removed". This regressor represented any activity associated with the dynamic noise background alone on those trials where the target was physically removed after seven seconds, whether the participant was reporting perceptual completion or not. Note that this condition is physically and perceptually similar to "onset". However, it always occurred at the end of the trial and was therefore not associated with any of the onset transients that would be expected at the beginning of the trial immediately after the onset of a full screen of dynamic noise. It is perceptually identical to "target filled-in" but differs in physical stimulation due to the absence of the target.

Periods between the first button press (initial fading) and the second button press (completely filled-in), were excluded from the fMRI analysis as they proved to be short (see Results) and were likely to represent a mixture of different percepts.

In the functional localizer, blocks were defined by the physical presence or absence of the target. Motion parameters defined by the realignment procedure were added to the model as six separate regressors of no interest. Multiple linear regression was

then used to generate parameter estimates for each regressor at every voxel for every participant. Data were high pass filtered (cut-off: 0.0078Hz) to remove low-frequency signal drifts.

4.2.7 Visual area localisation

Retinotopic mapping was essential to accurately delineate the regions within visual areas V1 and V2 which were directly stimulated by the target. This was necessary as the wide inter-subject anatomical variability of early visual areas precludes assignment of activations to visual areas based purely on normalised or averaged coordinates (Dougherty et al., 2003). To identify the boundaries of primary visual cortex, standard retinotopic mapping procedures were used (Sereno *et al.*, 1995;Teo *et al.*, 1997;Wandell *et al.*, 2000). Flashing checkerboard patterns covering either the horizontal or vertical meridian (Figure 4.2ai) were alternated with rest periods for five epochs of 10 volumes over two scanning runs, each lasting 155 volumes. SPM2 was used to generate activation maps for the horizontal and vertical meridians (Figure 4.2aii). Mask volumes for each region of interest were obtained by delineating the borders between visual areas using activation patterns from the meridian localizers. Standard definitions of V1 were followed together with segmentation and cortical flattening using the MrGray software (Teo *et al.*, 1997;Wandell *et al.*, 2000).

The mask volumes for right V1 and V2 were used, in conjunction with the functional localizer images, to identify voxels showing significant activation ($p < .05$ family-wise error corrected) for the comparison of trials where the target localizer was present, compared to rest periods, using the regression analysis described above. This

comparison identifies voxels activated by the peripheral target stimulus in each of the retinotopic areas determined by the independent meridian mapping procedure (Figure 4.2bii). Regions-of-interest in area V3 were only identified in three subjects, as the target was small (1.2 degrees) and eccentrically placed (8.75 degrees), making higher visual areas more difficult to co-localize.

To compare activation in the retinotopic target representation with control regions of retinotopic cortex that did not represent the target, activity was examined from regions of comparable voxel numbers representing comparable eccentricities from left ventral V1 and V2 (which represent the upper right visual quadrant) to produce control ROIs for each participant individually. In addition, activity in a larger control ROI that represented the entire right upper quadrant was also examined (compare with (Sterzer *et al.*, 2006)).

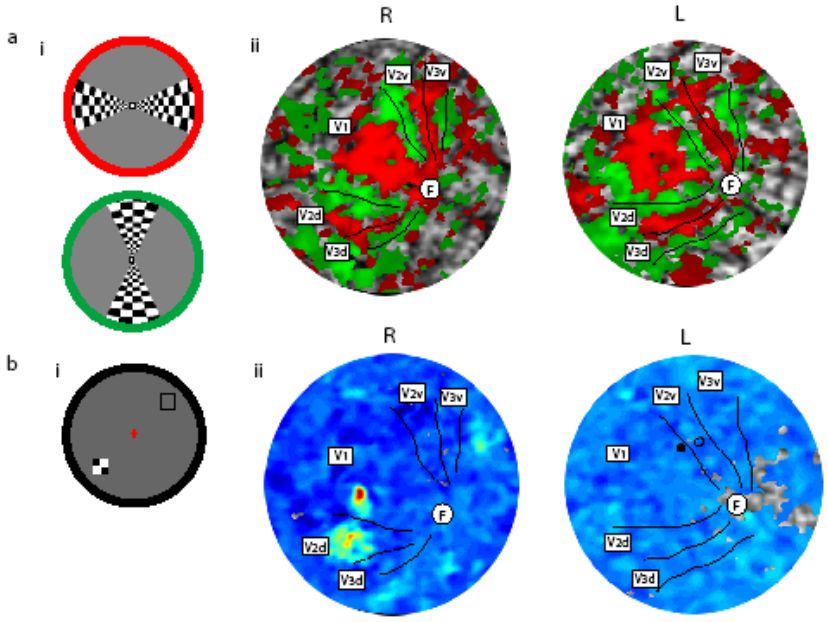

Figure 4.2 Stimulus representation in visual cortex. (ai) Visual stimuli used to map the horizontal and vertical meridians (Methods). (aii) The outline of individual visual areas V1, V2d, V2v, V3d, V3v and the fovea, determined using meridian mapping (see Methods) are shown on the flattened cortex for a representative participant (right and left visual cortex).

(bi) The visual stimulus used to localize the region of interest, with a checkerboard at the region of interest. (Note that the actual visual stimulus may have differed slightly in greyscale value and the checkerboard is not shown to scale). The open square indicates the part of the visual field represented by the control ROIs in V1 and in V2. (bii) Regions of interest (ROIs) in visual cortex representing the spatial location of the target were identified by combining functional localizer images with masks delineated for right V1 and V2 for each participant individually. The spatial distribution of target-specific stimulus-evoked activity (contrast of ROI localizer present versus absent, thresholded at $p<.05$, family-wise error corrected) is shown projected onto a flattened representation of right visual cortex for a representative participant. The spatial distribution of the control ROIs in V1 (closed figure) and in V2 (open figure) are shown projected onto the flattened representation of left visual cortex for the same representative participant.

The final analytic step was to extract from the independently defined target and control regions the regression parameters for each experimental condition arising from the analysis of the main experimental time-series. These were averaged across participants yielding estimates of percentage signal change for each condition averaged across V1 and V2 responding only to the target (target ROIs) or the control ROIs for every participant. In order to determine whether any differences in activity between the conditions were retinotopically specific, activity in the target ROIs was compared with activity in the control ROIs.

The statistical significance of any differences in activation within and between the regions was assessed with a repeated measures ANOVA, with region (target ROI and control ROI) and condition (onset, visible, filled-in, removed) as repeated factors, for V1 and V2 separately, with the Huynh-Feldt correction for non-sphericity where appropriate and post-hoc two-tailed t-tests.

4.3. Results

4.3.1 Behavioural Results

All participants reported reliable perceptual completion of the artificial scotoma throughout the main experiment, and that they were unable to distinguish between periods of perceptual completion where the target was physically present but perceptually filled-in by the dynamic noise backgrounds and those trials where the target was physically removed mid-way through the trial. No visual after-effects from

the flickering target in the main experiment were reported. Participants did not report perceptual filling-in of the functional localizer.

During scanning, perceptual filling-in of the artificial scotoma occurred for at least one second on 90.2% of trials (SEM 2.78%). The mean latency before participants began to report perceptual filling-in was 4.2s after trial onset (SEM 0.33s). After the onset of perceptual completion was reported, full perceptual disappearance occurred rapidly with a mean duration from beginning to fade to completely perceptually filled-in of 1.1s (SEM 0.24s). The mean duration of perceptual filling-in after the participants had reported completion was 5.0s (SEM 0.32s). Long-range infra-red eye tracking confirmed there were no systematic differences in total eye movements during the different perceptual conditions ($F(1.1,6.9)=.59$, $p=.49$, $\varepsilon=.38$).

4.3.2 Functional MRI analysis

Cortical activity specifically associated with the target in V1 and V2 was examined by combining functional localizer images with mask images for V1 and V2 to create target ROIs. The relatively eccentric location of the very small target (necessary to evoke reliable perceptual filling-in) makes such localisation challenging due to the cortical magnification factor, particularly for the smaller retinotopic visual areas. Nevertheless, for V1 and V2 the functional localizer was very effective. Two clear clusters of activation were identified ($p<.05$ family-wise error corrected for multiple comparisons) in all participants and these clusters were located within the mask regions of V1 and V2 (determined using independent retinotopic mapping) (see

Figure 4.2). It was therefore possible to be confident that activity measured within these target ROIs during the main experiment represented cortical activity associated with the target. The mean size of the target ROIs (at the conservative statistical threshold $p<.05$ FWE-corrected) was 3.25 voxels (SEM 0.34 voxels) in V1 and 7.75 voxels (SEM 1.55 voxels) in V2, reflecting the expectation that the target would activate a relatively small volume of cortical tissue. The activity in these target ROIs was compared with activity not directly related to the target in control ROIs. These were similar sizes in voxels to the target ROIs, at equivalent eccentricities but in the opposite hemisphere and responded to a small region in the right upper visual field. This is an area as far as possible from the target and contained dynamic noise at all times during the trial (Figure 4.2) (see Methods). The mean size of the control ROIs in V1 was 4.25 voxels (SEM 0.68 voxels) and 4.83 voxels (SEM 0.54 voxels) in V2.

Due to the very small size (1.12 degree) and eccentricity (8.75 degree) of the target, cortex specific to the target in V3 was only localised in three subjects. It is therefore not possible to draw any meaningful conclusions about the pattern of cortical activity in V3 during perceptual filling-in.

Signals extracted from the target ROIs in the main experiment were compared across each of the periods in every trial and participant reflecting the four experimental conditions (onset, target visible, target perceptually filled-in and target removed). Figure 4.3b shows BOLD signals from the target ROI in V1 and the control ROI in V1 associated with these different time periods A repeated measures ANOVA with the Huynh-Feldt correction for non-sphericity showed a main effect of region (target ROI or control ROI), $F(1,11)=5.0$, $p=.047$, a main effect of condition,

$F(2.2,24.7)=7.0$, $p=.003$, $\varepsilon=.75$ and an interaction of region and condition ($F(2.1,22.7)=6.2$, $p=.007$, $\varepsilon=.69$). These differences were due to a significant decrease in activity in the target ROI when the target became invisible after perceptual completion, ($t(11)=3.5$, $p=.005$). Importantly, activity for the now invisible but physically present target remained significantly elevated in the target ROI compared to time periods when the target was physically removed ($t(11)=6.8$, $p<.0005$). As would be expected, activity in the target ROI was also significantly greater when the target was visible than at the onset of the trial, before the target appeared ($t(11)=2.3$, $p=.040$); and activity in the target ROI was significantly greater during periods when the target was visible, compared to when it was physically removed ($t(11)=5.6$, $p<.0005$).

In the control region in V1v ipsilateral to the target, that represents regions of the visual field distant from the target location (which were stimulated instead by the dynamic noise background throughout), there were no significant differences between activity evoked at onset of the dynamic noise background and when the target was presented ($t(11)=-1.2$, $p=2.5$) nor any significant differences between the physically different but perceptually identical conditions of target perceptually filled-in and target removed ($t(11)=1.7$, $p=.12$). These findings indicate that physical presentation of the target evoked responses in the target ROI but not the control region, consistent with the known retinotopy of these structures and the functional localiser. However, it is interesting to note that in the control ROI, which was not stimulated by the target, there was a small but significant reduction in activity comparing periods in the trial where the target was present but subjects were not reporting perceptual completion and after the target was reported as perceptually complete and now invisible

($t(11)=2.8$, $p=.02$). On inspection this appeared to represent a more general suppression of signals during perceptual completion in regions not stimulated by the target (Figure 4.3b). There was also reduced activity in the control ROI after the target was removed compared to periods when the target had been visible ($t(11)=3.0$, $p=.013$), which may reflect suppression from the already completed target continuing when the target was removed. These findings are consistent with the notion that perceptual completion of the artificial scotoma might be associated to some extent with signals in V1 that were not completely restricted to the retinotopic target representation.

On pairwise comparisons, there were no significant differences in activity in target and control ROIs ($t(11)=1.6$, $p=.14$) evoked at onset of the dynamic noise background, nor in the periods when the target was physically removed ($t(11)=1.2$, $p=.25$). However, the activity evoked during trial periods when the target was visible differed significantly between target and control ROIs ($t(11)=3.1$, $p=.010$) as did the activity following reported perceptual completion in the target and control ROIs ($t(11)=2.5$, $p=.030$), thus confirming retinotopic specificity of these differential responses to the retinotopic representation of the target location in V1.

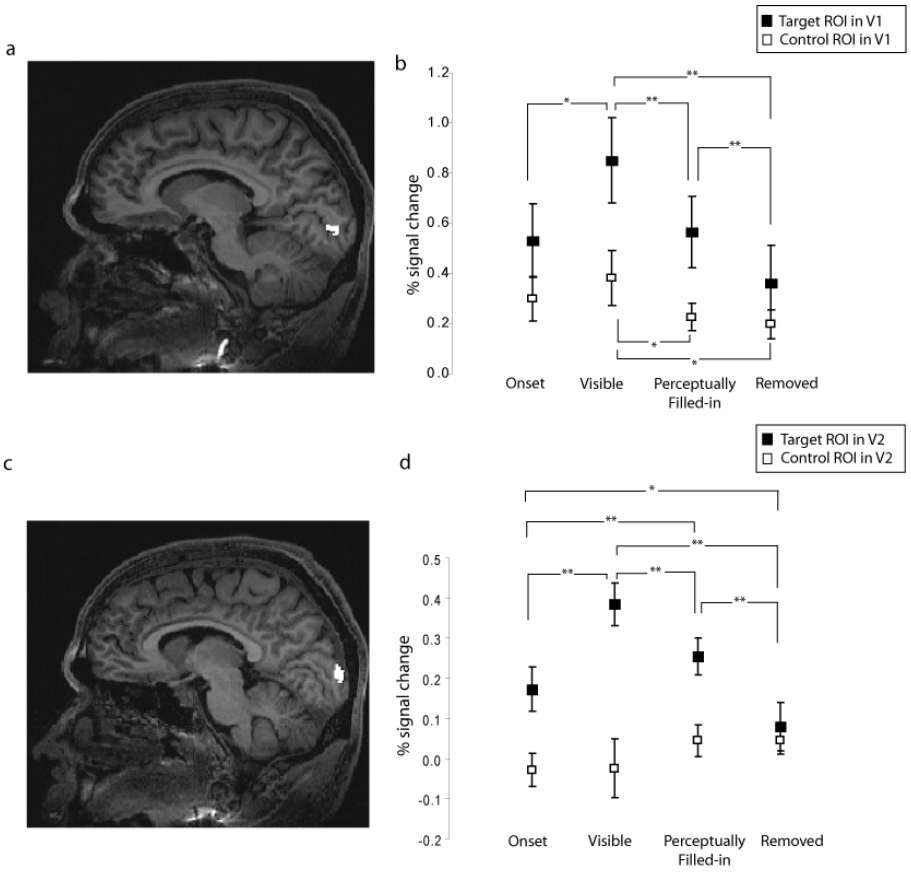

Figure 4.3 (a,b) Region-of-interest (ROI) in V1. (a) Voxels responding to the target within V1 (target ROI in V1), defined using the functional localizer, are displayed for a representative participant on a sagittal section of a T1-weighted structural image. The location of the target ROI in the upper bank of the right calcarine sulcus (corresponding to its location in the left lower visual field) is apparent. (b) BOLD signal change (percent relative to the global mean) averaged across all twelve participants (error bars = one SEM) in the target ROI within right V1 (closed squares) and for the equivalent sized control ROI in left V1 (open squares) plotted separately for each condition (onset; visible; perceptually filled-in; removed; see Methods and Figure 4.1 for definitions). Note that activity in the V1 target ROI decreased during perceptual filling-in, but that activity remained elevated compared to the baseline condition, when no target was present. In contrast, in the control ROI there was also a small but significant reduction in activity during perceptual completion but no further reduction in signal change when the target was physically absent. The symbol '**' indicates statistical significance ($p<.005$, 2-tailed t test) and the symbol '*' indicates statistical significance ($p<.05$, 2-tailed t test).

(c,d) Region-of-interest (ROI) in V2. (c) Voxels responding to the target within V2 (target ROI in V2), defined using the functional localizer, are displayed for a representative participant overlaid on a sagittal section of a T1-weighted structural image. (d) BOLD signal change (percent relative to the global mean) averaged across all twelve participants (error bars = one SEM) for each condition within the target ROI in right V2 (closed squares) and the equivalent sized control ROI in left V2v (open squares). The overall pattern of activity in the V2 target ROIs was similar to the V1 ROIs, with a significant decrease in activation when the participants reported perceptual completion of the target, compared to when they reported that the target was visible and a further decrease when the target was physically removed. In the control ROI however, there were no significant differences between the conditions. The symbol '**' indicates statistical significance ($p<.005$, 2-tailed t test) and the symbol '*' indicates statistical significance ($p<.05$, 2-tailed t test).

As a further control, activity in the whole of V1v ipsilateral to the target was also examined. This region responds to activity in the upper right quadrant, an area only stimulated by dynamic noise and not the target. Results were qualitatively unchanged compared to the smaller control ROI. A repeated measures ANOVA with the Huynh-Feldt correction for non-sphericity showed a main effect of region (target ROI or whole V1v), $F(1,11)=9.7$, $p=.010$, a main effect of condition, $F(2.2,23.8)=5.1$, $p=.012$, $\varepsilon=.72$ and an interaction of region and condition ($F(2.1,22.7)=14.3$, $p<.0005$, $\varepsilon=.68$). As for the smaller control ROI, a significant reduction in activity was also found when the target was reported as perceptually completed compared to when it was visible ($t(11)=2.2$, $p=.048$), despite the fact that the target was presented in the lower left quadrant, a region not represented by left V1v (Figure 4.4a).

Pairwise comparison showed no significant differences between activity evoked after the target was removed, comparing the target ROI in V1 and the whole of left V1v ($t(11)=1.3$, $p=.21$), but the levels of activity evoked by the onset periods, the target

visible and perceptually filled-in conditions were all greater in the target ROI ($t(11)=2.3$, $p=.041$, $t(11)=4.7$, $p=.001$, $t(11)=3.2$, $p=.008$).

Figure 4.3b shows BOLD signals in V2 associated with perceptual filling-in of the artificial scotoma. A repeated measures ANOVA with the Huynh-Feldt correction for non-sphericity showed a main effect of region (target ROI or control ROI), $F(1,11)=8.3$, $p=.015$, a main effect of condition (onset, target visible and target perceptually filled-in and target removed), $F(2.2,24.2)=5.3$, $p=.011$, $\varepsilon=.73$) and an interaction of region and condition ($F(3,33)=22.5$, $p<.0005$). As in V1, these differences were due to a significant decrease in activity in the target ROI when the target was perceptually filled-in ($t(11)=4.09$, $p=.002$); but activity evoked when the target was perceptually completed remained significantly elevated compared to when it was physically removed ($t(11)=6.4$, $p<.0005$). There was also significantly greater activity in the target ROI when the target was visible compared to when it was removed ($t(11)=8.8$, $p<.0005$), and compared to the onset periods, before the target had been presented ($t(11)=5.0$, $p<.0005$). In the target ROI in V2, there was also greater activity after perceptual completion had occurred compared to periods before the target had been presented ($t(11)=3.6$, $p=.004$) and activity was greater during the onset periods than after the target had been removed ($t(11)=2.9$, $p=.016$).

In V2, these changes were clearly restricted to the retinotopic location of the target, as responses of retinotopic regions of V2 that did not represent the target (control ROI in V2v) showed no significant differences between periods when the target was visible and after perceptual completion ($t(11)=1.3$, $p=.23$,) or between any other conditions. (Onset and visible: $t(11)=.067$, $p=.95$; onset and perceptually filled-in: $t(11)=2.1$,

p=.064; onset and removed: t(11)=1.8, p=.097; visible and removed: t(11)=1.2, p=.27, perceptually filled-in and removed: t(11)=.07, p=.95).

Furthermore, when the same conditions were compared between the two regions (target ROI in V2 compared to control ROI in V2v), there was no significant difference between the regions after the target was removed (t(11)=-.42, p=.68,) but there was a significant difference between the regions when the target was visible (t(11)=4.6, p=.001,) and when it was perceptually filled-in (t(11)=2.9, p=.015,). There was also a significant difference between the two regions before the target was presented (t(11)=2.6, p=.026).

Activity was also examined in the whole of left V2v compared to the target ROI in V2 (Figure 4.4b). A repeated measures ANOVA with the Huynh-Feldt correction for non-sphericity showed a main effect of region (target ROI or whole V2v), $F(1,11)=7.0$, $p=.023$, a main effect of condition, $F(2.2,23.8)=7.6$, $p=.002$, $\varepsilon=.73$ and an interaction of region and condition ($F(3,33)=43.0$, $p<.0005$). As in the small control ROI in V2v, no significant differences in activity were found in V2v between any of the conditions.

Pairwise comparison showed no significant difference between the target ROI in V2 and the whole of left V2v before the target was presented (onset) (t(11)=.89, p=.39) or after the target was removed (t(11)=1.0, p=.32), but the activity evoked by the target visible and perceptually filled-in conditions was greater in the target ROI (t(11)=5.2, p<.0005, t(11)=4.4, p=.001).

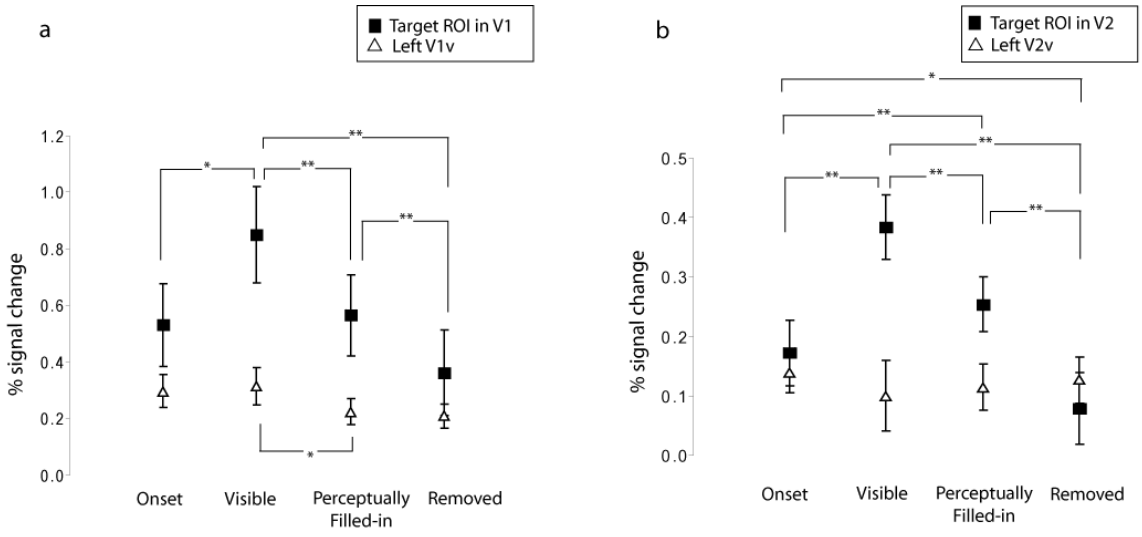

Figure 4.4 (a) Region of interest in V1 compared to whole left V1v. BOLD signal change (percent relative to the global mean) averaged across all twelve participants (error bars = one SEM) in the target ROI within right V1 (closed squares) and for the whole of left V1v ipsilateral to the target as a control ROI (open triangles) plotted separately for each condition (onset; visible; perceptually filled-in; removed; see Methods and Figure 4.1 for definitions). Note that activity in the target V1 ROI decreased when participants reported perceptual completion, but that activity remained elevated compared to the baseline condition, when no target was present. In contrast, in the whole of left V1v there was also a small but significant reduction in activity when participants reported perceptual completion but no further reduction in signal change when the target was physically absent. The symbol '**' indicates statistical significance ($p<.005$, 2-tailed t test) and the symbol '*' indicates statistical significance ($p<.05$, 2-tailed t test).

(b) Region of interest in V2 compared to whole left V2v. BOLD signal change (percent relative to the global mean) averaged across all twelve participants (error bars = one SEM) for each condition within the target ROI in right V2 (closed squares) and the whole of left V2v (open triangles). The overall pattern of activity in the V2 ROIs was similar to the V1 ROIs, with a significant decrease in activation when participants reported perceptual completion of the target, compared to when the target was visible and a further decrease when the target was physically removed. In the whole of V2v however, there were no significant differences between the conditions. The symbol '**' indicates

statistical significance ($p<.005$, 2-tailed t test) and the symbol '*' indicates statistical significance ($p<.05$, 2-tailed t test).

4.4 Discussion

The major finding in this study was that the behavioural report of perceptual completion of an artificial scotoma in humans was accompanied by reductions in BOLD signals representing the perceptually filled-in target in V1 and V2. In V1 (but not V2), regions of cortex distant from the target representation also showed subtle reductions in signal correlated with perceptual completion of the target, but these were significantly smaller than the reductions identified in the cortical locations corresponding to the target representation. The reductions in activity associated with perceptual completion of the target representation were not complete, as even after perceptual filling-in had occurred and the target was invisible, BOLD signals in the target representation remained elevated compared to when the target was physically removed. This is consistent with a persistent neural representation of the now invisible target in both V1 and V2.

4.4.1 Perceptual completion of an artificial scotoma is associated with reductions in BOLD signals

Perceptual filling-in of the target necessarily followed a period when the stimulus was visible. This raises the possibility that the decrease in signal observed comparing the visible and invisible (perceptually completed) target reflects a generalised decrease in V1 and V2 signals over time, or saturation of the BOLD signal evoked by the

dynamic noise background that attenuates over time. However, several aspects of these data make such a possibility unlikely. First, the decrease in signal which was observed was much greater for the cortical representation of the target compared to control ROIs (which represented regions stimulated by the dynamic random noise), and so cannot reflect a generalised adaptation of BOLD signals. Second, the BOLD signal within the target representation at the onset of each trial was lower than when the target was visible in both V1 ROI and V2 ROI. Thus the procedure can detect the small differences in retinotopic activity elicited by presentation of a small target on top of a dynamic noise background, and signals were not saturated by the dynamic noise background. Finally, a significant reduction in activity was observed during periods of trials when the target was physically removed compared to when the target was perceptually filled-in. This could not reflect a generalised adaptation over time during the experiment itself as the periods when the target was removed (during 'catch' trials, comprising 25% of the total trials) occurred at the same time periods during the trial as the periods when perceptual filling-in typically occurred. Taken together, these findings suggest that the differences in BOLD signal between conditions reflect changes in cortical activity rather than saturation or adaptation effects on haemodynamic responses.

4.4.2 Filled-in targets are associated with activity which is elevated compared to a no-target baseline

These data demonstrate that in regions responding to the target, activity was reduced during perceptual filling-in but remained elevated compared to periods when the target was physically removed. This finding of persistent elevation (relative to

physical absence of the target) after perceptual completion cannot be an artefact of averaging signals from trials with variable latency or duration of perceptual completion for several reasons. Although individual experiences of perceptual completion can be gradual and of variable latency, both latency and duration of perceptual completion were determined on a trial-by-trial basis for each participant by examining their multiple button press responses (see Methods). The construction of the regressors on a trial-by-trial basis ensured that only time-periods when the target was reported by participants as completely invisible were reported in this particular contrast. Periods of gradual fading were therefore excluded from the analysis and only the states before fading had commenced ('target visible') and after the target had become completely invisible ('target perceptually filled-in') were examined. In addition, participants were instructed to be conservative in their reports and only report perceptual completion when they were sure that the target was invisible.

4.4.3 Considering differences in activity in the control ROI in V1

In the control ROI in V1v, a region that responds to the upper right visual field where no target was presented there were no significant differences in activity between periods prior to the target being presented and during periods when the target was visible, consistent with the retinotopic organisation of V1. However, small but nevertheless significant reductions in activity were identified comparing periods before and after perceptual completion of the target had occurred. These differences were significantly smaller than in the target ROI, indicating a degree of retinotopic selectivity but not as complete as in V2. Interestingly, a significant reduction in

activity was also found in the control ROI in V1 when the target was physically removed compared to when it was visible. In a region whose retinotopy reflects regions of the visual field stimulated only by the dynamic background it might be expected that these two time-periods show comparable levels of activity. However, it should be noted that the target was physically removed at times during the trial when participants had typically already reported perceptual filling-in, so these time periods after the target was physically removed do not represent a true baseline, as any neural activity associated with the perceptual experience of filling-in may still be ongoing, and it might be expected that the reductions in activity seen during periods of perceptual completion would continue to be seen during these periods after the target is physically removed.

4.4.3 Possible mechanisms

One very influential model for underlying neural filling-in mechanisms associated with perceptual completion (Gerrits and Vendrik, 1970;Grossberg and Mingolla, 1985;Neumann et al., 2001;Grossberg and Hong, 2006) is that lateral spreading which causes neural filling-in of surfaces in normal vision, is inhibited by the boundaries of an image. This theory has been further developed on the basis of behavioural (De Weerd *et al.*, 1998) and single neuron studies in monkey (De Weerd *et al.*, 1995) as a possible neural mechanism underlying the perceptual completion of an artificial scotoma. The proposed neural model consists of two stages: a slow period during which figure-ground segregation fails due to adaptation of neurons responding to the boundary between target and background. This is followed by a faster process of

feature spreading. Note that such a model is purely neural and makes no specific predictions about how these neural phenomena are related to the phenomenal experience of perceptual completion. In the present study, the relatively low spatial resolution of fMRI means that it is not possible to unambiguously disentangle the potential contribution of these two hypothesised neural processes to the observed signal changes or the perceptual experience of completion reported by the participants. One possibility is that the target-specific reductions in activity observed in V1 and V2 during perceptual completion reflect specific inhibitory processes suppressing the target boundary. Such processes usually keep a uniform region segregated from the surrounding texture. This hypothesis would also be consistent with the increases in firing in some neurons associated with texture filling-in observed in monkey (De Weerd *et al.*, 1995) as BOLD contrast fMRI primarily reflects synaptic activity within a cortical area rather than spiking activity per se (Viswanathan and Freeman, 2007). The weaker non-retinotopic decreases in BOLD activity observed in V1, that have also been identified in a previous human fMRI study of luminance filling-in (Mendola *et al.*, 2006), may reflect the more general process of feature spreading that allows perceptual filling-in to occur. However, not all evidence is consistent with a two-stage theory of slow border adaptation followed by a rapid neural filling-in. For example, changing properties of the border between target and background by increasing spatial blur and stereoscopic disparity does not affect the latency at which human observers report perceptual completion of the target (Welchman and Harris, 2003). This is somewhat inconsistent with the notion that border adaptation must occur prior to perceptual completion of an artificial scotoma, although it is possible that such findings depend on the eccentricity of the target and indeed for other types of stimuli, changes in border contrast do influence time before

perceptual completion is reported (Sturzel and Spillmann, 2001). Further research is therefore required to establish both the nature of the neural processes underlying subjective reports of perceptual completion and their relationship to the retinotopic reductions in population-specific responses that have been observed here.

4.4.4 Comparison with previous studies

This study necessarily conflates (due to the relatively low spatial resolution of fMRI) the neural correlates of the flickering target and the background noise, which after perceptual filling-in has been reported appears to occupy the same location in visual space. Thus there are two distinct phenomenal aspects of completion taking place in the same location of the visual field; the disappearance of the target (although it remains physically present) and the appearance of the background (although it remains physically absent). In the previous chapter (chapter 3) (Weil *et al.*, 2007), MEG was used with an identical stimulus to isolate signals evoked by the target during perceptual completion by measuring signals at the frequency of the flickering target before and after perceptual completion. Such frequency 'tagged' signals were reduced but not eliminated in contralateral posterior sensors after perceptual filling-in, consistent with a locus for perceptual completion in visual cortex and a persistent representation of the invisible target. However the relatively low spatial resolution of MEG meant that it was not possible to determine the precise locus in visual cortex. Although BOLD contrast fMRI is an indirect measure of neuronal activity and reflects the activity across neuronal populations, the findings in this study converge strikingly with these previous results to unambiguously demonstrate that changes in neuronal

population signals associated with reported perceptual completion of an artificial scotoma can be identified in retinotopic representations of the target in V1 and V2. Importantly, the two studies show qualitatively the same pattern of findings despite employing two different methods of measuring neuronal population activity, MEG and fMRI. More research is needed to clarify the neuronal processes associated with the perceptual experience of filling-in and the role of individual components such as feature spread from the background and disappearance of the target.

These findings concerning perceptual completion of an artificial scotoma with dynamic luminance noise are broadly consistent with a recent fMRI study in humans of luminance filling-in with static homogenous backgrounds (Mendola *et al.*, 2006). In that earlier study, periods of perceptual invisibility were associated with reductions in activity in early visual cortex. However, the decreases in activity associated with luminance filling-in measured in that earlier study were not restricted to the target location and extended throughout V1 and V2 including to regions not stimulated by the luminance target. In contrast, the present study provides evidence that changes in activity after perceptual completion were retinotopically specific to the target representation in V1 and V2, but in addition V1 shows a weak general, non-retinotopic reduction in activity associated with perceptual filling-in. Furthermore, the data presented in this study go beyond this earlier work by showing that although activity in the target representation in V1 and V2 is reduced after it becomes invisible, activity remains elevated compared to when the target is physically removed. This indicates that a representation of the now invisible target persists in human V1 and V2, consistent with the previous observations using MEG (Chapter 3) (Weil et al 2007). Such an invisible representation is also consistent with the behavioural finding

that perceptually filled-in targets can nevertheless influence behaviour (Ramachandran and Gregory, 1991;Meng et al., 2005) and with the observation from very different paradigms that V1 can represent properties of invisible stimuli (Haynes and Rees, 2005;Kamitani and Tong, 2005). More generally, the broad consistency of these findings with earlier studies using different stimuli to elicit behavioural reports of perceptual completion suggest that a common mechanism may underlie the variety of target and background textures and artificial scotoma configurations that can elicit very similar perceptual experiences (Ramachandran & Gregory, 1991) but this will require further investigation.

4.5 Conclusion

These findings indicate that the earliest cortical stages of the human visual pathways show signals correlated with behavioural reports of perceptual completion of artificial scotomas. This suggests that the neural basis for such perceptual completion reflects a process manifest in signals from early visual cortex. Moreover, the persistent signal associated with the perceptually filled-in and now invisible target demonstrates the continued representation of this invisible target in early visual cortex. An important and unresolved issue is whether higher cognitive functions can influence this low-level process of perceptual filling-in. I will now turn to the second goal of this thesis, exploring the top-down influences on perception, starting by examining the top-down influences of perceptual filling-in.

CHAPTER 5: EFFECTS OF HIGHER COGNITIVE FUNCTIONS ON PERCEPTUAL FILLING-IN OF AN ARTIFICIAL SCOTOMA

5.1 Introduction

The previous two chapters (chapters 3 and 4) have explored the neural correlates of perceptual filling-in of an artificial scotoma. In particular, they have focused on activity in early visual cortex whilst such a stimulus is seemingly filled-in by a dynamic background, providing evidence for a low-level account of this phenomenon driven primarily by bottom-up sensory factors.

However, it has recently become apparent that directing spatial attention (a 'top-down' signal) to the target, can increase the probability that filling-in will occur (De Weerd et al., 2006). This provides some preliminary evidence that filling-in represents an interplay between top-down and bottom-up factors. Moreover, such evidence favours theoretical accounts of filling-in that propose it is an active process, rather than accounts that claim that filling-in merely reflects passive ignoring of information that is no longer represented in the brain (Dennett, 1991). Furthermore, if filling-in is an active process and affected by top-down signals, then manipulations of those signals by different tasks might affect filling-in differently, but whether this is the case is not yet known.

In this chapter, the influences of two contrasting manipulations of top-down signals on concurrent perception of an artificial scotoma were explored. Either perceptual or

working memory load were independently manipulated to examine how these affected the probability and onset of filling-in of a peripheral artificial scotoma. Similar load manipulations have been used to investigate processing of task-irrelevant stimuli using perceptual load (Rees et al., 1997;Bahrami et al., 2008;Schwartz et al., 2005) and working memory load manipulations (de Fockert et al., 2001;Lavie et al., 2004;Dalton et al., 2009) allowing specific predictions to be formed of the effects of these manipulations on the process of perceptual filling-in.

5.1.1 Lavie's load theory of selective attention applied to the process of perceptual filling-in

Lavie's load theory of selective attention and cognitive control (Lavie, 2005;Lavie et al., 2004) proposes that increasing the load of a perceptual task will consume capacity, thereby reducing resources dedicated to processing stimuli irrelevant to that task. Increasing perceptual load is operationally defined as either increasing the number of items that must be processed in the same task or, for the same number of items, making the perceptual task more demanding by increasing the number of stimulus features that must be processed (Lavie and de Fockert, 2003); within this theoretical framework, the terms perceptual load and attentional load are used interchangeably (see for example (Bahrami et al., 2007;Bahrami et al., 2008)). Indeed, both behavioural (Lavie and de Fockert, 2003;Bahrami et al., 2008) and neuroimaging (Schwartz et al., 2005;Bahrami et al., 2007) studies have consistently shown that increasing perceptual load reduces processing of stimuli outside the focus of attention.

If perceptual filling-in of artificial scotomas is an active process requiring attentional resources, then reducing the availability of such resources for processing both the target and background, by increasing the perceptual load of a concurrent task at fixation, should lead to a lower probability of filling-in and a delay in its onset. If, on the other hand, perceptual filling-in is a form of passive ignoring, as previously suggested (Dennett, 1991), opposite effects on these measures should be expected, because a reduction in attentional resources should make it easier to ignore missing information.

To compare the effects of two different types of top-down signal, working memory load was also manipulated while examining perceptual filling-in of an artificial scotoma (see also (Macdonald and Lavie, 2008)). Importantly, by comparing how perceptual filling-in varied in association with two different concurrent tasks, any general effects of performing a concurrent task per se on perceptual filling-in was controlled for. Load theory proposes that increasing working memory load can have the opposite effect to that of increasing perceptual load in tasks where certain stimuli must be attended while others are ignored, because working memory is part of the executive control mechanism prioritizing stimulus processing. Hence, exhausting the capacity of working memory reduces the ability to maintain prioritization of current behavioural goals, leading to more processing of irrelevant distractors (Lavie et al., 2004;de Fockert et al., 2004;de Fockert et al., 2001). However, in the paradigm used in this study there were no distractors, only a primary task of working memory and a secondary task of monitoring perceptual filling-in of a figure placed on a background. It was hypothesized that in perceptual filling-in, the background may play an analogous role to a distractor; in such a case, increasing working memory load may

impair the relative processing priorities of the target and background, increasing the salience of the background and affecting perception in the same way as for distractor processing, thus shortening the latency and increasing the probability of perceptual filling-in. Alternatively, if without distractors, working memory served only to consume resources and divert attention away from the perceptual filling-in task, working memory load would, like perceptual load, delay and reduce the probability of perceptual filling-in.

5.2 Methods

5.2.1 Participants

Twelve volunteers participated in experiment 1 (mean age 27.8 years, range 19-37 years, 5 female, 10 right handed) and ten participated in experiment 2 (mean age 26.6 years, range 21-32 years, 4 female, 10 right handed). All had normal or corrected-to-normal vision and gave written informed consent to participate in the study, which was approved by the local ethics committee.

5.2.2 Stimuli

Visual stimuli were presented on a gamma-calibrated CRT display (21" Sony GDM-F520; 800x600 resolution; 60 Hz refresh rate), placed in a darkened room, with participants wearing headphones for experiment 2. Participants' heads were

supported by a chin rest to ensure a fixed viewing distance of 57cm. Stimulus display and response collection were controlled by Matlab 6.5.1 (Mathworks Inc.) using the COGENT 2000 toolbox (www.vislab.ucl.ac.uk/Cogent2000/index.html). Stimuli consisted of full-field random dynamic achromatic noise (subtending 33º x 25º; mean luminance of 23.3cd/m^2) and a flickering peripheral target. To generate random dynamic noise, 30 arrays of 200x200 pixels were created, each measuring 0.165º x 0.124º with a grey-scale randomly assigned at the start of each run. The 30 arrays were then presented in a random order at the screen refresh rate (60Hz). The target figure was a small flickering achromatic square (1.12º x 1.12º) superimposed on the background in the lower left visual field at 9.43º eccentricity (8º across, 5º down) flickering between black (luminance 0.51cd/m^2) and white (luminance 80.9cd/m^2) at a rate of 7.5Hz (8 screen refresh cycles per presentation). The lower half of the visual field was chosen for placement of the target figure, as perceptual filling-in is more robust in the lower visual field (Mendola et al., 2006). The figure was flickered to avoid stimulus-contingent after-effects.

5.2.3 Perceptual filling-in procedure

On each trial, participants were presented with a screen of dynamic noise. After 3s, a flickering target figure appeared in the near periphery, on the background of the dynamic noise. Participants were instructed to fixate centrally (see specific instructions for each experiment below) and to indicate the appearance of the peripheral figure using three different keyboard buttons on the standard PC keyboard. When the figure first appeared they were required to press one button ('1' on the

keypad). If the figure disappeared (through perceptual filling-in) then participants were required to press a second button ('2' on the keypad). Participants indicated any re-appearance of the figure by a third button-press ('3' on the keypad). These button presses were used to define the latency of perceptual filling-in (time until perceptual filling-in) and the reaction times to the appearance of the target at the beginning of each trial. The probability of perceptual filling-in was defined as the proportion of trials during which the figure was perceptually filled-in for at least 1000 ms (until reappearance of the figure or the end of the trial). Participants were encouraged to be conservative in their responses and only report perceptual filling-in once the figure had completely disappeared.

Trials lasted 15 seconds and were followed by a 500ms interval during which a grey screen (luminance 21.8cd/m^2) was presented. Participants completed 4 blocks for experiment 1 (for 3 participants, data were recorded but not saved for 2 blocks for technical reasons) and 2 blocks for experiment 2. Each block comprised 30 trials and participants received quantitative feedback at the end of every block consisting of the percentage of trials where they had reported perceptual filling-in for longer than one second. Participants were encouraged to blink between trials and during specific rest periods between blocks, but were not told to abstain from blinking during the rest of the experiment. All participants received training prior to testing, to ensure they could experience disappearance of the stimulus and assign consistent responses to the different perceptual states.

5.2.4 Eye movement recording and analysis

During testing, eye position and pupil diameter were continually sampled at 250Hz using a high-speed video eye tracker (Cambridge Research Systems Ltd, Kent, England, www.crsltd.com). Eye tracking data were analyzed with Matlab. Blinks and periods of signal loss were removed from the data. Eye position (defined as the mean position of the eye) and eye movements (defined as the variance around eye position) were then computed for each participant under each load (low / high) and visibility condition (peripheral target visible / perceptually filled-in). A repeated measures ANOVA was used to establish whether eye position and eye movements differed between the various experimental conditions. For experiment 1 (perceptual load task), eye movements were recorded and analysed for all twelve participants. For experiment 2 (working memory task), eye movements were recorded for all ten participants but could only be analysed for 8 participants for technical reasons.

5.2.5 Experiment 1 - Perceptual Load

Whilst participants monitored the appearance and perceptual filling-in of the peripheral figure, they concurrently performed a perceptual task which has been previously shown to allow effective manipulation of perceptual load (Schwartz et al., 2005). This task required a serial visual search on a stream of targets presented at fixation. Crosses spanning 0.52º (vertical line) by 0.22º (horizontal line) were presented at fixation on a rectangular black background (1.3º x 1º). Crosses could appear in any of six colours (red, green, yellow, blue, cyan and purple) and two

orientations (upright or inverted; the horizontal line of the cross was placed 0.25º – 1 pixel – above or below the centre of the vertical line, see Figure 5.1a). Each cross was displayed for 250 ms followed by a blank period of 500 ms before the appearance of the next cross. Perceptual load was manipulated so that for identical stimulus streams, participants performed either a low-load feature search (responding to red crosses among other cross colours), or a high-load conjunction search (responding to either upright yellow or inverted green crosses, but not the opposite conjunctions). Note that this study only examined dual-task conditions with concurrent performance of the perceptual load and filling-in tasks, contrasting two different levels of perceptual load. Crucially, this enabled the isolation of the effect of perceptual load independently from performance of a concurrent task per se. A comparison of filling-in monitoring with and without a perceptual load task would instead have been confounded by a difference in the number of tasks and the need for executive task coordination, which was not the case here.

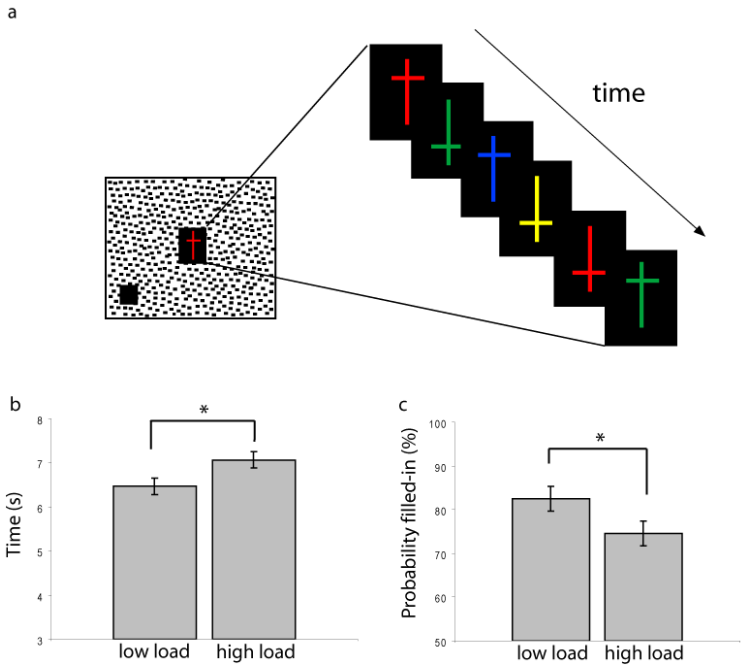

Figure 5.1. Experiment 1: Effect of perceptual load on perceptual filling-in. (a) Procedure. Participants reported the appearance and then perceptual filling-in of a peripheral achromatic figure using button-presses. The figure flickered between black and white. At the same time, participants viewed a series of central coloured crosses and monitored for the appearance of cross targets defined either according to their colour (red crosses, low perceptual load) or colour and orientation (upright yellow or inverted green crosses, high perceptual load). **(b,c) Results.** (b) Increasing perceptual load altered the latency of perceptual filling-in onset. Latency of perceptual filling-in increased in the high (versus low) load perceptual task. (c) Probability of perceptual filling-in was reduced by high (versus low) perceptual load. Data shown are averaged across twelve participants, with error bars representing standard error of the mean difference and '*' indicating statistical significance ($p<.05$, 2-tailed t test).

Participants responded with a button-press whenever a cross target was detected (down arrow on finger pad).

Half of the participants used their left hand to respond to the fixation task and their right hand to report filling-in; this was switched for the other participants, to ensure that handedness bias was not introduced.

5.2.6 Experiment 2 - Working Memory Load

Each trial began with presentation of a grey screen with a central red fixation cross while participants listened to a sequence of five numbers (1 to 5), always preceded by "zero", presented through headphones. Working memory load was manipulated by either presenting the number sequence in ascending order (low load) or in random order (high load). Participants committed the number sequence to memory. This was followed by the 15-second perceptual filling-in task, which was identical to that in experiment 1. Full-screen dynamic noise was presented and after 3 seconds, a peripheral target was added to the display. Participants monitored the target for perceptual filling-in while fixating centrally, using button presses to indicate what they perceived. Different to experiment 1, there was no central perceptual task and participants fixated on a small static red cross (0.4^{o} x 0.4^{o}; see Figure 5.2a). At the end of the perceptual filling-in task, participants were presented with a grey screen and heard the word 'probe' followed by a digit chosen randomly from the original memory set. They then had 3.5 seconds to report the digit that followed the probe in the original memory set by pressing the appropriate key on the keyboard's number pad. The last digit in the memory set was never the probe and all sets began with "0" to ensure that all five digits between 1 and 5 were used as responses in both conditions. A new trial began at the end of the response period. This working memory load manipulation has been used in previous studies (de Fockert et al.,

2001;Dalton et al., 2009). In the low load condition the task is relatively easy. However, this approach has the advantage of avoiding any confound introduced by using dissimilar set sizes, which would have been the case if an alternative method of manipulating the number of digits held in working memory had been used. Although the low-load condition imposes relatively small demands on working memory, participants were still required to remember which type of trial they were performing. Thus the dual task and response requirements were fully matched across both working memory load conditions.

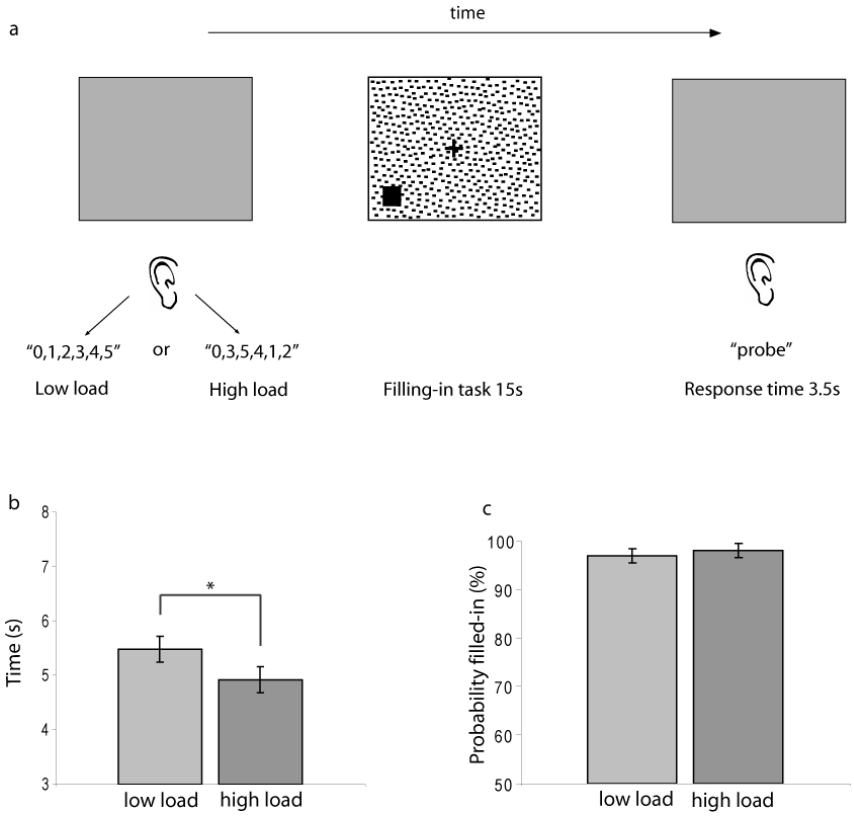

Figure 5.2. Experiment 2: Effect of working memory load on perceptual filling-in. (a) Procedure Participants viewed a grey screen whilst hearing a sequence of 5 numbers, always preceded by '0'. The sequence was either presented in ascending order (low working memory load) or random order (high working memory load). Presentation of this sequence was followed by the perceptual filling-in task (see Figure 5.1 and Methods for full details), where participants reported the appearance and then

perceptual filling-in of a peripheral figure, whilst retaining the previously presented number sequence in working memory. After fifteen seconds of monitoring the filling-in display, participants then viewed another grey screen and heard the word 'probe', followed by a number from the original memory set. They then had 3.5 seconds to report the digit that followed the probe number in the original memory set. **(b,c) Results.** The effect of high (versus low) working memory load on perceptual filling-in was in the opposite direction to that of high (versus low) perceptual load: (b) Latency of perceptual filling-in was reduced under high (versus low) working memory load. (c) The probability of perceptual filling-in was not affected by high (versus low) working memory load, but note it was already close to ceiling under low load. Data shown are averaged across ten participants, with error bars representing standard error of the mean difference and '*' indicating statistical significance ($p<.05$, 2-tailed t test).

5.3 Results

5.3.1 Experiment 1

5.3.1.1 Perceptual load

The perceptual load manipulation was effective: Mean reaction times to target crosses were faster for low perceptual load (483 ms) compared to high perceptual load (568 ms; $t(11)= 7.7$, SEM=11.1 ms , $p<.0005$). There was also a higher mean percentage of correctly detected central targets (hit rate) for the low load (93%) compared to the high load (88%; $t(11)= 3.2$, SEM=1.4%, $p=.009$), ruling out a speed-accuracy trade-off.

5.3.1.2 Effect of perceptual load on perceptual filling-in

Increasing perceptual load reduced participants' ability to initiate perceptual filling-in (Fig. 5.1b). The mean probability of perceptual filling-in was reduced under high perceptual load (75%) compared to low load (83%; t(11)=2.8, SEM=2.8%, p=.017). Mean latency of perceptual filling-in was greater for higher perceptual load (7066 ms) than low perceptual load (6468 ms; t(11)= 3.1, SEM=191.8 ms, p=.01).

To gauge the effect of perceptual load on reaction times, rather than on perceptual filling-in, the reaction times to the physical appearance of the flickering target were also measured. Mean reaction times to the appearance of the target were slower under high perceptual load (1006 ms) than under low perceptual load (909 ms; t(11)=3.4, SEM=28.2 ms, p=.006). However, the magnitude of the difference between the time to perceptual filling-in under high versus low load was far greater (598 ms) than for noting the appearance of the target (96 ms). This suggests that although high load does increase reaction times to a target, it has a greater effect on perceptual filling-in than could be attributed to reaction time alone.

5.3.1.3 Eye position data

A repeated measures ANOVA on the mean eye position data showed no main effect of visibility condition (target visible or perceptually filled-in; F(1,11)=1.4, MSE=0.16 p=.26) or perceptual load (low or high; F(1,11)=1.8, MSE=0.07, p=.21), and no interaction between condition and load (F(1,11)=1.7, MSE=0.04, p=.22). A similar ANOVA conducted on the variance of eye movements also showed no main effects of visibility condition (F(1,11)=1.5, MSE=1.16, p=.25) or perceptual load (F(1,11)=0.94, MSE=1.56 p=.35) and no interaction between condition and load

(F(1,11)=0.47,MSE=0.31, p=.51). Thus the effects of perceptual load on the latency and probability of perceptual filling-in cannot be attributed to differences in fixation or eye movements.

5.3.2 Experiment 2

5.3.2.1 Working memory load

The working memory manipulation was effective: Mean reaction times were faster for low working memory load (679 ms) than for high working memory load (1267 ms; t(9)=5.6, SEM=106 ms , p<.0005). Accuracy was also better for low working memory load with a higher mean percentage of correct trials for the low load (99%) than the high load condition (82%; t(9)=3.2, SEM= 5.4%, p=.01), ruling out a speed-accuracy trade-off.

5.3.2.2 Effect of working memory load on perceptual filling-in

The effect of working memory load on the latency of perceptual filling-in was in the opposite direction to that of perceptual load (Fig 5.2b). Mean latency of perceptual filling-in (time until perceptual filling-in) was shorter for high (4796 ms) than for low working memory load (5428 ms; t(9)= 2.36, SEM=237 ms, p=.042). In contrast to the effect of perceptual load on probability of perceptual filling-in, there was no difference in the mean probability of perceptual filling-in between high (97%) and low working memory load (98%; t(9) =.71, SEM=1.5%, p=.49). There were also no differences in mean reaction times to the appearance of the target between high (787

ms) and low working memory load (1011 ms; t(9)=.87, SEM=256 ms, p=.40). The present results are unlikely to be due to the different levels of load affecting participants' response criteria, as the effect of perceptual load on response times to physical events (target onset) was an order of magnitude smaller than the effect on filling in (Experiment 1) and there was no effect of working memory load on such response times (Experiment 2). Future research could rule out the possibility of criterion shifts entirely, using additional conditions in which targets physically disappeared as well.

5.3.2.3 Eye position data

A repeated measures ANOVA on the mean eye position data showed no main effect of condition (target visible or perceptually filled-in; F(1,7)=0.51,MSE=1.76, p=.50) or load (low or high; F(1,7) =0.47,MSE=2.53, p=.51), and no interaction between condition and load (F(1,7)=0.25,MSE=1.82, p=.63). A similar ANOVA conducted on the variance of eye movements also showed no main effect of condition (F(1,7)=0.29,MSE=9.0, p=.61) or load (F(1,7) =1.1,MSE=24.6, p=.34) and no interaction between condition and load (F(1,7)=0.23,MSE=9.2, p=.65). Thus the effects of working memory load on the latency and duration of perceptual filling-in cannot be attributed to differences in fixation or eye movements.

5.4 Discussion

In this study, the effect of manipulating perceptual load and working memory load on the latency and probability of perceptual filling-in of an artificial scotoma was examined. Opposite effects for manipulations of perceptual load and working memory load were found on the latency and probability of perceptual filling-in of an artificial scotoma. Increasing concurrent perceptual load increased the latency and lowered the probability of perceptual filling-in of artificial scotomas. Conversely, perceptual filling-in occurred earlier when concurrent working memory load was increased. Taken together, these results demonstrate contrasting effects of different types of top-down signals on the perceptual completion of an artificial scotoma.

5.4.1 Effect of perceptual load on perceptual filling-in

The finding that increasing perceptual load reduced the likelihood that participants would report initiation of perceptual filling-in is consistent with the predictions of load theory (Lavie, 2005) and now extends the theory's scope to the phenomenon of perceptual filling-in. Perceptual completion is more likely to take place when spatial attention is directed to the perceptually filled-in target (De Weerd et al., 2006). If perceptual filling-in is indeed an active process requiring top-down control, then increasing perceptual load reduces the processing capacity available for the peripheral target, making perceptual filling-in less probable. Low perceptual load leaves more processing resources, allowing perceptual filling-in to occur. Thus these findings are consistent with perceptual filling-in being an active process, although whether it occurs through an isomorphic or a symbolic mechanism cannot be deduced from the data presented here.

5.4.2 Effect of working memory load on perceptual filling-in

A second proposal in load theory addresses the way working memory determines stimulus processing priorities. This predicts that high working memory load can have an opposite effect to that of high perceptual load in situations where different stimuli compete for processing resources. Depleting the capacity of active cognitive control reduces the ability to maintain prioritisation of behavioural goals, leading to increased processing of distractors (Lavie et al, 2004). In the present context of perceptual filling-in whilst performing a working memory task, there were no irrelevant distractors; participants held a number sequence in working memory whilst monitoring the perceptual filling-in of a figure placed on a dynamic noise background. Moreover, reducing attention to the target is known to impair filling-in (De Weerd et al., 2006). Therefore, how is it possible to account for the finding of enhanced perceptual filling-in with increased working memory load? Load theory can instead provide some insight into the mechanism of perceptual filling-in itself. Despite the fact that the background was not defined as a distractor, the working memory load manipulation may have altered the relative salience of the target and the background. Under conditions of increased working memory load in a concurrent task, and a breakdown in the prioritisation of processing competing stimuli, the dynamic twinkling background may have become more salient compared to the target, causing an increase in breakdown of figure-ground segregation and enhanced perceptual filling-in. This suggestion that perceptual filling-in is more likely when

the background is more salient than the target is consistent with previous findings that perceptual filling-in is enhanced by a dynamic twinkling background compared to a static but noisy background and enhanced for a static compared to a uniform background (Spillmann and Kurtenbach, 1992). Moreover, filling-in is also enhanced for reduced luminance, motion and contrast differences between the target and background (Welchman and Harris, 2001) and impaired for more salient red targets, compared to green targets (De Weerd et al., 2006). I therefore propose that working memory load may impact on perceptual filling-in by modulating the relative saliency of the background and the target. An alternative hypothesis is that higher working memory load produces a state of generally increased alertness or arousal that in itself enhances perceptual filling-in (note, however, that there is no reason to assume working memory load has this effect but perceptual load does not). Future work could disentangle these two hypotheses by explicitly contrasting the effects of manipulations of arousal and working memory load on perceptual filling-in.

Although there was a decreased probability of perceptual filling-in when perceptual load was increased, there was no difference in probability of perceptual filling-in when working memory load was increased. However, the probability of perceptual filling-in was already at ceiling in the low memory-load task, so the effects of high working memory load could not increase the probability of perceptual filling-in any further. In order to increase the power to detect a difference in probability of filling-in in the working memory load task, the perceptual filling-in target could be made larger or less eccentric, making perceptual filling-in less likely. Nevertheless, in the present study the perceptual filling-in stimulus parameters were kept constant for the two manipulations in order to be able to contrast their effects.

5.4.3 Comparison with previous work examining effects of spatial attention on perceptual filling-in

These findings are broadly consistent with a recent behavioural study (De Weerd et al., 2006) showing that directing spatial attention to the features of a figure increases the probability of it being perceptually filled-in by a textured background, compared to unattended figures. This study goes beyond this work as the effects of exhausting processing resources with a second, unrelated task were examined, rather than specifically directing spatial attention to the target itself. In this way, it was possible to explore the role of attentional capacity for perceptual filling-in. An attentional effect on the latency of perceptual completion was also found, whereas De Weerd et al (2006) did not. That study, however, directed attention without exhausting it. It is possible that in contrast, the perceptual load manipulation in the study presented in this chapter depleted processing capacity under high load to an extent that made it possible to detect this effect.

The role of attention in modulating perceptual completion in humans has only rarely been studied in other forms of perceptual filling-in. A study of colour fading during fixation (Lou, 1999) showed that attended discs were more likely to fade than unattended discs. Similarly, a recent behavioural study of motion induced blindness (Scholvinck and Rees, 2009a) showed that attended, rather than unattended targets are more likely to disappear and that increasing perceptual load is associated with reduced

periods of invisibility. Future work could examine to what extent these other forms of perceptual completion share common feedback mechanisms with perceptual filling-in of artificial scotomas.

5.5 Conclusion

This chapter has demonstrated that the effects of manipulating two different types of load in concurrent perceptual and working memory tasks have opposite effects on the latency of perceptual filling-in of an artificial scotoma. This provides new evidence for top-down influences from higher cognitive functions on the processes of perceptual filling-in and also suggests that such perceptual filling-in reflects an active process. The next chapter will turn to a different and unusual form of perceptual completion, which occurs in the context of brain injury, and will explore the integration of information from object sensitive areas in the damaged brain.

CHAPTER 6: THE NEURAL CORRELATES OF FILLING-IN ACROSS THE VERTICAL MERIDIAN IN A PATIENT WITH HEMIANOPIA

6.1 Introduction

The previous chapters (chapters 3, 4 and 5) have examined filling-in in normal human vision. Here I will investigate a different type of filling-in that occurs following brain injury. Hemianopic completion is a form of perceptual completion where contours straddling the vertical meridian are perceived as complete in patients with hemianopia (Poppelreuter, 1917;Sergent, 1988;WARRINGTON, 1962). Its defining characteristic is that the patient reports as complete both incomplete (partial) stimuli (here referred to as paracompletion), as well as complete contours (here referred to as veridical completion), when the stimulus overlaps the vertical meridian defining the medial border of their hemianopia. It differs from blindsight in that completion leads to perceptual awareness of a complete contour, rather than the ability to respond unconsciously but accurately to stimuli placed within the perimetrically blind hemifield. Hemianopic completion is not seen when incomplete stimuli are presented elsewhere in the visual field.

6.1.1 Possible mechanisms for hemianopic completion

Three types of explanation have been advanced concerning the neural mechanisms underlying hemianopic completion (Walker and Mattingley, 1997;McCarthy et al.,

2006) . First, it has been suggested that completion is a constructive process, reflecting the operation of processes that in healthy individuals can lead to the perception of a complete form from partial information (e.g. modal or amodal completion). Alternatively, hemianopic completion might be secondary to spatial inattention and thus reflects lack of awareness of 'missing' sensory evidence. Finally, it is possible that hemianopic completion can be explained by the presence of residual vision within the hemianopia or serious flaws in the methodology used for testing.

In this chapter, high field functional MRI (fMRI) was used to study the neural basis of hemianopic completion in a single individual who has been particularly well investigated behaviourally (McCarthy *et al.*, 2006). Importantly, systematic testing in this individual reveals no evidence of any asymmetric attentional deficit or any residual vision that might contribute to the completion except at high contrast. These previous findings rule out a lateralized deficit of attention or residual vision contributing to his hemianopic completion. Therefore this study examined whether hemianopic completion might reflect a constructive neural process in higher visual areas in the absence of input from earlier retinotopic cortex.

6.1.2 Potential neural substrates for hemianopic completion

There are a number of potential neural substrates for such a constructive process. Modal completion refers to the interpolation of borders (termed illusory contours, IC) between inducing edges and associated brightness enhancement of the perceived figure, while amodal completion is the perception of a complete object behind an occluder. In healthy human subjects, there is general agreement that both processes

originate in ventral visual cortex, but some controversy over whether they share a common mechanism and whether perceptual completion is a process initiated at early stages of visual processing or commences at higher levels of the visual system (Murray *et al.*, 2004;Rauschenberger *et al.*, 2006). For example, while in humans early retinotopic areas V1/V2 are activated by illusory contours (Ffytche and Zeki, 1996;Seghier et al., 2000;Larsson et al., 1999), other studies implicate object-sensitive ventral visual regions anterior to retinotopic visual cortex such as the lateral occipital cortex (LOC) in IC processing (Mendola et al., 1999;Stanley and Rubin, 2003;Ritzl et al., 2003;Murray et al., 2004), amodal completion (Murray *et al.*, 2004;Weigelt *et al.*, 2007) and dynamic shape integration of an object moving behind occluders (Yin *et al.*, 2002) . While these studies implicate higher visual areas in illusory contour perception, they cannot be used to test a hypothesis of a constructive process in higher visual areas in the absence of early visual input as retinotopic cortex is always present and stimulated. POV lacks almost all retinotopic visual cortex contralateral to the stimulus, allowing such a hypothesis to be tested.

Brain activity associated with hemianopic completion was therefore measured in the patient in both retinotopic early visual cortex and higher areas of ventral visual cortex. The incomplete figure was chosen following preliminary trials to generate completion of the semicircle (paracompletion) on around 50% of trials. Importantly, the comparison was made between brain activity evoked by identical partial contours that either did or did not lead to behavioural reports of perceptual completion. It was thus possible to compare trials during which identical visual stimulation led to two different perceptual outcomes, avoiding the problem of stimulus confound (Frith *et al.*, 1999). By contrasting these two situations, brain regions were sought that

reflected the process of perceptual completion independent from variation in physical stimulation. It was hypothesised that perceptual completion would be associated with differential neural activity (compared to non-completion) in either retinotopic visual cortex or areas consistent with LOC and that activity in higher visual areas in the absence of activity in earlier retinotopic cortex might reflect a constructive process for hemianopic completion.

6.2 Materials and Methods

6.2.1 Case Report

POV is a 71 year-old right-handed man who presented 16 years prior to the study with a three year history of paroxysmal visual field disturbances and six month history of headaches. Visual field testing at the time revealed a right-sided homonymous paracentral scotoma and after investigation he underwent a craniotomy to excise a tentorial meningioma. Five days post-operatively, he exhibited a large right-sided homonymous scotoma with sparing along the vertical meridian superiorly and inferiorly and in the outer periphery.

Imaging postoperatively revealed a left occipital cavity with damage to most of the left calcarine sulcus (apart from the most anterior portion) and involvement of the left posterior fusiform gyrus. He made a good recovery and continued to live independently. However, he noticed that he often made errors regarding the size and shape of objects extending into his blind hemifield. This was explored

psychophysically and he demonstrates hemianopic completion that cannot be accounted for by spatial inattention or residual vision (McCarthy *et al.*, 2006). This previous study documented responses to complete and half shapes presented within the left, right and central visual field. For these stimuli presented in the left visual field, POV responded correctly on 94% of occasions. He detected the presence of stimuli presented entirely within the right visual field on 19% of presentations (the authors note very long latencies of > 3s for these presentations). For stimuli presented within the centre of the visual field, POV reported as complete 38% of whole shapes and 22% of half shapes.

Fifteen years following the excision, he continues to demonstrate hemianopic completion. At the time of the investigations performed here, he remains fully ambulant and living independently in the community. Structural MRI is unchanged (see Figure 6.1a) with a large left occipital cavity extending into the left occipital horn of the lateral ventricle. Visual field testing using the Humphrey Field Analyser (30-2 Full Threshold protocol; Model 750i, Zeiss) demonstrated a large right homonymous hemianopia with thresholds of <0 dB extending from the vertical meridian to 30 degrees laterally, 18 degrees superiorly and 20 degrees inferiorly (see Figure 6.1b), which has remained stable for fifteen years. Previous detailed neuropsychological testing revealed no significant intellectual or cognitive deficits and no evidence of neglect on line bisection tasks, digit cancellation and drawing tasks(McCarthy et al., 2006). There were no other neurological abnormalities.

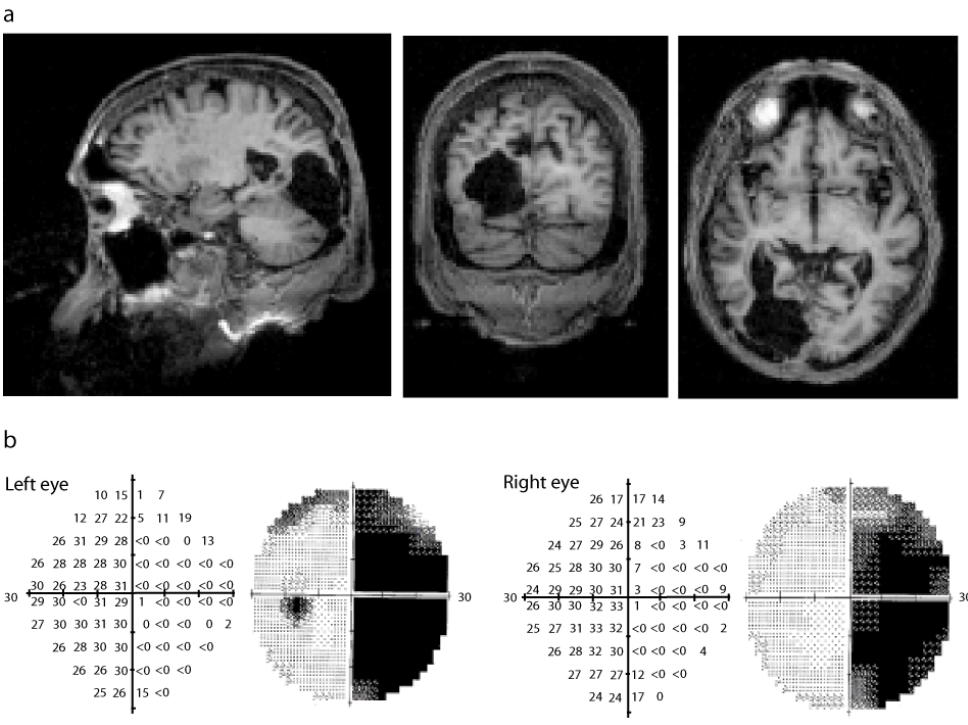

Figure 6.1 (a) Anatomical location of the lesion. Three sections (sagittal, coronal and axial) are shown through POV's T1-weighted MRI. A large cystic lesion is seen in the left occipital lobe which is in communication with the left lateral ventricle, involves most of the occipital lobe and extends anteriorly to involve parts of the inferior temporal lobe. In the coronal and axial sections, the left hemisphere is shown on the left. **(b) Visual Field testing**. Humphrey Field Analyser plots for POV measured at the time of testing on Humphrey Visual Field Analyser, 30-2 Full Threshold protocol, demonstrating a large right homonymous hemianopia. Locations marked as '<0' represent locations where the brightest stimulus did not elicit a response. These areas are marked in black. Note that fields are presented to 30 degrees eccentricity. POV has residual vision on perimetry beyond 30 degrees but the stimulus was at 4.5 degrees eccentricity and the field of view in the MRI scanner is approximately 20 degrees eccentricity.

POV gave his informed consent to participate in this study and also for the publication of this clinical history, which was approved by the Institute of Neurology, University College London Ethics Committee. The initials POV are not transparently related to his name.

6.2.2 Stimuli

Visual stimuli (see Figure 6.2a) consisted of either a semicircular contour that appeared grey (radius 4.5 degrees and line width 0.16 degrees; luminance 6.5 cd/m^2) or a matching grey circular contour drawn around a fixation point (comprising a black square 0.4 x 0.4 degrees surrounding a central white square 0.2 x 0.2 degrees) and presented on a grey background (luminance 8.5 cd/m^2) The centre point of the semicircular or circular contour was shifted relative to the fixation point to lie one degree lateral to fixation in the blind (right) hemifield. When a semicircular contour was shown, it was always placed within the sighted (left) hemifield and extended by one degree into the blind field. Thus physical stimulation was identical in the sighted (left) visual field for semicircular and circular contours, and differed only in the blind (right) visual field.

Stimuli were projected using an LCD projector (NEC LT158, refresh rate 60Hz, screen resolution 640x480) onto a circular projection screen at the rear of the scanner. POV viewed the screen via a mirror positioned within the head coil. All stimuli were presented with MATLAB 6.5.1 (Mathworks Inc.) using the COGENT 2000 toolbox (www.vislab.ucl.ac.uk/Cogent2000/index.html).

6.2.3 Procedure

Each trial started with presentation of a fixation point on a blank grey screen for 750ms. For the first 250ms, the central square within the fixation target was coloured

red, to alert POV that the trial was starting and to encourage central fixation. This was followed by presentation for 100 ms of either a semicircular contour in the sighted (left) visual field (on 70% of trials) or presentation of a complete circular contour (on 10% of trials). After stimulus offset, POV was required to report his percept within 2500 ms by pressing one of three buttons with his right hand ('1', '2' or '3' on the keypad). Pilot behavioural studies indicated that these stimuli and presentation times reliably evoked one of three clearly distinct percepts in POV: a semicircular contour, a circular contour or a patchy (incomplete) circular contour. POV was encouraged to be conservative in his responses and only report the perception of a circular contour when he was sure of this perception. These button presses were used on a trial-by-trial basis to define the percept associated with each physical stimulus presentation. On 20% of trials, no stimulus was presented ('null trials') and fixation maintained in order to assess baseline activity. On these trials POV was not required to respond. Each trial was followed by an intertrial interval of 1900 ms.

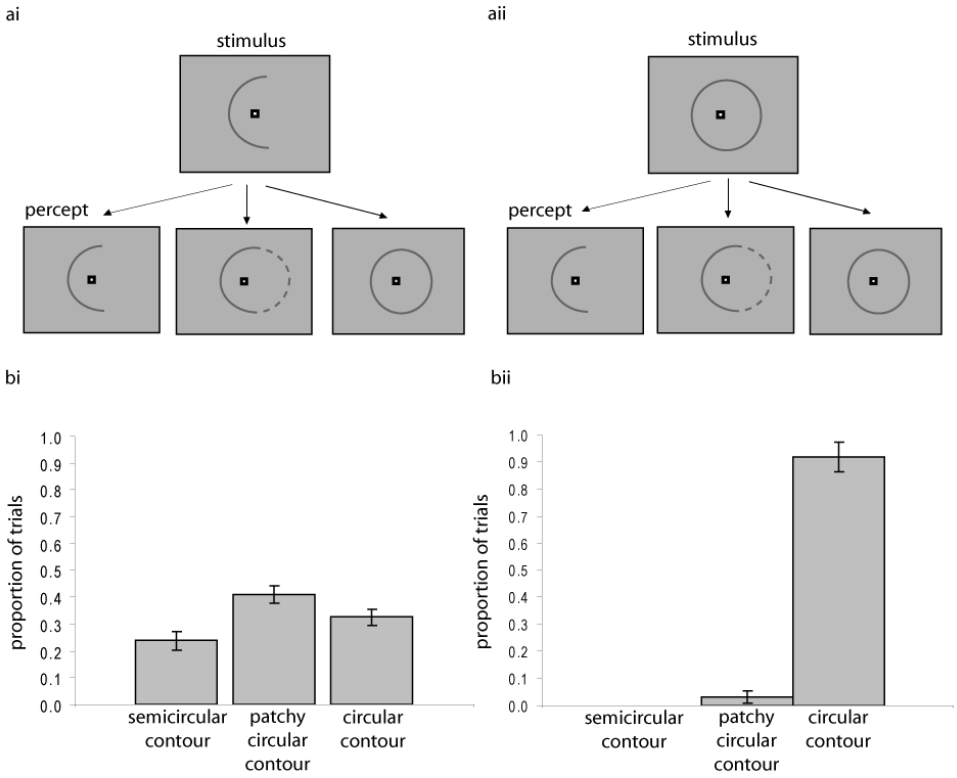

Fig 6.2 (a) Stimuli and percepts. POV was shown either (i) a semicircular contour (70% of trials) or (ii) a complete circular contour (10% of trials). In each case the centre of the circle or semicircle was shifted 1 degree into the blind hemifield. Stimulus duration was 100 ms. For each trial POV perceived a semicircular contour, a patchy circular contour or a complete circular contour. The perception of a complete circular contour on a trial when a semicircular contour had been presented constituted hemianopic completion. 20% of trials were null trials when only a blank screen with fixation point was presented. **(b) Behavioural results.** bi) Proportion of trials when a semicircle was presented when each percept was reported. bii) Proportion of trials when a circle was presented when each percept was reported.

Trials were arranged into blocks of ten. The order of presentation of a semicircular contour, circular contour or null trial within each block was selected randomly for each block. Each scanning session consisted of 3 blocks of 10 trials. Sessions were kept short at the request of POV to minimise the time he was in the scanner and due to fatigue. POV completed a total of 20 sessions, spread over 5 days. This arrangement

allowed the number of trials to be maximised whilst minimising the duration of individual scanning sessions.

6.2.4 Functional MRI scanning

A 3T Siemens Allegra system was used to acquire both T2*-weighted echo planar (EPI) images with blood oxygenation level dependent contrast (BOLD) and T1-weighted anatomical images. Each EPI image comprised of thirty-six 3-mm axial slices with an in-plane resolution of 3×3mm. The main experiment was split into 20 runs, each consisting of 87 volumes. The first five volumes of each run were discarded to allow for T1 equilibration effects. Volumes were acquired continuously with a TR of 2.34 s per volume.

During scanning, eye position and pupil diameter were continually sampled at 60 Hz using long-range infrared video-oculography (ASL 504LRO Eye Tracking System, Mass) and monitored on-line via a video screen to ensure that POV maintained fixation.

6.2.5 Data analysis

Functional imaging data were analyzed using Statistical Parametric Mapping software (SPM5, Wellcome Trust Centre for Imaging Neuroscience, University College London). Slices were corrected for acquisition time using the most caudal slice as reference. All image volumes were realigned spatially to the first and resulting image

volumes were coregistered to POV's structural scan and smoothed with a Gaussian kernel (FWHM 6mm).

Trial-specific regressors were created for each of the possible combinations of percept and physical stimulus type by generating delta functions that represented trial onsets and convolving with a synthetic haemodynamic response. There were thus six different regressors of experimental interest defined according to stimulus (semicircle or circle) and accompanying reported percept (semicircular contour, patchy circle or circle) (See Table 6.1).

1. Semicircular stimulus, semicircular contour percept
2. Semicircular stimulus, patchy circle percept
3. Semicircular stimulus, circle contour percept
4. Circle stimulus, semicircular contour percept
5. Circle stimulus, patchy circle percept
6. Circle stimulus, circle percept

	Stimulus		
Percept		Semicircle	Circle
	Semicircle	1	4
	Patchy circle	2	5
	Circle	3	6

Table 6.1 Possible combinations of presented stimuli and percepts. Numbers refer to regressors in list above.

In addition, null trials were modelled to provide an implicit baseline. Motion parameters defined by the realignment procedure were employed as six separate regressors of no interest. All regressors were entered into a multiple linear regression model and parameter estimates determined for all brain voxels. Data were high pass filtered (cut-off: 0.0078Hz) to remove low-frequency signal drifts and a mask of POV's grey matter (produced using SPM segmentation) was explicitly applied. Appropriately weighted linear contrasts between the experimental conditions identified activated areas on a voxel-wise basis. The resulting set of t values constituted a Statistical Parametric Map (SPM{T}) which was globally thresholded at a level of $p<.001$, uncorrected for multiple comparisons. Here only those loci that survived a statistical threshold of $p<.05$ after correction for multiple comparisons are reported for the volume examined.

6.2.6 Retinotopic analyses

To identify the boundaries of retinotopic visual cortical areas, standard retinotopic mapping procedures were used (Sereno *et al.*, 1995;Teo *et al.*, 1997;Wandell *et al.*, 2000). Flashing checkerboard patterns covering either the horizontal or vertical meridian were alternated with rest periods for five epochs of 10 volumes over two scanning runs, each lasting 155 volumes. SPM5 was used to generate activation maps for the horizontal and vertical meridians. Mask volumes for each region of interest were obtained by delineating the borders between visual areas using activation patterns from the meridian localizers. Only contralesional visually responsive

retinotopic areas could be identified, corresponding to the size and location of his existing lesion (see Figure 6.1a). Standard definitions of V1-V3 were followed, together with segmentation and cortical flattening using the MrGray software (Teo *et al.*, 1997;Wandell *et al.*, 2000). This was used to define a number of retinotopic regions of interest. Appropriately weighted linear contrasts were then used between the experimental conditions from the main analysis (above) to identify activated voxels within each retinotopic region of interest, effecting a small volume correction (SVC) for multiple comparisons within that region at a threshold of $p<.05$, family-wise error corrected.

6.2.7 Whole brain analysis

Apart from the retinotopic analyses, in order to facilitate reporting of any activations in a common stereotactic space, the multiple regression analysis was repeated after spatial normalisation of each image volume to the standard template for the Montreal Neurological Institute (MNI) using the unified segmentation algorithm in SPM5 for spatial normalisation. This has been validated as the most sensitive and robust method for normalising lesioned brains (Crinion *et al.*, 2007). Appropriately weighted linear contrasts were then used between the experimental conditions from the main analysis (above) to identify activated voxels and report those surviving a single-voxel p-threshold of $p<.05$, family-wise error corrected for multiple comparisons. To identify areas of ventral visual cortex that were visually-responsive, a small volume correction ($p<.05$, FWE-corrected) was used based on those voxels that showed differential responses to conditions where visual stimuli were presented (i.e. experimental conditions 1-6, above) versus null trials that were also within 20mm

of previously reported (Grill-Spector *et al.*, 2000;Spiridon *et al.*, 2006;Avidan *et al.*, 2002;Murray *et al.*, 2003;Lerner *et al.*, 2002;Downing *et al.*, 2007;Eger *et al.*, 2008) mean stereotactic coordinates of LOC (see e.g.(Yin *et al.*, 2002) for a similar approach).

6.2.8 Eye tracking analysis

Eye tracking data recorded during scanning were analyzed with MATLAB 7 (Mathworks Inc., Sherborn, MA). Blinks and periods of signal loss were removed from the data. Mean eye position in the horizontal and vertical directions relative to fixation was then computed separately for the stimulation presentation period of each trial within each condition. A positive value in the horizontal direction indicated movement into the right (blind) hemifield. A one-way ANOVA was used to establish whether mean eye position in the horizontal and vertical direction deviated significantly between conditions.

6.3 Results

6.3.1 Behavioural findings

On trials when a semicircular contour was presented, POV reported perceiving a semicircular contour (i.e. veridical perception) on 24% (SEM = 4%) of trials, a patchy circular contour (i.e. partial paracompletion) on 41% (SEM = 3%) and a circular contour (i.e. full paracompletion) on 33% (SEM = 3%) of occasions (see Figure 6.2b).

Thus POV showed hemianopic completion on 33% of trials. On trials where a circular contour was presented, POV perceived a circular contour (i.e. veridical completion, despite part of the contour falling into his blind hemifield) on 92% (SEM = 5%) of times and a patchy circle on 3% (SEM = 2%) of times. He did not perceive a semicircular contour on any of these trials. He also never responded to a null trial (i.e. occasions when no visual stimulus was presented). Mean reaction times for trials when the semicircular contour was presented were 971 ms (SEM = 167 ms) for the perception of a semicircle, 1269 ms (SEM = 180 ms) for the patchy circle and 1047 ms (SEM = 132 ms) for a circular contour. The mean reaction time for the perception of a circular contour on trials when a circular contour was presented was 978 ms (SEM = 159 ms). There was no significant difference in reaction times for any of the presentations or perceptions apart from the perception of a patchy circle (only ever perceived during presentation of a semicircular contour) which differed significantly from perception of a semicircular contour ($t(15)=7.1$, $p<.005$) and a circular contour ($t(15)=5.1$, $p<.005$) during presentation of a semicircular contour and from perception of a circle during presentation of a circle ($t(15)=5.4$, $p<.005$). In all cases, perception of a patchy circle was associated with slower reaction times. This may have been because, as a hybrid between a circular and semicircular contour, a longer decision process was required in responding to the percept.

6.3.2 Eye tracking analysis

Long-range infra-red eye tracking confirmed there were no systematic differences across different trial types in mean eye position in the horizontal direction ($F(3,291)=1.3$, $p=.27$ and no systematic differences in mean eye position in the

vertical direction ($F(3,291)=0.25$, $p=.86$. Mean eye position in the horizontal direction relative to fixation was 0.35 degrees (SEM = 0.10 degrees) during trials where a semicircular contour was presented and a semicircular contour was perceived, 0.67 degrees (SEM = 0.18 degrees) during trials where a semicircular contour was presented and a patchy circle was perceived, 0.33 degrees (SEM = 0.09 degrees) during trials where a semicircular contour was presented and a circle was perceived and 0.43 degrees (SEM = 0.18 degrees) during trials where a circular contour was presented and a circle was perceived.

Mean eye position in the vertical direction was 0.028 degrees (SEM = 0.063 degrees) during trials where a semicircular contour was presented and a semicircular contour was perceived, 0.097 degrees (SEM = 0.085 degrees) during trials where a semicircular contour was presented and a patchy circle was perceived, 0.030 degrees (SEM = 0.066 degrees) during trials where a semicircular contour was presented and a circle was perceived and 0.007 degrees (SEM = 0.084 degrees) during trials where a circular contour was presented and a circle was perceived. Thus there were no systematic differences in movement toward or away from the blind hemifield between the different conditions, although with a slight tendency across all conditions towards eccentric fixation into the blind hemifield.

6.3.3 Functional MRI

Examination of the retinotopic data confirmed areas identifiable as V1-V3 in the undamaged right hemisphere. In the damaged left hemisphere, the occipital lesion extended throughout areas homologous to these right hemisphere retinotopic

structures and no clear retinotopic organisation was apparent (within the limits of the visual field of view of approximately 20 degrees in the MRI scanner).

Data from the main experiment were next examined for a number of different statistical comparisons:

a. Same physical stimulation, different percept: Hemianopic completion (paracompletion, 3-1 in Table 6.1)

Stimulus-specific activation of cortical areas by hemianopic completion (specifically paracompletion) was revealed by statistical comparisons between trials when a semicircular contour was displayed but POV reported perception of a circular contour, versus trials when a semicircular contour was displayed and he reported perception of a semicircle. Note that for this comparison, the visual stimulus was identical in both conditions and only the conscious percept differed. Any differences in BOLD signal between these two conditions reflect neural activity specifically associated with the percept during hemianopic completion that was not confounded by any changes in physical stimulation.

No significant clusters of activity were found within right, undamaged visual cortex in visual areas V1-V3 for this comparison, although when these areas were examined for activity in all conditions compared to the null condition, each visual area showed a significant cluster of activity (within V1, $p<.0005$ family-wise error corrected, t=7.11, k=24, when correcting for V1 as a small volume; within V2, $p<.0005$ family-wise error corrected, t=7.85, k=17, when correcting for V2 as a small volume; within V3,

p<.0005 family-wise error corrected, t=5.56, k=1, when correcting for V3 as a small volume). Thus retinotopic areas V1-V3 show strong activation to visual stimulation (versus no visual stimulation) but do not show any significant differential activation associated with hemianopic completion.

In contrast, anterior to retinotopic visual cortex this comparison revealed strong differential activation in the lingual gyrus in the right occipital cortex (Brodmann area 19) (maximum coordinates [32, -62 4], t=4.01, *p*<.0005 uncorrected, *p*=.040 small volume family-wise error corrected; see Figure 6.3a and for the time-courses of activation see Figure 6.3b). This is 17.5 mm away from the mean of previously reported coordinates of lateral occipital complex from 7 previous studies (see Methods).

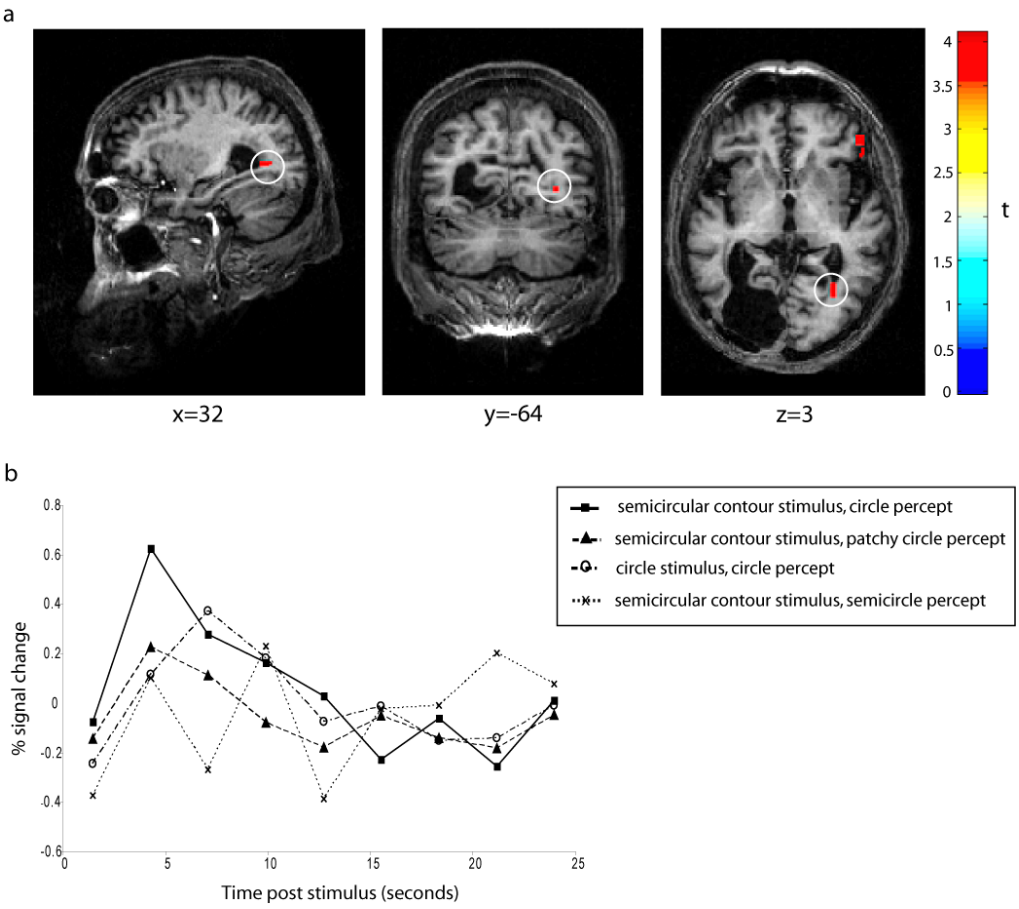

Fig 6.3 (a) Areas activated by hemianopic completion. The location of the most significant activations during hemianopic completion revealed by comparison of trials when a circle was perceived with trials when a semicircle was perceived, during presentation of a semicircle (paracompletion). All activations are shown superimposed on POV's T1-weighted anatomical image. $p<.001$ uncorrected. The white ring indicates strong differential activation for this condition when corrected for the small volume of a 20mm sphere centred on the mean MNI coordinates of the lateral occipital complex, t=4.01, p<.0005 uncorrected, $p=.04$ family-wise error corrected. In the coronal and axial sections, the left hemisphere is represented on the left. The colour of the activation represents the *t* value, as indicated by the scale bar. **(b) Timecourse of event-related activity**. The change in BOLD contrast as a function of peristimulus time is plotted for the peak voxel.

Figure 6.4 provides a more detailed comparison of percentage signal change between the different conditions at the peak voxel of activation in this cluster at 2TR following

stimulus presentation. No other brain regions showed significant activity after correction for multiple comparisons.

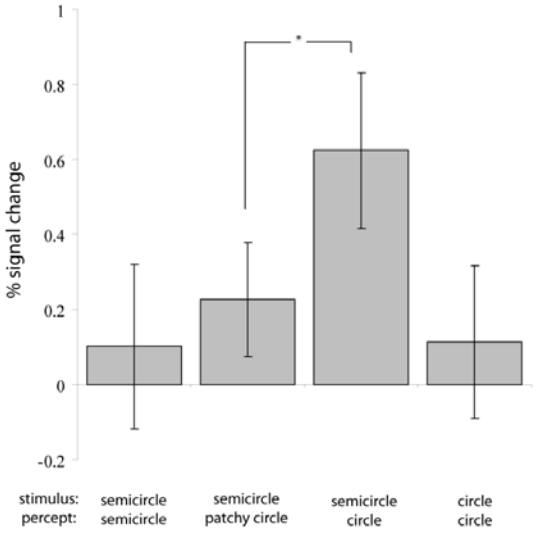

Fig 6.4 Percentage signal change at peak voxel across four experimental conditions at 2TR following stimulus presentation (see Methods for details). This voxel was selected on the basis of showing a significant difference in activity (see Results for details of statistical comparison) comparing perception of a circle (paracompletion) with perception of a semicircle (no completion). Activity in this voxel at this time point also differed significantly comparing the perception of a circle (paracompletion) with perception of a patchy circle ($t(3)=4.0$, $p=.029$). Error bars represent standard error of the mean for activity over 4 runs. The symbol '*' indicates statistical significance ($p<.05$, 2-tailed t test).

It was not possible to examine equivalent differential responses to the veridical type of hemianopic completion (i.e. trials when a circular contour was displayed and POV reported a circular contour, versus trials when a circular contour was displayed and he reported a semicircular contour) as there were no trials on which POV was shown a circular contour and he reported a semicircular contour.

b. Same percept, different stimulation: comparison of the two types of hemianopic completion; paracompletion and veridical completion (3-6 in Table 6.1)

Next, the two types of hemianopic completion: paracompletion and veridical completion were compared to look for differential BOLD activity which might suggest a difference in cortical location for the two phenomena. However, the comparison of trials when a semicircular contour was shown and a circle was perceived (paracompletion) with trials when a circle was shown and a circle was perceived (veridical completion) revealed no significant activation at a threshold of $p<.05$, FWE-corrected. These data were further inspected at the lower threshold of $p<0.001$, uncorrected but this also revealed no significant activation. The absence of activity in this comparison suggests that there is no difference in neuronal activity when POV is shown a circle or a semicircle and sees a circle and therefore hemianopic completion of the circle is unlikely to be due to residual vision, although, especially in a single subject case study, it is always difficult to be certain that no difference exists between conditions based on the lack of statistical significance.

c. Different stimulation, different percepts: no hemianopic completion (1-6 in Table 6.1)

The final examination was of brain areas differentially activated by the comparison of the perception of a circle when a circle was presented with the perception of a semicircle when a semicircle was presented. Note that for this comparison both the percept and the stimulus differ, so any differences in brain activation might reflect

either stimulus-driven or percept-associated changes. This comparison revealed significant activation in the right putamen (MNI coordinates 26, 6, 2; $p<.005$ family-wise error corrected) and in the prefrontal cortex, insula and caudate on whole brain analysis (for details see Table 6.2). Importantly, whole brain analysis did not reveal activation in visual cortex and examination of the same small volume used in the critical contrast of interest ('a' above) revealed no areas of activation meeting the family-wise error threshold for that small volume. However, this absence of evidence of differences in activity should be interpreted with caution in this single subject study, which may have limited power to detect differences in activity where they exist.

Location	**Coordinates [x,y,z] (MNI space)**	**Number of voxels in cluster**	***t* value**	***p* value**
Right ventral putamen	26, 6, 2	52	6.12	<.0005
Right prefrontal cortex	52, 34, -6	35	5.59	.001
Left caudate	-10, 0, 8	39	5.58	.001
Left superior temporal gyrus	-52, -56, 12	28	5.57	.002
Right insula	36, -2, 8	29	5.56	.002
Left posterior insula	-34, -24, 8	28	5.47	.003
Anterior cingulate cortex	10, 46, -8	14	5.35	.005
Left thalamus	-6, -16, 10	17	5.28	.006
Left putamen	-26, -4, 2	21	5.17	.011

Table 6.2 Veridical perception of a circle versus semicircle. Coordinates and t values for event-related activation associated with the comparison of veridical perception of a circle and a semicircle ($p < .05$ family-wise error corrected).

6.4 Discussion

In this study, the neural correlates of hemianopic completion have been demonstrated in POV by comparing fMRI responses on trials where he showed completion of a semicircular stimulus with trials where an identical visual stimulus was displayed but he did not show completion. Retinotopic mapping demonstrated no consistent retinotopic areas in left occipital cortex, consistent with the location and extent of his lesion (Figure 6.1a). In right occipital cortex retinotopic areas could be identified and were visually responsive, but did not show significant differential activity associated with hemianopic completion. Such differential activity was instead identified anterior to retinotopic cortex in the lingual gyrus in the right occipital cortex, contralateral to the lesion, ipsilateral to the illusory edge of the stimulus. This region was located in visually-responsive ventral visual cortex near to reported coordinates for the human lateral occipital complex (Grill-Spector *et al.*, 2000;Spiridon *et al.*, 2006;Lerner *et al.*, 2002;Avidan *et al.*, 2002;Murray *et al.*, 2003;Downing *et al.*, 2007;Eger *et al.*, 2008). No difference was found in neural activity in POV between the two forms of hemianopic completion (paracompletion and veridical completion) which suggests that in POV, these two forms of hemianopic completion are likely to be due to similar processes.

6.4.1 Comparison with previous studies

Previous studies of hemianopic completion in patients have been confounded by problems of residual vision within the blind hemifield (WILLIAMS and Gassell, 1962;Torjussen, 1978), eye movements toward the blind hemifield (WILLIAMS and

Gassell, 1962), eccentric fixation (Sergent, 1988;Bender and Teuber, 1946) and visual neglect (Sergent, 1988;WARRINGTON, 1962). These problems were avoided in this study in several ways. First, the main comparison of interest was the completion of the incomplete form of a semicircular contour (paracompletion). Thus any perception of a circular contour could not be due to residual vision, eye movements or eccentric fixation, as no circular contour was ever presented on such trials. The possibility of residual vision in POV was also ruled out through careful (and repeated) visual field testing, which demonstrated a stable dense hemianopia with no preserved islands of visual function. Eye position from fixation was also monitored throughout scanning and no significant differences were found between experimental conditions, thus ruling out the possibility that differences in eye position could account for these findings. It should also be noted that visual stimuli were presented for only 100 ms, which is too rapid for eye movements to be planned and subsequently executed into the blind hemifield. Completion in POV could also not be attributed to blindsight (Marcel, 1998;Jackson, 1999) as the critical comparison reflects the comparison of partial stimuli for which there is no stimulus physically present in the blind hemifield that might give rise to a behavioural report in the absence of perception. Finally, completion cannot be attributed to spatial inattention as POV shows no evidence of neglect on formal clinical assessment.

6.4.2 Hemianopic completion processes may be similar to those involved in illusory contour formation

The principal finding is that contralesional visually-sensitive areas of ventral visual cortex near to reported coordinates for the lateral occipital complex (LOC) were

differentially activated on trials resulting in hemianopic completion versus physically identical trials that did not result in completion. Low-level physical properties of visual stimulation were controlled for by comparing physically identical stimuli that gave rise to two different percepts. The finding that activation was located in ventral visual cortex anterior to retinotopic cortex and close to LOC coordinates is consistent with the prior hypothesis that regions involved in the perception of objects are specifically involved in hemianopic completion. These findings further suggest that hemianopic completion may reflect higher level processes similar to illusory contour perception in healthy volunteers, with the edges of the semicircular contour here acting as inducing edges for completion. It should be noted however, that this process may differ from illusory contour perception in that no low level visual processes seem to be involved here (and indeed POV's lesion encompasses visual areas V1-V3). Furthermore, although the observed right hemisphere activity was close to coordinates for LOC, it cannot be unequivocally established that this activity fell within POV's lateral occipital complex, in part because after a substantial cortical lesion, reorganisation may have occurred such that normal structural and functional anatomy is not entirely preserved.

6.4.3 Could hemianopic completion arise due to failure of reciprocal inhibition from other brain regions?

One possible mechanism underlying such a proposal is that LOC (or abutting regions of visually-sensitive ventral occipital cortex anterior to retinotopic cortex) may construct a unitary visual percept, uniting the two lateralised hemifield maps from

retinotopic visual cortex earlier in the visual processing pathway (Tootell et al., 1998b). Importantly, POV has an extensive occipital lesion that encompasses most of the left retinotopic visual cortex and extends into the inferior temporal gyrus (see Figure 6.1a). This is likely to deprive ipsilesional ventral visual cortex of input from the contralesional hemifield. It is possible that reorganisation may have occurred causing undamaged, contralesional ventral visual cortex to compensate for this lack of input. Hemianopic completion may therefore be the result of unopposed activity of contralesional visually-sensitive ventral occipital areas by a breakdown in reciprocal inhibition between the left and right hemispheres. This may explain why hemianopic completion is not a universal phenomenon, and is not always observed in patients with homonymous hemianopia(Poppelreuter, 1917;Sergent, 1988;Walker and Mattingley, 1997) . It is possible that for hemianopic completion to occur, unopposed activity of contralesional areas of ventral occipital cortex is also required. It can therefore be hypothesised that sufficient damage to retinotopic cortex to deprive ipsilesional visually-sensitive cortex anterior to retinotopic areas of input might be the necessary and sufficient criteria for hemianopic completion. Such a hypothesis should be tested in future work.

6.4.4 Stimulation of the blind hemifield in patients with hemianopia but no hemianopic completion

In patients with homonymous hemianopia who do not experience hemianopic completion, stimulation of the blind field can lead to activation of extrastriate cortex in the undamaged (ipsilateral) hemisphere. Of note, Nelles and colleagues examined

cortical activity during stimulation of the blind hemifield in 13 patients with homonymous hemianopias secondary to occipital lobe strokes (Nelles *et al.*, 2007). Stimulation of the hemianopic visual field induced greater ipsilateral (contralesional) activation of extrastriate visual cortex in Brodmann area 18, although they did not specifically examine which retinotopic visual area this reflected. Another study also reported that stimulation of the blind hemifield in a patient with blindsight resulted in activation in ipsilateral occipital lobe (Bittar *et al.*, 1999) in V5 and V3/V3A. Those studies differ significantly from the study presented in this chapter in that they report stimulation within the blind hemifield in the absence of any corresponding perception rather than completion of partial stimuli into the blind hemifield. Nevertheless, they suggest that ipsilateral activation of visual cortex to stimulation of the blind hemifield may be a more generalised effect of plasticity following occipital lobe damage that may have wider implications for patients with damage to the visual pathways. Specifically, the intact hemisphere may play a role in mediating blindsight or in the rehabilitation of visual abilities in the blind field. The mechanism for such a role for the ipsilateral hemisphere could arise from cortical plasticity through adaptation or reorganisation of cortical tissue, or via new connections (Bridge *et al.*, 2008), or alternatively, via existing subcortical neural pathways and structures such as the superior colliculi.

6.4.5 Limitations of this study

There are several limitations to this study. Results are reported for a single patient and it is not clear whether these results generalise to other patients with hemianopic completion. It should also be noted that POV reported perceiving a complete circle on

most trials when he was presented with a circle, despite a large dense hemianopia. Although the edges of the semicircle stimulus were aligned to the edges of his hemianopia, it is possible that the edges of the circle extended closer to the edges of the deficit and were therefore more powerful inducers of completion than the semicircle. It is also more difficult to interpret activity during this condition. The perception of a complete circle when presented with a circular contour (despite his hemianopia) could be due to hemianopic completion (in the same way as the semicircular contour showed completion) or other causes for example residual vision or eccentric fixation. Importantly, no difference in neural activity were found between trials showing veridical and paracompletion, suggesting that in POV hemianopic completion of the complete circle was not due to these other causes.

6.5 Conclusion

The event-related fMRI findings in this study show that hemianopic completion is associated with increased activation in contralesional visually-sensitive ventral occipital cortex anterior to retinotopic areas and near to the lateral occipital complex. This may occur due to unopposed activity of contralesional object-sensitive areas in the absence of input from destroyed retinotopic cortex.

CHAPTER 7: INFLUENCES OF REWARD ON VISUAL CORTEX ACTIVITY

7.1 Introduction

The first section of this thesis (Chapters 3-6) examined the integration of bottom-up and top-down signals in the process of perceptual filling-in. This chapter will now turn to an intriguing and relatively underexplored area of top-down processing of visual information; the influence of reward feedback on visual cortex activity in the absence of concurrent visual stimulation.

7.1.1 The effect of reward on visual task performance and visual cortex activity

Reward can influence performance and brain activity on tasks requiring sensory discrimination. For instance, in somatosensory discrimination tasks, reward modulates primary somatosensory cortex activity in both humans (Pleger *et al.*, 2008) and other mammals (Pantoja *et al.*, 2007). However, it is less clear whether (and how) reward can modulate activity associated with visual discriminations in visual cortices.

In humans, there is now some evidence that activity in visual cortex can be enhanced by reward expectation (Krawczyk *et al.*, 2007;Small *et al.*, 2005) and may track the value of visual stimuli during decision tasks (Serences, 2008). But these studies either did not assess how reward for performance in explicitly perceptual tasks affects

distinct identified areas within visual cortex (including retinotopically mapped regions)(Krawczyk *et al.*, 2007;Small *et al.*, 2005), or they did not dissociate the possible modulatory effects of reward or object value on visually evoked responses, from any impact of reward receipt *independent* of visual stimulation upon visual areas (Serences, 2008).

In this chapter, 3T fMRI was used in humans to examine whether and how rewards given for performance on a visual discrimination task can influence BOLD signals in different areas of human visual cortex. Participants were required to discriminate the orientation of two achromatic gratings presented successively in one visual field, while ignoring similar (but independently-oriented) gratings in the other visual field. Subjects received financial reward for each correct judgement only at trial end, as indicated by auditory feedback. Critically, in contrast to previous studies on the effects of reward or value on task performance and brain activity (Krawczyk et al., 2007;Small et al., 2005;Serences, 2008), the event-related fMRI design made it possible to distinguish BOLD signals associated with visual discrimination of the gratings from those attributable to later (non-visual) reward feedback. Furthermore, because retinotopic mapping of early visual areas V1-V3 was used, and lateralised representations of the visual targets within these areas were identified, it was possible to specifically assess any impact of the reward manipulations for early retinotopic regions, as well as for higher areas of visual cortex, during administration of rewards in the absence of any concurrent visual stimulation.

7.2 Materials and Methods

7.2.1 Participants

Twelve neurologically normal right-handed adults (20 to 32 years old, five females), with normal or corrected vision by self-report, gave written informed consent to participate in the study, which was approved by the local ethics committee.

7.2.2 Stimuli

Each visual display (see Fig. 7.1a) comprised two achromatic circular grating patches drawn from a set of similar gratings (see below). Each patch subtended 4 degrees in diameter (spatial frequency 3 cycles per degree, luminance 0.10 to 13.64 cd/m^2) presented in the left and right upper quadrants (one grating in each quadrant), at an eccentricity of 6.41 degrees (5 degrees along the horizontal meridian, 4 degrees vertically). The background was a uniform gray screen of luminance 3.66 cd/m^2. A central fixation point (black square measuring 0.4 degrees diameter, luminance 0.10 cd/m^2, with central white square, 0.2 degrees diameter, luminance 13.64 cd/m^2) was present throughout the experiment.

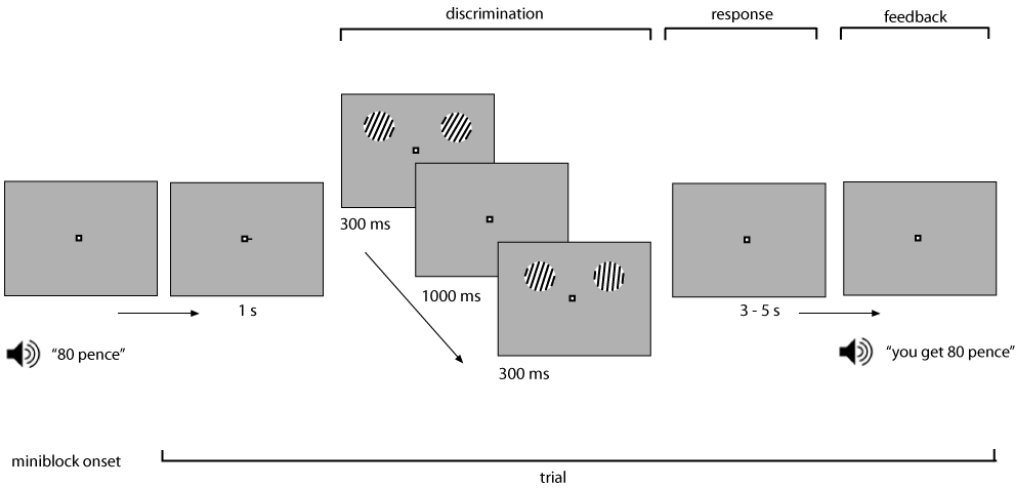

Figure 7.1. Procedure. Trials were grouped into short 'mini-blocks' of four with 2 possible reward levels: 10 pence or 80 pence per correct discrimination. At the onset of each mini-block, participants heard an auditory cue informing them of the reward level for that mini-block. The onset of each trial began with a small visual cue directing participants to attend covertly to either the left or right grating. Attended side remained constant throughout the mini-block. This was followed by the visual stimuli to discriminate: participants fixated centrally whilst attending to one side and were shown bilateral gratings for 300 ms, followed by a uniform grey screen, and then a further pair of bilateral gratings with different orientations. The task was to decide, for the attended side only, which display (first or second) contained the grating with the more vertical orientation. Participants were given 3-5 seconds to respond using a key press. This was followed by auditory feedback, informing participants of the amount won for a correct response, e.g. "You get 80 pence"; or for an incorrect response: "You get zero pence". Jittering the separation of reward delivery from the discrimination task, together with the different levels of reward and the rewarded or no-reward outcome, made it possible to dissociate haemodynamic responses that were specific to the delivery of reward from responses associated with the visual discrimination (see main text). The inter-trial interval was 3-5 seconds.

The stimulus set comprised ten different gratings orientated in steps of one degree (four subjects) or two degrees (eight subjects) away from vertical in either the clockwise or anticlockwise direction. Differences in orientation were determined on a per-participant basis to match individual performance levels, by means of pilot testing

implemented as a practice session in the scanner (without financial reward). Participants could only proceed to the main experiment if they achieved an accuracy of approximately 75% correct responses. The task was made easier or more difficult using larger or smaller orientation differences according to the participant's individual score during this initial piloting and pre-selection.

Stimuli were projected using an LCD projector (NEC LT158, refresh rate 60Hz, screen resolution 640x480) onto a circular projection screen at the rear of the scanner. Participants viewed the screen via a mirror positioned within the head coil. All stimuli were presented via MATLAB 6.5.1 (Mathworks Inc.), using the COGENT 2000 toolbox (www.vislab.ucl.ac.uk/Cogent2000/index.html). Auditory stimuli were recorded using a Behringer two channel mixer and presented using COGENT via etymotic headphones.

7.2.3 Procedure

Participants performed a temporal two-alternative forced-choice orientation-discrimination task (Fig. 7.1a). On each trial a pair of gratings was presented in the upper left and right visual fields for 300ms, followed after an interval of 1000ms by a second pair of gratings presented at the same location for 300ms (see Figure 7.1a). Participants were required to fixate centrally while attending either the upper-left or upper-right location, to discriminate which of the two gratings presented successively at that location (first or second) was oriented closer to vertical. Three to five seconds after presentation of the second grating (randomly jittered), participants received

auditory feedback indicating the amount won. This consisted of a recorded female voice informing them "you get 10 pence" or "you get 80 pence" following a correct discrimination, depending on the reward magnitude for that block; or "you get zero pence" for an incorrect discrimination. Thus, the visual discrimination phase of the trial, when the gratings were presented, was separated from the later reward-phase of the trial, when only auditory feedback was given. BOLD signal attributable to reward-phase feedback was decorrelated from that due to the visual stimulus presentation by including a temporal jitter of 3-5 seconds between visual stimulus and reward administration, by using different reward levels, and by titrating task difficulty to yield 60%-80% correct responses (and hence a large proportion of trials with no-reward feedback). The inter-trial interval was three to five seconds, again randomly jittered. Every correct response was followed by reward and every incorrect response by non-reward (0 pence), in order to maximise the learning effect of rewarded trials.

On each trial, the orientation of the first grating on the attended side was chosen randomly from the pool of possible orientations for that subject (see stimulus description above). The second grating on that side was chosen from the remainder of the stimulus set with the same direction of rotation. Thus, both gratings on one side were always oriented in either a clockwise direction, or an anti-clockwise direction, for any one trial. But the difference in orientation between the two successive gratings could vary, with two levels of discrimination difficulty. The stimuli consisted of easy (2-8 degrees difference in orientation) and difficult discriminations (1-2 degrees difference in orientation), titrated according to individual participants' ability, with equal numbers of trials in each group (easy or difficult). The orientation of the

gratings in each hemifield was always different, but otherwise independent. The difficulty factor was randomly assigned for each trial within a block.

Two magnitudes of possible financial reward were investigated: 10 or 80 pence for each correct discrimination. Each magnitude was tested for each hemifield over 40 trials in total for each participant. Four successive trials of a particular reward magnitude were grouped into mini-blocks, otherwise randomly determined. Each such mini-block also included one 'rest' trial. Rest trials consisted of only a uniform grey screen (luminance 3.66 cd/m^2) with a central fixation point but no gratings and no auditory feedback. The sequential position of the rest trials within each mini-block was assigned randomly.

The onset of each mini-block was signalled by an auditory cue ("10 pence" or "80 pence"), indicating the level of reward for each correct discrimination within that mini-block. This was followed by a visual cue directing participants to attend to either the left or right grating for all of the subsequent trials in that mini-block. This visual cue consisted of a small black horizontal bar (0.2 by 0.1 degrees, luminance 0.10 cd/m^2) immediately to either the left or right side of the fixation point.

Gratings were always presented in both the right and left hemifield, but participants were directed to attend covertly only to the one side that had to be judged (and was rewarded for a correct discrimination) in a given mini-block, by the small bar at the start of each such mini-block (see above), with side of covert attention decided randomly for each block. The brief grating presentations, at unpredictable

orientations, minimized any after-effects. Participants indicated their judgement using one or other of two possible button presses with their right hand.

Participants were reimbursed for participation according to the summed reward across 50% of randomly chosen trials, after scanning. Thus the financial rewards were real.

7.2.4 Functional MRI scanning

A 3T Siemens Allegra system was used to acquire T2*-weighted echo planar (EPI) images with BOLD contrast. T1-weighted anatomical images were acquired using a 1.5T Siemens Sonata system. Each EPI image comprised of forty 3-mm axial slices covering the whole cerebrum with an in-plane resolution of 3×3mm. The main experiment was split into five runs, each consisting of 243-260 volumes (duration of the run differed slightly between participants due to the jittering between stimulus presentation and feedback, and the intertrial jittering). The first five volumes of each run were discarded to allow for T1 equilibration effects. Volumes were acquired continuously with a TR of 2.4 s per volume.

The main experiment was followed by four further functional imaging runs to independently functionally localize the retinotopic representations of the peripheral gratings in particular, for subsequent region-of-interest (ROI) analyses (see below). Participants fixated centrally while viewing a circular checkerboard the same size and location as each grating in the main experiment (4 degrees diameter at 6.41 degrees eccentricity, 5 degrees across, 4 degrees up), contrast-reversing at 10Hz on a uniform

grey background (luminance 3.66 cd/m^2); see Fig 7.2(c). This checkerboard stimulus was presented for 5 volumes on either side, interleaved with rest periods lasting for 3 volumes with a uniform grey screen and no checkerboard displayed. That whole sequence was then repeated 8 times for each run. A central fixation point was present throughout, with fixation confirmed by eye-tracking, as for the main experiment also (see below). This stimulus localizer procedure comprised 140 volumes in total (fMRI sequence and parameters were identical to the main experiment). This was followed by two further runs to functionally localize the borders of retinotopic visual areas V1, V2 and V3. Flashing checkerboard patterns covering either the horizontal or vertical meridian (see Fig 7.2 (a)) were alternated with rest periods for five epochs of 10 volumes over two scanning runs, each lasting 155 volumes. Finally, a Siemens standard double-echo gradient-echo fieldmap sequence was acquired for distortion correction of the EPI images. (Echo times: 10.0 and 12.46 ms, TR = 1020 ms, matrix size = 64x64, 64 slices covering the whole head, voxel size = 3x3x3mm).

7.2.5 Eye tracking

During scanning, eye position and pupil diameter were continually sampled at 60Hz using long-range infrared video-oculography (ASL 504LRO Eye Tracking System, Mass) to ensure participants maintained fixation. Eye position was monitored on-line via a video screen, for all participants, and this confirmed good adherence to the fixation requirement. Eye position was recorded to disk and subsequently analyzed for six participants (see below), but was not stored for the other six due to technical problems.

7.2.6 fMRI whole brain analyses

Functional imaging data were analyzed using Statistical Parametric Mapping software (SPM5, Wellcome Trust Centre for Imaging Neuroscience, University College London). EPI images were corrected for geometric distortions caused by susceptibility-induced field inhomogeneities. A combined approach was used which corrects for both static distortions and changes in these distortions due to head motion (Andersson *et al.*, 2001;Hutton *et al.*, 2002). The static distortions were calculated for each participant by processing the fieldmap, using the FieldMap toolbox implemented in SPM5. The images were then realigned and unwarped using SPM5 (Andersson *et al.*, 2001), using procedures that allow the measured static distortions to be included in the estimation of distortion changes associated with head motion. Images were then spatially normalised to the standard template for the Montreal Neurological Institute (MNI), using the unified segmentation algorithm in SPM5 for spatial normalisation and smoothed with a Gaussian kernel (FWHM 10mm), in accord with the standard SPM approach.

Trial-specific regressors were created by generating delta functions that represented trial onsets for each of the combinations of attended hemifield (left or right) and reward magnitude (high or low) during the visual-phase of each trial; and for each of the combinations of attended hemifield (left or right), reward magnitude (high or low) and whether or not reward was given for the feedback-phase. These were convolved with a synthetic haemodynamic response. In addition, rest trials were modelled for

both the visual- and feedback phases to reduce residual error in the estimation of the event-related haemodynamic response function (Dale, 1999). Motion parameters defined by the realignment procedure were employed as six separate regressors of no interest. Data were high- pass filtered (cut-off: 0.0078Hz) to remove low-frequency signal drifts; the regressors were then entered into a multiple linear regression model, and parameter estimates determined for all brain voxels.

Appropriately weighted linear contrasts were conducted between the experimental conditions of interest, and corresponding parameters were estimated on a voxel-wise basis. The resulting set of t values constituted a Statistical Parametric Map (SPM{T}), which was assessed in two different ways. For the whole brain analyses, where there was a prior hypothesis, appropriate small volume corrections were used (using a threshold of $p<0.05$, corrected for multiple comparisons across the small volume examined) (Worsley, 2003) based on the PickAtlas (http://www.fmri.wfubmc.edu/cms/software#PickAtlas) to independently define anatomical regions of interest. These comprised subcortical areas previously described as being activated by reward, (specifically ventral striatum) (Elliott *et al.*, 2000;O'Doherty *et al.*, 2001;Knutson *et al.*, 2001); plus areas known to be activated by visual stimuli (specifically, the occipital lobe). For all other areas a more conservative correction was used across the whole brain volume at a cluster threshold of $p<0.05$, family-wise error corrected.

7.2.7 fMRI retinotopic analyses

In addition to whole-brain group analyses, activation was also examined within retinotopic regions-of-interest (ROIs) in early visual cortex, corresponding to the visual field locations of the visual stimuli, as separately localized. In accordance with standard practice, these analyses were carried out on an individual-participant basis without spatial normalisation and with a correspondingly smaller degree of spatial smoothing. Image volumes for each participant were realigned spatially to the first and resulting image volumes were coregistered for each participant to their own structural scan and smoothed with a Gaussian kernel (FWHM 6mm) to improve signal to noise. Trial-specific regressors were generated using the same procedure as in the whole brain analysis, followed by multiple linear regression (using SPM5, as above) to produce voxel-wise estimates of activation for each experimental condition.

To identify the boundaries of retinotopic visual cortices V1-V3, standard retinotopic mapping procedures were used (Sereno et al., 1995;Teo et al., 1997;Wandell et al., 2000). SPM5 was used to generate activation maps for the horizontal and vertical meridians. Mask volumes for each region of interest were obtained by delineating the borders between visual areas using activation patterns from the meridian localizers. Standard definitions of V1, V2 and V3 were followed, together with segmentation and cortical flattening using Freesurfer (http://surfer.nmr.mgh.harvard.edu/). Please note that for all ROI analyses, only 11 (out of a total of 12) participants were included, as one participant had moved between the main functional experiment and the localiser experiment such that their occipital pole was mislocated to lie outside the range of the main scanned volume.

The mask volumes for V1, V2 and V3, in conjunction with the functional localizer images for stimulus-responsive regions, were used to identify voxels showing significant activation (T = 2.5, with some variability across participants to ensure contiguous collection of voxels) for the comparison of trials where the target localizer was present, compared to rest periods, using the regression analysis described above. This comparison identifies voxels activated by the grating stimulus in each of the retinotopic areas as determined by the independent meridian mapping procedure. The final analytic step was to extract from these independently defined ROIs the regression parameters for each experimental condition arising from the analysis of the main experimental time-series. These were averaged across participants, yielding estimates of percentage signal change for each condition, averaged across voxels in V1, V2 or V3 that responded to the visual field location corresponding to the gratings for every participant.

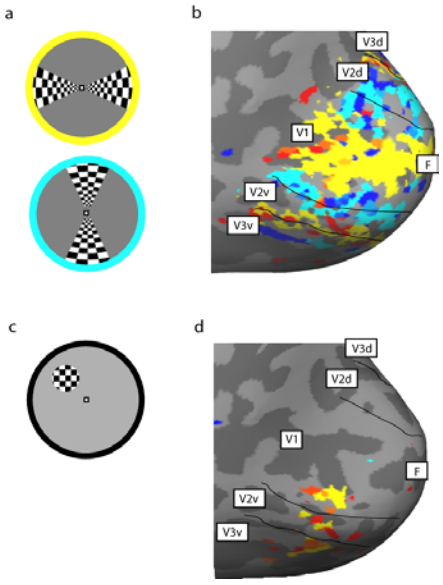

Figure 7.2. Stimulus representation in visual cortex (a) Illustration of flickering checkerboard visual stimuli used to map the horizontal and vertical meridians. **(b)** The outline of individual visual

areas V1, V2d, V3d, V3v and V3d determined using meridian mapping are shown on the surface of the right hemisphere for a representative participant. **(c)** Illustration of the flickering visual stimulus used to localise the stimulus responsive ROI within retinotopic cortex as appropriate for a left-sided grating, using a checkerboard at the visual field location of interest. An equivalent checkerboard was presented within the right visual field instead, to localise the stimulus-responsive ROI for a right-sided grating. Note that the actual visual stimulus may have differed slightly in greyscale value and the checkerboard is not shown to scale. **(d)** Regions of interest (ROIs) in visual cortex representing the spatial location of the peripheral target were identified by combining functional localizer images with masks delineated for V1-V3 for each participant individually. The spatial distribution of target-specific stimulus evoked activity (contrast of ROI localizer presented on left versus right side, threshold t=2.5) is shown projected onto the inflated surface of the posterior aspect of the right hemisphere, for a representative participant.

The statistical significance of any differences in activation during the main experiment within the ROIs defined by the independent localiser scans was assessed with separate repeated-measures ANOVAs, with condition (attended side, reward level, reward received or not) as repeated factors, for each of the ROIs in V1, V2 and V3 separately.

7.2.8 Eye tracking analysis

Eye-tracking data recorded during scanning were analyzed with MATLAB 7 (Mathworks Inc., Sherborn, MA). Blinks and periods of signal loss were removed from the data. Mean eye position in the horizontal and vertical directions relative to fixation was then computed separately for the visual- and reward-feedback phase of each trial within each condition. A positive value in the horizontal direction indicated

a shift into the right hemifield. A repeated-measures ANOVA, was used to establish whether mean eye position deviated significantly between conditions.

7.3 Results

7.3.1 Behavioral data

Increased monetary reward was associated with improved accuracy of visual discrimination for easier trials ($t(11)=2.3$, $p=.048$), but not for the most difficult trials where the difference in orientation between successive gratings was smallest ($t(11)=0.46$, $p=.65$); see Fig 1b. The accuracy of visual discrimination did not differ between right and left hemifields ($t(11)=0.87$ $p=.44$, ns); see Fig 7.3c.

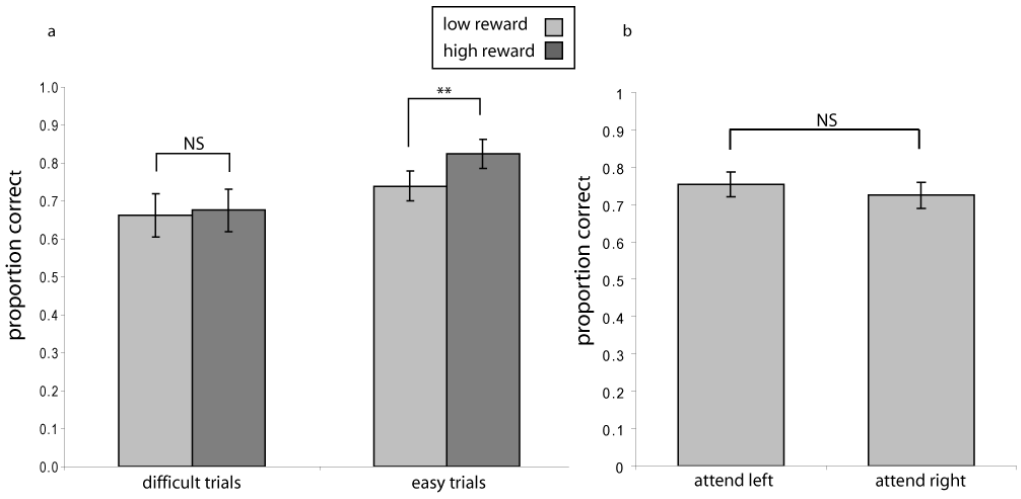

Figure 7.3 (a) Higher reward levels were associated with improved accuracy in the visual discrimination task for the easier but not the hardest trials. **(b)** There were no differences in accuracy for visual discrimination of gratings attended in the left or right hemifields. Error bars = one standard

error of the difference between paired conditions. The symbol '**' indicates statistical significance ($p<.05$, 2-tailed paired t-test), NS, not significant.

The effect of receiving a reward on a given trial on the discrimination accuracy of a subsequent trial was also considered (Pleger *et al.*, 2008;Pleger *et al.*, 2009). There was an increase in the conditional probability of the next trial being correct after receiving a reward on the previous trial, compared to not receiving a reward on the previous trial ($t(11)=2.36$, $p=.038$, 2-tailed t-test); see Fig 7.4. This pattern did not significantly differ for higher versus lower rewarded trials ($F(1,11)=0.11$, $p=.75$, n.s).

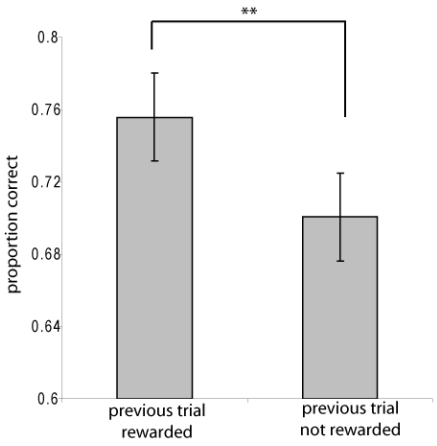

Figure 7.4 Trial-to-trial effects of receiving reward. (a) Behavioral results. Receiving reward was associated with improved accuracy on the subsequent trial, compared to after a trial that had not been rewarded. Group means of 12 participants are shown. Error bars indicate the standard error of the difference between paired conditions and the symbol '**' indicates statistical significance. ($p<.05$, 2-tailed paired t test).

7.3.2 Functional MRI data

Three related sets of analyses were performed on the data. These focused on the visual discrimination phase of each trial, the reward phase and finally on trial-to-trial

effects. In each case the convention is used of reporting ROI-based results in retinotopic visual cortical areas V1-V3 first, followed by results from the whole-brain analyses outside these retinotopic areas.

7.3.2.1. Visual discrimination phase

The visual discrimination phase consisted of presentation of lateralised grating stimuli, one of which (the attended side) was discriminated. No reward feedback (for correct versus incorrect trials) was presented during this phase, though it would be possible to anticipate the overall level of reward that could be gained as participants were aware whether that trial was in a high or low reward block. It was therefore anticipated that retinotopic effects of spatial attention would be found in visual cortex for the ROI-based analyses, but no effect of future reward (i.e. correct versus incorrect trials) would be seen, and there were no specific hypotheses regarding the effects of reward anticipation.

Comparing the effect of attending to the left or right grating revealed a main effect of attention for contralateral (versus ipsilateral) attention in the retinotopic representations of the stimulus location in V1 ($F(1,10)=16.0$, $p=.003$), V2 ($F(1,10)=19.3$, $p=.001$) and V3 ($F(1,10)=26.1$, $p<.005$); see Fig. 7.5. This is consistent with previous findings (e.g. (Kastner et al., 1998;Martinez et al., 1999a;Buchel et al., 1998;Silver et al., 2007). There were no effects of contralateral (versus ipsilateral) attention outside retinotopic cortex on whole-brain analysis (all $p>0.05$, corrected for multiple comparisons).

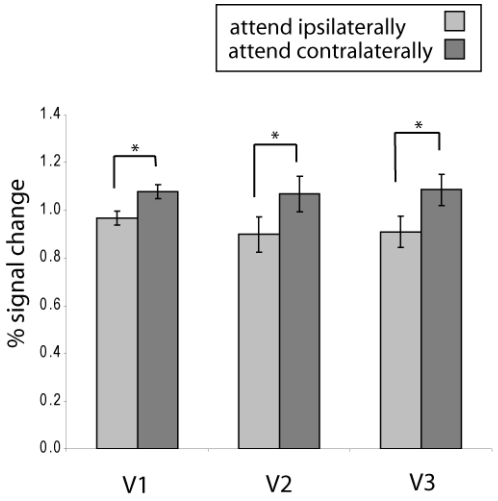

Figure 7.5 Differences in brain activity during visual discrimination. BOLD signal change (percent relative to the global mean) averaged across 11 retinotopically mapped participants, for the ROIs responding to the grating stimuli in V1, V2, V3 during the visual-discrimination phase of the trial. Responses are plotted separately for gratings attended in the contralateral or ipsilateral hemifields. Error bars are standard error of the difference between paired conditions and the symbol '*' indicates statistical significance ($p<.05$, 2-tailed paired t-test).

During the discrimination phase of the trial, participants had not yet been informed whether they were correct (or not) and so did not know whether they would receive a reward on that trial. Consistent with this, no differences in activity were detected (all $p>0.4$ in retinotopic ROIs) in the discrimination phase on trials that would later be rewarded (i.e. correct) versus not rewarded (i.e. incorrect). Similarly, there were no significant differences in activity in visual cortex on whole-brain analysis outside retinotopic visual cortex (all $p>0.1$, corrected).

Finally, significant differences in brain activity were identified comparing the discrimination phase of trials in high (versus low) reward blocks, irrespective of whether those trials would be rewarded during the feedback phase. In retinotopic

ROIs there was no main effect of anticipated reward level in V1, but there was a main effect of reward level in V2 ($F(1,10)=5.7$, $p=.038$) and a trend in V3 ($F(1,10)=3.5$, $p=.09$) Outside retinotopic cortex, whole-brain analysis revealed significant activation within the ventral striatum (coordinates [-12 20 0], $t=4.22$, $p=.039$ small-volume corrected), left superior temporal gyrus (coordinates [-60, 12, 2], $t = 5.37$, $p<.005$ fwe-corrected), left cingulate gyrus (coordinates [-8, 18, 42], $t=5.21$, $p=.005$ fwe-corrected) and right inferior frontal gyrus (coordinates [48, 26, -6], $t=4.56$, $p=.025$ fwe-corrected). There was also an interaction between easy and hard difficulty level and reward level in V1 ($F(1,10)=5.1$, $p=.048$), resembling the interaction observed in the behavioral data (see Fig. 7.3a).

Taken together, these findings are consistent with attentional modulation of stimulus representations in visual cortex during task performance, which may partially relate to the reward value of the perceptual discrimination in the different reward conditions (see also (Serences, 2008)). Importantly, the inability to identify any significant difference between correct (rewarded) and incorrect (non-rewarded) trials at the point of discrimination suggests that any effects in visual cortex seen at the later phase of (non-visual) reward delivery (see below) do not reflect an attentional or value-modulation difference between trials that are later rewarded and not rewarded.

7.3.2.2. Reward feedback phase

The effect of reward during the (non-visual) reward-feedback phase of each trial was examined next. Note that during this phase of the trial, participants were given

auditory feedback via headphones whilst viewing a grey screen (present throughout the experiment), but were not shown any visual stimuli. As there was no visual stimulation during this phase, it was hypothesised that any effects of lateralised attention from the earlier part of the trial would be minimal. The specific interest in these analyses focused on any differences between correct (rewarded) and incorrect (not-rewarded) trials, which now became apparent to participants at this phase of the trial, plus any effects of high (versus low) reward.

In retinotopic cortex, stimulus-responsive ROIs did not show any significant ($p<0.05$) main effect of reward (versus no reward) in V1, V2 or V3 (see leftmost three bars in Fig. 7.6b). There was also no main effect of attention (contralateral versus ipsilateral), nor interactions between reward and attention for the ROIs in V1 and V2. For the ROI in V3, there was a main effect of attending to the contralateral side during the feedback period ($F(1,10)=9.9$, $p=.01$) and an interaction between reward and side attended ($F(1,10)=13.4$, $p=.004$), suggesting that reward had some lateralised effects on V3 that could not be identified in V1 and V2.

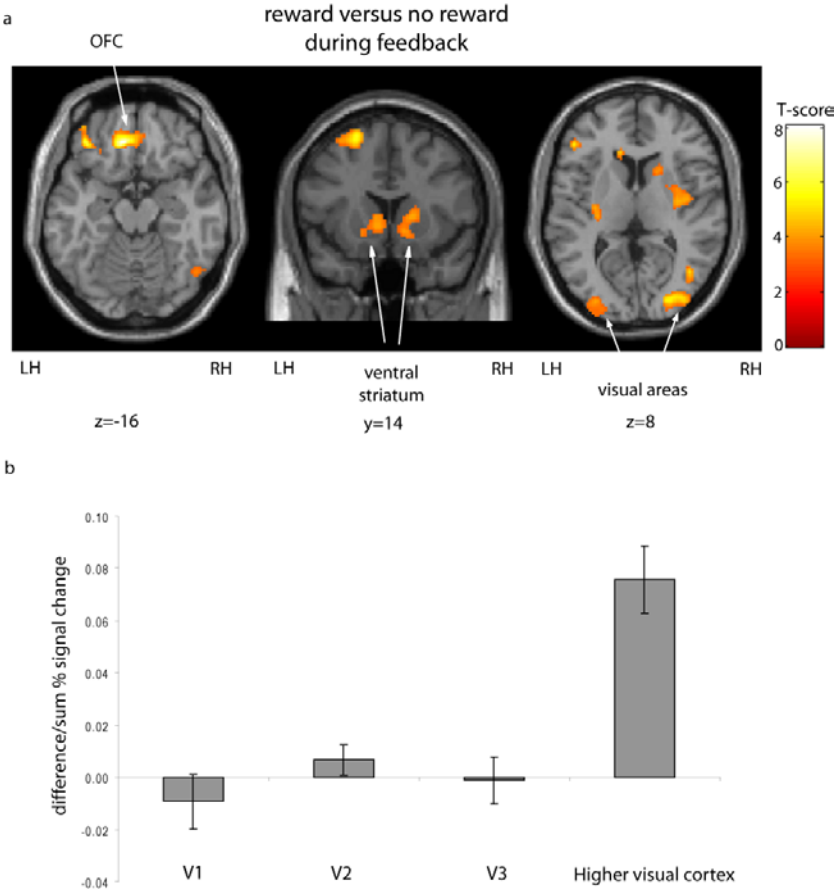

Figure 7.6 Changes in brain activity during reward feedback. (a) Whole brain analysis reveals cortical regions showing increased BOLD signal for rewarded versus non-rewarded trials, during the (auditory) feedback-phase of the trial. Activations are projected onto axial, coronal and axial MRI slices of a T1-weighted canonical brain, thresholded at p<.005 uncorrected for display. See Results for coordinates, p-values and t scores. **(b)** In visual ROIs, the difference in percent signal change between rewarded versus non-rewarded trials is shown, divided by the sum of activation for the ROIs in V1, V2 and V3 and for higher visual cortex (as identified on whole brain analysis). Error bars are standard error of the difference between paired conditions

In contrast to these effects of reward (versus no reward) on retinotopic cortex, whole brain analysis revealed many more areas responding differentially to reward (versus no reward). Importantly, activation of higher visual areas beyond retinotopic cortex was found (coordinates [28, -88, 8], t=5.41, p=.005 and [-30, -88, 6], t=4.35, p=.046,

small volume corrected; see Fig 7.6). The visual areas activated by this contrast (rewarded versus unrewarded trials during non-visual feedback) were lateral and anterior to the ROIs in V1-V3 (see Fig. 7.7). The peak coordinates ([-30, -88, 6] and [28, -88, 8]) fell within the range of area LO1, a region of the lateral occipital complex which shows robust orientation-selective adaptation to gratings defined by luminance, contrast and orientation cues (Larsson and Heeger, 2006;Larsson et al., 2006). It is therefore likely that the regions activated during the feedback period of rewarded trials are close to, or within, part of the lateral occipital complex.

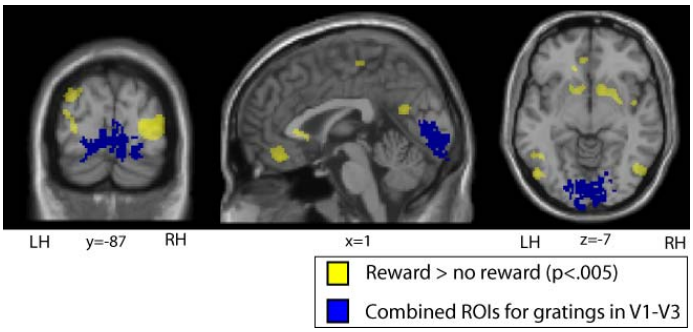

Figure 7.7 Cortical regions showing increased BOLD signal for rewarded versus non-rewarded trials during the feedback phase of the trial (threshold: p<.005 uncorrected) shown in yellow, along with the combined ROIs for the gratings in V1, V2 and V3 for 11 participants (shown in blue), all projected onto coronal, sagittal and axial MRI slices of a T1-weighted canonical brain at the coordinates shown. Note that the regions responding to rewarded trials are anterior and lateral to the regions responding to the gratings within V1-3.

In addition to these visual areas anterior to V1-V3, significant activation was also identified for rewarded trials (versus unrewarded trials) in left ventral striatum, an area previously associated with reward and reward prediction (Elliott *et al.*, 2000;O'Doherty *et al.*, 2001;Knutson *et al.*, 2001) (coordinates [-6, 14, -2], t=4.09, p=.049 and [16, 16, 4], t=4.04, p=.099 small volume corrected; see Fig 7.6a).

Differential reward-related activation was also detected in orbitofrontal cortex (coordinates [-8, 38, -16], t=8.06 p=.067, fwe corrected on whole brain analysis). A full list of areas activated by the contrast of reward (versus no reward) is given in Table 7.1.

Location	**Coordinates [x,y,z] (MNI space) of peak voxel**	**Number of voxels in cluster**	**T value**	***p* value**
Orbitofrontal cortex	-8, 38, -16	461	8.06	.067
Ventral striatum: left	-6, 14, -2	112	4.09	.015*
right	16, 16, 4	61	4.04	.033*
Right putamen	32, -10, 4	786	6.74	.005
Left middle frontal gyrus	-22, 14, 62	681	5.63	.012
Left superior parietal lobe	-28, -68, 48	573	5.13	.027
Right visual region	28, -88, 8	524	5.41	.005*
Left visual region	-30, -88, 6	286	4.35	.046*

* small volume corrected (see Methods).

Table 7.1. Reward versus no reward during (auditory) feedback phase

Finally effects of reward magnitude (high versus low reward) in either retinotopic cortex or on whole brain analysis were considered. No significant (all p>0.05) differential activation was found for this contrast in retinotopic ROIs. On whole brain analysis significant activation was identified in left precuneus (coordinates [-14, -46, 34], t=6.52, p<.005 fwe-corrected), in the left substantia nigra (coordinates [-10, -20, -16], t=5.59, p=.001 fwe-corrected) and left medial frontal gyrus (coordinates [0, 40, 42], t=3.86 p=.017 fwe-corrected).

Importantly, several aspects of the design and results presented thus far argue against purely 'attentional' interpretations of the observed reward effects, or interpretations based on previously observed 'value-based' modulations (Serences, 2008). First,

there was no effect of correct/incorrect in higher visual areas during the discrimination phase of the trial (see above), when participants viewed the gratings and effects of contralateral attention were observed. Thus any differences between reward/ no reward during non-visual reward feedback could not have arisen due to a carry-over of generalised alertness, increased attention, or value-based processing increases during the visual discrimination task. Second, during the feedback-period, visual input did not differ between conditions, as the feedback was always given auditorily, with participants merely fixating an unchanging point on an otherwise uniform grey screen.

Taken together, these data show that in the reward phase of the trial, the most prominent effects of reward (versus no reward) were observed not in retinotopic ROIs, but in bilateral retinotopic visual cortex immediately anterior to V1-V3 (consistent with the putative anatomical location of LO1), plus areas of striatum and prefrontal cortex previously implicated in reward processing.

7.3.2.3. Trial-to-trial effects

Finally, the effect of receiving a reward on a given trial on brain activity on a subsequent trial was considered (Pleger *et al.*, 2008;Pleger *et al.*, 2009) given the behavioral findings above that reward improved discrimination accuracy on a subsequent trial. The trial-to-trial impact of receiving reward was linked to BOLD activity in visual cortex during the visual-discrimination-phase for the next trial (cf.(Pleger et al., 2008), for a somatosensory analogue). In retinotopic visual cortex, the ROI analysis revealed a significant interaction between the direction of attention

(contralateral versus ipsilateral) in the discrimination phase of a trial, and whether the previous trial had been rewarded (or not) in V1 ($F(1,10)=5.42$, $p=.042$). Paired t-tests confirmed that this interaction was driven by higher responses for contralateral compared to ipsilateral attention in the previously rewarded trials ($t(1,10)=2.3$, $p=.043$ and $t(1,10)=1.075$, $p=.31$ for contralateral compared to ipsilateral attention in the previously non-rewarded trials; see Fig.7.8 for plot of activity evoked in each condition).

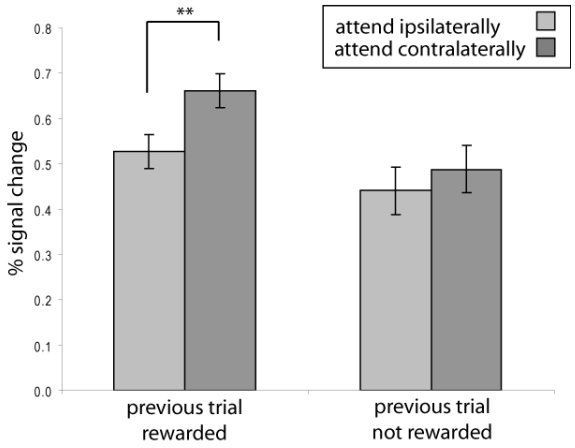

Figure 7.8 Effect of rewarded trials on percent signal change in V1. BOLD signal change (percent relative to the global mean) averaged across 11 retinotopically mapped participants, for the V1 stimulus-responsive ROI, during the visual-discrimination phase of the trial, shown for trials subsequent to reward receipt, or to non-reward, separately when attending to ipsilateral or contralateral gratings. Note that for trials preceded by reward receipt, there is a greater difference in percent signal change between attending to a contralateral versus ipsilateral grating, than after unrewarded trials. Error bars indicate the standard error of the difference between paired conditions and the symbol '**' indicates statistical significance ($p<.05$, 2-tailed paired t test).

No similar interactions were found either in V2 ($F(1,10)=0.80$, $p=.39$) or V3 ($F(1,10)=0.02$, $p=.9$). Similarly, on whole brain analysis, there were no significant clusters of activation for this interaction of previously rewarded trials with attended

side. Critically, this effect of reward (vs no reward) was not seen in retinotopic visual areas during the feedback phase of the trial itself. This suggests that reward administration on the previous trial affects subsequent BOLD responses of retinotopic areas to visual stimuli specifically at the previously rewarded location, rather than resulting in general feedback-related activity to retinotopic visual areas. This argues against accounts of the findings in terms of general resetting signals related to trial end (Jack et al., 2006), or carry-over effects from the reward phase of previous trials, which would not be spatially specific.

Taken together, these data show that receiving reward was associated with improved performance on a subsequent trial and significantly enhanced activity on that subsequent trial in attended stimulus-specific representations in primary visual cortex.

7.3.3 Eye tracking analysis

Long-range infra-red eye tracking confirmed there were no significant differences (all $p>.3$) between different trial types in mean eye position in the horizontal direction (our stimuli were arranged horizontally), neither in the discrimination phase nor the reward phase of the trial.

Pupil size was slightly but significantly larger during unrewarded compared to rewarded trials in the reward feedback phase (2.1% larger in the unrewarded trials, $F(1,5)=7.5$, $p=.04$). Note that this difference cannot account for the changes in BOLD signals observed during the feedback phase, which were in the opposite direction (i.e. greater BOLD signal on rewarded versus unrewarded trials, while the pupil size

differences observed would result in slightly *less* retinal illumination on rewarded versus unrewarded trials).

	Condition	Mean eye position x direction (degrees) (± SEM)	Mean eye position y direction (degrees) (± SEM)	Mean pupil size (% compared to mean) (± SEM)
Discrimination	Low reward level attend left	-0.01 (0.43)	0.12 (0.15)	99.5 (0.61)
	Low reward level attend right	-1.18 (1.95)	0.92 (0.64)	99.1 (0.70)
	High reward level attend left	0.94 (0.42)	0.38 (0.22)	99.4 (0.40)
	High reward level attend right	0.77 (0.35)	0.57 (0.35)	98.9 (0.72)
Feedback	Rewarded Low reward level attend left	-1.38 (1.73)	0.29 (0.61)	99.3 (0.31)
	Rewarded Low reward level attend right	-0.12 (0.49)	-0.27 (0.31)	99.9 (0.87)
	Rewarded High reward level attend left	1.96 (1.68)	-0.06 (0.41)	99.6 (0.36)
	Rewarded High reward level attend right	0.45 (0.27)	0.21 (0.49)	98.6 (0.79)
	Not rewarded Low reward level attend left	-0.48 (0.58)	-0.11 (0.31)	101.2 (0.96)
	Not rewarded Low reward level attend right	1.07 (0.46)	0.26 (0.39)	102.1 (1.1)
	Not rewarded High reward level attend left	-0.44 (1.0)	0.42 (0.94)	102.0 (1.0)
	Not rewarded High reward level attend right	0.80 (0.99)	0.20 (0.88)	100.5 (1.2)

Table 7.2 Eye position data. Mean eye position for six participants in the vertical (x) and horizontal (y) position from fixation, measured in visual degrees and mean pupil

size (measured as % compared to the mean for all trials) for each condition at each phase within a trial. SEM is standard error of the mean.

7.4 Discussion

In this chapter, brain activity associated with lateralised visual discrimination was dissociated from brain activity associated with subsequent (non-visual) receipt of financial reward, as signalled by auditory feedback; and from the influence of reward receipt upon brain activity for the subsequent trial. Activity in parts of visual cortex was found to be modulated at all three of these successive phases, but the anatomical locus and nature of these modulations had a specific relationship to different processes associated with visual discrimination and reward.

During visual discrimination (before reward delivery), activity in retinotopic ROIs representing the visual gratings was modulated by spatial attention, in accord with previous findings that retinotopic cortex can be modulated by spatial attention during task performance. For retinotopic areas, anticipation of high (versus low) reward modulated activity only in V2 (with a trend in V3); whereas higher visual areas (anterior to retinotopic areas V1-V3) showed no effects of reward level during the visual-discrimination phase (when attentional effort associated with reward incentive might conceivably have arisen, but did not). Furthermore, there were no effects of correct (versus incorrect) discrimination in any visual areas during visual discrimination, suggesting that any effects of reward (and correctness) seen during the

feedback-phase of the trial were not due to a carry-over of differences in signal arising during discrimination.

As the trial progressed, auditory feedback signalled reward when no visual stimuli were present. Although there were no differences in visual stimulation at this point (in contrast to previous observations of reward/value modulations of sensory processing (Krawczyk et al., 2007;Small et al., 2005;Serences, 2008)), significant activity increases were nevertheless observed in higher visual areas for rewarded versus non-rewarded trials. The signals in higher visual areas reflect a categorical effect of reward or reward valence feedback, rather than just trial end, or resetting (Jack et al., 2006) as that would affect correct and incorrect trials equally. Moreover, the signals seen in this study are associated with activity in ventral striatum and OFC, regions activated by reward.

The higher visual areas activated for rewarded versus non-rewarded trials were anterior and lateral to retinotopic V3 (Fig 7.7), overlapping with coordinates identified previously as part of the lateral occipital complex (Larsson and Heeger, 2006). This area is sensitive to the orientation of gratings (Larsson *et al.*, 2006) similar to those used in the current study, but its responses are not strongly lateralised with respect to field of presentation. The observation of feedback-associated activation of this area may therefore be consistent with effects of reward on neural representations of oriented stimuli at this intermediate level of visual processing. In contrast, no effect of reward (or reward level) was found on earlier (lateralised) retinotopic representations, in areas V1 and V2 that are known to contain neural populations selective for stimulus orientation (Hubel and Wiesel, 1968;Kamitani and

Tong, 2005). These observations thus indicate both that reward feedback can modulate higher visual cortex even in the absence of visual stimulation, and that its effects on neural populations representing a stimulus differ qualitatively at different levels of the visual system.

7.4.1 Comparison with previous studies of reward influences on visual processing

The findings presented here provide new evidence that parts of human visual cortex can be modulated by reward feedback, even when this is delivered non-visually. In addition to modulating visual cortex, the comparison of reward and non-reward feedback also activated ventral striatum and orbitofrontal cortex. These areas are consistently activated in a variety of reward paradigms (Elliott *et al.*, 2000;O'Doherty *et al.*, 2001;Knutson *et al.*, 2001), confirming their role as key nodes in a reward network. The findings that reward also affects visual cortex are consistent with a small, emerging number of studies exploring possible impacts of reward for mammalian visual cortex. For example, pairing a visual stimulus with subsequent reward leads to a proportion of neurons in rat primary visual cortex expressing activity that predicts reward timing (Shuler and Bear, 2006). In humans, reward is associated with improved visual performance (Seitz *et al.*, 2009) and visual cortex activity is increased by reward expectation (Krawczyk *et al.*, 2007;Small *et al.*, 2005). However, unlike the present work, those recent studies did not dissociate reward feedback from the visual discrimination itself, and therefore did not demonstrate that non-visual reward signals per se can evoke visual cortex activation.

This work also differs fundamentally from previous work in non-human primates showing that neurons in parietal cortex represent the value of competing choices (Sugrue et al., 2004;Platt and Glimcher, 1999) and a recent fMRI study in humans showing value-based modulation as early in the visual processing pathway as V1 (Serences, 2008). Those studies characterised the effects of value tied to a particular stimulus or region of space, whereas in the study presented here, the effects of overall reward magnitude in visual cortex were examined (analogous to (Pleger et al., 2008) in the somatosensory domain). The design of the study presented here also made it possible to examine the effects of reward feedback and how this influenced discrimination ability on subsequent trials, rather than just the effects of reward magnitude at the time of choice.

7.4.2 Possible mechanisms for reward feedback to visual cortex

This study shows for the first time that non-visual reward feedback following visual discrimination can lead to enhanced BOLD signals in (higher) visual cortex. Such signals may reflect a 'teaching signal', possibly propagated via feedback connections from areas involved directly in reward processing and involving neuromodulators such as dopamine (see (Pleger *et al.*, 2009)) and noradrenaline. This study thus suggests a hypothesis that could be formally tested in future studies, using effective connectivity analysis in conjunction with pharmacological manipulations. Dopamine is released following stimuli that predict reward,(Romo and Schultz, 1990) and noradrenergic neurons may respond to unpredicted more than predicted rewards (Foote *et al.*, 1980;Aston-Jones *et al.*, 1994). Although dopaminergic innervation of

the visual cortex is relatively sparse (Berger *et al.*, 1988), even primate visual cortices receive at least some dopaminergic fibres (Berger and Gaspar, 1994). Feedback messages carried by dopamine and/or noradrenergic neurons might influence the efficacy of synaptic transmission, providing a potential mechanism for how behavioral learning via reward feedback (Schultz and Dickinson, 2000) may result in improved visual perception, via enhanced sensitivity to relevant stimulus features.

7.4.3 Trial-to-trial effects of reward

Attention directed to the lateralised gratings modulated retinotopic activity during discrimination, but no evidence was found for lateralised modulation by reward signals in V1 or V2 (which instead were associated with bilateral modulation of higher visual areas and lateralised modulation in V3). What mechanisms could explain how reward signals delivered to higher visual areas might subsequently influence neural activity associated with task performance in a lateralized discrimination? One possibility is that the neuronal representations modulated in higher visual cortex have some critical role in task performance (potentially consistent with their role in representing orientation, see (Larsson *et al.*, 2006). But the data presented here also provide tentative support for an alternative mechanism: Receiving reward on the preceding trial was associated with improved accuracy for the visual discrimination on the subsequent trial, indicating a trial-to-trial behavioral effect of reward. Moreover, during the visual-discrimination phase of the next trial following a rewarded trial, enhanced BOLD signals were found associated with the stimulus representation in primary visual cortex contralateral to the attended grating (see Fig

7.8). This indicates that receiving a reward at the end of one trial (which affects higher visual cortex) was associated not only with more accurate visual discrimination on the next trial, but also with enhanced signals in lateralised early retinotopic cortex representing the task-relevant stimulus during the discrimination phase of the next trial. Thus, the reward signals observed in higher visual areas during the reward phase of a trial may lead to interplay between those higher visual areas and lateralised stimulus representations in earlier visual cortex that process the task-relevant stimulus on a subsequent trial. Such an account remains possible rather than proven, but might be tested in future variations of this paradigm, e.g. with causal interventions such as transcranial magnetic stimulation, targeting specific visual areas at different timepoints during and between trials.

7.4.4 Comparison with previous studies showing effects of reward on somatosensory processing

The work presented here may be compared to the effects of reward feedback on somatosensory cortex (Pleger *et al.*, 2008;Pleger *et al.*, 2009). These showed lateralised reactivation of primary somatosensory cortex during reward feedback, unlike the study presented here which shows bilateral activation of higher visual areas, with effects contralateral to the stimulus only for the subsequent trial. It is possible that the differences between these studies reflect differences in the architecture by which reward signals affect different sensory cortices (possibly due to anatomical proximity of somatosensory cortex to reward areas, different levels of dopaminergic innervation, and/or a more hierarchical organisation of processing in

visual cortex). Alternatively, the differences may reflect the specific task and stimuli in each experiment. Although the task presented here was intended to be optimised for evoking primary visual cortex responses, it is possible that discriminating the orientations of two gratings presented sequentially requires input from higher visual areas (Larsson *et al.*, 2006), that may be more efficient for sustained representation. The role of learning might also differ, as in the current study there were larger numbers of possible combinations of gratings in the task, than for the somatosensory stimuli used in (Pleger *et al.*, 2008). Finally, the somatosensory studies found effects of reward magnitude on signals in human primary somatosensory cortex which may reflect increased power, as these studies used four different levels of reward whereas this study used two levels. But despite these differences, there were also clear similarities between the two studies, including: responses of ventral striatum and orbitofrontal cortex to reward, clear findings that sensory cortices (whether somatosensory or visual) can be affected by reward feedback, and presence of trial-to-trial effects, whereby receipt of reward on one trial led to an enhanced response in contralateral primary cortex for the discrimination-phase of the next trial, as well as to better performance.

7.5 Conclusion

In this chapter, evidence has been presented for top-down reward-associated feedback signals in higher visual areas, even without concurrent visual stimulation, and also that rewarded trials are associated with improved behavioral performance and increased activity in human primary visual cortex during the discrimination period of

a subsequent trial. I have thus provided new evidence consistent with a teaching signal being propagated (possibly from ventral striatum and/or orbitofrontal cortex) to higher visual areas, and ultimately impacting on contralateral primary visual cortex during discrimination for the next trial after reward receipt. Having documented such influences of rewarding visual discrimination in the human brain, further work is now needed to characterise whether these influences may be task-dependent, or reflect a more general architecture for reward influences on visual processing.

CHAPTER 8: GENERAL DISCUSSION

8.1 Introduction

The experimental studies in this thesis explore the integration of bottom-up and top-down signals in visual processing of perceptual filling-in, where the visual system interpolates information across visual space where that information is physically absent; and in the processing of reward feedback in the absence of concurrent visual stimulation. This general discussion will review the findings of the experimental chapters and will consider the implication of these findings in the context of normal perception and in visual perception following damage to visual structures. Finally I will consider further experimental studies that could be used to test hypotheses generated from the studies presented here. The experimental studies can be grouped according to whether they examine the perceptual completion of artificial scotomas (Chapters 3,4,5), hemianopic completion (Chapter 6) or the influence of reward on visual processing (Chapter 7).

8.2 Perceptual filling-in of artificial scotomas

The first part of this thesis is concerned with perceptual filling-in of artificial scotomas. These occur when a uniform target is placed in the near periphery on the background of dynamic twinkling noise. After a few seconds of central fixation, the target will perceptually fill-in to be replaced by the background. The neural processes

involved in this form of perceptual completion are not yet clear. Detection thresholds for Gabor patches presented within artificial scotomas are elevated by dynamic noise surrounds (Mihaylov *et al.*, 2007) and during Troxler fading observers are less able to detect a probe presented within a perceptually filled-in target (Lleras and Moore, 2006). These findings are consistent with suppression of neural responses during perceptual filling-in, although this has not previously been measured in humans during perceptual completion of artificial scotomas.

8.2.1 Neural responses during perceptual completion of artificial scotomas measured using MEG

Chapter 3 examined neural responses during perceptual completion of an artificial scotoma using MEG. By tagging the target at a known frequency, responses specific to that target could be examined. In this way a fundamental problem of investigating filling-in was circumvented, as it is often unclear whether recorded responses are related to the filled-in target or to the background. The major finding was that responses specific to the target were reduced when the target was perceptually filled-in, consistent with stronger neural representation for visible compared to invisible stimuli and suggesting that perceptual filling-in is associated with suppression of neural responses. Although the spatial resolution of MEG is too to low detect whether these responses were specific to the spatial location of the target, these findings are consistent with the isomorphic theory of perceptual filling-in, as they demonstrate that responses specific to the frequency of the flickering target are reduced during the experience of perceptual completion and that perceptual filling-in is an active (albeit suppressive) process.

This reduction in responses during perceptual filling-in may reflect a reduced neural response to a now invisible target. Alternatively, the suppression of responses from the target might be causing it to become invisible. Disentangling whether the reduction in responses to the invisible target is the cause or effect of it becoming invisible has important implications for understanding the processing of invisible stimuli. Does a target become invisible, causing a reduction in target-specific neural responses or does the process of perceptual filling-in cause a suppression in neural responses, which causes it to become invisible? This might be addressed by exploring more closely the timecourse of responses following perceptual filling-in but this is limited by the current methods. Unlike for a visible stimulus, when the exact time of presentation is known by the experimenter, the point when a target becomes invisible due to filling-in is known only by the participant. He or she can communicate this using for example button press responses, but these are inherently delayed compared to the time point of invisibility. It is therefore not possible to determine accurately the time at which a target becomes invisible. It might be possible to approximate this by using participant-specific reaction times to determine as closely as possible the point at which the target fills-in and then examine the power of stimulus-specific responses before and after the point of transition between the target being visible and filled-in as has been done previously (Scholvinck and Rees, 2009b). However, this remains an approximation and would still be unlikely to be accurate enough to shed light on the temporal unfolding of the neural responses at the point of transition from visible to invisible.

A second important finding of the experiment in Chapter 3 was that although the responses to the target were reduced after it became invisible, they were still greater than a no-target baseline. This is consistent with a persistent neural representation for the now invisible stimulus and suggests that, in common with previous reports of neural responses to other invisible stimuli (Moutoussis and Zeki, 2002;Fang and He, 2005), even when a target becomes invisible as it is perceptually filled-in by its background, it continues to evoke responses within visual cortex.

Although the target was flickered in this study, allowing the measurement of responses specific to the target, the background was not flickered. Thus, from the experiment presented here, it is not possible to determine the neural activity of responses specific to the background. This is of particular relevance for perceptual filling-in of artificial scotomas, as the background perceptually fills-in the region previously occupied by the target. It would be of great interest if, for example, in contrast with signals specific to the target, background signals increased during perceptual filling-in. Future work could therefore examine responses specific to the background during perceptual filling-in. This could be done by flickering the target and the background at different frequencies and examining changes in power at each of these frequencies after perceptual filling-in has occurred. An alternative strategy might be to repeat the paradigm but this time flickering the background and not the target. This would require a larger target and a restricted background (more similar to the display used in (De Weerd *et al.*, 1998) so that the background to target ratio is lower than for a whole screen of background), to increase sensitivity to detect possible changes in power as perceptual filling-in takes place.

Another issue which might be explored using the superior temporal resolution of MEG, is that of the precise temporal dynamics which take place during perceptual filling-in of an artificial scotoma. One influential model for the neural mechanism underlying filling-in (Gerrits and Vendrik, 1970;Grossberg and Mingolla, 1985) is that the lateral spreading which causes neural filling-in of surfaces in normal vision is inhibited by the boundaries of an image. This theory has been further developed on the basis of single cell recordings in monkeys (De Weerd *et al.*, 1995) and behavioural studies in humans (De Weerd *et al.*, 1998) to explain the possible mechanisms underlying perceptual filling-in of an artificial scotoma. The suggested model consists of two stages: a slow period during which adaptation of the neurons responding to the boundary between the target and the background causes the failure of figure-ground segregation. This is then followed by the faster process of featural spreading. Therefore a specific question arising from this MEG experiment might be whether there is any evidence for this two-stage process, with a slow breakdown in the boundary of the target and then a faster spread of neural activity. This might be addressed using a similar paradigm to that used in Chapter 3, but instead of flickering the whole target at one frequency, flickering the border and the interior of the target at different frequencies and looking for a dissociation in their responses immediately prior to the time when perceptual filling-in is reported.

8.2.2 The anatomical locus of perceptual completion of artificial scotomas

Chapter 4 explored the anatomical location of perceptual filling-in of artificial scotomas. Behavioural and neurophysiological studies have been consistent with a locus in early retinotopic cortex (De Weerd *et al.*, 1998;De Weerd *et al.*, 1995) but

this had not yet been explicitly demonstrated in humans. I showed that the behavioural report of perceptual filling-in of an artificial scotoma is accompanied by reductions in BOLD signals representing the filled-in target in V1 and in V2. This lends further weight to the active neural hypothesis for perceptual completion and argues against other theories of perceptual filling-in, especially Dennet's ignoring an absence (Dennett, 1991), but also the symbolic theory (labelling an area as more of the same (O'Regan, 1992)), and even the suggestion that filling-in involves 'sewing up' of the filled-in region (Kapadia *et al.*, 1994), as this chapter presents evidence of retinotopic (or point-for-point) reductions in BOLD signal in the cortical representation of the target during perceptual filling-in.

Moreover, the BOLD responses to the perceptually filled-in target were greater than the no-target baseline, providing evidence for the persistent representation of the invisible target at the retinotopic location corresponding to the target in visual space. These findings, consistent with those presented in Chapter 3 using MEG, provide converging evidence from different experimental modalities that during perceptual filling-in, the now invisible filled-in target continues to evoke responses within visual cortex.

Interestingly, there was a subtle but important difference in responses to perceptual completion between V1 and V2. In V2, the reduction in activity was exclusive to the retinotopic representation of the target. However, in V1, a reduction in BOLD signal was also seen in regions not responding to the target. It is possible that these differences represent distinct roles for V1 and V2 in perceptual filling-in. The target-specific reductions in activity observed in V1 and V2 might reflect specific inhibitory

processes suppressing the target boundary so that it is no longer segregated from the surrounding texture. The weaker, non-retinotopic decreases in activity observed only in V1, might instead reflect the more general process of feature spreading which allows filling-in to take place. Such a hypothesis might be tested by examining activity related specifically to the border of the target and comparing this to activity within the target's interior (as above). It might also be interesting to specifically examine activity related to the region surrounding the target.

An important issue not addressed by the experiment in Chapters 3 and 4 is the question of possible underlying neural mechanisms mediating perceptual completion. Spillmann and Werner (Spillmann and Werner, 1996) have proposed three possible candidate mechanisms of long-rage interactions to account for the phenomenon: The first is a feedforward circuit whereby spatially separated signals converge at higher levels, to produce output where a perceptually filled-in surface is indistinguishable from a real surface. The second involves recruitment of intrinsic horizontal connections to allow interactions within one visual region, to provide links between stimulated regions. The third model involves long-range feedback projections from higher regions to group cell responses at lower levels. These three models could be tested by performing functional connectivity analyses, such as psychophysiological interactions or dynamic causal modelling which are methods to assess the functional relationships between different brain regions.

An intriguing alternative model for understanding the findings in Chapters 3 and 4 is that proposed by Friston (Friston, 2005). This describes all hierarchical sensory processing in an empirical Bayes framework, whereby the role of backward

connections is to provide contextual feedback to earlier stages in the cortical processing pathway, by minimising prediction error. This is the difference between the observed input and that predicted by the generative model and inferred causes. Where an earlier cortical stage (say for example V1) finds a surprising input, an error signal is passed to the next stage (here this would be V2). If this input can be explained by V2, a suppressive signal passes back to V1, otherwise an error signal is passed to successively higher stages until the surprising finding can be explained. Thus any evoked response can be understood as a transient expression of prediction error which is then suppressed by predictions from higher cortical areas. Friston uses this model to interpret previous observations that when disparate elements form coherent shapes (Murray et al., 2002b) increases in activity are seen in LOC, but reductions are seen in primary visual cortex. He suggests that this reduced activity in V1 is a result of grouping processes performed in higher areas. The findings presented in Chapter 4 (and also in Chapter 3) are consistent with this model. The reductions in activity in V1 and V2 may be due to predictive suppression from higher cortical regions. Perhaps the more generalised suppression seen beyond the retinotopic ROIs in V1 during perceptual filling-in also reflects suppressive signals from higher cortical regions explaining away the prediction error, although it is not entirely clear why there would be a difference between V1 and V2 for suppression within and beyond the ROIs. It is of course possible that the absence of a generalised reduction in activity outside the retinotopic location of the target in V2 is a false negative finding and that there are in reality no differences in the pattern of responses between V1 and V2 during perceptual filling-in. This might be addressed by repeating the experiment with more participants.

The fMRI study of perceptual filling-in described in Chapter 4 examined activity within early retinotopic regions during perceptual filling-in of artificial scotomas, but was not optimised to detect modulations of activity in higher cortical regions during this process, particularly during the transitions from not filled-in to perceptually filled-in. For example, during binocular rivalry, perceptual switches are associated with increased activity in parietal and frontal regions (Lumer *et al.*, 1998) and in motion induced blindness perceptual switches are associated with increased activity in left frontal cortex (Scholvinck and Rees, 2009b). A further extension of this study might therefore explore this question of top-down involvement in perceptual filling-in in more detail, by examining the transitions between not filled-in and perceptually filled-in on a whole brain analysis. This might involve the use of reaction time data to determine as accurately as possible the point at which perceptual filling-in occurred.

8.2.3 Top-down involvement in perceptual completion of artificial scotomas

This question of top-down involvement in perceptual filling-in was addressed in the behavioural study described in Chapter 5. The major finding was that two different manipulations of high-level cognitive functions had contrasting effects on perceptual filling-in of an artificial scotoma. Increasing perceptual load caused filling-in to occur with longer latency and lower probability; conversely, increasing working memory load caused filling-in to occur earlier (although probability of filling-in was unaffected with the stimulus parameters used here). These findings were interpreted in the context of load theory (Lavie *et al.*, 2004). By increasing perceptual load, there was reduced processing capacity available for the peripheral target, making filling-in less probable. This is consistent with recent work showing that directing spatial

attention to a target makes it more likely to perceptually fill-in (De Weerd *et al.*, 2006).

The second proposal in load theory addresses the way that working memory determines stimulus processing priorities. This predicts that high working memory load will have the opposite effect to that of perceptual load where stimuli compete for processing resources. According to the theory, higher working memory load depletes the capacity of active cognitive control and reduces the ability to maintain prioritisation of behavioural goals, causing increased processing of distractors (de Fockert *et al.*, 2001). However, in the paradigm presented in Chapter 5, where perceptual filling-in was taking place whilst participants performed a working memory task, there were no irrelevant distractors. To account for the enhanced perceptual filling-in I hypothesised that the relative salience of the target and the background might have been modulated by the working memory manipulation. Under the conditions of increased working memory load and the breakdown in prioritisation of behavioural goals, the dynamic twinkling noise might have become more salient compared to the target. More salient backgrounds are more likely to promote filling-in as a dynamic background is associated with enhanced filling-in compared to a static background and a textured background is associated with enhanced filling-in compared to uniform backgrounds. I therefore propose that working memory load impacts on perceptual filling-in by modulating the relative saliency of the background and the target. Such a hypothesis could be tested by directly examining the relative salience of the target and background during the working memory manipulation, for example using response times to stimulus features.

An alternative hypothesis is that increased working memory load instead simply causes an increased state of alertness or arousal. This could be tested in future work by manipulating arousal. For example it might be possible to compare perceptual filling-in at different times during the day or night. Alternatively measures of general alertness could be recorded during the working memory load manipulation, such as response times to peripheral targets. It should be noted that reaction times to the *appearance* of the peripheral target did not differ between the high and low working memory load manipulation suggesting that, for this measure of alertness, there was no difference between the two levels.

One possible problem with this experiment is whether the working memory and perceptual load tasks actually affect perceptual filling-in, or instead simply alter the response criterion made by the participants. It is possible that with higher load the response criterion changes and this affects the latency of responses. In other words, the findings reflect processing at the decisional level instead of the perceptual experience of filling-in. This would involve a change in response criterion in different directions for the two different load tasks. That is, a higher response criterion during high perceptual load and lower response criterion during high working memory load, but this is still a possible explanation. It is challenging to explicitly test this hypothesis using the current paradigm, as this would require a measure of hits and misses to quantify the response criterion and there are no clear hits or misses for perceptual completion as it is a subjective experience. However, a close approximation could be achieved by having the target physically disappear for brief intermittent periods (during the time when it is known to be visible and not

filled-in) and measuring hits and misses (as well as reaction times) for this disappearance under the different load conditions. If there were no significant differences in response criterion or reaction times between the high and low loads, then the findings presented in this chapter could be attributed to perceptual and working memory load effects on perceptual completion, and not to any decisional process.

Taken together, these studies have shown that perceptual filling-in of an artificial scotoma takes place in early retinotopic cortex, in V1 and V2. Together with previous studies showing that perceptual filling-in is strongly modulated by stimulus-related properties such as eccentricity and contrast (De Weerd et al., 1998;Welchman and Harris, 2001) this suggests that it is essentially a bottom-up process. I have also shown that during perceptual filling-in, stimulus specific activity is reduced, although not down to a no-target baseline and I have provided some evidence consistent with a two-stage process for filling-in, involving breakdown of target boundaries followed by a more rapid non-specific spread of feature filling-in. In addition, I have also demonstrated that this low-level process is influenced in a top-down manner by high-level functions such as perceptual load and even working memory.

Future work could specifically explore commonalities between perceptual filling-in of artificial scotomas and other forms of filling-in, in particular evidence for featural spread of filling-in limited or not limited by stimulus boundaries. For example, comparing filling-in across artificial and real scotomas. Here, an intriguing difference is that where perceptual filling-in occurs across real scotomas, it is instantaneous, with patients experiencing a surface as complete, despite their retinal disease. It might be

possible to retinotopically map the scotoma, using the twinkle after-effect experienced by patients with scotomas to localise the scotoma (Crossland *et al.*, 2007) and then examining responses in the scotoma regions of interest whilst patients view a patterned stimulus. This question is further complicated by the question of whether remapping occurs following retinal scotomas, which is still hotly debated (Baker *et al.*, 2008;Dilks *et al.*, 2007).

8.3 Hemianopic completion

Chapter 6 examined a different form of perceptual completion: hemianopic completion, which occurs in the context of hemianopia and is characterised by the patient reporting as complete both complete and incomplete contours, where the completed stimulus straddles the vertical meridian. I examined fMRI responses in a patient with a dense right-sided homonymous hemianopia following surgery to excise a meningioma. BOLD responses were compared for trials where a semicircle was reported as a complete circle, with trials where the semicircle was reported as a semicircle. Differential activity was shown in the lingual gyrus in the right occipital cortex, contralateral to the patient's lesion, ipsilateral to the illusory edge of the stimulus and close to reported coordinates for the human lateral occipital complex.

The paradigm avoided problems of residual vision and eye movements toward the blind hemifield, as the main comparison of interest was the completion of the incomplete semicircle, where no stimulus was present in the blind hemifield. Furthermore, neglect was ruled out as a confound as the patient had been extensively

behaviourally tested prior to scanning (McCarthy *et al.*, 2006) and showed no evidence of neglect on formal testing.

Based on the experimental findings, I proposed that hemianopic completion might result due to unopposed activity of contralesional visually-sensitive ventral-occipital areas, whereby, each side predicts a completed form based on the information from earlier retinotopic regions and this is verified by reciprocal feedback between left and right hemispheres. In this patient, with an extensive occipital lesion encompassing most of the left retinotopic visual cortex and extending into the inferior temporal gyrus, this reciprocal feedback might be impaired, causing hemianopic completion (see Fig 8.1). Specifically the absence of negative feedback from ipsilesional higher visual areas to contralesional higher visual areas may result in relatively increased activity and the erroneous perception of a circle. Thus hemianopic completion might represent an example of perceptual completion caused by absence of top-down or lateral feedback signals.

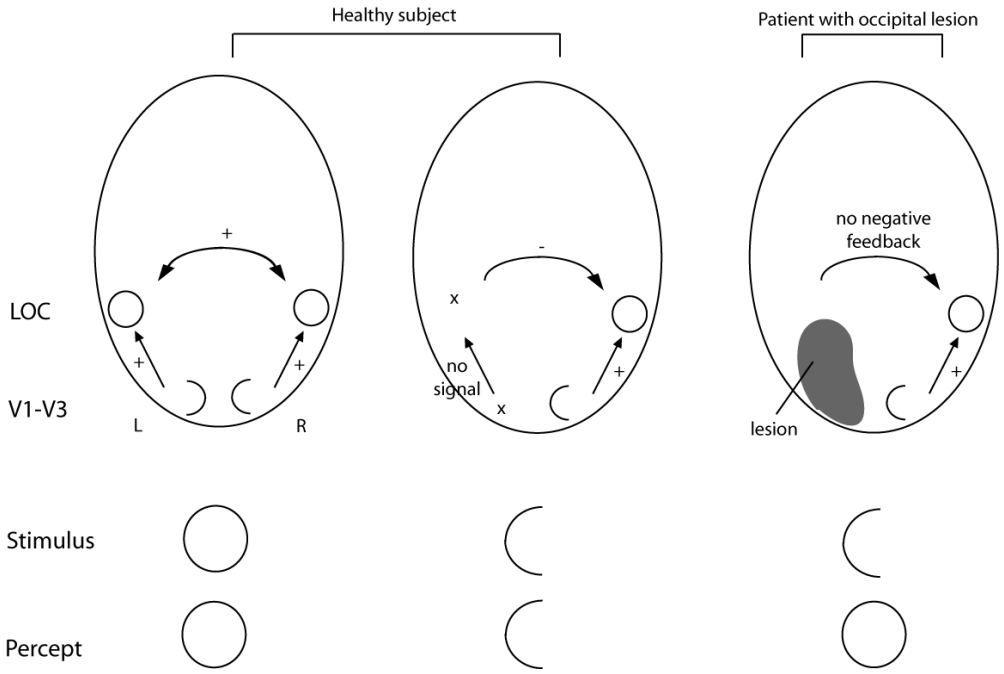

Figure 8.1 Model for hemianopic completion. In healthy subjects, presentation of a semicircle might cause negative feedback to the ipsilateral LOC contralateral to the side of the semicircle due to absence of input from ipsilateral V1-V3 (as no semicircle is present in the opposite hemifield). This suppresses any assumed completed circle and the semicircle is perceived. However, in patients experiencing hemianopic completion, there is no negative feedback to contralesional LOC, so the assumed circle is perceived and relatively increase activity is seen in contralesional LOC.

Such a hypothesis could be specifically tested in several ways: in the first instance, this single-patient study could be extended by looking for activation during hemianopic completion in several patients showing this phenomenon. Transcranial magnetic stimulation might also be used to specifically target ventral-occipital regions during or immediately following perception of a semicircle in normal observers, to attempt to provoke hemianopic completion. In patients with hemianopia following stroke, lesion overlap studies might be used to look for differences in lesion anatomy between patients showing hemianopic completion and those that do not.

Walker and Mattingley (in their commentary on Pessoa's guide to perceptual filling-in (Pessoa *et al.*, 1998)) have suggested several other possible explanations for hemianopic completion: They suggest that it might be a form of amodal completion in which the hemianopic region is treated as a large occluder (similar to models for the blind spot proposed by Durgin (Durgin *et al.*, 1995)). Alternatively, it might reflect top-down activations of stored object representations, reducing the threshold for detecting stimuli falling in the blind field. Interestingly, they contrast hemianopic completion with pathological completion occurring in patients with parietal neglect which they describe as being consistent with the brain ignoring an absence of information, similar to the model suggested by Dennet (Dennett, 1991) for filling-in in general.

Taken together, the findings presented in Chapter 6 demonstrate that during hemianopic completion, there is increased activity in contralesional visually sensitive ventral occipital cortex anterior to retinotopic regions and near to the lateral occipital complex. This increase in activity is in contrast with the reduction in activity seen during perceptual filling-in of an artificial scotoma. This could be because a contour is perceived where it does not actually exist, unlike the case of perceptual filling-in of artificial scotomas where the target is not perceived and is instead replaced by the background. Alternatively, in the light of the model proposed by Friston (Friston, 2005) and also the model describe above, this might be because hemianopic completion is a pathological form of completion where the usual suppressive feedback signals are impaired, leading to abnormally increased activity and the illusion of a contour where it does not actually exist.

8.4 Effect of reward on human visual processing

In the second section of this thesis, in Chapter 7, I explored further the role of top-down signals in perception by examining a different form of top-down influence: the role of reward feedback on visual processing. Two recent studies have demonstrated that reward has direct modulatory effects on somatosensory processing, with reward feedback causing lateralised increases in activity in primary somatosensory cortex (Pleger *et al.*, 2008), which can be modulated by dopamine (Pleger *et al.*, 2009). However, the effects of reward feedback on visual processing have been less well explored as studies of reward influence on visual processing have not dissociated reward receipt from visual stimulation (Krawczyk *et al.*, 2007;Serences, 2008). In Chapter 7, I used fMRI to examine whether reward can modulate activity in visual cortex. Critically, I used an event-related design which allowed me to separate out the visual discrimination task from reward feedback to specifically examine responses in visual cortex during reward feedback. Furthermore, by using retinotopic mapping of early visual areas, I was able to examine responses within these early retinotopic regions during reward feedback and in other phases of the trial. I found that reward feedback (as signalled auditorily) increased BOLD signal in visual areas beyond retinotopic cortex, in addition to activity in regions known to be modulated by reward. Furthermore, when correct visual performance led to reward, this in turn led to enhanced visual activity contralateral to the judged stimulus on the next trial, for retinotopic representations of the judged visual stimuli in primary visual cortex.

This study therefore provides evidence that reward can influence visual processing both directly (at the point of reward feedback) and indirectly (during the next visual discrimination) as another form of top-down control. This finding makes evolutionary sense, as for an animal to maximise reward outcomes, it is sensible to optimise rewarded behaviour and therefore to use reward outcomes to feed back and improve performance in tasks associated with later rewards. However, this has not been previously demonstrated and the sensory cortices are not traditionally thought of as being part of the reward network, despite the fact that primate visual cortices receive at least some dopaminergic fibres (Berger and Gaspar, 1994). Thus the findings in this experiment might be useful when considering the relationship between perception and learned behaviour.

Several aspects of this study raise important questions which could be addressed by further investigations. The finding that reward feedback causes bilateral activation in higher visual areas, beyond retinotopic cortex and yet lateralised effects on the next trial raises the question of whether these reward-associated modulations of higher visual areas are specific to the orientation discrimination task used in Chapter 7, or whether they are related to reward feedback associated with any visual task. Further studies could therefore explore effects of reward feedback on visual cortex activation following different perceptual tasks such as spatial acuity or contrast perception tasks which might be predicted to involve early retinotopic cortex. It would also be interesting to explore whether these reward effects seen in somatosensory and visual domains extend to other modalities such as auditory processing.

The finding that receiving a reward on one trial was associated with enhanced signal in lateralised primary visual cortex on the next trial provides evidence consistent with a teaching signal propagated from reward-responsive areas such as ventral striatum and/ or orbitofrontal cortex, to higher visual areas and then primary visual cortex on the next trial. This hypothesis could be tested in future studies, for example using a causal intervention such as transcranial magnetic stimulation (TMS) to target specific visual areas at specific timepoints during and between trials, or by combining TMS with fMRI. Alternatively, the timecourse of such a teaching signal could be explored using neurophysiological techniques such as EEG or MEG to examine the timing of responses in visual areas following reward. Such a model could also be tested using dynamic causal modelling of either the fMRI or MEG data of the same paradigm.

The mechanisms of reward feedback to visual areas could be further explored using a pharmacological manipulation of the paradigm. If the effect of reward is mediated by dopamine signals, such feedback might be enhanced by direct administration of dopamine, or inhibited by a dopamine antagonist such as risperidone or olanzapine (see (Pleger *et al.*, 2009) for a similar study in the somatosensory domain). It might also be interesting to look at the impact of reward feedback on visual processing in targeted patient groups with damage to specific reward-associated structures, such as focal basal ganglia lesions or Parkinson disease, where visual processing is largely unaffected.

8.5 Conclusion

In summary, the findings presented in this thesis provide evidence for bottom-up and top-down interactions in perceptual filling-in and explore the integration of top-down and bottom-up signals following reward feedback. I have shown that stimuli present in the outside world can be rendered invisible by processes taking place in early retinotopic cortex, but that this process is modulated by higher cognitive functions; and that higher cognitive functions such as reward can directly impact on visual processing in early retinotopic cortex. The examples explored within this thesis have relevance for visual processing in general. I began this thesis by considering the complexity of visual information with which the visual system is presented at each moment and the enormous task of translating this into a series of meaningful objects and scenes. Much of this information is fragmented and requires organisation and interpolation by higher visual regions feeding back to inform processes taking place earlier in the visual pathways. Similarly, information from other higher cognitive functions such as reward outcome can be used to attune visual processing in early retinotopic regions. The studies presented in this thesis demonstrate the integration of signals from bottom-up and top-down processes within the areas of perceptual completion and reward processing. The consequences of these interactions and the underlying mechanisms require further study. However, the existence of these interactions adds weight to current models of both perceptual completion and reward processing and should be considered when exploring other areas of human perception, as it is only through integration from multiple levels that visual information can be successfully processed.

Reference List

1. Aine C, Huang M, Stephen J, Christner R (2000) Multistart algorithms for MEG empirical data analysis reliably characterize locations and time courses of multiple sources. Neuroimage 12: 159-172.

2. Akgoren N, Fabricius M, Lauritzen M (1994) Importance of nitric oxide for local increases of blood flow in rat cerebellar cortex during electrical stimulation. Proc Natl Acad Sci U S A 91: 5903-5907.

3. Albert MK (2007) Mechanisms of modal and amodal interpolation. Psychol Rev 114: 455-469.

4. Allman JM, Kaas JH (1971) A representation of the visual field in the caudal third of the middle tempral gyrus of the owl monkey (Aotus trivirgatus). Brain Res 31: 85-105.

5. Alvarenga DP, Couto MF, Pessoa VF (2008) Filling in at partially deafferented visual cortex. Br J Ophthalmol 92: 1257-1260.

6. Anderson AK, Christoff K, Stappen I, Panitz D, Ghahremani DG, Glover G, Gabrieli JD, Sobel N (2003) Dissociated neural representations of intensity and valence in human olfaction. Nat Neurosci 6: 196-202.

7. Anderson BL, Singh M, Fleming RW (2002) The interpolation of object and surface structure. Cognit Psychol 44: 148-190.

8. Andersson JL, Hutton C, Ashburner J, Turner R, Friston K (2001) Modeling geometric deformations in EPI time series. Neuroimage 13: 903-919.

9. Ashburner J, Friston KJ (1999) Nonlinear spatial normalization using basis functions. Hum Brain Mapp 7: 254-266.

10. Aston-Jones G, Rajkowski J, Kubiak P, Alexinsky T (1994) Locus coeruleus neurons in monkey are selectively activated by attended cues in a vigilance task. J Neurosci 14: 4467-4480.

11. Attwell D, Iadecola C (2002) The neural basis of functional brain imaging signals. Trends Neurosci 25: 621-625.

12. Attwell D, Laughlin SB (2001) An energy budget for signaling in the grey matter of the brain. J Cereb Blood Flow Metab 21: 1133-1145.

13. Avidan G, Harel M, Hendler T, Ben Bashat D, Zohary E, Malach R (2002) Contrast sensitivity in human visual areas and its relationship to object recognition. J Neurophysiol 87: 3102-3116.

14. Awater H, Kerlin JR, Evans KK, Tong F (2005) Cortical representation of space around the blind spot. J Neurophysiol 94: 3314-3324.

15. Bahrami B, Carmel D, Walsh V, Rees G, Lavie N (2008) Unconscious orientation processing depends on perceptual load. J Vis 8: 12-10.

16. Bahrami B, Lavie N, Rees G (2007) Attentional load modulates responses of human primary visual cortex to invisible stimuli. Curr Biol 17: 509-513.

17. Baillet S, Mosher JC, Leahy RH (2001) Electronic brain mapping. IEEE Signal Processing Magazine 18: 14-30.

18. Baker CI, Dilks DD, Peli E, Kanwisher N (2008) Reorganization of visual processing in macular degeneration: replication and clues about the role of foveal loss. Vision Res 48: 1910-1919.

19. Baker CI, Peli E, Knouf N, Kanwisher NG (2005) Reorganization of visual processing in macular degeneration. J Neurosci 25: 614-618.

20. Bakin JS, Nakayama K, Gilbert CD (2000) Visual responses in monkey areas V1 and V2 to three-dimensional surface configurations. J Neurosci 20: 8188-8198.

21. Balleine BW, Killcross AS, Dickinson A (2003) The effect of lesions of the basolateral amygdala on instrumental conditioning. J Neurosci 23: 666-675.

22. Beck DM, Rees G, Frith CD, Lavie N (2001) Neural correlates of change detection and change blindness. Nat Neurosci 4: 645-650.

23. Bender MB, Teuber HL (1946) Phenomena of fluctuation, extinction and completion in visual perception. Archives of Neurology and Psychiatry 55: 627-658.

24. Berger B, Gaspar P (1994) Comparative anatomy of the catecholaminergic innervation of rat and primate cerebral cortex. In: Phylogeny and development of catecholamine systems in the CNS of vertebrates (Smeets WJAJ, Reiner A, eds), pp 293-325. Cambridge: Cambridge University Press.

25. Berger B, Trottier S, Verney C, Gaspar P, Alvarez C (1988) Regional and laminar distribution of the dopamine and serotonin innervation in the macaque cerebral cortex: a radioautographic study. J Comp Neurol 273: 99-119.

26. Berkley MA, Debruyn B, Orban G (1994) Illusory, motion, and luminance-defined contours interact in the human visual system. Vision Res 34: 209-216.

27. Bittar RG, Ptito M, Faubert J, Dumoulin SO, Ptito A (1999) Activation of the remaining hemisphere following stimulation of the blind hemifield in hemispherectomized subjects. Neuroimage 10: 339-346.

28. Blood AJ, Zatorre RJ, Bermudez P, Evans AC (1999) Emotional responses to pleasant and unpleasant music correlate with activity in paralimbic brain regions. Nat Neurosci 2: 382-387.

29. Bonneh YS, Cooperman A, Sagi D (2001) Motion-induced blindness in normal observers. Nature 411: 798-801.

30. Boselie F, Wouterlood D (1992) A critical discussion of Kellman and Shipley's (1991) theory of occlusion phenomena. Psychol Res 54: 278-285.

31. Boynton GM, Engel SA, Glover GH, Heeger DJ (1996) Linear systems analysis of functional magnetic resonance imaging in human V1. J Neurosci 16: 4207-4221.

32. Bressan P, Mingolla E, Spillmann L, Watanabe T (1997) Neon color spreading: a review. Perception 26: 1353-1366.

33. Bressan P, Vallortigara G (1991) Illusory depth from moving subjective figures and neon colour spreading. Perception 20: 637-644.

34. Bridge H, Thomas O, Jbabdi S, Cowey A (2008) Changes in connectivity after visual cortical brain damage underlie altered visual function. Brain 131: 1433-1444.

35. Buchel C, Josephs O, Rees G, Turner R, Frith CD, Friston KJ (1998) The functional anatomy of attention to visual motion. A functional MRI study. Brain 121 (Pt 7): 1281-1294.

36. Buffart H, Leeuwenberg E (1981) Coding theory of visual pattern completion. J Exp Psychol Hum Percept Perform 7: 241-274.

37. Burr DC (1987) Implications of the Craik-O'Brien illusion for brightness perception. Vision Res 27: 1903-1913.

38. Busch NA, Debener S, Kranczioch C, Engel AK, Herrmann CS (2004) Size matters: effects of stimulus size, duration and eccentricity on the visual gamma-band response. Clin Neurophysiol 115: 1810-1820.

39. Calford MB, Chino YM, Das A, Eysel UT, Gilbert CD, Heinen SJ, Kaas JH, Ullman S (2005) Neuroscience: rewiring the adult brain. Nature 438: E3-E4.

40. Campbell FW, Robson JG (1961) A fresh approach to stabilised retinal images. J Physiol 158: 1-11.

41. Carelli P, Leoni R (1986) Localization of biological sources with arrays of superconducting gradiometers. J Appl Phys 59: 645-650.

42. Cavada C, Goldman-Rakic PS (1989) Posterior parietal cortex in rhesus monkey: II. Evidence for segregated corticocortical networks linking sensory and limbic areas with the frontal lobe. J Comp Neurol 287: 422-445.

43. Chen Y, Seth AK, Gally JA, Edelman GM (2003) The power of human brain magnetoencephalographic signals can be modulated up or down by changes in an attentive visual task. Proc Natl Acad Sci U S A 100: 3501-3506.

44. Chino Y, Smith EL, III, Zhang B, Matsuura K, Mori T, Kaas JH (2001) Recovery of binocular responses by cortical neurons after early monocular lesions. Nat Neurosci 4: 689-690.

45. Chino YM, Kaas JH, Smith EL, III, Langston AL, Cheng H (1992) Rapid reorganization of cortical maps in adult cats following restricted deafferentation in retina. Vision Res 32: 789-796.

46. COHEN HB (1961) The effect of contralateral visual stimulation on visibility with stabilized retinal images. Can J Psychol 15: 212-219.

47. Cohen MA, Grossberg S (1984) Neural dynamics of brightness perception: features, boundaries, diffusion, and resonance. Percept Psychophys 36: 428-456.

48. Colby CL, Duhamel JR, Goldberg ME (1996) Visual, presaccadic, and cognitive activation of single neurons in monkey lateral intraparietal area. J Neurophysiol 76: 2841-2852.

49. Corbetta M, Miezin FM, Dobmeyer S, Shulman GL, Petersen SE (1990) Attentional modulation of neural processing of shape, color, and velocity in humans. Science 248: 1556-1559.

50. Cornsweet T (1970) Visual perception. New York: Academic Press.

51. Cosmelli D, David O, Lachaux JP, Martinerie J, Garnero L, Renault B, Varela F (2004) Waves of consciousness: ongoing cortical patterns during binocular rivalry. Neuroimage 23: 128-140.

52. Cowey A (1964) PROJECTION OF THE RETINA ON TO STRIATE AND PRESTRIATE CORTEX IN THE SQUIRREL MONKEY, SAIMIRI SCIUREUS. J Neurophysiol 27: 366-393.

53. Craik KJW (1966) Brightness discrimination, borders and subjetcive brightness. In: The nature of psychology pp 94-97. Cambridge: Cambridge University Press.

54. Crinion J, Ashburner J, Leff A, Brett M, Price C, Friston K (2007) Spatial normalization of lesioned brains: performance evaluation and impact on fMRI analyses. Neuroimage 37: 866-875.

55. Crossland MD, Bex PJ (2009) Spatial alignment over retinal scotomas. Invest Ophthalmol Vis Sci 50: 1464-1469.

56. Crossland MD, Dakin SC, Bex PJ (2007) Illusory stimuli can be used to identify retinal blind spots. PLoS One 2: e1060.

57. Dakin SC, Bex PJ (2003) Natural image statistics mediate brightness 'filling in'. Proc Biol Sci 270: 2341-2348.

58. Dale AM (1999) Optimal experimental design for event-related fMRI. Hum Brain Mapp 8: 109-114.

59. Dale AM, Fischl B, Sereno MI (1999) Cortical surface-based analysis. I. Segmentation and surface reconstruction. Neuroimage 9: 179-194.

60. Dalton P, Lavie N, Spence C (2009) The role of working memory in tactile selective attention. Q J Exp Psychol (Colchester) 62: 635-644.

61. Davey MP, Maddess T, Srinivasan MV (1998) The spatiotemporal properties of the Craik-O'Brien-Cornsweet effect are consistent with 'filling-in'. Vision Res 38: 2037-2046.

62. Davis G, Driver J (1994) Parallel detection of Kanizsa subjective figures in the human visual system. Nature 371: 791-793.

63. Davis G, Driver J (2003) Effects of modal versus amodal completion upon visual attention: a function for filling-in? In: Filling-in. From preceptula completion to cortical reorganization (Pessoa L, De Weerd P, eds), pp 128-150. Oxford University Press.

64. Davis TL, Kwong KK, Weisskoff RM, Rosen BR (1998) Calibrated functional MRI: mapping the dynamics of oxidative metabolism. Proc Natl Acad Sci U S A 95: 1834-1839.

65. de Fockert J, Rees G, Frith C, Lavie N (2004) Neural correlates of attentional capture in visual search. J Cogn Neurosci 16: 751-759.

66. de Fockert JW, Rees G, Frith CD, Lavie N (2001) The role of working memory in visual selective attention. Science 291: 1803-1806.

67. De Weerd P (2006) Perceptual filling-in: More than the eye can see. Prog Brain Res 154: 227-245.

68. De Weerd P, Desimone R, Ungerleider LG (1998) Perceptual filling-in: a parametric study. Vision Res 38: 2721-2734.

69. De Weerd P, Gattass R, Desimone R, Ungerleider LG (1995) Responses of cells in monkey visual cortex during perceptual filling-in of an artificial scotoma. Nature 377: 731-734.

70. De Weerd P, Smith E, Greenberg P (2006) Effects of Selective Attention on Perceptual Filling-in. J Cogn Neurosci 18: 335-347.

71. DeAngelis GC, Anzai A, Ohzawa I, Freeman RD (1995) Receptive field structure in the visual cortex: does selective stimulation induce plasticity? Proc Natl Acad Sci U S A 92: 9682-9686.

72. Della LC, Chelazzi L (2006) Visual selective attention and the effects of monetary rewards. Psychol Sci 17: 222-227.

73. Dennett D (1991) Consciousness explained. Boston: Little, Brown and Company.

74. Denys K, Vanduffel W, Fize D, Nelissen K, Peuskens H, Van Essen D, Orban GA (2004) The processing of visual shape in the cerebral cortex of human and nonhuman primates: a functional magnetic resonance imaging study. J Neurosci 24: 2551-2565.

75. Desimone R (1996) Neural mechanisms for visual memory and their role in attention. Proc Natl Acad Sci U S A 93: 13494-13499.

76. Devinck F, Hansen T, Gegenfurtner KR (2007) Temporal properties of the chromatic and achromatic Craik-O'Brien-Cornsweet effect. Vision Res 47: 3385-3393.

77. Dilks DD, Serences JT, Rosenau BJ, Yantis S, McCloskey M (2007) Human adult cortical reorganization and consequent visual distortion. J Neurosci 27: 9585-9594.

78. Disbrow EA, Slutsky DA, Roberts TP, Krubitzer LA (2000) Functional MRI at 1.5 tesla: a comparison of the blood oxygenation level-dependent signal and electrophysiology. Proc Natl Acad Sci U S A 97: 9718-9723.

79. DITCHBURN RW, GINSBORG BL (1952) Vision with a stabilized retinal image. Nature 170: 36-37.

80. Dolan RJ, Fink GR, Rolls E, Booth M, Holmes A, Frackowiak RS, Friston KJ (1997) How the brain learns to see objects and faces in an impoverished context. Nature 389: 596-599.

81. Donner TH, Sagi D, Bonneh YS, Heeger DJ (2008) Opposite neural signatures of motion-induced blindness in human dorsal and ventral visual cortex. J Neurosci 28: 10298-10310.

82. Dougherty RF, Koch VM, Brewer AA, Fischer B, Modersitzki J, Wandell BA (2003) Visual field representations and locations of visual areas V1/2/3 in human visual cortex. J Vis 3: 586-598.

83. Downing PE, Wiggett AJ, Peelen MV (2007) Functional magnetic resonance imaging investigation of overlapping lateral occipitotemporal activations using multi-voxel pattern analysis. J Neurosci 27: 226-233.

84. Driver J, Davis G, Russell C, Turatto M, Freeman E (2001a) Segmentation, attention and phenomenal visual objects. Cognition 80: 61-95.

85. Driver J, Vuilleumier P, Eimer M, Rees G (2001b) Functional magnetic resonance imaging and evoked potential correlates of conscious and unconscious vision in parietal extinction patients. Neuroimage 14: S68-S75.

86. Durgin FH, Tripathy SP, Levi DM (1995) On the filling in of the visual blind spot: some rules of thumb. Perception 24: 827-840.

87. Eger E, Ashburner J, Haynes JD, Dolan RJ, Rees G (2008) fMRI activity patterns in human LOC carry information about object exemplars within category. J Cogn Neurosci 20: 356-370.

88. Elliott R, Friston KJ, Dolan RJ (2000) Dissociable neural responses in human reward systems. J Neurosci 20: 6159-6165.

89. Elliott R, Newman JL, Longe OA, William Deakin JF (2004) Instrumental responding for rewards is associated with enhanced neuronal response in subcortical reward systems. Neuroimage 21: 984-990.

90. Engel SA, Glover GH, Wandell BA (1997) Retinotopic organization in human visual cortex and the spatial precision of functional MRI. Cereb Cortex 7: 181-192.

91. Engel SA, Rumelhart DE, Wandell BA, Lee AT, Glover GH, Chichilnisky EJ, Shadlen MN (1994) fMRI of human visual cortex. Nature 369: 525.

92. Essen DC, Zeki SM (1978) The topographic organization of rhesus monkey prestriate cortex. J Physiol 277: 193-226.

93. Fang F, He S (2005) Cortical responses to invisible objects in the human dorsal and ventral pathways. Nat Neurosci 8: 1380-1385.

94. Fawcett IP, Barnes GR, Hillebrand A, Singh KD (2004) The temporal frequency tuning of human visual cortex investigated using synthetic aperture magnetometry. Neuroimage 21: 1542-1553.

95. Felleman DJ, Van Essen DC (1991) Distributed hierarchical processing in the primate cerebral cortex. Cereb Cortex 1: 1-47.

96. Ffytche DH, Zeki S (1996) Brain activity related to the perception of illusory contours. Neuroimage 3: 104-108.

97. Fiorani JM, Rosa MG, Gattass R, Rocha-Miranda CE (1992) Dynamic surrounds of receptive fields in primate striate cortex: a physiological basis for perceptual completion? Proc Natl Acad Sci U S A 89: 8547-8551.

98. Fischl B, Dale AM (2000) Measuring the thickness of the human cerebral cortex from magnetic resonance images. Proc Natl Acad Sci U S A 97: 11050-11055.

99. Fischl B, Liu A, Dale AM (2001) Automated manifold surgery: constructing geometrically accurate and topologically correct models of the human cerebral cortex. IEEE Trans Med Imaging 20: 70-80.

100. Fischl B, Salat DH, Busa E, Albert M, Dieterich M, Haselgrove C, van der KA, Killiany R, Kennedy D, Klaveness S, Montillo A, Makris N, Rosen B,

Dale AM (2002) Whole brain segmentation: automated labeling of neuroanatomical structures in the human brain. Neuron 33: 341-355.

101. Fischl B, Salat DH, van der Kouwe AJ, Makris N, Segonne F, Quinn BT, Dale AM (2004) Sequence-independent segmentation of magnetic resonance images. Neuroimage 23 Suppl 1: S69-S84.

102. Fischl B, Sereno MI, Dale AM (1999) Cortical surface-based analysis. II: Inflation, flattening, and a surface-based coordinate system. Neuroimage 9: 195-207.

103. Foote SL, Aston-Jones G, Bloom FE (1980) Impulse activity of locus coeruleus neurons in awake rats and monkeys is a function of sensory stimulation and arousal. Proc Natl Acad Sci U S A 77: 3033-3037.

104. Fox PT, Raichle ME (1986) Focal physiological uncoupling of cerebral blood flow and oxidative metabolism during somatosensory stimulation in human subjects. Proc Natl Acad Sci U S A 83: 1140-1144.

105. Fox PT, Raichle ME, Mintun MA, Dence C (1988) Nonoxidative glucose consumption during focal physiologic neural activity. Science 241: 462-464.

106. Friedman HS, Zhou H, von der HR (1999) Color filling-in under steady fixation: behavioral demonstration in monkeys and humans. Perception 28: 1383-1395.

107. Friston K (2005) A theory of cortical responses. Philos Trans R Soc Lond B Biol Sci 360: 815-836.

108. Friston KJ (1995) Spatial registration and normalization of images. Hum Brain Mapp 3: 165-189.

109. Friston KJ, Glaser DE, Henson RN, Kiebel S, Phillips C, Ashburner J (2002) Classical and Bayesian inference in neuroimaging: applications. Neuroimage 16: 484-512.

110. Friston KJ, Josephs O, Rees G, Turner R (1998) Nonlinear event-related responses in fMRI. Magn Reson Med 39: 41-52.

111. Friston KJ, Williams S, Howard R, Frackowiak RS, Turner R (1996) Movement-related effects in fMRI time-series. Magn Reson Med 35: 346-355.

112. Frith C, Perry R, Lumer E (1999) The neural correlates of conscious experience: an experimental framework. Trends Cogn Sci 3: 105-114.

113. Galambos R (1992) A comparison of certain gamma band brain rhythms in cat and man. In: Induced rhythms in the brain (Basar E, Bullock T, eds), pp 201-216.

114. Gandhi SP, Heeger DJ, Boynton GM (1999) Spatial attention affects brain activity in human primary visual cortex. Proc Natl Acad Sci U S A 96: 3314-3319.

115. Gattass R, Gross CG, Sandell JH (1981) Visual topography of V2 in the macaque. J Comp Neurol 201: 519-539.

116. Gattass R, Nascimento-Silva S, Soares JG, Lima B, Jansen AK, Diogo AC, Farias MF, Botelho MM, Mariani OS, Azzi J, Fiorani M (2005) Cortical visual areas in monkeys: location, topography, connections, columns, plasticity and cortical dynamics. Philos Trans R Soc Lond B Biol Sci 360: 709-731.

117. Gattass R, Sousa AP, Gross CG (1988) Visuotopic organization and extent of V3 and V4 of the macaque. J Neurosci 8: 1831-1845.

118. Gerrits HJ, Timmerman GJ (1969) The filling-in process in patients with retinal scotomata. Vision Res 9: 439-442.

119. Gerrits HJ, Vendrik AJ (1970) Simultaneous contrast, filling-in process and information processing in man's visual system. Exp Brain Res 11: 411-430.

120. Giannikopoulos DV, Eysel UT (2006) Dynamics and specificity of cortical map reorganization after retinal lesions. Proc Natl Acad Sci U S A 103: 10805-10810.

121. Gilbert CD, Sigman M (2007) Brain states: top-down influences in sensory processing. Neuron 54: 677-696.

122. Gilbert CD, Wiesel TN (1992) Receptive field dynamics in adult primary visual cortex. Nature 356: 150-152.

123. Goebel R, Khorram-Sefat D, Muckli L, Hacker H, Singer W (1998) The constructive nature of vision: direct evidence from functional magnetic resonance imaging studies of apparent motion and motion imagery. Eur J Neurosci 10: 1563-1573.

124. Gottfried JA, O'Doherty J, Dolan RJ (2002) Appetitive and aversive olfactory learning in humans studied using event-related functional magnetic resonance imaging. J Neurosci 22: 10829-10837.

125. Graf EW, Adams WJ, Lages M (2002) Modulating motion-induced blindness with depth ordering and surface completion. Vision Res 42: 2731-2735.

126. Grill-Spector K, Kushnir T, Hendler T, Edelman S, Itzchak Y, Malach R (1998) A sequence of object-processing stages revealed by fMRI in the human occipital lobe. Hum Brain Mapp 6: 316-328.

127. Grill-Spector K, Kushnir T, Hendler T, Malach R (2000) The dynamics of object-selective activation correlate with recognition performance in humans. Nat Neurosci 3: 837-843.

128. Gross J, Schmitz F, Schnitzler I, Kessler K, Shapiro K, Hommel B, Schnitzler A (2004) Modulation of long-range neural synchrony reflects temporal limitations of visual attention in humans. Proc Natl Acad Sci U S A 101: 13050-13055.

129. Grossberg S (1994) 3-D vision and figure-ground separation by visual cortex. Percept Psychophys 55: 48-121.

130. Grossberg S (1997) Cortical dynamics of three-dimensional figure-ground perception of two-dimensional pictures. Psychol Rev 104: 618-658.

131. Grossberg S (2003) Filling-in the forms: Surface and boundary interactions in visual cortex. In: Filling-In: from perceptual completion to cortical reorganization (Pessoa L, De Weerd P, eds), pp 13-37. Oxford University Press.

132. Grossberg S, Hong S (2006) A neural model of surface perception: lightness, anchoring, and filling-in. Spat Vis 19: 263-321.

133. Grossberg S, Mingolla E (1985) Neural dynamics of form perception: boundary completion, illusory figures, and neon color spreading. Psychol Rev 92: 173-211.

134. Haenny PE, Maunsell JH, Schiller PH (1988) State dependent activity in monkey visual cortex. II. Retinal and extraretinal factors in V4. Exp Brain Res 69: 245-259.

135. Halgren E, Mendola J, Chong CD, Dale AM (2003) Cortical activation to illusory shapes as measured with magnetoencephalography. Neuroimage 18: 1001-1009.

136. Hamalainen M, Hari R (2002) Magnetoencephalographic characterization of dynamic brain activation. In: Brain mapping: the methods (Toga AW, Mazziotta JC, eds), pp 230-253. Academic Press.

137. Hamalainen M, Hari R, Ilmoniemi RJ, Knuutila J, Lounasmaa OV (1993) Magnetoencephalography - theory, instrumentation and applictions to noninvasive studies of the wokring human brain. Reviews of Modern Physics 65: 413-497.

138. Hardage L, Tyler CW (1995) Induced twinkle aftereffect as a probe of dynamic visual processing mechanisms. Vision Res 35: 757-766.

139. Haruno M, Kuroda T, Doya K, Toyama K, Kimura M, Samejima K, Imamizu H, Kawato M (2004) A neural correlate of reward-based behavioral learning in caudate nucleus: a functional magnetic resonance imaging study of a stochastic decision task. J Neurosci 24: 1660-1665.

140. Haynes JD, Rees G (2005) Predicting the stream of consciousness from activity in human visual cortex. Curr Biol 15: 1301-1307.

141. Haynes JD, Rees G (2006) Decoding mental states from brain activity in humans. Nat Rev Neurosci 7: 523-534.

142. Heeger DJ, Ress D (2002) What does fMRI tell us about neuronal activity? Nat Rev Neurosci 3: 142-151.

143. Hegde J, Fang F, Murray SO, Kersten D (2008) Preferential responses to occluded objects in the human visual cortex. J Vis 8: 16.

144. Heinrich SP, Bach M (2001) Adaptation dynamics in pattern-reversal visual evoked potentials. Doc Ophthalmol 102: 141-156.

145. Herrmann CS (2001) Human EEG responses to 1-100 Hz flicker: resonance phenomena in visual cortex and their potential correlation to cognitive phenomena. Exp Brain Res 137: 346-353.

146. Herrmann CS, Bosch V (2001) Gestalt perception modulates early visual processing. Neuroreport 12: 901-904.

147. Herrmann CS, Grigutsch M, Busch NA (2005) EEG oscillations and wavelet analysis. In: Event-Related Potentials (Handy TC, ed), pp 229-259. Cambridge, Massachusetts: MIT Press.

148. Hirsch J, DeLaPaz RL, Relkin NR, Victor J, Kim K, Li T, Borden P, Rubin N, Shapley R (1995) Illusory contours activate specific regions in human visual cortex: evidence from functional magnetic resonance imaging. Proc Natl Acad Sci U S A 92: 6469-6473.

149. Hofstoetter C, Koch C, Kiper DC (2004) Motion-induced blindness does not affect the formation of negative afterimages. Conscious Cogn 13: 691-708.

150. Hoge RD, Atkinson J, Gill B, Crelier GR, Marrett S, Pike GB (1999) Investigation of BOLD signal dependence on cerebral blood flow and oxygen consumption: the deoxyhemoglobin dilution model. Magn Reson Med 42: 849-863.

151. Holland PC, Gallagher M (2004) Amygdala-frontal interactions and reward expectancy. Curr Opin Neurobiol 14: 148-155.

152. Holmes G (1918) DISTURBANCES OF VISION BY CEREBRAL LESIONS. Br J Ophthalmol 2: 353-384.

153. Horton JC, Hoyt WF (1991) The representation of the visual field in human striate cortex. A revision of the classic Holmes map. Arch Ophthalmol 109: 816-824.

154. Hsu LC, Yeh SL, Kramer P (2004) Linking motion-induced blindness to perceptual filling-in. Vision Res 44: 2857-2866.

155. Hsu LC, Yeh SL, Kramer P (2006) A common mechanism for perceptual filling-in and motion-induced blindness. Vision Res 46: 1973-1981.

156. Huang MX, Aine C, Davis L, Butman J, Christner R, Weisend M, Stephen J, Meyer J, Silveri J, Herman M, Lee RR (2000) Sources on the anterior and posterior banks of the central sulcus identified from magnetic somatosensory evoked responses using multistart spatio-temporal localization. Hum Brain Mapp 11: 59-76.

157. Hubel DH, Wiesel TN (1965) RECEPTIVE FIELDS AND FUNCTIONAL ARCHITECTURE IN TWO NONSTRIATE VISUAL AREAS (18 AND 19) OF THE CAT. J Neurophysiol 28: 229-289.

158. Hubel DH, Wiesel TN (1968) Receptive fields and functional architecture of monkey striate cortex. J Physiol 195: 215-243.

159. Hung CP, Ramsden BM, Chen LM, Roe AW (2001) Building surfaces from borders in Areas 17 and 18 of the cat. Vision Res 41: 1389-1407.

160. Hutton C, Bork A, Josephs O, Deichmann R, Ashburner J, Turner R (2002) Image distortion correction in fMRI: A quantitative evaluation. Neuroimage 16: 217-240.

161. Huxlin KR, Saunders RC, Marchionini D, Pham HA, Merigan WH (2000) Perceptual deficits after lesions of inferotemporal cortex in macaques. Cereb Cortex 10: 671-683.

162. Jack AI, Shulman GL, Snyder AZ, McAvoy M, Corbetta M (2006) Separate modulations of human V1 associated with spatial attention and task structure. Neuron 51: 135-147.

163. Jackson SR (1999) Pathological perceptual completion in hemianopia extends to the control of reach-to-grasp movements. Neuroreport 10: 2461-2466.

164. Jensen O, Hari R, Kaila K (2002) Visually evoked gamma responses in the human brain are enhanced during voluntary hyperventilation. Neuroimage 15: 575-586.

165. Johnson JS, Olshausen BA (2005) The recognition of partially visible natural objects in the presence and absence of their occluders. Vision Res 45: 3262-3276.

166. Josephson BD (1962) Possible new effects in superconductive tunnelling. Phys Lett **1**: 251-253.

167. Kamitani Y, Tong F (2005) Decoding the visual and subjective contents of the human brain. Nat Neurosci 8: 679-685.

168. Kanizsa G (1979) Organization in vision. New York: Praeger.

169. Kanwisher N, McDermott J, Chun MM (1997) The fusiform face area: a module in human extrastriate cortex specialized for face perception. J Neurosci 17: 4302-4311.

170. Kapadia MK, Gilbert CD, Westheimer G (1994) A quantitative measure for short-term cortical plasticity in human vision. J Neurosci 14: 451-457.

171. Kastner S, De Weerd P, Desimone R, Ungerleider LG (1998) Mechanisms of directed attention in the human extrastriate cortex as revealed by functional MRI. Science 282: 108-111.

172. Kastner S, Pinsk MA (2004) Visual attention as a multilevel selection process. Cogn Affect Behav Neurosci 4: 483-500.

173. Kastner S, Pinsk MA, De Weerd P, Desimone R, Ungerleider LG (1999) Increased activity in human visual cortex during directed attention in the absence of visual stimulation. Neuron 22: 751-761.

174. Kellman PJ, Shipley TF (1991) A theory of visual interpolation in object perception. Cogn Psychol 23: 141-221.

175. Kellman PJ, Yin C, Shipley TF (1998) A common mechanism for illusory and occluded object completion. J Exp Psychol Hum Percept Perform 24: 859-869.

176. Kiebel SJ, Holmes AP (2003) The general linear model. In: Human Brain Function (Ashburner J, Friston KJ, Penny WD, eds), pp 1-58.

177. Kingdom F, Moulden B (1988) Border effects on brightness: a review of findings, models and issues. Spat Vis 3: 225-262.

178. Knutson B, Fong GW, Adams CM, Varner JL, Hommer D (2001) Dissociation of reward anticipation and outcome with event-related fMRI. Neuroreport 12: 3683-3687.

179. Knutson B, Fong GW, Bennett SM, Adams CM, Hommer D (2003) A region of mesial prefrontal cortex tracks monetarily rewarding outcomes: characterization with rapid event-related fMRI. Neuroimage 18: 263-272.

180. Komatsu H (2006) The neural mechanisms of perceptual filling-in. Nat Rev Neurosci 7: 220-231.

181. Komatsu H, Kinoshita M, Murakami I (2002) Neural responses in the primary visual cortex of the monkey during perceptual filling-in at the blind spot. Neurosci Res 44: 231-236.

182. Koob GF, Everitt B, Robbins TW (2008) Reward, motivation and addiction. In: Fundamental Neuroscience (Squire L, Berg D, Bloom F, eds), pp 987-1016. Elsevier.

183. Krauskopf J, Riggs LA (1959) Interocular transfer in the disappearance of stabilised images. American Journal of Psychology 72: 248-252.

184. Krawczyk DC, Gazzaley A, D'Esposito M (2007) Reward modulation of prefrontal and visual association cortex during an incentive working memory task. Brain Res 1141: 168-177.

185. Kringelbach ML, O'Doherty J, Rolls ET, Andrews C (2003) Activation of the human orbitofrontal cortex to a liquid food stimulus is correlated with its subjective pleasantness. Cereb Cortex 13: 1064-1071.

186. Kruggel F, Herrmann CS, Wiggins CJ, von Cramon DY (2001) Hemodynamic and electroencephalographic responses to illusory figures: recording of the evoked potentials during functional MRI. Neuroimage 14: 1327-1336.

187. Kwong KK, Belliveau JW, Chesler DA, Goldberg IE, Weisskoff RM, Poncelet BP, Kennedy DN, Hoppel BE, Cohen MS, Turner R, . (1992) Dynamic magnetic resonance imaging of human brain activity during primary sensory stimulation. Proc Natl Acad Sci U S A 89: 5675-5679.

188. LaBar KS, Gitelman DR, Parrish TB, Kim YH, Nobre AC, Mesulam MM (2001) Hunger selectively modulates corticolimbic activation to food stimuli in humans. Behav Neurosci 115: 493-500.

189. LANSING RW (1964) Electroencephalographic correltaes of binocular rivalry in man. Science 146: 1325-1327.

190. Larsson J, Amunts K, Gulyas B, Malikovic A, Zilles K, Roland PE (1999) Neuronal correlates of real and illusory contour perception: functional anatomy with PET. Eur J Neurosci 11: 4024-4036.

191. Larsson J, Heeger DJ (2006) Two retinotopic visual areas in human lateral occipital cortex. J Neurosci 26: 13128-13142.

192. Larsson J, Landy MS, Heeger DJ (2006) Orientation-selective adaptation to first- and second-order patterns in human visual cortex. J Neurophysiol 95: 862-881.

193. Lavie N (2005) Distracted and confused?: selective attention under load. Trends Cogn Sci 9: 75-82.

194. Lavie N, de Fockert JW (2003) Contrasting effects of sensory limits and capacity limits in visual selective attention. Percept Psychophys 65: 202-212.

195. Lavie N, Hirst A, de Fockert JW, Viding E (2004) Load theory of selective attention and cognitive control. J Exp Psychol Gen 133: 339-354.

196. Lee TS, Nguyen M (2001) Dynamics of subjective contour formation in the early visual cortex. Proc Natl Acad Sci U S A 98: 1907-1911.

197. Legatt AD, Arezzo J, Vaughan HG, Jr. (1980) Averaged multiple unit activity as an estimate of phasic changes in local neuronal activity: effects of volume-conducted potentials. J Neurosci Methods 2: 203-217.

198. Lerner Y, Harel M, Malach R (2004) Rapid completion effects in human high-order visual areas. Neuroimage 21: 516-526.

199. Lerner Y, Hendler T, Malach R (2002) Object-completion effects in the human lateral occipital complex. Cereb Cortex 12: 163-177.

200. Lleras A, Moore CM (2006) What you see is what you get: functional equivalence of a perceptually filled-in surface and a physically presented stimulus. Psychol Sci 17: 876-881.

201. Logothetis NK, Pauls J, Augath M, Trinath T, Oeltermann A (2001) Neurophysiological investigation of the basis of the fMRI signal. Nature 412: 150-157.

202. Lou L (1999) Selective peripheral fading: evidence for inhibitory sensory effect of attention. Perception 28: 519-526.

203. Luck SJ, Chelazzi L, Hillyard SA, Desimone R (1997) Neural mechanisms of spatial selective attention in areas V1, V2, and V4 of macaque visual cortex. J Neurophysiol 77: 24-42.

204. Lumer ED, Friston KJ, Rees G (1998) Neural correlates of perceptual rivalry in the human brain. Science 280: 1930-1934.

205. Lumer ED, Rees G (1999) Covariation of activity in visual and prefrontal cortex associated with subjective visual perception. Proc Natl Acad Sci U S A 96: 1669-1673.

206. Macdonald JS, Lavie N (2008) Load induced blindness. J Exp Psychol Hum Percept Perform 34: 1078-1091.

207. Magistretti PJ, Pellerin L (1999) Cellular mechanisms of brain energy metabolism and their relevance to functional brain imaging. Philos Trans R Soc Lond B Biol Sci 354: 1155-1163.

208. Malkova L, Gaffan D, Murray EA (1997) Excitotoxic lesions of the amygdala fail to produce impairment in visual learning for auditory secondary reinforcement but interfere with reinforcer devaluation effects in rhesus monkeys. J Neurosci 17: 6011-6020.

209. Malonek D, Dirnagl U, Lindauer U, Yamada K, Kanno I, Grinvald A (1997) Vascular imprints of neuronal activity: relationships between the dynamics of cortical blood flow, oxygenation, and volume changes following sensory stimulation. Proc Natl Acad Sci U S A 94: 14826-14831.

210. Malonek D, Grinvald A (1996) Interactions between electrical activity and cortical microcirculation revealed by imaging spectroscopy: implications for functional brain mapping. Science 272: 551-554.

211. Marcel AJ (1998) Blindsight and shape perception: deficit of visual consciousness or of visual function? Brain 121 (Pt 8): 1565-1588.

212. Marquardt DW (1963) An algorithm for least-squares estimation of non-linear parameters. J Soc Indust Appl Math 11: 431-441.

213. Martinez A, Anllo-Vento L, Sereno MI, Frank LR, Buxton RB, Dubowitz DJ, Wong EC, Hinrichs H, Heinze HJ, Hillyard SA (1999b) Involvement of striate and extrastriate visual cortical areas in spatial attention. Nat Neurosci 2: 364-369.

214. Martinez A, Anllo-Vento L, Sereno MI, Frank LR, Buxton RB, Dubowitz DJ, Wong EC, Hinrichs H, Heinze HJ, Hillyard SA (1999a) Involvement of striate and extrastriate visual cortical areas in spatial attention. Nat Neurosci 2: 364-369.

215. Martinez-Conde S, Macknik SL, Troncoso XG, Dyar TA (2006) Microsaccades counteract visual fading during fixation. Neuron 49: 297-305.

216. Masuda Y, Dumoulin SO, Nakadomari S, Wandell BA (2008) V1 projection zone signals in human macular degeneration depend on task, not stimulus. Cereb Cortex 18: 2483-2493.

217. Mathiesen C, Caesar K, Akgoren N, Lauritzen M (1998) Modification of activity-dependent increases of cerebral blood flow by excitatory synaptic activity and spikes in rat cerebellar cortex. J Physiol 512 (Pt 2): 555-566.

218. Matsumoto M, Komatsu H (2005) Neural responses in the macaque v1 to bar stimuli with various lengths presented on the blind spot. J Neurophysiol 93: 2374-2387.

219. Mattingley JB, Davis G, Driver J (1997) Preattentive filling-in of visual surfaces in parietal extinction. Science 275: 671-674.

220. Mattout J, Phillips C, Penny WD, Rugg MD, Friston KJ (2006) MEG source localization under multiple constraints: an extended Bayesian framework. Neuroimage 30: 753-767.

221. McCarthy RA, James-Galton M, Plant GT (2006) Form completion across a hemianopic boundary: behindsight? Neuropsychologia 44: 1269-1281.

222. Mendola JD, Conner IP, Sharma S, Bahekar A, Lemieux S (2006) fMRI Measures of Perceptual Filling-in in the Human Visual Cortex. J Cogn Neurosci 18: 363-375.

223. Mendola JD, Dale AM, Fischl B, Liu AK, Tootell RB (1999) The representation of illusory and real contours in human cortical visual areas revealed by functional magnetic resonance imaging. J Neurosci 19: 8560-8572.

224. Meng M, Remus DA, Tong F (2005) Filling-in of visual phantoms in the human brain. Nat Neurosci 8: 1248-1254.

225. Meyer GE, Dougherty T (1987) Effects of flicker-induced depth on chromatic subjective contours. J Exp Psychol Hum Percept Perform 13: 353-360.

226. Michotte A, Thines G, Crabbe G (1991) Amodal completion of perceptual structures. In: Michotte's experimental phenomonelogy of perception (Thines G, Costall A, Butterworth G, eds), pp 140-167. Hillsdale, NJ: Erlbaum.

227. Mihaylov P, Manahilov V, Simpson WA, Strang NC (2007) Induced internal noise in perceptual artificial scotomas created by surrounding dynamic noise. Vision Res 47: 1479-1489.

228. Mikami A, Newsome WT, Wurtz RH (1986) Motion selectivity in macaque visual cortex. I. Mechanisms of direction and speed selectivity in extrastriate area MT. J Neurophysiol 55: 1308-1327.

229. Mintun MA, Lundstrom BN, Snyder AZ, Vlassenko AG, Shulman GL, Raichle ME (2001) Blood flow and oxygen delivery to human brain during functional activity: theoretical modeling and experimental data. Proc Natl Acad Sci U S A 98: 6859-6864.

230. Mitzdorf U (1987) Properties of the evoked potential generators: current source-density analysis of visually evoked potentials in the cat cortex. Int J Neurosci 33: 33-59.

231. Montaser-Kouhsari L, Landy MS, Heeger DJ, Larsson J (2007) Orientation-selective adaptation to illusory contours in human visual cortex. J Neurosci 27: 2186-2195.

232. Montaser-Kouhsari L, Moradi F, Zandvakili A, Esteky H (2004) Orientation-selective adaptation during motion-induced blindness. Perception 33: 249-254.

233. Moran J, Desimone R (1985) Selective attention gates visual processing in the extrastriate cortex. Science 229: 782-784.

234. Motter BC (1993) Focal attention produces spatially selective processing in visual cortical areas V1, V2, and V4 in the presence of competing stimuli. J Neurophysiol 70: 909-919.

235. Motter BC (1994) Neural correlates of attentive selection for color or luminance in extrastriate area V4. J Neurosci 14: 2178-2189.

236. Moutoussis K, Zeki S (2002) The relationship between cortical activation and perception investigated with invisible stimuli. Proc Natl Acad Sci U S A 99: 9527-9532.

237. Murakami I (1995) Motion aftereffect after monocular adaptation to filled-in motion at the blind spot. Vision Res 35: 1041-1045.

238. Murakami I, Komatsu H, Kinoshita M (1997) Perceptual filling-in at the scotoma following a monocular retinal lesion in the monkey. Vis Neurosci 14: 89-101.

239. Murray MM, Foxe DM, Javitt DC, Foxe JJ (2004) Setting boundaries: brain dynamics of modal and amodal illusory shape completion in humans. J Neurosci 24: 6898-6903.

240. Murray MM, Imber ML, Javitt DC, Foxe JJ (2006) Boundary completion is automatic and dissociable from shape discrimination. J Neurosci 26: 12043-12054.

241. Murray MM, Wylie GR, Higgins BA, Javitt DC, Schroeder CE, Foxe JJ (2002a) The spatiotemporal dynamics of illusory contour processing: combined high-density electrical mapping, source analysis, and functional magnetic resonance imaging. J Neurosci 22: 5055-5073.

242. Murray SO, Kersten D, Olshausen BA, Schrater P, Woods DL (2002b) Shape perception reduces activity in human primary visual cortex. Proc Natl Acad Sci U S A 99: 15164-15169.

243. Murray SO, Olshausen BA, Woods DL (2003) Processing shape, motion and three-dimensional shape-from-motion in the human cortex. Cereb Cortex 13: 508-516.

244. Nakayama K, Shimojo S (1992) Experiencing and perceiving visual surfaces. Science 257: 1357-1363.

245. Nakayama K, Shimojo S, Ramachandran VS (1990) Transparency: relation to depth, subjective contours, luminance, and neon color spreading. Perception 19: 497-513.

246. Nakayama K, Shimojo S, Silverman GH (1989) Stereoscopic depth: its relation to image segmentation, grouping, and the recognition of occluded objects. Perception 18: 55-68.

247. Nelles G, de Greiff A, Pscherer A, Forsting M, Gerhard H, Esser J, Diener HC (2007) Cortical activation in hemianopia after stroke. Neurosci Lett 426: 34-38.

248. Neumann H, Pessoa L, Hansen T (2001) Visual filling-in for computing perceptual surface properties. Biol Cybern 85: 355-369.

249. Nieder A (2002) Seeing more than meets the eye: processing of illusory contours in animals. J Comp Physiol A Neuroethol Sens Neural Behav Physiol 188: 249-260.

250. O'Brien V (1958) Contour perception, illusion and reality. J Opt Soc Am 48: 112-119.

251. O'Craven KM, Rosen BR, Kwong KK, Treisman A, Savoy RL (1997) Voluntary attention modulates fMRI activity in human MT-MST. Neuron 18: 591-598.

252. O'Doherty J, Kringelbach ML, Rolls ET, Hornak J, Andrews C (2001) Abstract reward and punishment representations in the human orbitofrontal cortex. Nat Neurosci 4: 95-102.

253. O'Doherty J, Winston J, Critchley H, Perrett D, Burt DM, Dolan RJ (2003) Beauty in a smile: the role of medial orbitofrontal cortex in facial attractiveness. Neuropsychologia 41: 147-155.

254. O'Doherty JP (2004) Reward representations and reward-related learning in the human brain: insights from neuroimaging. Curr Opin Neurobiol 14: 769-776.

255. O'Doherty JP, Deichmann R, Critchley HD, Dolan RJ (2002) Neural responses during anticipation of a primary taste reward. Neuron 33: 815-826.

256. O'Regan JK (1992) Solving the "real" mysteries of visual perception: the world as an outside memory. Can J Psychol 46: 461-488.

257. Ogawa S, Lee TM, Nayak AS, Glynn P (1990) Oxygenation-sensitive contrast in magnetic resonance image of rodent brain at high magnetic fields. Magn Reson Med 14: 68-78.

258. Ogawa S, Tank DW, Menon R, Ellermann JM, Kim SG, Merkle H, Ugurbil K (1992) Intrinsic signal changes accompanying sensory stimulation: functional brain mapping with magnetic resonance imaging. Proc Natl Acad Sci U S A 89: 5951-5955.

259. Ohtani Y, Okamura S, Shibasaki T, Arakawa A, Yoshida Y, Toyama K, Ejima Y (2002) Magnetic responses of human visual cortex to illusory contours. Neurosci Lett 321: 173-176.

260. Pantoja J, Ribeiro S, Wiest M, Soares E, Gervasoni D, Lemos NA, Nicolelis MA (2007) Neuronal activity in the primary somatosensory thalamocortical loop is modulated by reward contingency during tactile discrimination. J Neurosci 27: 10608-10620.

261. Paradiso MA, Hahn S (1996) Filling-in percepts produced by luminance modulation. Vision Res 36: 2657-2663.

262. Pastor MA, Artieda J, Arbizu J, Valencia M, Masdeu JC (2003) Human cerebral activation during steady-state visual-evoked responses. J Neurosci 23: 11621-11627.

263. Pauling L, Coryell CD (1936) The Magnetic Properties and Structure of Hemoglobin, Oxyhemoglobin and Carbonmonoxyhemoglobin. Proc Natl Acad Sci U S A 22: 210-216.

264. Pavlov IP (1927) Conditioned relexes. Oxford: Oxford University Press.

265. Perna A, Tosetti M, Montanaro D, Morrone MC (2005) Neuronal mechanisms for illusory brightness perception in humans. Neuron 47: 645-651.

266. Pessoa L, Thompson E, Noe A (1998) Finding out about filling-in: a guide to perceptual completion for visual science and the philosophy of perception. Behav Brain Sci 21: 723-748.

267. Petrovic P, Pleger B, Seymour B, Kloppel S, De Martino B, Critchley H, Dolan RJ (2008) Blocking central opiate function modulates hedonic impact and anterior cingulate response to rewards and losses. J Neurosci 28: 10509-10516.

268. Phillips C, Rugg MD, Friston KJ (2002) Anatomically informed basis functions for EEG source localization: combining functional and anatomical constraints. Neuroimage 16: 678-695.

269. Pillow J, Rubin N (2002) Perceptual completion across the vertical meridian and the role of early visual cortex. Neuron 33: 805-813.

270. Pinna B, Grossberg S (2005) The watercolor illusion and neon color spreading: a unified analysis of new cases and neural mechanisms. J Opt Soc Am A Opt Image Sci Vis 22: 2207-2221.

271. Platt ML, Glimcher PW (1999) Neural correlates of decision variables in parietal cortex. Nature 400: 233-238.

272. Pleger B, Blankenburg F, Ruff CC, Driver J, Dolan RJ (2008) Reward facilitates tactile judgments and modulates hemodynamic responses in human primary somatosensory cortex. J Neurosci 28: 8161-8168.

273. Pleger, B., Ruff, C. C., Blankenburg, F., Kloeppel, S., Driver, J., and Dolan, R. J. Dopaminergic reward influences on somatosensory decision making. PLoS Biology . 2009.
Ref Type: In Press

274. Poppelreuter W (1917) Disturbances of lower and higher visual capacities caused by occipital damage: with special reference to the psychological, pedagogical, industrial and social implications. Translated by Zihl, J. Oxford: Clarendon Press.

275. Portin K, Vanni S, Virsu V, Hari R (1999) Stronger occipital cortical activation to lower than upper visual field stimuli. Neuromagnetic recordings. Exp Brain Res 124: 287-294.

276. Powers WJ, Hirsch IB, Cryer PE (1996) Effect of stepped hypoglycemia on regional cerebral blood flow response to physiological brain activation. Am J Physiol 270: H554-H559.

277. PRITCHARD RM, HERON W, HEBB DO (1960) Visual perception approached by the method of stabilized images. Can J Psychol 14: 67-77.

278. Proverbio AM, Zani A (2002) Electrophysiological indexes of illusory contours perception in humans. Neuropsychologia 40: 479-491.

279. Ramachandran VS (1992) Filling in the blind spot. Nature 356: 115.

280. Ramachandran VS, Gregory RL (1991) Perceptual filling in of artificially induced scotomas in human vision. Nature 350: 699-702.

281. Ramachandran VS, Ruskin D, Cobb S, Rogers-Ramachandran D, Tyler CW (1994) On the perception of illusory contours. Vision Res 34: 3145-3152.

282. Ramnani N, Miall RC (2003) Instructed delay activity in the human prefrontal cortex is modulated by monetary reward expectation. Cereb Cortex 13: 318-327.

283. Ramsden BM, Hung CP, Roe AW (2001) Real and illusory contour processing in area V1 of the primate: a cortical balancing act. Cereb Cortex 11: 648-665.

284. Rauschenberger R, Liu T, Slotnick SD, Yantis S (2006) Temporally unfolding neural representation of pictorial occlusion. Psychol Sci 17: 358-364.

285. Redies C, Crook JM, Creutzfeldt OD (1986) Neuronal responses to borders with and without luminance gradients in cat visual cortex and dorsal lateral geniculate nucleus. Exp Brain Res 61: 469-481.

286. Redies C, Spillman L (1982) The neon color effect in the Ehrenstein illusion. Perception 10: 667-681.

287. Rees G, Friston K, Koch C (2000) A direct quantitative relationship between the functional properties of human and macaque V5. Nat Neurosci 3: 716-723.

288. Rees G, Frith CD, Lavie N (1997) Modulating irrelevant motion perception by varying attentional load in an unrelated task. Science 278: 1616-1619.

289. Reich LN, Levi DM, Frishman LJ (2000) Dynamic random noise shrinks the twinkling aftereffect induced by artificial scotomas. Vision Res 40: 805-816.

290. Rensink RA, Enns JT (1998) Early completion of occluded objects. Vision Res 38: 2489-2505.

291. Ress D, Heeger DJ (2003) Neuronal correlates of perception in early visual cortex. Nat Neurosci 6: 414-420.

292. RIGGS LA, RATLIFF F, CORNSWEET JC, CORNSWEET TN (1953) The disappearance of steadily fixated visual test objects. J Opt Soc Am 43: 495-501.

293. Ritzl A, Marshall JC, Weiss PH, Zafiris O, Shah NJ, Zilles K, Fink GR (2003) Functional anatomy and differential time courses of neural processing for explicit, inferred, and illusory contours. An event-related fMRI study. Neuroimage 19: 1567-1577.

294. Roe AW, Lu HD, Hung CP (2005) Cortical processing of a brightness illusion. Proc Natl Acad Sci U S A 102: 3869-3874.

295. Rolls ET, Sienkiewicz ZJ, Yaxley S (1989) Hunger Modulates the Responses to Gustatory Stimuli of Single Neurons in the Caudolateral Orbitofrontal Cortex of the Macaque Monkey. Eur J Neurosci 1: 53-60.

296. Romo R, Schultz W (1990) Dopamine neurons of the monkey midbrain: contingencies of responses to active touch during self-initiated arm movements. J Neurophysiol 63: 592-606.

297. Sakaguchi Y (2001) Target/surround asymmetry in perceptual filling-in. Vision Res 41: 2065-2077.

298. Sakaguchi Y (2006) Contrast dependency in perceptual filling-in. Vision Res 46: 3304-3312.

299. Samar VJ, Bopardikar A, Rao R, Swartz K (1999) Wavelet analysis of neuroelectric waveforms: a conceptual tutorial. Brain Lang 66: 7-60.

300. Sary G, Chadaide Z, Tompa T, Koteles K, Kovacs G, Benedek G (2007) Illusory shape representation in the monkey inferior temporal cortex. Eur J Neurosci 25: 2558-2564.

301. Sasaki Y, Watanabe T (2004) The primary visual cortex fills in color. Proc Natl Acad Sci U S A 101: 18251-18256.

302. Sawamura H, Georgieva S, Vogels R, Vanduffel W, Orban GA (2005) Using functional magnetic resonance imaging to assess adaptation and size invariance of shape processing by humans and monkeys. J Neurosci 25: 4294-4306.

303. Scholvinck ML, Rees G (2009a) Attentional influences on the dynamics of motion-induced blindness. J Vis 9: 38-39.

304. Scholvinck ML, Rees G (2009b) Neural Correlates of Motion-induced Blindness in the Human Brain. J Cogn Neurosci.

305. Schultz W, Dickinson A (2000) Neuronal coding of prediction errors. Annu Rev Neurosci 23: 473-500.

306. Schwartz S, Vuilleumier P, Hutton C, Maravita A, Dolan RJ, Driver J (2005) Attentional load and sensory competition in human vision: modulation of fMRI responses by load at fixation during task-irrelevant stimulation in the peripheral visual field. Cereb Cortex 15: 770-786.

307. Schwartz WJ, Smith CB, Davidsen L, Savaki H, Sokoloff L, Mata M, Fink DJ, Gainer H (1979) Metabolic mapping of functional activity in the hypothalamo-neurohypophysial system of the rat. Science 205: 723-725.

308. Seghier M, Dojat M, Delon-Martin C, Rubin C, Warnking J, Segebarth C, Bullier J (2000) Moving illusory contours activate primary visual cortex: an fMRI study. Cereb Cortex 10: 663-670.

309. Seghier ML, Vuilleumier P (2006) Functional neuroimaging findings on the human perception of illusory contours. Neurosci Biobehav Rev 30: 595-612.

310. Segonne F, Dale AM, Busa E, Glessner M, Salat D, Hahn HK, Fischl B (2004) A hybrid approach to the skull stripping problem in MRI. Neuroimage 22: 1060-1075.

311. Segonne F, Pacheco J, Fischl B (2007) Geometrically accurate topology-correction of cortical surfaces using nonseparating loops. IEEE Trans Med Imaging 26: 518-529.

312. Seitz AR, Kim D, Watanabe T (2009) Rewards evoke learning of unconsciously processed visual stimuli in adult humans. Neuron 61: 700-707.

313. Sekular A, Palmer S, Flynn C (1994) Local and global processes in visual completion. Psychol Sci 5: 260-267.

314. Senkowski D, Rottger S, Grimm S, Foxe JJ, Herrmann CS (2005) Kanizsa subjective figures capture visual spatial attention: evidence from electrophysiological and behavioral data. Neuropsychologia 43: 872-886.

315. Serences JT (2008) Value-based modulations in human visual cortex. Neuron 60: 1169-1181.

316. Sereno MI, Dale AM, Reppas JB, Kwong KK, Belliveau JW, Brady TJ, Rosen BR, Tootell RB (1995) Borders of multiple visual areas in humans revealed by functional magnetic resonance imaging. Science 268: 889-893.

317. Sergent C, Baillet S, Dehaene S (2005) Timing of the brain events underlying access to consciousness during the attentional blink. Nat Neurosci 8: 1391-1400.

318. Sergent J (1988) An investigation into perceptual completion in blind areas of the visual field. Brain 111 (Pt 2): 347-373.

319. Sheth BR, Sharma J, Rao SC, Sur M (1996) Orientation maps of subjective contours in visual cortex. Science 274: 2110-2115.

320. Shuler MG, Bear MF (2006) Reward timing in the primary visual cortex. Science 311: 1606-1609.

321. Shulman RG, Rothman DL (1998) Interpreting functional imaging studies in terms of neurotransmitter cycling. Proc Natl Acad Sci U S A 95: 11993-11998.

322. Silver MA, Ress D, Heeger DJ (2007) Neural correlates of sustained spatial attention in human early visual cortex. J Neurophysiol 97: 229-237.

323. Singh M (2004) Modal and amodal completion generate different shapes. Psychol Sci 15: 454-459.

324. Sirotin YB, Das A (2009) Anticipatory haemodynamic signals in sensory cortex not predicted by local neuronal activity. Nature 457: 475-479.

325. Sled JG, Zijdenbos AP, Evans AC (1998) A nonparametric method for automatic correction of intensity nonuniformity in MRI data. IEEE Trans Med Imaging 17: 87-97.

326. Small DM, Gitelman D, Simmons K, Bloise SM, Parrish T, Mesulam MM (2005) Monetary incentives enhance processing in brain regions mediating top-down control of attention. Cereb Cortex 15: 1855-1865.

327. Small DM, Gregory MD, Mak YE, Gitelman D, Mesulam MM, Parrish T (2003) Dissociation of neural representation of intensity and affective valuation in human gustation. Neuron 39: 701-711.

328. Smirnakis SM, Brewer AA, Schmid MC, Tolias AS, Schuz A, Augath M, Inhoffen W, Wandell BA, Logothetis NK (2005) Lack of long-term cortical reorganization after macaque retinal lesions. Nature 435: 300-307.

329. Smith A, Over R (1975) Tilt aftereffects with subjective contours. Nature 257: 581-582.

330. Smith AT, Over R (1979) Motion aftereffect with subjective contours. Percept Psychophys 25: 95-98.

331. Smith AT, Singh KD, Williams AL, Greenlee MW (2001) Estimating receptive field size from fMRI data in human striate and extrastriate visual cortex. Cereb Cortex 11: 1182-1190.

332. Somers DC, Dale AM, Seiffert AE, Tootell RB (1999) Functional MRI reveals spatially specific attentional modulation in human primary visual cortex. Proc Natl Acad Sci U S A 96: 1663-1668.

333. Soto D, Humphreys GW, Rotshtein P (2007) Dissociating the neural mechanisms of memory-based guidance of visual selection. Proc Natl Acad Sci U S A 104: 17186-17191.

334. Spencer KM (2005) Averaging, detection and classification of single-trial ERPs. In: Event-Related Potentials (Handy TC, ed), pp 209-227. Cambridge, Massachussets: MIT Press.

335. Spillman L, De Weerd P (2003) Mechanisms of surface completion: Perceptual filling-in of texture. In: Filling-in: From perceptual completion to cortical reorganisation (Pessoa L, De Weerd P, eds), pp 81-105. New York: Oxford University Press.

336. Spillmann L, Kurtenbach A (1992) Dynamic noise backgrounds facilitate target fading. Vision Res 32: 1941-1946.

337. Spillmann L, Otte T, Hamburger K, Magnussen S (2006) Perceptual filling-in from the edge of the blind spot. Vision Res 46: 4252-4257.

338. Spillmann L, Werner JS (1996) Long-range interactions in visual perception. Trends Neurosci 19: 428-434.

339. Spiridon M, Fischl B, Kanwisher N (2006) Location and spatial profile of category-specific regions in human extrastriate cortex. Hum Brain Mapp 27: 77-89.

340. Spitzer H, Desimone R, Moran J (1988) Increased attention enhances both behavioral and neuronal performance. Science 240: 338-340.

341. Stanley DA, Rubin N (2003) fMRI activation in response to illusory contours and salient regions in the human lateral occipital complex. Neuron 37: 323-331.

342. Sterzer P, Haynes JD, Rees G (2006) Primary visual cortex activation on the path of apparent motion is mediated by feedback from hMT+/V5. Neuroimage 32: 1308-1316.

343. Sturzel F, Spillmann L (2001) Texture fading correlates with stimulus salience. Vision Res 41: 2969-2977.

344. Sugita Y (1999) Grouping of image fragments in primary visual cortex. Nature 401: 269-272.

345. Sugrue LP, Corrado GS, Newsome WT (2004) Matching behavior and the representation of value in the parietal cortex. Science 304: 1782-1787.

346. Sunness JS, Liu T, Yantis S (2004) Retinotopic mapping of the visual cortex using functional magnetic resonance imaging in a patient with central scotomas from atrophic macular degeneration. Ophthalmology 111: 1595-1598.

347. Tailby C, Metha A (2004) Artificial scotoma-induced perceptual distortions are orientation dependent and short lived. Vis Neurosci 21: 79-87.

348. Takeichi H, Shimojo S, Watanabe T (1992) Neon flank and illusory contour: interaction between the two processes leads to color filling-in. Perception 21: 313-324.

349. Tanaka K (1993) Neuronal mechanisms of object recognition. Science 262: 685-688.

350. Teo PC, Sapiro G, Wandell BA (1997) Creating connected representations of cortical gray matter for functional MRI visualization. IEEE Trans Med Imaging 16: 852-863.

351. THOMPSON JM, WOOLSEY CN, TALBOT SA (1950) Visual areas I and II of cerebral cortex of rabbit. J Neurophysiol 13: 277-288.

352. Tong F, Engel SA (2001) Interocular rivalry revealed in the human cortical blind-spot representation. Nature 411: 195-199.

353. Tononi G, Srinivasan R, Russell DP, Edelman GM (1998) Investigating neural correlates of conscious perception by frequency-tagged neuromagnetic responses. Proc Natl Acad Sci U S A 95: 3198-3203.

354. Tootell RB, Hadjikhani N, Hall EK, Marrett S, Vanduffel W, Vaughan JT, Dale AM (1998a) The retinotopy of visual spatial attention. Neuron 21: 1409-1422.

355. Tootell RB, Mendola JD, Hadjikhani NK, Ledden PJ, Liu AK, Reppas JB, Sereno MI, Dale AM (1997) Functional analysis of V3A and related areas in human visual cortex. J Neurosci 17: 7060-7078.

356. Tootell RB, Mendola JD, Hadjikhani NK, Liu AK, Dale AM (1998b) The representation of the ipsilateral visual field in human cerebral cortex. Proc Natl Acad Sci U S A 95: 818-824.

357. Tootell RB, Reppas JB, Kwong KK, Malach R, Born RT, Brady TJ, Rosen BR, Belliveau JW (1995) Functional analysis of human MT and related visual cortical areas using magnetic resonance imaging. J Neurosci 15: 3215-3230.

358. Torjussen T (1978) Visual processing in cortically blind hemifields. Neuropsychologia 16: 15-21.

359. Treue S, Martinez Trujillo JC (1999) Feature-based attention influences motion processing gain in macaque visual cortex. Nature 399: 575-579.

360. Treue S, Maunsell JH (1996) Attentional modulation of visual motion processing in cortical areas MT and MST. Nature 382: 539-541.

361. Tripathy SP, Levi DM, Ogmen H (1996) Two-dot alignment across the physiological blind spot. Vision Res 36: 1585-1596.

362. Troxler D (1804) Ueber das Verschwinden gegebener Gegenstande innerhalb unseres Gesichtkreises. In: Ophthalmische Bibliothek pp 1-119. Jena: F Frommann.

363. Tse PU (1999) Volume completion. Cogn Psychol 39: 37-68.

364. Turner R, Howseman A, Rees GE, Josephs O, Friston K (1998) Functional magnetic resonance imaging of the human brain: data acquisition and analysis. Exp Brain Res 123: 5-12.

365. Turner R, Le Bihan D, Moonen CT, Despres D, Frank J (1991) Echo-planar time course MRI of cat brain oxygenation changes. Magn Reson Med 22: 159-166.

366. Ungerleider LG, Gaffan D, Pelak VS (1989) Projections from inferior temporal cortex to prefrontal cortex via the uncinate fascicle in rhesus monkeys. Exp Brain Res 76: 473-484.

367. Ungerleider LG, Haxby JV (1994) 'What' and 'where' in the human brain. Curr Opin Neurobiol 4: 157-165.

368. Ungerleider LG, Mishkin M (1982) Two cortical visual systems. In: Analysis of visual behavior (Ingle DJ, Goodale MA, Mansfield RJW, eds), pp 549-586. Cambridge, MA: MIT Press.

369. van Lier R, van der HP, Leeuwenberg E (1994) Integrating global and local aspects of visual occlusion. Perception 23: 883-903.

370. van Lier R, Vergeer M, Anstis S (2009) Filling-in afterimage colors between the lines. Curr Biol 19: R323-R324.

371. van Tuijl HF (1975) A new visual illusion: neonlike color spreading and complementary color induction between subjective contours. Acta Psychol (Amst) 39: 441-445.

372. Vandenberghe R, Duncan J, Arnell KM, Bishop SJ, Herrod NJ, Owen AM, Minhas PS, Dupont P, Pickard JD, Orban GA (2000) Maintaining and shifting attention within left or right hemifield. Cereb Cortex 10: 706-713.

373. Varin D (1971) Fenomeni di contrasto e diffusione cromatica nell'organizzazione spaziale del campo percettivo. Rivista di Psicologia 65: 101-128.

374. Viswanathan A, Freeman RD (2007) Neurometabolic coupling in cerebral cortex reflects synaptic more than spiking activity. Nat Neurosci 10: 1308-1312.

375. Von der Heydt R, Friedman H, Zhou H (2003) Searching for the Neural Mechanism of Color Filling-in. In: Filling-In. From Perceptual completion to cortical reorganisation (Pessoa L, De Weerd P, eds), pp 106-127. New York: Oxford University Press.

376. Von der Heydt R, Peterhans E (1989) Mechanisms of contour perception in monkey visual cortex. I. Lines of pattern discontinuity. J Neurosci 9: 1731-1748.

377. von Helmholtz, H. Ueber einige Gesetze der Vertheilung elektrischer Strome in korperlichen Leitern, mit Anwendung auf die thierisch-elektrischen Versuche. Ann.Phys.Chem. 89, 211. 1853.
Ref Type: Internet Communication

378. Vrba J, Robinson SE (2001) Signal processing in magnetoencephalography. Methods 25: 249-271.

379. Vuilleumier P, Valenza N, Landis T (2001) Explicit and implicit perception of illusory contours in unilateral spatial neglect: behavioural and anatomical correlates of preattentive grouping mechanisms. Neuropsychologia 39: 597-610.

380. Walker R, Mattingley JB (1997) Ghosts in the machine? Pathological Visual Completion Phenomena in the Damaged Brain. Neurocase 3: 313-335.

381. WALLS GL (1954) The filling-in process. Am J Optom Arch Am Acad Optom 31: 329-341.

382. Wandell BA (1999) Computational neuroimaging of human visual cortex. Annu Rev Neurosci 22: 145-173.

383. Wandell BA, Chial S, Backus BT (2000) Visualization and measurement of the cortical surface. J Cogn Neurosci 12: 739-752.

384. WARRINGTON EK (1962) The completion of visual forms across hemianopic field defects. J Neurol Neurosurg Psychiatry 25: 208-217.

385. Watanabe T, Harner AM, Miyauchi S, Sasaki Y, Nielsen M, Palomo D, Mukai I (1998) Task-dependent influences of attention on the activation of human primary visual cortex. Proc Natl Acad Sci U S A 95: 11489-11492.

386. Watanabe T, Sato T (1989) Effects of luminance contrast on color spreading and illusory contour in the neon color spreading effect. Percept Psychophys 45: 427-430.

387. Watanabe T, Takeichi H (1990) The relation between color spreading and illusory contours. Percept Psychophys 47: 457-467.

388. Weigelt S, Singer W, Muckli L (2007) Separate cortical stages in amodal completion revealed by functional magnetic resonance adaptation. BMC Neurosci 8: 70.

389. Weil RS, Kilner JM, Haynes JD, Rees G (2007) Neural correlates of perceptual filling-in of an artificial scotoma in humans. Proc Natl Acad Sci U S A 104: 5211-5216.

390. Welchman AE, Harris JM (2001) Filling-in the details on perceptual fading. Vision Res 41: 2107-2117.

391. Welchman AE, Harris JM (2003) Is neural filling-in necessary to explain the perceptual completion of motion and depth information? Proc Biol Sci 270: 83-90.

392. Wilkswo JPJ (1989) In: Advances in Biomagnetism (Williamson SJ, et al., eds), pp 1-18. New York/ London: Plenum.

393. WILLIAMS D, Gassell MM (1962) Visual function in patients with homonymous hemianopia. I. The visual fields. Brain 85: 175-250.

394. Worsley KJ (2003) Developments in random field theory. In: Human Brain Function (Frackowiak RS, Friston K, Frith C, Dolan RJ, Price C, Zeki S, Penny WD, eds), pp 881-886. Elsevier Academic Press.

395. Yang G, Chen G, Ebner TJ, Iadecola C (1999) Nitric oxide is the predominant mediator of cerebellar hyperemia during somatosensory activation in rats. Am J Physiol 277: R1760-R1770.

396. Yang G, Iadecola C (1996) Glutamate microinjections in cerebellar cortex reproduce cerebrovascular effects of parallel fiber stimulation. Am J Physiol 271: R1568-R1575.

397. Yin C, Shimojo S, Moore C, Engel SA (2002) Dynamic shape integration in extrastriate cortex. Curr Biol 12: 1379-1385.

398. Zeki S, Watson JD, Lueck CJ, Friston KJ, Kennard C, Frackowiak RS (1991) A direct demonstration of functional specialization in human visual cortex. J Neurosci 11: 641-649.

399. Zener K (1937) The significance of behavior accompanying conditioned salivary secretion for theories of the conditioned response. Am J Psychol 50: 384-403.

400. Zepeda A, Vaca L, Arias C, Sengpiel F (2003) Reorganization of visual cortical maps after focal ischemic lesions. J Cereb Blood Flow Metab 23: 811-820.

401. Zur D, Ullman S (2003) Filling-in of retinal scotomas. Vision Res 43: 971-982.